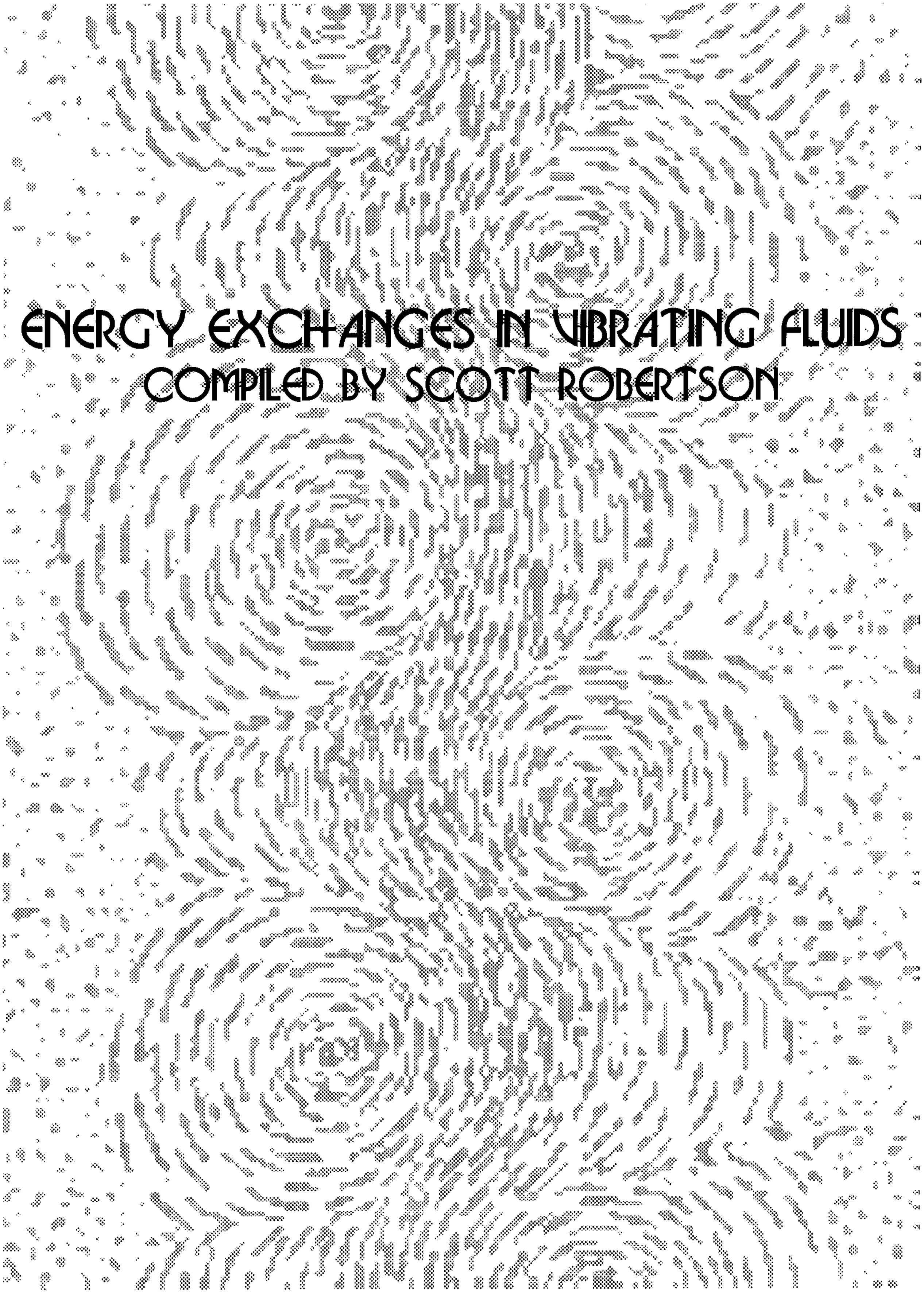

ENERGY EXCHANGES IN VIBRATING FLUIDS

COMPILED BY SCOTT ROBERTSON

PNEUMATIC OPTIONS
www.AirCarAccess.com

ENERGY EXCHANGES IN VIBRATING FLUIDS

CONTENTS

Vortex rings formed by pulsating fluid ....front cover

Resonators 1

Resonance in piping 54

Waterhammer 59

Wave dynamics 95

Vortex rings 114

Resonating jets 128

Noise reduction 150

Conceptual Physics, Paul G. Hewitt, 6th ed., 1989
Harper-Collins, p. 346-7 Resonance

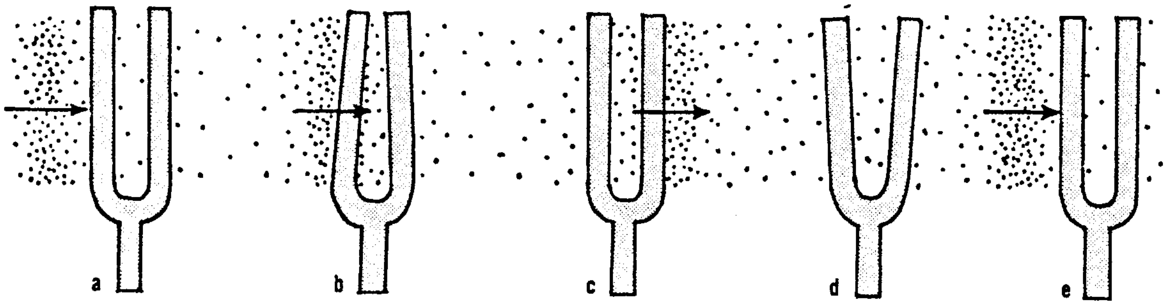

Figure 19-12
Stages of resonance. (*a*) The first compression meets the fork and gives it a tiny and momentary push; (*b*) the fork bends and then (*c*) returns to its initial position just at the time a rarefaction arrives and (*d*) overshoots in the opposite direction. Just when it returns to its initial position (*e*) the next compression arrives to repeat the cycle. Now it bends farther because it is moving.

If the forks are not adjusted for matched frequencies, the timing of pushes is off, and resonance will not occur. When you tune your radio set, you are similarly adjusting the natural frequency of the electronics in the set to match one of the many surrounding signals. The set then resonates to one station at a time instead of playing all stations at once.

Resonance is not restricted to wave motion. It occurs whenever successive impulses are applied to a vibrating object in rhythm with its natural frequency. In 1831, cavalry troops marching across a footbridge near Manchester, England, inadvertently caused the bridge to collapse when they marched in rhythm with the bridge's natural frequency. Since then, it has become customary to order troops to "break step" when crossing bridges. A more recent bridge disaster was caused by wind-generated resonance (Figure 19-13).

The effects of resonance are all about us. Resonance underscores not only the sound of music, but the color of autumn leaves, the height of ocean tides, the operation of lasers, and a vast multitude of phenomena that add to the beauty of the world about us.

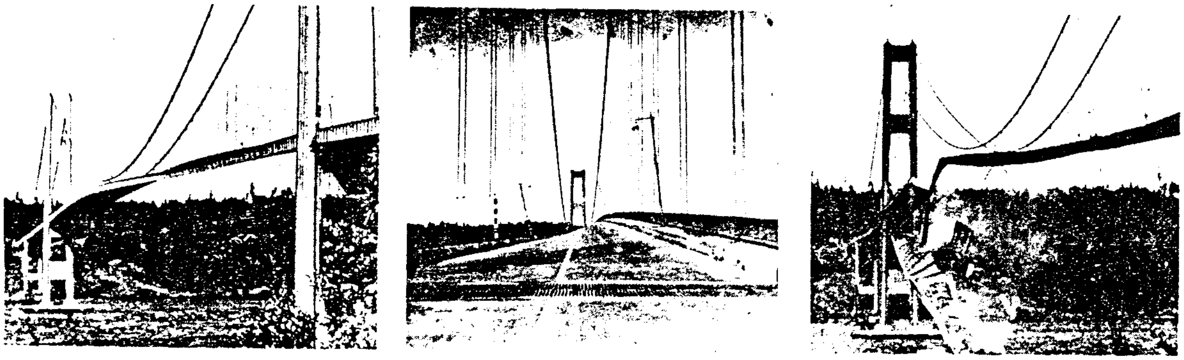

Figure 19-13
In 1940, four months after being completed, the Tacoma Narrows Bridge in the state of Washington was destroyed by wind-generated resonance. The mild gale produced a fluctuating force in resonance with the natural frequency of the bridge, steadily increasing the amplitude until the bridge collapsed.

Interference

Sound waves, like any waves, can be made to exhibit interference. Recall that wave interference was discussed in the last chapter. A comparison of interference for transverse waves and longitudinal waves is shown in Figure 19-14. In either case, when the crests of one wave overlap the crests of another wave, increased amplitude results. Or when the crest of one wave overlaps the trough of another wave, decreased amplitude results. In the case of sound, the crest of a wave corresponds to a compression, and the trough of a wave corresponds to a rarefaction. Interference occurs for both transverse and longitudinal waves.

An interesting case of sound interference is illustrated in Figure 19-15. If you are an equal distance from two sound speakers that emit identical tones of constant frequency, the sound is louder because the effects of the two speakers add. The compressions and rarefactions of the tones arrive in step, or in phase. However, if you move to the side so that the paths from the speakers to you differ by a half wavelength, then the rarefactions from one speaker will be filled in by the compres-

Figure 19-14
Wave interference for transverse and longitudinal waves.

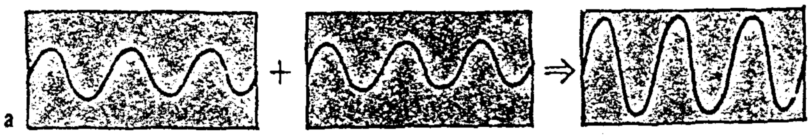

The superposition of two identical transverse waves in phase produces a wave of increased amplitude.

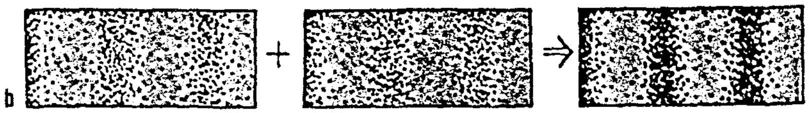

The superposition of two identical longitudinal waves in phase produces a wave of increased intensity.

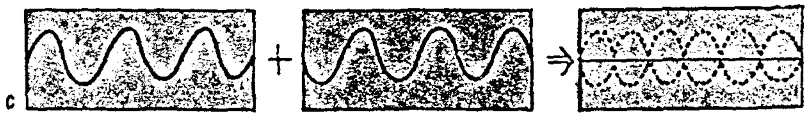

Two identical transverse waves that are out of phase destroy each other when they are superimposed.

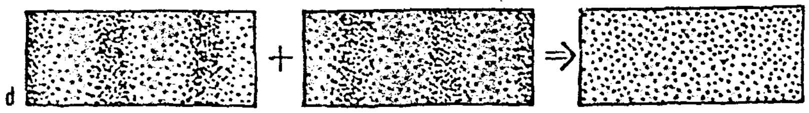

Two identical longitudinal waves that are out of phase destroy each other when they are superimposed.

sions from the other speaker. This is destructive interference. It is just as if the crest of one water wave exactly filled in the trough of another water wave. If the region is devoid of any reflecting surfaces, little or no sound will be heard!

Predicting Flow-Induced Vibrations in a Convoluted Hose

A composite model was constructed from two less accurate models.

Marshall Space Flight Center, Alabama

A composite mathematical model predicts approximately the frequencies and modes of vibrations induced by flows of various fluids in a convoluted hose (see figure). This model was constructed from two older approximate models that were complementary to each other. One of the older models did not adequately account for interactions between the hose structures and the fluids and therefore gave accurate predictions only in cases in which the fluids had little effect or in which the fluids acted as simple additional mass loads that were parts of the hose structures. The other older model accounted for fluid/structure interactions but was applicable only to hoses made of steel.

Like the second-mentioned older model, the composite model is based partly on a spring-and-lumped-mass representation of dynamics that involve the springiness and mass of a convolution of the hose and the density of the fluid in the hose. The Laplace-transformed equations of coupled motion of the lumped masses and springs lead to the following fourth-order equation for the complex frequencies of the vibrational modes:

In this equation, s is the Laplace-transform complex frequency, K is the spring stiffness of a convolution, rf is the mass density of the fluid, A is a cross-sectional area of a convolution, C is called the "fluid capacitance" (analogous to electrical capacitance) and is a measure of the energy and momentum associated with the change in the amount of fluid in a convolution during flexing of the hose, and L is called "fluid inertance" (analogous to both inertia and electrical inductance) and is a function of the dimensions of a convolution. The solution of this equation consists of two sets of complex roots associated with two frequencies. The resonant frequencies predicted by this model are generally lower than those observed in experiments.

This work was done by Stuart A. Harvey of Rockwell International Corp. for **Marshall Space Flight Center**. *For further information,* ***write in 101*** *on the TSP Request Card.*
MFS-29969

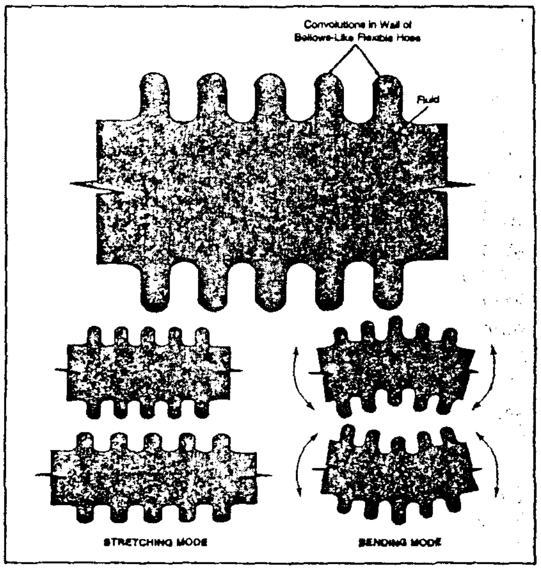

Vibrations In Both Stretching and Bending modes can occur when the flow of fluid in the hose interacts with the convolutions.

p. 94

Impulses which, occurring singly or at irregular intervals, are incapable of producing any noticeable effects may, when made regularly, under favorable circumstances, yield astonishing results. The rattling of church windows by air waves generated by a particular pipe of the organ, a bridge strained or broken by the regular tramp of soldiers or by the trotting of horses, the vibration of a six or eight story building by a wagon rumbling over the pavement, a factory vibrated to a dangerous degree by machinery contained within its walls, a mill shaken from foundation to roof by air waves generated by water falling over a dam, are all familiar examples of the power of regular or harmonic vibrations.

Harmonic vibrations result from regularly recurring impulses, which may be very slight indeed, but when the effects of the impulses are added one to another, the accumulation of power is sometimes very great.

To secure cumulative effects, the impulses must not only be regular in their occurrence, but the body receiving the impulses must be able to respond, its vibratory period must correspond with the period of the impulses, and, further than this, the impulses must bear a certain relation to a particular phase of the vibration, in order that they may act upon the vibrating body in such a way as to augment its motion rather than diminish it.

There are railroad bridges that vibrate alarmingly when crossed by locomotives running at a certain speed, the vibrations being caused by the comparatively slight lack of balance in the driving wheels and connecting rods. For this reason the speed is restricted on such bridges.

During the early tests of the East River bridge between New York and Brooklyn, it was found that the structure was so massive and its vibratory period so slow that it could not be injuriously affected by the marching of men or the trotting of horses; consequently, travel proceeds on this bridge as upon any highway.

A well known English physicist is reported to have said that with suitable appliances he could break an iron girder by pelting it with pith balls. An experiment of this kind would certainly show in a striking manner the effects of very slight rhythmic impulses. As it is manifestly impracticable to perform such an experiment, an easier method of illustrating harmonic vibrations must be sought.

In the accompanying engravings, Fig. 132 shows how a bar of steel may be set in active vibration by drops of water. The bar is supported at nodal points upon angular pieces of wood. Above the center of the bar is arranged a faucet, which communicates with the water supply. The bar is first vibrated by hand, and the faucet is adjusted so that the water drops in unison with the vibrations of the bar. The motion of the bar is then stopped, and the water is allowed to drop on it. The bar soon begins to vibrate, and in a short time the vibration acquires considerable amplitude. In Fig. 133 is shown an experiment in which the intermittent pull of an electro-magnet is made to accomplish the

FIG. 132

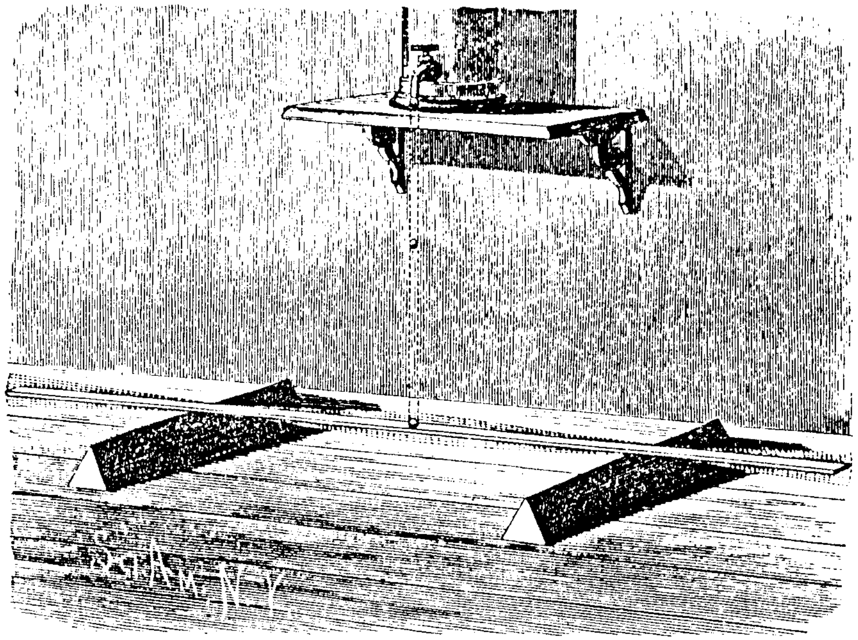

Harmonic Vibration.

same thing. In this case the steel bar forms a part of the circuit. The magnet is provided with a light wooden spring-pressed arm, carrying a contact point and a conductor. This arm is arranged to follow the bar up and down through the upper half of its excursion, breaking the contact at the median position of the bar. The magnet becomes alternately magnetized and demagnetized, and the bar is alternately pulled down and released. The bar used in these experiments is ¼ inch thick, 1¼ inches wide, and 8 feet long. A much larger bar might be used. Without doubt, even an iron girder of great size and weight might be set in active vibration by the same means.

FIG. 133.

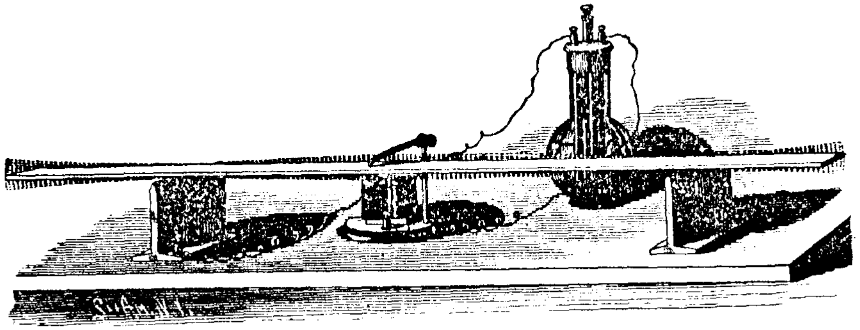

Vibration by Magnetic Impulse.

FIG. 147.

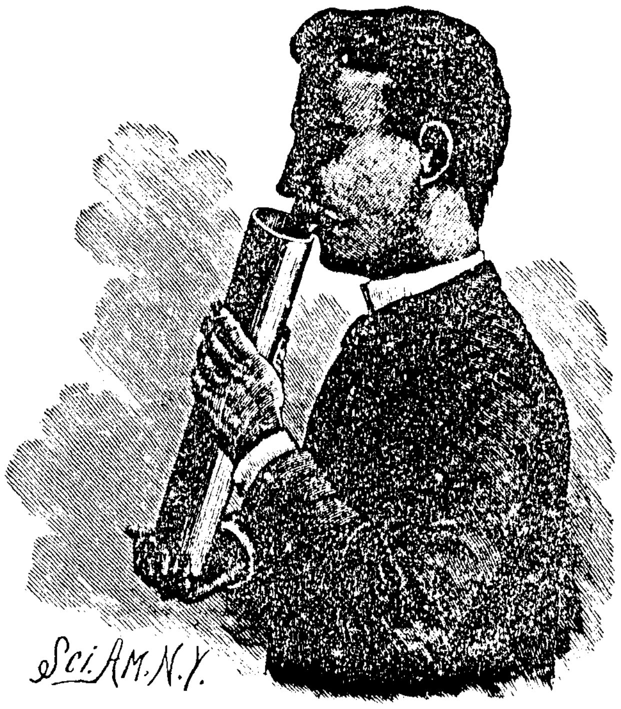

Re-enforcement of Vocal Sounds.

RE-ENFORCEMENT OF SOUND.

The re-enforcement of sounds by the vibration of confined masses of air may be readily investigated without apparatus, that is, such apparatus as is commonly employed in acoustical experiments. A very simple experiment illustrating the fact that a sound may be strengthened by a confined body of air is illustrated in Fig. 147. The only requisite for tnis experiment is a paper tube 16 or 18 inches long and about 3 inches in diameter, or, in the absence of such a tube, a sheet of thick paper rolled into a tube will answer. This tube should be held with one end near the mouth, the opposite end being closed by the palm of the hand. By making a sound continuously with the voice, gradually rising in pitch, for example by singing O, with the voice rising from the lowest note it is capable of making, toward the highest note, a point will be found where the sound is largely increased. This increase of sound will occur at the same point in the scale each time the experi-

FIG. 148.

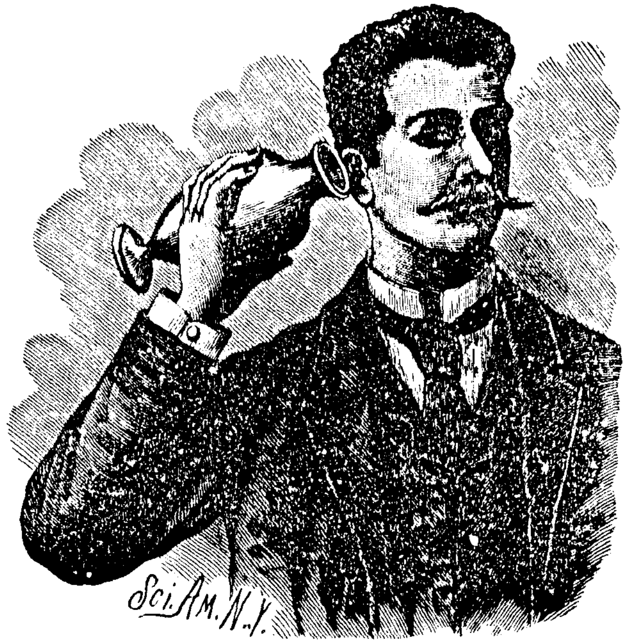

Selective Power of a Resonant Vessel.

ment is tried with the same tube, thus showing that the dimensions of the tube are in some way related to the re-enforced note, and to that only. It will also be noticed that the vibrations of the air in the resonant tube not only affect the auditory apparatus, but also have sufficient power to be plainly perceptible to the sense of touch, the vibrations being felt by the hand.

Another very simple experiment showing the same phenomenon in a different way is illustrated in Fig. 148. In this case the resonant vessel consists of a vase. Any vessel of substantially the same form may be used. The size is not very material, but by making several trials of different vessels a particular one will be found which will yield better results than others on account of being of the correct dimensions. The experiment consists in holding the vase obliquely in close proximity to the ear, then running the chromatic scale upon any instrument having sufficient range, preferably upon a piano or organ. Some note of the scale will sound much louder than any of the others. By tilting the vase slightly in one direction or the other, so as to cause the ear to partly close the mouth of the vase, the resonant qualities may possibly be improved, as the movement of the vase in this manner amounts to tuning the resonator.

In Fig. 149 is represented an experiment in which the mouth is employed as a resonator, and an ordinary tea bell as the source of the sound. The tuning is effected by moving the tongue back and forth, also by opening or closing the lips. By a few trials a position of the mouth will be found which will cause it to respond to the sound of the bell and act as an efficient resonator.

The familiar instrument shown in Fig. 150 is used in connection with the mouth as a resonator. In this example the reed of the Jew's harp is made to yield a variety of tones, dependent upon the adjustment of the mouth and the force of the breath. The fundamental note of the reed is the clearest and best, and always distinctly heard. The forced overtones are less satisfactory, but suffice for playing tunes that are recognizable.

The experiment with the bell, represented in Fig. 151, is very striking, and is easily performed. The bell is simply an old fashioned clock bell or gong fastened on the end of a small wooden handle by a common wood screw. The resonator is a paper tube of about two-thirds the diameter of the bell, provided with a movable portion or diaphragm, as shown at A. Although the bell may be set in vibration by rapping it with the knuckles or striking it with a large sized rubber eraser, it may be more satisfactorily sounded by drawing a well resined bow over its edge. The bell is held over the mouth of the paper tube, and the diaphragm is moved up or down in the tube until a position is reached in which the bell will yield a full tone, which is much louder than it is capable of giving when used without the resonator. The diaphragm is then fastened by means of sealing wax or glue.

To re-enforce one of the overtones of the bell, the opposite end of the tube is gradually shortened by paring off narrow strips from its edge until it responds to the high tone which the bell is capable of giving out when bowed in a particular way. Now, by causing the bell to vibrate strongly and placing it near opposite ends of the resonator in alternation, it will be found that the deeper cavity will respond only to the grave note of the bell, while the shallower cavity will re-enforce only the overtone to which it is tuned. In this experiment it will be found a little more convenient to have separate resonators for the different tones.

FIG. 149.

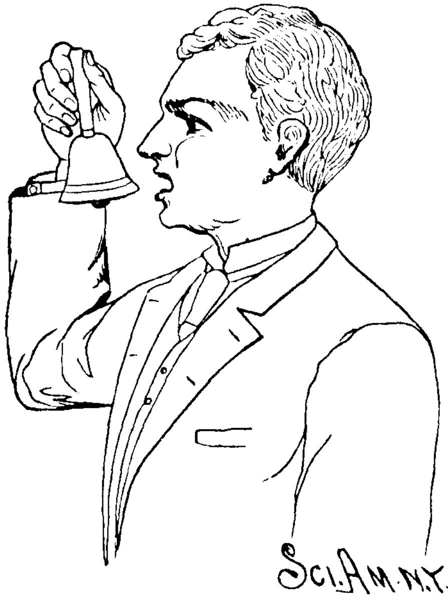

The Mouth used as a Resonator.

FIG. 150.

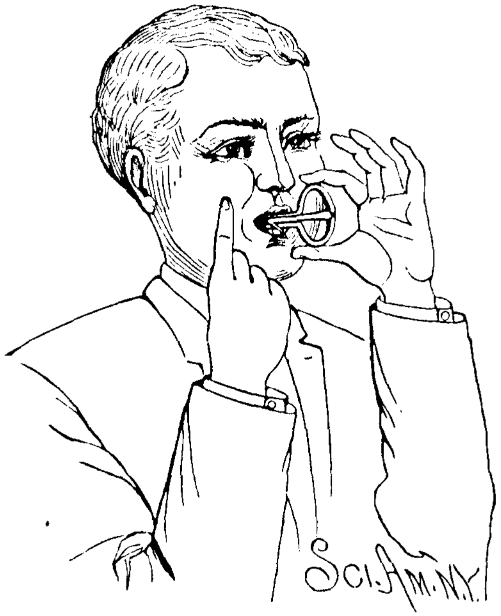

Experiment with the Jew's Harp

In Fig. 152 is shown an experiment which is substantially the same as that just described in connection with the bell. In this case two tuning forks, A and C, are used as sound producers, and to each fork is adapted a resonator consisting of a paper tube about ⅝ inch in diameter and 8 or 10 inches long. Each tube is tuned to the fork in connection with which it is to be used by inserting a cork and moving it until the length of the inclosed air column is such as to respond to the fork. It will be found that the A resonator will respond only to the A fork, and the C resonator will re-enforce only the sound of the C fork.

Fig. 151.

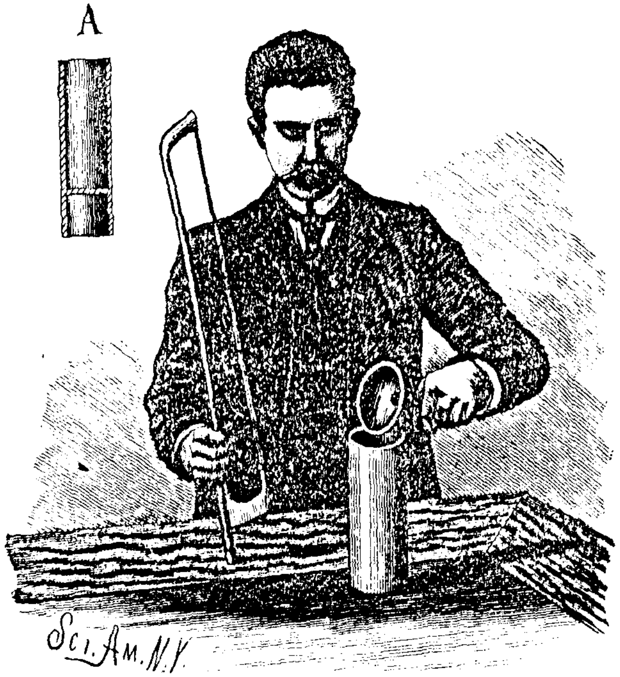

Bell and Resonator.

Fig. 152.

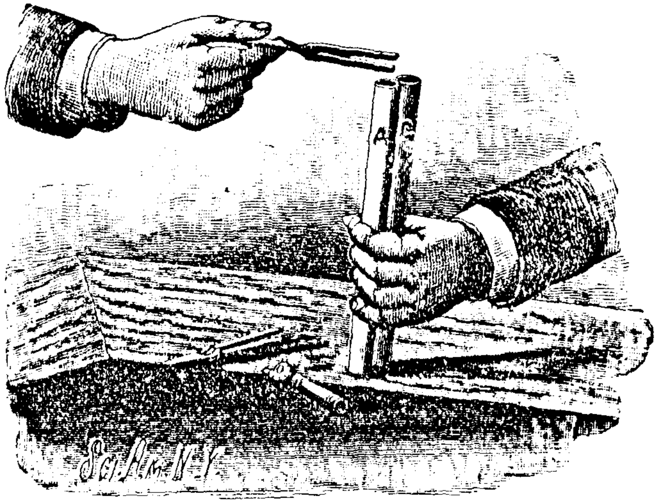

Tuning Forks and Resonant Tubes.

In all these cases the resonant tube or cavity corresponds in depth to about one-quarter of a wave length of the particular sound which it is adapted to re-enforce. The wave proceeding from the sounding body strikes the bottom of the resonant chamber and is reflected back in time to proceed with the other half of the wave moving in the opposite direction, greatly augmenting its volume.

The combination of two series of sound waves may be made to produce silence if the relation of the two series be such that the air condensations of one series coincide with the rarefactions of the other series. This may be demonstrated by holding a tuning fork over its appropriate resonator and turning it until the plane of vibration of the fork is at an angle of 45° with the axis of the resonating tube. By placing the fork in the same position relative to the ear, the same phenomenon may be observed without the resonator.

A SIREN FOR MEASURING VELOCITIES.

In this instrument advantage is taken of the well known fact that for every tone a resonator may be provided that will respond to and re-enforce the vibrations producing that tone. The length of a closed resonant tube is one-fourth that of the sound wave to which it responds. The length of an open resonant tube is one-half that of the sound wave to which it responds. It is obvious that a telescopic tube may be adjusted to respond to different pitches. Knowing the number of vibrations required per second to produce a certain pitch, it is comparatively an easy matter to determine the rate of any series of regular air vibrations by adjusting the tube to such a length as to cause it to respond to the vibrations.

In Fig. 172 is shown a resonant tube supported over a small fan wheel. The fan has ten blades, so that during one revolution it sends ten puffs of air up the tube. By gradually increasing the velocity of the fan a speed will be reached

Fig. 172.

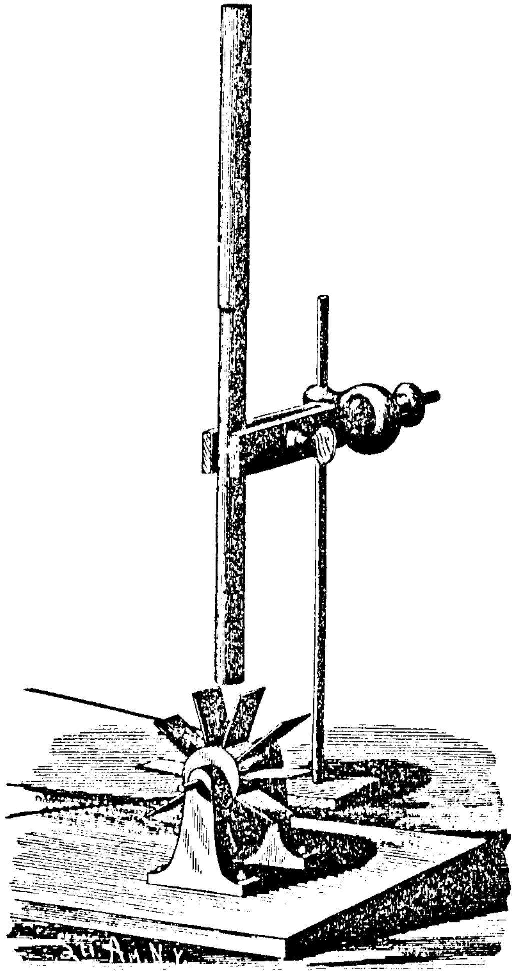

Determining Speed by Resonance.

Fig. 173.

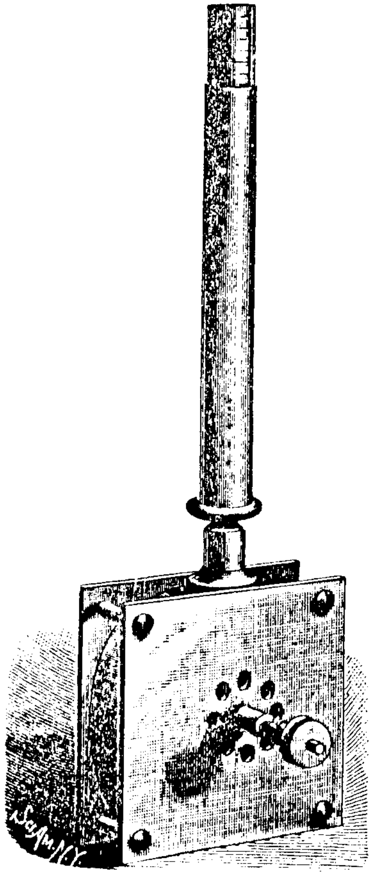

Siren for Measuring Velocities.

at which the tube yields a low but distinct musical tone. If, for example, this tone corresponds to middle *c*, it is known that 261 puffs of air are made in the tube, and that since there are ten blades to the fans, the number of revolutions of the fan shaft must be $261 \div 10 = 26{\cdot}1$ per second, or 1,566 revolutions per minute.

In Fig. 173 is illustrated a siren constructed on this principle. The parts of this instrument are shown in detail in Fig. 174. It consists of a circular casing containing a rotary fan which draws in air at the center and discharges it through an opening in the top of the casing. The blades of the fan are arranged radially upon opposite sides of the disk, and the fan is encircled by a perforated rim, which fits the circular casing and acts as a valve in controlling the escape of air. The perforations of the rim correspond in number and position with the fan blades.

Fig. 174.

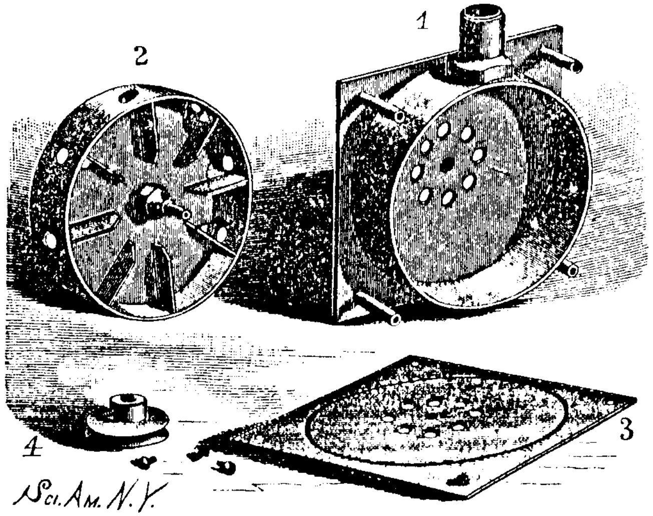

Details of the Siren.

The discharge opening of the casing is provided with a socket for receiving a resonator. The resonator shown

Fig. 175.

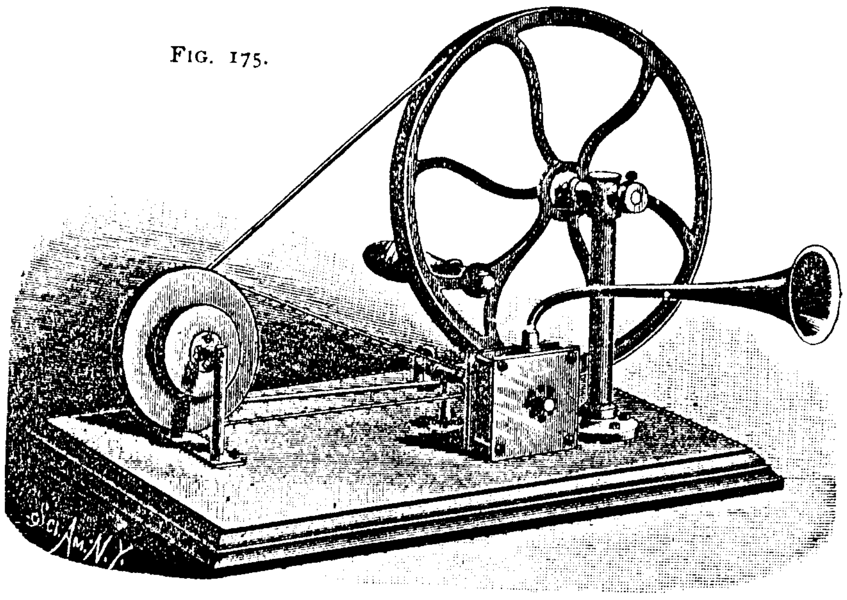

Centrifugal Siren.

in Fig. 173 consists of a pair of tubes made to slide telescopically one within the other, the inner one being graduated to indicate the different lengths required for different pitches, and consequently for different speeds. As the fan revolves, the air drawn in through the holes at the center of the casing is thrown ontward by centrifugal force, thus maintaining a pressure of air at the periphery of the fan. The holes in the rim of the fan allow the air to escape in regular puffs, the frequency of which depends upon the velocity of the fan. These puffs produce sounds varying in pitch and intensity with the speed of the fan, and the resonating tube re-enforces the particular note to which it is tuned, so that when a speed is reached corresponding with the adjustment of the tube, the fact is known by the superior strength of that particular note. Any change of speed may be detected by the lessening of the intensity of the sound and the change of pitch.

The siren is shown in Fig. 175 in connection with mechanism for driving it by hand. It is provided with a revolution counter and with a trumpet-shaped resonator. It is designed to be used in the same manner as the siren of Cagniard Latour, and, like that instrument, it yields sounds under water.

AIAA Journal, Aug. 1974, Vol. 12, No. 8, p. 1076-107

Experimental Investigation of a Cylindrical Resonator

James H. T. Wu,* P. Perry Ostrowski,† Rafik A. Neemeh,‡ and Patrick H. W. Lee§
McGill University, Montreal, Canada

Similar to a conventional resonance tube, a cylindrical resonator is investigated experimentally for producing high pressure and temperature gases. A quartz pressure transducer was used to determine pressure at the center of the resonator disk and a schlieren system to observe internal and external shock waves. A peak pressure nearly 3 times the jet stagnation pressure is observed and the internal shock waves are shown to be somewhat nonsymmetric and eccentric.

Introduction

STUDY of fluid oscillations associated with the operation of a simple resonance tube was initiated by Hartmann.[1] This device consists of a closed-end tube mounted with its open end facing an underexpanded fluid jet. Spark schlieren[2] and shadow photography[3,4] has shown that the resonant cycle is characterized by alternate periods of inflow and outflow from the tube which correspond to the appearance of an internal travelling shock wave and expansion waves. Thompson[4,5] has introduced a wave diagram analysis based on appropriate boundary conditions at the tube mouth. A more recent investigation[6] has improved Thompson's theory and used streak schlieren photographs to demonstrate that the traveling shock wave is internally generated.

It is well-known that the structure of the exciting jet strongly affects the performance of a simple resonance tube.[3] At a pressure ratio less than 4, underexpanded choked jets have a repetitive cellular appearance and resonance occurs only if the tube mouth is placed in the downstream half of each jet cell. This half cell is termed "the intervals of instability". Smith and Powell[3] have shown that higher harmonic resonant frequencies are obtained with the cavity mouth located near the midpoint of a jet cell and that the fundamental frequency is obtained at the downstream end.

Current interest[7,8] in aerodynamic resonators is focused on their use as a high-temperature device or igniter by taking advantage of the repeated irreversible shock heating of the indigenous fluid which remains permanently trapped inside a straight or tapered tube. It is noted that end wall temperatures of the order of 400°C can be achieved with gaseous nitrogen[7] and 1200°C with helium.[8]

The present investigation demonstrates a working device based on a combination of principles given by Hartmann[1] and Guderley.[9] Amplification of the internal shock wave can be accomplished by employing a cylindrical resonator cavity excited by a circumferential fluid jet. The resonant cycle is then characterized by a cylindrical implosion-explosion process which has a significantly greater potential for generation of high temperature and pressure than the conventional plane shock wave. Since all significant shock amplification occurs in a comparatively small region surrounding the implosion center, the cylindrical symmetry of the imploding wave is crucial to the successful operation of this device. Accordingly, the aim of this investigation is to examine the operating characteristics of such a cylindrical configuration. To this end, spark schlieren and shadow photography is employed to observe the nature of the external flowfield (exciting jets) as well as the internal flowfield (traveling shock wave). The resonant frequency and pressure amplitude are measured with a pressure transducer located at the geometric center of one resonator disk. Acoustic theory is used for a rough estimate of the resonant frequency.

Acoustic Theory

Despite the fact that strong traveling shocks may appear inside the resonator cavity, acoustic theory may be employed to give an estimate of the resonant frequency. Essentially, the internal waves are taken to be acoustic in nature so that the wave motion is then described by the linear wave equation. In cylindrical coordinates this procedure yields the well-known solution for the perturbation velocity potential,[10] which is written in terms of the familiar Bessel functions. Application of the boundary conditions (the particle velocity at the center must be zero and the perturbation pressure is zero at the resonator mouth i.e., $r = r_o$) yields the condition $Jo(2\pi f r_o/c) = 0$ where f is the frequency and c the local sound speed. The first root of the Bessel function then gives the fundamental frequency of acoustic vibration: $f = c/2.615 r_o$.

Experiments

A cross-sectional view of the cylindrical resonator is presented in Fig. 1. Two circular disks 2.65 in. in diameter with a lip chamfer of 45° are separated by a gap to form the resonator cavity. These disks are supported by a hollow (for schlieren viewing) threaded rod which is held in place by a threaded tightening ring so that the disk gap is adjustable. The resonator cavity is surrounded by a cylindrical plenum chamber 7.5 in. in

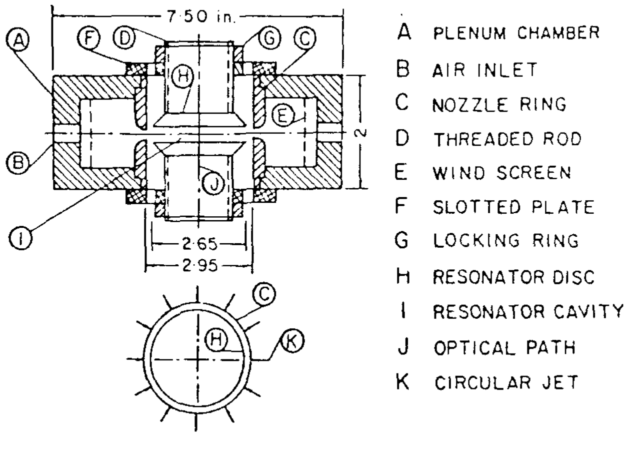

Fig. 1 Schematic of the cylindrical resonator.

Received September 10, 1973; revision received January 29, 1974. This work was supported by the National Research Council of Canada under Grant A-1255 and donations by C. R. Whyte and R. N. Lawson. A version of this work was presented at the 11th Biennial Fluid Dynamics Symposium on Advanced Problems and Methods in Fluid Dynamics, Sopot-Kamienny Potok, Poland, 1973.

Index categories: Shock Waves and Detonations; Nonsteady Aerodynamics; Nozzle and Channel Flow.

* Associate Professor.

† Research Engineer.

‡ Research Engineer; also Assistant Professor, Loyola College, Montreal, Canada.

§ Research Assistant.

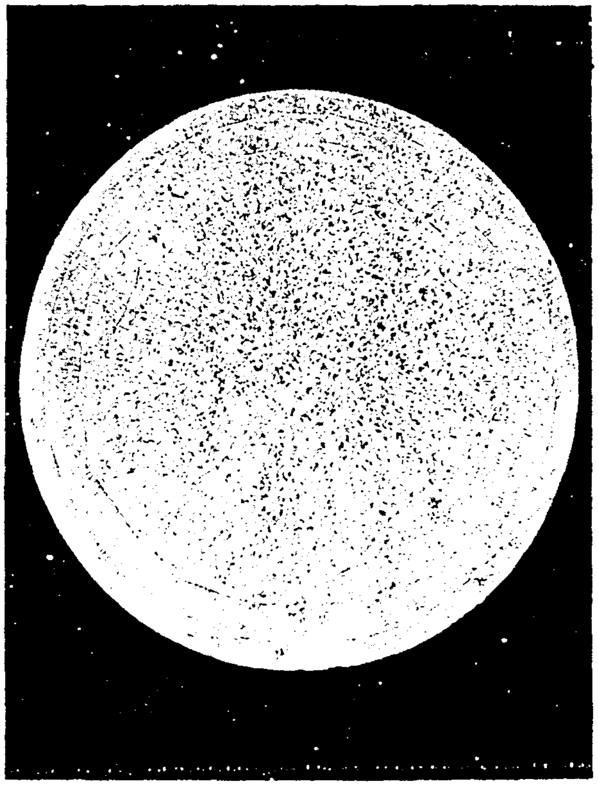

Fig. 2 A typical spark shadowgraph showing jet cells (pressure ratio = 3.94).

diameter fitted with five compressed air inlets connected to a common supply. A narrow slit 0.030 in. wide with a $\frac{1}{4}$ in. rounded entrance in the inner wall of the plenum serves as a nozzle for the exciting jet which is directed radially towards the resonator cavity. The device is constructed entirely of aluminum except for the central portion of the resonator disks which are fitted with Plexiglas windows for schlieren viewing.

The most important physical parameters which affect the acoustic or thermal output of the resonator are the nozzle width and diameter, jet stagnation pressure, resonator disk gap and diameter, and the resonator material. The present study is largely a qualitative one and an extensive parametric program to maximize the resonator output has not been undertaken. Instead, a nozzle diameter of 2.95 in. and nozzle width of 0.030 in. were arbitrarily chosen and resonator disks of 2.75 and 2.65 in. were tested separately. The latter were found to yield a consistently higher resonant pressure amplitude for all jet pressures. Similarly, a resonator disk gap of 0.068 in. was also found to be superior to any other value in this regard. These values were then held fixed for the balance of the tests despite the fact that they were not determined from an exhaustive parametric study.

With the resonator geometry thus fixed, the test procedure was largely concerned with adjusting the jet stagnation pressure. As the pressure is increased, each jet cell is lengthened and the effective location of the resonator mouth is then altered. For the present investigation, three series of tests were performed. First, flash shadowgraphy was employed to examine the jet cell dimensions with the resonator disks removed. Second, a $\frac{3}{8}$ in. quartz pressure transducer (pcb Piezotronics Inc., Model 101A) was mounted in the center of one resonator disk so that the pressure history could be recorded on an oscilloscope (Tektronix Model 555). Finally, the resonator disks were fitted with Plexiglas windows and the resonant cycle was examined via spark schlieren photography. The windows gave a 1.5-in.-diam field of view at the geometric center of the resonator cavity and the optical axis was normal to the resonator disks.

Results and Discussion

The structure of the exciting jet alone (resonator disks removed) is shown in Fig. 2 for a stagnation pressure ratio of 3.94. In this view, three jet cells are visible with the first exhibiting the highest degree of circular symmetry. Since cell symmetry is crucial to the operation of this device, it appears to be best to design the resonator to operate on the first or outermost cell of the exciting jet.

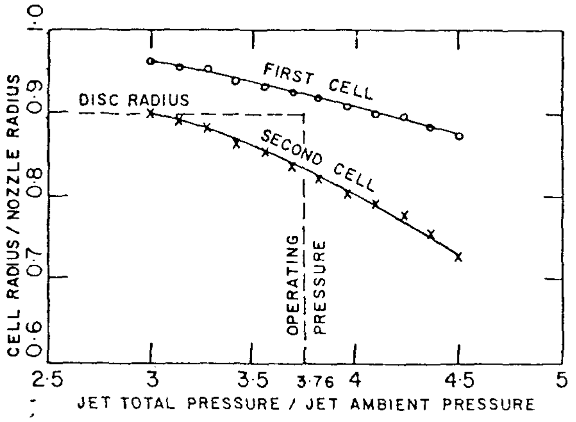

Fig. 3 Jet cell radius vs jet pressure ratio (nozzle radius = 1.475 in. and nozzle width = 0.03 in.).

Figure 3 shows the jet cell measurements taken from several shadowgraphs similar to that of Fig. 2 for jet pressure ratios between 3.0 and 4.5. It can be seen that cell length increases for higher pressure ratios and the second cell is longer than the first. Now, with the resonator disk in place, resonance is observed to commence at a pressure ratio of 3.76. When this operating point is superimposed on the figure, it surprisingly falls into the first half of the second jet cell which is theoretically outside the "intervals of instability." Yet resonance persists. The possible reason for this is that the jet structure is altered when the resonator disks are in place, as the disks are chamfered with some bluntness. This type of behavior has been observed for simple resonance tubes as well.[3]

The pressure history at the center of one resonator disk is presented in Fig. 4 for jet pressure ratios between 3.69 and 5.19. Resonance begins very abruptly at a pressure ratio of 3.76 and thereafter the pressure amplitude (P_{max}-P_{min}) falls rapidly and becomes only about one fourth its initial level at a pressure ratio of 5.19, as in Fig. 5. At the onset of resonance, the pressure trace is seen to exhibit periodically a very steep rise which implies the existence of a strong internal imploding-exploding shock wave. The peak pressure of approximately 163 psia is nearly three times the jet stagnation pressure of 55 psia. In addition, the subsequent expansion phase of the resonant cycle is seen to take place in three distinct stages because of wave

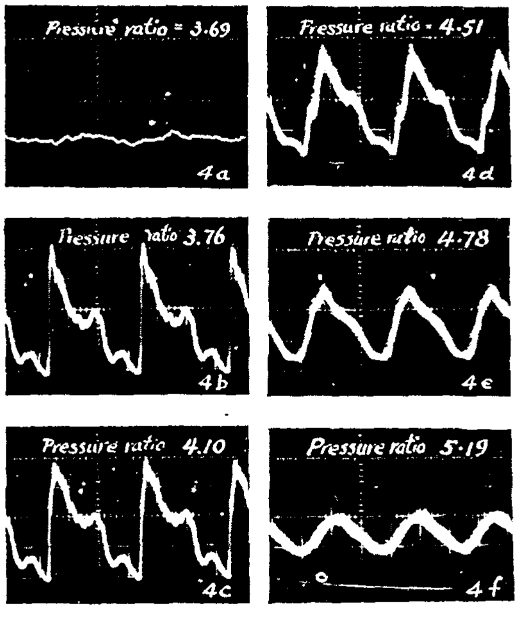

Fig. 4 Pressure measurements at the disk center.

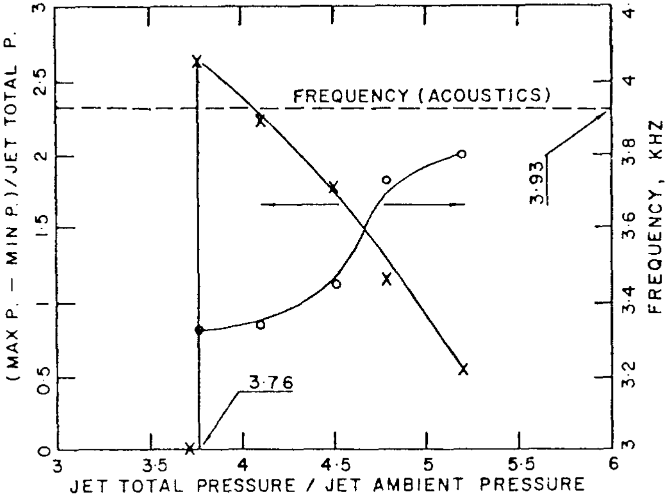

Fig. 5 Pressure amplitude vs jet pressure ratio (3.76 is a minimum value for resonance).

interaction within the confined converging region. As the jet pressure ratio is increased, the waveform gradually becomes distorted until eventually the motion appears to be entirely acoustic. It is implied from Fig. 3 that this behavior is due to lengthening of the jet cell structure so that eventually the resonator mouth is effectively located in the upstream half of the cell and resonance cannot be maintained in this stable interval.

According to the oscilloscope traces, the resonant frequency is 3.33 kcps, which is about 15% lower than the acoustic frequency of 3.93 kcps with $c = 1135$ fps and $r_o = 1.325$ in. Attempting to account for shock heating effects by raising c above its ambient value makes the discrepancy even larger. Thus it appears that the shock-wave speeds with respect to the disk are subsonic over a considerable segment of the resonant cycle. Not surprisingly, the frequency measured from Fig. 4f is only 4% lower than the theoretical acoustic value (see Fig. 5).

Schlieren photographs, taken randomly but arranged in time sequence to illustrate pertinent features of the resonant cycle for a jet pressure ratio of 3.76, are presented in Fig. 6. These clearly show a nearly circular internal shock wave. Although whether this wave is imploding or exploding has not been determined experimentally, Figs. 6b and 6c are assumed to show the imploding wave as the enclosed flowfield appears quiescent, while Figs. 6d and 6e are thought to show the exploding shock for the opposite reason. Figures 6a and 6d show in- and outflow of the resonant cycle as the external shock is pushed far upstream against the impulse of the exciting jet, respectively.

Figure 6 also yields some qualitative information regarding the resonator performance. The internal shock, although nearly circular, is not perfectly so and is characterized by the appearance of several Mach reflections[11] around its periphery. The shock wave does not appear to collapse to the geometric center of the disks, therefore it seems likely that the resonator performance (i.e., pressure amplitude or temperature) can be increased by refining the design. It is noted that the appearance of a burn close to the center of the Plexiglas windows (small dark area in the photographs) indicates that the internal shock creates high temperature and collapses into a fairly small region.

Conclusions

A cylindrical resonator operating on an imploding-exploding cycle has been demonstrated experimentally. To achieve resonant conditions, the resonator disks must be precisely aligned relative to the exciting jet nozzle and the disk gap must be adjusted until the pressure amplitude is maximized. This type of "tuning" is required because a systematic experimental program to define the effect of various geometric parameters such as nozzle width and radius, disk gap and radius, etc., has not been completed.

The higher acoustic potential of the present device over conventional resonance tubes is demonstrated as a pressure rise of nearly 3 times the jet stagnation pressure has been measured at the center of the resonator cavity. Acoustic theory yields a fair estimate of the resonant frequency as the measured value is about 15% lower.

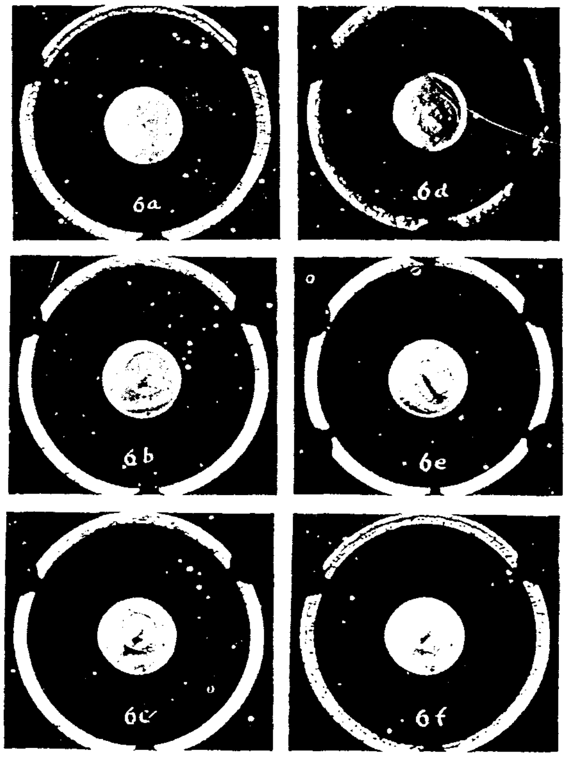

Fig. 6 Schlieren photographs showing shock waves (jet pressure ratio = 3.76 and total pressure = 55 psia).

Shadow and schlieren photographs show that 1) without the resonator disks, the jet from the circular nozzle has clearly defined jet cells of nearly circular shape, and 2) with the disks in place, the imploding and exploding shock waves in the central region of the disks are somewhat eccentric and characterized by the appearance of Mach reflections along the main shock profile. Although the cylindrical resonator is ultimately intended for high temperature generation, temperature measurements have been delayed until the shock wave eccentricity is improved.

References

[1] Hartmann, J., "On the Production of Acoustic Waves by Means of an Air Jet of a Velocity Exceeding that of Sound," *Philosophical Magazine*, Vol. 11, 1931, pp. 329–334.

[2] Vrebalovich, T., "Resonance Tubes in a Supersonic Flow Field," TR 32-378, 1962, Jet Propulsion Lab., Pasadena, Calif.

[3] Smith, T. J. B. and Powell, A., "Experiments Concerning the Hartmann Whistle," Rept. 64-62, 1964, Univ. of California, Berkeley, Calif.

[4] Thompson, P. A., "Resonance Tubes," Sc.D. thesis, 1960, MIT, Cambridge, Mass.

[5] Thompson, P. A., "Jet-Driven Resonance Tube," *AIAA Journal*, Vol. 2, No. 7, July 1964, pp. 1230–1233.

[6] Wu, J. H. T., Neemah, R. A., and Ostrowski, P. P., "Resonance Tubes in Underexpanded Sonic Jets," *CASI Transactions*, Vol. 6, No. 1, 1973, pp. 26–35.

[7] Phillips, B. R. and Pavli, A. J., "Resonance Tube Ignition of Hydrogen-Oxygen Mixtures," TN D-6354, 1971, NASA.

[8] Corrado, A. P., Rakowsky, E. L., and Marchese, V. P., "Resonance Tube Heating," private communication based on Abstract for American Physics Society Fluid Dynamics meeting, Nov. 1972, Boulder, Colo.

[9] Guderley, G., "Powerful Spherical and Cylindrical Compression Shocks in the Neighbourhood of the Centre of the Sphere and of the Cylinder Axis," *Luftfahrtforschung*, Vol. 19, 1942.

[10] Morse, P. M. and Ingard, K. U., *Theoretical Acoustics*, McGraw-Hill, New York, 1968.

[11] Whitham, G. B., "A New Approach to Problems of Shock Dynamics, Part I, Two-Dimensional Problems," *Journal of Fluid Mechanics*, Vol. 4, 1958, pp. 145–171.

AIAA JOURNAL
Feb. 1978
VOL. 16, NO. 2
p. 184-186

Technical Notes

TECHNICAL NOTES are short manuscripts describing new developments or important results of a preliminary nature. These Notes cannot exceed 6 manuscript pages and 3 figures; a page of text may be substituted for a figure and vice versa. After informal review by the editors, they may be published within a few months of the date of receipt. Style requirements are the same as for regular contributions (see inside back cover).

Aerothermodynamic Characteristics of a Resonance Tube Driven by a Subsonic Jet

C. E. G. Przirembel*
Rutgers University, New Brunswick, N.J.
and
L. S. Fletcher†
University of Virginia, Charlottesville, Va.

Introduction

A RESONANCE tube, in its simplest form, is a cylindrical or rectangular tube closed at one end and facing a coaxial fluid jet at the open end. If appropriate geometric and fluid conditions are satisfied by the jet/tube combination, the fluid within the tube is excited to violent harmonic motion. If the tube is sufficiently long, the intense periodic oscillations give rise to strong thermal effects which result in resonance tube endwall temperatures significantly higher than the corresponding jet stagnation temperatures. For subsonic and low Mach number supersonic jets, the fundamental resonance frequency is independent of the jet Mach number $M_{\rm jet}$ and can be approximated by $f = C/4L$, where C is the speed of sound of the jet and L is the length of the resonance tube.

Previous experimental and analytical work, reviewed by Przirembel and Fletcher,[1] was concerned primarily with resonance tubes driven by supersonic and underexpanded, choked jets. For subsonic jets, only very limited experimental data have been reported. Savory[2] has observed fluid oscillations for subsonic jets, when the resonance tube is supported axially by a cylindrical rod passing through the nozzle. The fluid dynamics of this flowfield have been analyzed by Broucher, Maresca, and Bournay.[3] Sprenger[4] was able to obtain oscillating flows with jet Mach numbers as low as 0.52 by placing a thin thread across the jet axis. Vrebalovich[5] observed oscillations in a cavity placed in a subsonic flowfield by locating a ring trip upstream of the tube mouth. More recently Przirembel, Fletcher, and Wolf[6] have observed resonance in two-dimensional resonance tubes driven by a subsonic, two-dimensional jet, without the introduction of any tripping device.

Experimental Program

A simple schematic of the axisymmetric nozzle/resonance tube model and pertinent geometrical parameters are shown in Fig. 1. The air jet was generated by a simple, converging nozzle with a contraction ratio of 3 to 1. The nozzle exit diameter was 0.375 in. (0.953 cm).

The resonance tube had an inside diameter d of 0.375 in. (0.953 cm). The length L to diameter d ratio was 30 for all tests. The resonance tube endwall was designed and constructed to accommodate iron-constantan thermocouples for temperature measurements, and an orifice for pressure measurements.

Results and Discussion

The variable test parameters were the ratio of the separation distance between the nozzle exit and the resonance tube inlet to the nozzle exit diameter S/D, the ratio of the jet stagnation pressure to the ambient pressure P_0/P_a, the ratio of the diameter of the trip to the nozzle exit diameter b/D, and the separation distance of the trip wire from the nozzle exit x. The nominal jet stagnation temperature was the atmospheric temperature.

Of principal interest in this experimental investigation was the determination of the temperature and thermal effects in the vicinity of the resonance tube endwall. Figures 2 and 3 summarize some typical results for jet flows with and without a trip. From Fig. 2, it can be seen that there is no measurable increase in the endwall temperature above the jet stagnation temperature for a simple subsonic jet ($M_{\rm jet} = 0.73$). However, as a thin wire is placed across the center of the jet exit plane, there is a significant temperature increase. As the jet Mach number is increased in Fig. 3, there is some limited resonance tube heating without the trip. The shape of curves for flow in the presence of the trip are quite similar. The peak endwall temperature increases as the jet Mach number increases. These results are consistent with those reported by Sprenger.[4] Broucher et al.[3] have argued that the presence of the trip results in a stagnation pressure deficiency in the jet, which

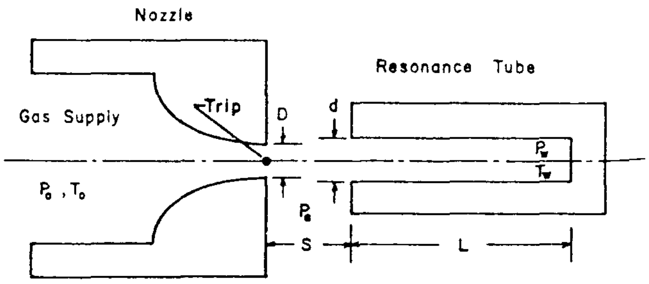

Fig. 1 Schematic of resonance tube model.

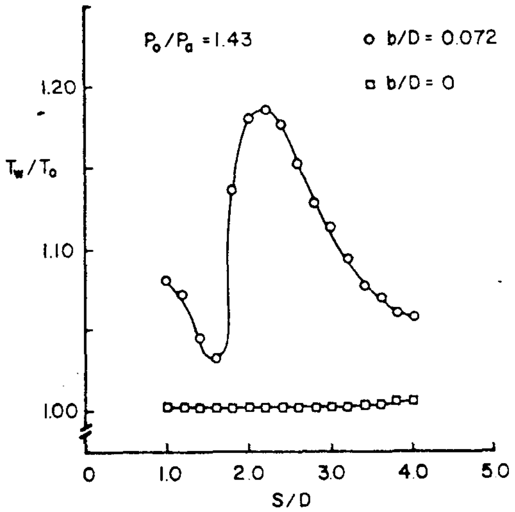

Fig. 2 Endwall temperature variation with S/D for $P_0/P_a = 1.43$.

Presented as Paper 77-236 at the AIAA 15th Aerospace Sciences Meeting, Los Angeles, Calif., Jan. 24-26, 1977; submitted July 18, 1977; revision received Oct. 6, 1977. Copyright © American Institute of Aeronautics and Astronautics, Inc., 1977. All rights reserved.

Index category: Nonsteady Aerodynamics.

*Associate Dean of Engineering. Associate Fellow AIAA.

†Professor and Chairman of Mechanical and Aerospace Engineering. Associate Fellow AIAA.

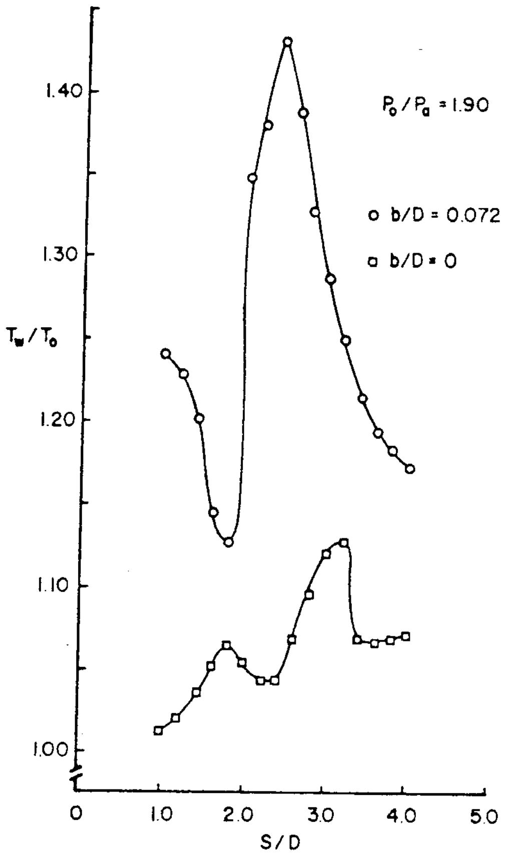

Fig. 3 Endwall temperature variation with S/D for $P_0/P_a = 1.90$.

allows the resonance tube outflow to penetrate the jet. From wake calculations for the trip immersed in the core of the jet, it can be shown that the maximum velocity defect is on the order of 20% for the maximum endwall temperatures. At the inlet plane for the resonance tube, the trip wake width is on the order of one-half the resonance tube diameter. By comparing the frequency of oscillation (286 Hz) and the shedding frequency (73,400 Hz) associated with the trip, there is no indication that the resonance condition is driven by the wake shedding process. The endwall pressure measurements showed a significant correlation with the endwall temperature curves, i.e., pressure increases occurred at the same S/D values as temperature increases.

The effect of the relative location of the trip wire x is shown in Fig. 4. As can be seen, there is a significant decrease in the maximum endwall temperature, as well as a shift in S/D as the wire is moved away from the jet exit plane. The jet centerline velocity defect increases very slightly at the resonance tube inlet. However, the mass flow of the jet entering the resonance tube decreases.

In order to determine the influence of trip diameter on the maximum endwall temperature, a series of experiments were performed which resulted in curves for different trip diameters similar to those shown in Figs. 2-4. For these experiments, the trips were placed at the exit plane of the nozzle. A summary of these results is presented in Fig. 5, where the maximum endwall temperatures are plotted for various trip diameters. The primary observation is that there is no distinct peak for a particular combination of wire diameter and jet velocity. Vortex shedding frequencies based on a Strouhal number of 0.21 do not provide any additional information on the mechanism of resonance since the estimated peaks appear independent of jet velocity. It should be noted that the calculated shedding frequencies are on the order of 200 times the frequency of oscillation in the resonance tube. From these observations it can be concluded that the oscillations in the resonance tube are not directly driven by the vortices shed from the trip.

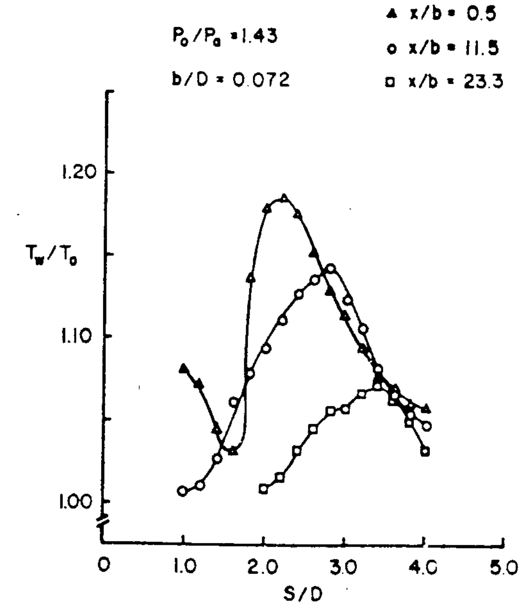

Fig. 4 Endwall temperature variation with S/D and relative location of trip for $P_0/P_a = 1.43$.

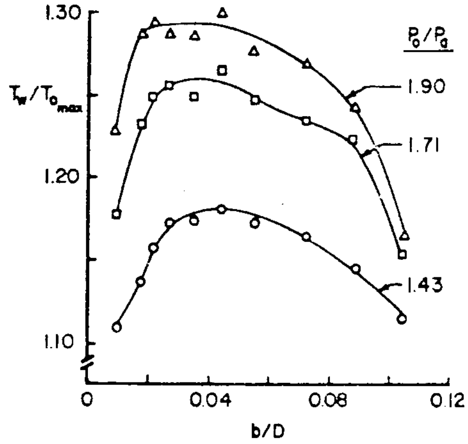

Fig. 5 Maximum endwall temperature variation with trip diameter.

As indicated earlier, Broucher et al.[3] have suggested that the best method to obtain oscillations in a resonance tube driven by a subsonic jet is to decrease the kinetic energy of the jet in the neighborhood of the axis in order to act upon the radial pressure distribution at the resonance tube entrance. Without detailed jet velocity and static pressure measurements near the resonance tube, it is not clear at this point if the present experimental results support their analysis. The wake defect of the present cylinder is still significant for the separation distances at which maximum endwall temperatures were measured. However, it is also possible that the trip wake vortices cause disturbances in the outer region of the jet and thereby initiate instabilities which ultimately lead to oscillations in the resonance tube.

Acknowledgment

The Rutgers Research Council provided partial financial support for this research.

References

[1] Przirembel, C. E. G. and Fletcher, L. S., "Aerothermodynamics of a Simple Resonance Tube," *AIAA Journal*, Vol. 15, Jan. 1977, pp. 101-104.

[2] Savory, L. E., "Experiments with the Hartmann Acoustic Generator," *Engineering*, Vol. 170, Aug. 1950, pp. 99, 137.

[3] Broucher, E., Maresca, C., and Bournay, M. H., "Fluid Dynamics of the Resonance Tube," *Journal of Fluid Mechanics*, Vol. 43, Part 2, 1970, pp. 369-384.

[4] Sprenger, H. S., "Über Thermische Effeckte bei Rezonnanzrohren," Mitteilungen Aus Dem Institut Fur Aerodyanamik An Der E.T.H., Zurich, Nr. 21, 1954, pp. 18-34.

[5] Vrebalovich, T., "Resonance Tubes in a Supersonic Flow Field," Jet Propulsion Lab., Pasadena, Calif., Rept. No. 32-378, 1972.

[6] Przirembel, C. E. G., Fletcher, L. S., and Wolf, D. E., "Thermodynamic Characteristics of a Blunt Two-Dimensional Resonance Tube," *AIAA Journal*, Vol. 15, July 1977, pp. 905-906.

AIAA Journal, Dec. 1984
Vol. 22, No. 12, p. 1823-1825

Thermal Performance of a Logarithmic-Spiral Resonance Tube

Rafik A. Neemeh,* P. Perry Ostrowski,†
and James H.T. Wu‡
Concordia University, Montreal, Canada

Introduction

THE simple Hartmann-Sprenger tube consists of a closed-end tube that is excited by an underexpanded gas jet facing its open end to produce violent, cyclic fluid oscillations internally and externally. Although this phenomenon has been known for some time, the heat generation capability of this device has been exploited only relatively recently.[1] Sprenger experimented to demonstrate that end-wall temperatures well in excess of the exciting jet stagnation temperature could be achieved with a uniform tube. Although it was suspected that this temperature rise resulted from nonlinear wave motion, this was not verified until spark shadowgraphs[2] clearly showed the existence of internal traveling shock waves. Streak schlieren photography[3] has shown that these are generated during the inflow phase of each cycle and that when higher harmonics are driven, several traveling shocks are present simultaneously.

Once it was recognized that thermal effects in the simple Hartmann-Sprenger tube resulted mainly from repeated shock heating of the fluid trapped inside, it became evident that the thermal performance could be enhanced either by strengthening the internal shock or increasing the frequency of the oscillations. This may be accomplished by a variety of methods, such as minimizing the tube length, employing a light driving gas, or contouring the tube profiles to accelerate the traveling shock. Thus far, it appears that no attempt has been made to formally optimize the internal geometry in order to maximize the thermal performance; therefore, tube shapes have been selected rather arbitrarily. Tapered tubes have commonly been employed to yield end-wall temperatures as high as 725°C using air[4] and 540°C with hydrogen.[5] A cylindrical resonator that operates on a shock implosion-explosion cycle has been devised by Wu et al.[6] in order to take advantage of the significant shock amplification that may be achieved through symmetrical implosion.

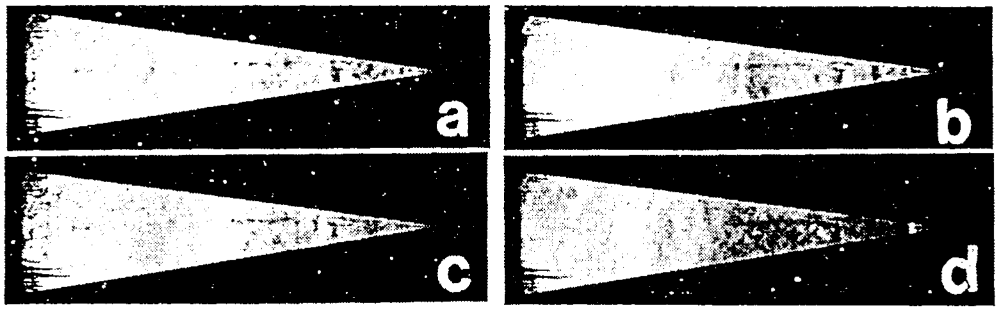

Fig. 1 Spark schlieren photographs of the shock motion within the tapered cavity, $P_{oj}/P_a = 1.92$, $h/d = 0.85$.

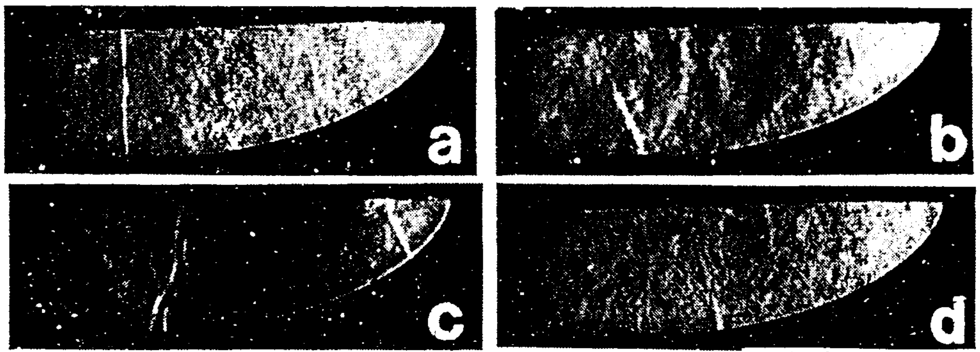

Fig. 2 Spark schlieren photographs of the shock motion within the logarithmic spiral cavity, $P_{oj}/P_a = 1.92$, $h/d = 0.85$.

The present Note investigates the thermal performance of a Hartmann-Sprenger tube with a two-dimensional logarithmic spiral internal contour. This particular profile was selected on the basis of prior shock tube studies,[7] which have shown that the shock motion in such area contractions yields cylindrical implosion and is, therefore, attractive for the present application. For experimental convenience, only two-dimensional shapes are tested, and performance is judged on the basis of spark schlieren photographs, end-wall temperatures, and piezoelectric pressure measurements.

Experiments

All tests were conducted with air as the working fluid. Flow visualization was accomplished with tubes of rectangular cross section (5.1 × 25.4 mm at the entrance) which were excited by an underexpanded jet from a converging nozzle with the same exit dimensions. Cavities with rectangular, 10-deg tapered, and logarithmic spiral wall contours with

---

Received Dec. 12, 1983; revision received Jan. 27, 1984. Copyright © 1984 by R. A. Neemeh. Published by the American Institute of Aeronautics and Astronautics with permission.

*Associate Professor, Department of Mechanical Engineering. Member AIAA.

†Research Associate, Department of Mechanical Engineering.

‡Distinguished Research Associate, Department of Mechanical Engineering. Member AIAA.

respective lengths of 15.2, 13.1, and 13.3 cm were tested. A single spark schlieren photograph was obtained for each test. Piezoelectric pressures were measured at different locations.

Temperature measurements were conducted with a second set of tubes, 17.8-cm long and 10.2-mm square at the entrance, whose walls were constructed with an asbestos compound. The tapered and spiral tubes have instrumentation ports 2.5-mm wide by 12.7-mm long for which chromelalumel thermocouples are located at the port midpoints. Each cavity is excited by an underexpanded air jet of diameter $d = 10.2$ mm.

Results and Discussion

Spark schlieren photographs of the shock propagation in the tapered and logarithmic spiral tubes are presented in Figs. 1 and 2, respectively, for a jet pressure ratio of 1.92 and a nozzle to cavity separation $h/d = 0.85$. Figure 1 is seen to be characterized by the appearance of Mach reflection due to the inclination of the channel walls, whereas Fig. 2 is observed to exhibit a curved shock normal to the wall surfaces with no reflected shocks trailing behind. Here, the shock appears to eventually collapse into a relatively small region.

Piezoelectric pressure measurements were carried out near the focus of the logarithmic spiral channel. From the recorded pressure histories, the pressure rise across the incident shock is found to increase, while that ahead of the shock decreases as the shock proceeds toward the vertex of the spiral which yields significant shock amplification. The pressure rise across the shock becomes twice that observed in the parallel tube walls. Thus, it appears that the logarithmic spiral cavity exhibits much better shock amplification than the square cavity.

The thermal performance of the three insulated tubes is shown in Fig. 3, which presents the maximum measured end-wall temperature vs jet pressure ratio. It is evident from the figure that the logarithmic spiral profile consistently achieves a higher temperature than the tapered tube over the entire range of jet pressures employed for the present tests. The increment in thermal performance is roughly constant. This implies that the shock amplification in the logarithmic spiral tube is significantly greater than in the tapered and rectangular tubes. It is evident from Fig. 3 that the peak thermal performance of the logarithmic spiral tubes employed in the present tests is rather low (320°C) compared to that obtained by other investigators,[4,5] but it is possible that higher temperatures may be achieved using a longer tube length. Nevertheless, the present results are useful from a comparative rather than absolute standpoint.

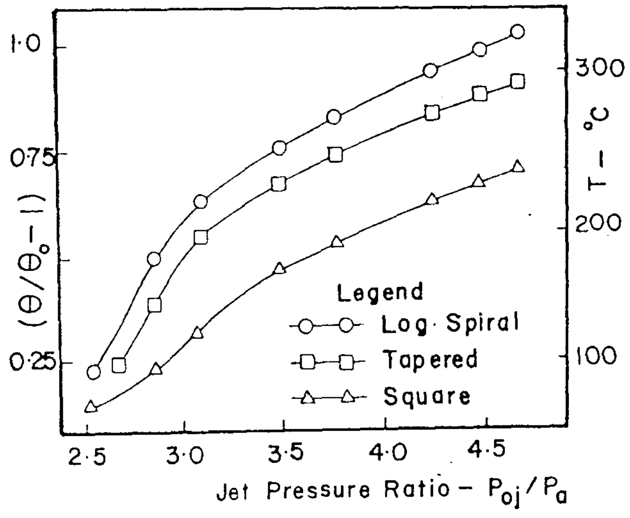

Fig. 3 End-wall temperatures.

Tests were also conducted to determine those locations of the tube mouth relative to the nozzle that produced maximum end-wall temperatures. Results for the logarithmic spiral profile at the jet pressure ratio of 3.77 show that the maximum temperature varies periodically with the nozzle-tube separation h due to the periodic structure of the exciting jet. The highest temperatures were recorded at $h/d = 1.7$. This means that the peak corresponds to a location where the tube mouth is situated downstream of the first pressure cell. This result differs from the findings of Przirembel and Fletcher.[8] However this difference might be explained by the fact that in their case, the open-end walls were rounded in contrast to the 30-deg chamfered entrances of the present tests.

Conclusion

Thermocouple measurements have demonstrated that a Hartmann-Sprenger tube with a logarithmic spiral profile achieves a significantly greater base temperature than a 10-deg tapered tube or a rectangular tube of comparable length. This improved performance is interpreted to result from a higher degree of shock amplification which produces a greater entropy rise in the shock-heated indigenous gas that remains trapped inside the tube. Therefore, it appears that an axisymmetric logarithmic spiral tube could be used to improve the performance further.

Acknowledgments

The work was supported by the Natural Sciences and Engineering Research Council of Canada under Grant A-4206. The assistance of M.N. Elabdin is acknowledged.

References

[1] Brocher, E., "Heat Transfer and Equilibrium Temperature Near the End Plate of a Hartmann-Sprenger Tube," *Shock Tube and Shock Wave Research*, University of Washington Press, Seattle, Wash., 1977, pp. 66-73.

[2] Hall, I.M. and Berry, C.J., "On the Heating Effect in a Resonance Tube," *Journal of the Aerospace Sciences*, Vol. 26, April 1959, p. 253.

[3] Wu, J.H.T., Neemeh, R.A., and Ostrowski, P.P., "Resonance Tubes in Underexpanded Sonic Jets," *CASI Transactions*, Vol. 6, March 1973, pp. 26-35.

[4] McAlevy, R.F. and Pavlak, A., "Tapered Resonance Tubes: Some Experiments," *AIAA Journal*, Vol. 8, March 1970, pp. 571-572.

[5] Phillips, B.R. and Pavli, A.J., "Resonance Tube Ignition of Hydrogen-Oxygen Mixtures," NASA TN D-6354, 1971.

[6] Wu, J.H.T., Ostrowski, P.P., Neemeh, R.A., and Lee, P.H.W., "Experimental Investigation of a Cylindrical Resonator," *AIAA Journal*, Vol. 12, Aug. 1974, pp. 1076-1078.

[7] Wu, J.H.T., Archer, R.D., and Molder, S.M., "Shock Propagation in a Two-Dimensional Symmetric Logarithmic Spiral Channel," *Recent Developments in Shock Tube Research*, Stanford University Press, Stanford, Calif., 1973, pp. 604-612.

[8] Przirembel, C.E.G. and Fletcher, L.S., "Aerothermodynamics of a Simple Resonance Tube," *AIAA Journal*, Vol. 15, Jan. 1977, pp. 101-104.

The Theory of Sound
John William Strutt
Vol. 2, 2nd ed., 1896
London, McMillan p. 170-235

CHAPTER XVI.

THEORY OF RESONATORS.

303. IN the pipe closed at one end and open at the other we had an example of a mass of air endowed with the property of vibrating in certain definite periods peculiar to itself in more or less complete independence of the external atmosphere. If the air beyond the open end were entirely without mass, the motion within the pipe would have no tendency to escape, and the contained column of air would behave like any other complex system not subject to dissipation. In actual experiment the inertia of the external air cannot, of course, be got rid of, but when the diameter of the pipe is small, the effect produced in the course of a few periods may be insignificant, and then vibrations once excited in the pipe have a certain degree of persistence. The narrower the channel of communication between the interior of a vessel and the external medium, the greater does the independence become. Such cavities constitute resonators; in the presence of an external source of sound, the contained air vibrates in unison, and with an amplitude dependent upon the relative magnitudes of the natural and forced periods, rising to great intensity in the case of approximate isochronism. When the original cause of sound ceases, the resonator yields back the vibrations stored up as it were within it, thus becoming itself for a short time a secondary source. The theory of resonators constitutes an important branch of our subject.

As an introduction to it we may take the simple case of a stopped cylinder, in which a piston moves without friction. On the further side of the piston the air is supposed to be devoid of inertia, so that the pressure is absolutely constant. If now the piston be set into vibration of very long period, it is clear that the contained air will be at any time very nearly in the equilibrium condition (of uniform density) corresponding to the momentary position of the piston. If the mass of the piston be very considerable in comparison with that of the included air, the natural vibrations resulting from a displacement will occur nearly as if the air had no inertia; and in deriving the period from the kinetic and potential energies, the former may be calculated without allowance for the inertia of the air, and the latter as if the rarefaction and condensation were uniform. Under the circumstances contemplated the air acts merely as a spring in virtue of its resistance to compression or dilatation; the form of the containing vessel is therefore immaterial, and the period of vibration remains the same, provided the capacity be not varied.

When a gas is compressed or rarefied, the mechanical value of the resulting displacement is found by multiplying each infinitesimal increment of volume by the corresponding pressure and integrating over the range required. In the present case it is of course only the difference of pressure on the two sides of the piston which is really operative, and this for a small change is proportional to the alteration of volume. The whole mechanical value of the small change is the same as if the expansion were opposed throughout by the *mean*, that is half the final, pressure; thus corresponding to a change of volume from S to $S + \delta S$, since $p = a^2\rho$,

$$V = p \cdot \frac{\delta S}{2S} \cdot \delta S = \tfrac{1}{2}\rho a^2 \frac{(\delta S)^2}{S} \;\ldots\ldots\ldots\ldots\ldots\ldots(1)^1.$$

If A denote the area of the piston, M its mass, and x its linear displacement, $\delta S = Ax$, and the equation of motion is

$$M\ddot{x} + \frac{\rho a^2 A^2}{S} x = 0 \;\ldots\ldots\ldots\ldots\ldots\ldots\ldots\ldots(2),$$

indicating vibrations, whose periodic time is

$$\tau = 2\pi \div aA\sqrt{\frac{\rho}{MS}} \;\ldots\ldots\ldots\ldots\ldots\ldots\ldots(3).$$

Let us now imagine a vessel containing air, whose interior communicates with the external atmosphere by a narrow aperture or neck. It is not difficult to see that this system is capable of vibrations similar to those just considered, the air in the neighbourhood of the aperture supplying the place of the piston. By sufficiently increasing S, the period of the vibration may be made as long as we please, and we obtain finally a state of things in

---

[1] Compare (12) § 245.

which the kinetic energy of the motion may be neglected except in the neighbourhood of the aperture, and the potential energy may be calculated as if the density in the interior of the vessel were uniform. In flowing through the aperture under the operation of a difference of pressure on the two sides, or in virtue of its own inertia after such pressure has ceased, the air moves approximately as an incompressible fluid would do under like circumstances, provided that the space through which the kinetic energy is sensible be very small in comparison with the length of the wave. The suppositions on which we are about to proceed are not of course strictly correct as applied to actual resonators such as are used in experiment, but they are near enough to the mark to afford an instructive view of the subject and in many cases a foundation for a sufficiently accurate calculation of the pitch. They become rigorous only in the limit when the wave-length is indefinitely great in comparison with the dimensions of the vessel.

[On the above principles we may at once calculate the pitch of a resonator of volume S, whose cavity communicates with the external air by a long cylindrical neck of length L and area A. The mass of the aerial piston is ρAL; so that (3) gives as the period of vibration

$$\tau = \frac{2\pi}{a}\sqrt{\left(\frac{LS}{A}\right)} \text{ ....}(4);$$

or, if λ be the length of plane waves of the same pitch,

$$\lambda = a\tau = 2\pi\sqrt{\left(\frac{LS}{A}\right)} \text{ ....}(5).$$

If the cross-section of the neck be a circle of radius R, $A = \pi R^2$, and we obtain the formula (8) of § 307.]

304. The kinetic energy of the motion of an incompressible fluid through a given channel may be expressed in terms of the density ρ, and the rate of transfer, or current, $\dot{X}$, for under the circumstances contemplated the character of the motion is always the same. Since T necessarily varies as ρ and as $\dot{X}^2$, we may put

$$T = \tfrac{1}{2}\rho\frac{\dot{X}^2}{c} \text{ ....} (1),$$

where the constant c, which depends only on the nature of the channel, is a linear quantity, as may be inferred from the fact that the dimensions of $\dot{X}$ are 3 in space and -1 in time. In fact, if ϕ be the velocity-potential,

$$T = \tfrac{1}{2}\rho\iiint\left[\frac{d\phi^2}{dx^2} + \frac{d\phi^2}{dy^2} + \frac{d\phi^2}{dz^2}\right] dx\, dy\, dz = \tfrac{1}{2}\rho\iint \phi\,\frac{d\phi}{dn}\,dS,$$

by Green's theorem, where the integration is to be extended over a surface including the whole region through which the motion is sensible. At a sufficient distance on either side of the aperture, ϕ becomes constant, and if the constant values be denoted by ϕ_1 and ϕ_2, and the integration be now limited to that half of S towards which the fluid flows, we have

$$T = \tfrac{1}{2}\rho\,(\phi_1 - \phi_2)\iint\frac{d\phi}{dn}\,dS = \tfrac{1}{2}\rho\,(\phi_1 - \phi_2)\,\dot{X}.$$

Now, since within S ϕ is determined linearly by its surface values, $\iint\frac{d\phi}{dn}\,dS$, or $\dot{X}$, is proportional to $(\phi_1 - \phi_2)$. If we put $\dot{X} = c\,(\phi_1 - \phi_2)$, we get as before $T = \tfrac{1}{2}\rho\dot{X}^2/c$.

Fig. 58.

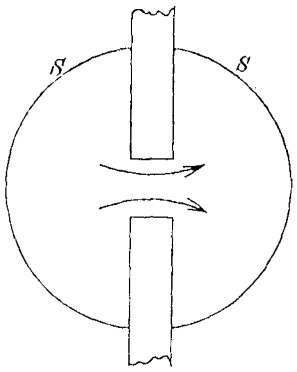

The nature of the constant c will be better understood by considering the electrical problem, whose conditions are mathematically identical with those of that under discussion. Let us suppose that the fluid is replaced by uniformly conducting material, and that the boundary of the channel or aperture is replaced by insulators. We know that if by battery power or otherwise, a difference of electric potential be maintained on the two sides, a steady current through the aperture of proportional magnitude will be generated. The ratio of the total current to the electromotive force is called the *conductivity* of the channel, and thus we see that our constant c represents simply this conductivity [illegible] the supposition that the specific conducting power of the hypothetical substance is unity. The same thing may be otherwise expressed by saying that c is the side of the cube, whose resistance between opposite faces is the same as that of the channel. In the sequel we shall often avail ourselves of the electrical analogy.

When c is known, the proper tone of the resonator can be easily deduced. Since

$$V = \tfrac{1}{2}\rho a^2\frac{X^2}{S}, \quad T = \tfrac{1}{2}\rho\frac{\dot{X}^2}{c} \text{ ....} (2),$$

the equation of motion is

$$\ddot{X} + \frac{a^2 c}{S} X = 0 \text{..........................(3)},$$

indicating simple oscillations performed in a time

$$\tau = 2\pi \div \sqrt{\frac{a^2 c}{S}} \text{......................(4)}.$$

If N be the frequency, or number of complete vibrations executed in the unit time,

$$N = \frac{a}{2\pi} \sqrt{\frac{c}{S}} \text{..........................(5)}.$$

The wave-length λ, which is the quantity most closely connected with the dimensions of the cavity, is given by

$$\lambda = \frac{a}{N} = 2\pi \sqrt{\frac{S}{c}} \text{...................... (6)},$$

and varies directly as the linear dimension. The wave-length, it will be observed, is a function of the size and shape of the resonator only, while the frequency depends also upon the nature of the gas; and it is important to remark that it is on the nature of the gas in and near the channel that the pitch depends and not on that occupying the interior of the vessel, for the inertia of the air in the latter situation does not come into play, while the compressibility of all gases is very approximately the same. Thus in the case of a pipe, the substitution of hydrogen for air in the neighbourhood of a node would make but little difference, but its effect in the neighbourhood of a *loop* would be considerable.

Hitherto we have spoken of the channel of communication as single, but if there be more than one channel, the problem is not essentially altered. The same formula for the frequency is still applicable, if as before we understand by c the whole conductivity between the interior and exterior of the vessel. When the channels are situated sufficiently far apart to act independently one of another, the resultant conductivity is the simple sum of those belonging to the separate channels; otherwise the resultant is less than that calculated by mere addition.

If there be two precisely similar channels, which do not interfere, and whose conductivity taken separately is c, we have

$$N = \sqrt{2} \times \frac{a}{2\pi} \sqrt{\frac{c}{S}} \text{.................... (7)},$$

shewing that the note is higher than if there were only one channel in the ratio $\sqrt{2} : 1$, or by rather less than a fifth—a law observed by Sondhauss and proved theoretically by Helmholtz in the case, where *the channels of communication consist of simple* holes in the infinitely th[illegible] of the reservoir.

305. The investigation of the conductivity for various kinds of channels is an important part of the theory of resonators; but in all except a very few cases the accurate solution of the problem is beyond the power of existing mathematics. Some general principles throwing light on the question may however be laid down, and in many cases of interest an approximate solution, sufficient for practical purposes, may be obtained.

We know (§§ 79, 242) that the energy of a fluid flowing through a channel cannot be greater than that of any fictitious *motion giving the same total current*. Hence, if the channel be narrowed in any way, or any obstruction be introduced, the conductivity is thereby diminished, because the alteration is of the nature of an *additional constraint*. *Before the change the fluid* was free to adopt the distribution of flow finally assumed. In cases where a rigorous solution cannot be obtained we may use the minimum property to estimate an inferior limit to the conductivity; the energy calculated from a hypothetical law of flow can never be less than the truth, and must exceed it unless the hypothetical and the actual motion coincide.

Another general principle, which is of frequent use, may be more conveniently stated in electrical language. The quantity with which we are concerned is the *conductivity of a certain conductor* composed of matter of unit specific conductivity. The principle is that if the conductivity of any part of the conductor be increased that of the whole is increased, and if the *conductivity* of any part be diminished that of the whole is diminished, exception being made of certain very particular cases, where no alteration ensues. In its passage through a conductor electricity distributes itself, so that the energy dissipated is for a given total current the least possible (§ 82). If now the specific resistance of any part be diminished, the total dissipation would be less than before, even if the distribution of currents remained unchanged. *A fortiori* will this be the case, when the currents redistribute themselves so as to make the dissipation a minimum. If an infinitely thin lamina of matter stretching across the channel be made perfectly conducting, the resistance of the whole will be diminished, unless the lamina coincide with one of the undisturbed equipotential surfaces. In the excepted case no effect will be produced.

306. Among different kinds of channels an important place must be assigned to those consisting of simple apertures in unlimited plane walls of infinitesimal thickness. In practical applications it is sufficient that a wall be very thin in proportion to the dimensions of the aperture, and approximately plane within a distance from the aperture large in proportion to the same quantity.

On account of the symmetry on the two sides of the wall, the motion of the fluid in the plane of the aperture must be normal, and therefore the velocity-potential must be constant; over the remainder of the plane the motion must be exclusively tangential, so that to determine ϕ on one side of the plane we have the conditions (i) $\phi = \text{constant}$ over the aperture, (ii) $d\phi/dn = 0$ over the rest of the plane of the wall, (iii) $\phi = \text{constant}$ at infinity.

Since we are concerned only with the differences of ϕ we may suppose that at infinity ϕ vanishes. It will be seen that conditions (ii) and (iii) are satisfied by supposing ϕ to be the potential of attracting matter distributed over the aperture; the remainder of the problem consists in determining the distribution of matter so that its potential may be constant over the same area. The problem is mathematically the same as that of determining the distribution of electricity on a charged conducting plate situated in an open space, whose form is that of the aperture under consideration, and the conductivity of the aperture may be expressed in terms of the *capacity* of the plate of the statical problem. If ϕ denote the constant potential in the aperture, the electrical resistance (for one side only) will be

$$\phi_1 \div \iint \frac{d\phi}{dn}\, d\sigma,$$

the integration extending over the area of the opening.

Now $\iint \frac{d\phi}{dn}\, d\sigma = 2\pi \times$ (whole quantity of matter distributed), and thus, if M be the capacity, or charge corresponding to unit-potential, the total resistance is $(\pi M)^{-1}$. Accordingly for the conductivity, which is the reciprocal of the resistance,

$$c = \pi M \text{ ....} (1).$$

So far as I am aware, the ellipse is the only form of aperture for which c or M can be determined theoretically[1], in which case the result is included in the known solution of the problem of determining the distribution of charge on an ellipsoidal conductor. From the fact that a shell bounded by two concentric, similar and similarly situated ellipsoids exerts no force on an internal particle, it is easy to see that the superficial density at any point of an ellipsoid necessary to give a constant potential is proportional to the perpendicular (p) let fall from the centre upon the tangent plane at the point in question. Thus if ρ be the density, $\rho = \kappa p$; the whole quantity of matter Q is given by

$$Q = \iint \rho\, dS = \kappa \iint p\, dS = 4\pi\kappa abc \text{ ....} (2),^{2}$$

so that
$$\rho = \frac{Qp}{4\pi\, abc} \text{ ....} (3).$$

In the usual notation

$$p = 1 \div \sqrt{\frac{x^2}{a^4} + \frac{y^2}{b^4} + \frac{z^2}{c^4}},$$

or, since
$$z^2/c^2 = 1 - x^2/a^2 - y^2/b^2,$$

$$p = c \div \sqrt{1 - \frac{x^2}{a^2} - \frac{y^2}{b^2} + \frac{c^2x^2}{a^4} + \frac{c^2y^2}{b^4}}\,.$$

If we now suppose that c is infinitely small, we obtain the particular case of an elliptic plate, and if we no longer distinguish between the two surfaces, we get

$$\rho = \frac{Q}{2\pi ab} \div \sqrt{1 - \frac{x^2}{a^2} - \frac{y^2}{b^2}} \text{ ....} (4).$$

We have next to find the value of the constant potential (P). By considering the value of P at the centre of the plate, we see that

$$P = \iint \frac{\rho\, dS}{r} = \iint \rho\, dr\, d\theta.$$

Integrating first with respect to r, we have

$$\int_0^r \rho\, dr = Q \div 4a\sqrt{(1 - e^2\cos^2\theta)},$$

e being the eccentricity; and thus

$$P = \frac{Q}{a}\int_0^{\frac{1}{2}\pi} \frac{d\theta}{\sqrt{(1 - e^2\cos^2\theta)}} = \frac{Q}{a} F(e),$$

where F is the symbol of the complete elliptic function of the first order. Putting $P=1$, we find

---

[1] The case of a resonator with an elliptic aperture was considered by Helmholtz (Crelle, Bd. 57, 1860), whose result is equivalent to (8).

[2] $2c$ being for the moment the third principal axis of the ellipsoid.

$$\frac{c}{\pi}=M=\frac{a}{F(e)}\ldots\ldots\ldots\ldots(5),$$

as the final expression for the capacity of an ellipse, whose semi-major axis is a and eccentricity is e. In the particular case of the circle, $e=0$, $F(e)=\frac{1}{2}\pi$, and thus for a circle of radius R,

$$c=2R\ldots\ldots\ldots\ldots(6).$$

If the capacity of the resonator be S, we find from (6) § 304

$$\lambda=\pi\sqrt{\left(\frac{2S}{R}\right)}\ldots\ldots\ldots\ldots(7).$$

The area of the ellipse (σ) is given by

$$\sigma=\pi a^2\sqrt{(1-e^2)},$$

and hence in terms of σ

$$\frac{1}{c}=\frac{1}{2}\sqrt{\left(\frac{\pi}{\sigma}\right)}\cdot\frac{2F(e)\,(1-e^2)^{\frac{1}{4}}}{\pi}\ldots\ldots\ldots\ldots(8).$$

When e is small, we obtain by expanding in powers of e previous to integration,

$$F(e)=\tfrac{1}{2}\pi\left\{1+\frac{1^2}{2^2}e^2+\frac{1^2.3^2}{2^2.4^2}e^4+\frac{1^2.3^2.5^2}{2^2.4^2.6^2}e^6+\ldots\right\}\ldots..(9),$$

whence

$$\frac{2F(e)\,(1-e^2)^{\frac{1}{4}}}{\pi}=1-\frac{e^4}{64}-\frac{e^6}{64}+\ldots$$

Neglecting e^8 and higher powers, we have therefore

$$c=2\sqrt{\left(\frac{\sigma}{\pi}\right)}\cdot\left(1+\frac{e^4}{64}+\frac{e^6}{64}+\ldots\right)\ldots\ldots\ldots\ldots(10).$$

From this result we see that, if its eccentricity be small, the conductivity of an elliptic aperture is very nearly the same as that of a circular aperture *of equal area*. Among various forms of aperture of given area there must be one which has a minimum conductivity, and, though a formal proof might be difficult, it is easy to recognise that this can be no other than the circle. An inferior limit to the value of c is thus always afforded by the conductivity of the circle of equal area, that is $2\sqrt{(\sigma/\pi)}$, and when the true form is nearly circular, this limit may be taken as a close approximation to the real value.

The value of λ is then given by

$$\lambda=2^{\frac{1}{2}}\pi^{\frac{5}{4}}\sigma^{-\frac{1}{4}}S^{\frac{1}{2}}\ldots\ldots\ldots\ldots(11).$$

In order to shew how slightly a moderate eccentricity affects the value of c, I have calculated the following short table with the aid of Legendre's values of $F(e)$. Putting $e=\sin\psi$, we have $\cos\psi$ as the ratio of axes, and for the conductivity

$$c=2\sqrt{\left(\frac{\sigma}{\pi}\right)}\cdot\frac{\pi}{2\sqrt{(\cos\psi)}\,.\,F(\sin\psi)}.$$

ψ.	$e=\sin\psi$.	$b:a=\cos\psi$.	$\pi\div 2F(e)\,(1-e^2)^{\frac{1}{4}}$.
0°	·00000	1·00000	1·0000
20°	·34204	·93969	1·0002
30°	·50000	·86603	1·0013
40°	·64279	·76604	1·0044
50°	·76604	·64279	1·0122
60°	·86603	·50000	1·0301
70°	·93969	·34202	1·0724
80°	·98481	·17365	1·1954
90°	1·00000	·00000	∞

The value of the last factor given in the fourth column is the ratio of the conductivity of the ellipse to *that of a circle of equal area*. It appears that even when the ellipse is so eccentric that the ratio of the axes is 2 : 1, the conductivity is increased by only about 3 per cent., which would correspond to an alteration of little more than a comma (§ 18) in the pitch of a resonator. There seems no reason to suppose that this approximate independence of shape is a property peculiar to the ellipse, and we may conclude with some confidence that in the case of any moderately elongated oval aperture, the conductivity may be calculated from the area alone with a considerable degree of accuracy.

If the area be given, there is no superior limit to c. For suppose the area σ to be distributed over n equal circles sufficiently far apart to act independently. The area of each circle is σ/n, and its conductivity is $2\,(n\pi)^{-\frac{1}{2}}\sigma^{\frac{1}{2}}$. The whole conductivity is n times as great, and therefore increases indefinitely with n. As a general rule, the more the opening is elongated or broken up, the greater will be the conductivity for a given area.

To find a superior limit to the conductivity of a given aperture we may avail ourselves of the principle that any addition to the aperture must be attended by an increase in the value of c. Thus in the case of a square, we may be sure that c is less than for the circumscribed circle, and we have already seen that it is greater than for the circle of equal area. If b be the side of the square,

$$\frac{2b}{\sqrt{\pi}} < c < \sqrt{2}\, b.$$

The tones of a resonator with a square aperture calculated from these two limits would differ by about a whole tone; the graver of them would doubtless be much the nearer to the truth. This example shews that even when analysis fails to give a solution in the mathematical sense, we need not be altogether in the dark as to the magnitudes of the quantities with which we are dealing.

In the case of similar orifices, or systems of orifices, c varies as the linear dimension.

307. Most resonators used in practice have necks of greater or less length, and even when there is nothing that would be called a neck, the thickness of the side of the reservoir cannot always be neglected. We shall therefore examine the conductivity of a channel formed by a cylindrical boring through an obstructing plate bounded by parallel planes, and, though we fail to solve the problem rigorously, we shall obtain information sufficient for most practical purposes. The thickness of the plate we shall call L, and the radius of the cylindrical channel R.

Fig. 59.

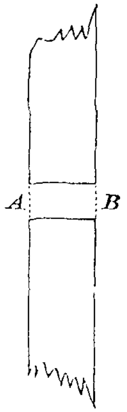

Whatever the resistance of the channel may be, it will be lessened by the introduction of infinitely thin discs of perfect conductivity at A and B, fig. 59. The effect of the discs is to produce constant potential over their areas, and the problem thus modified is susceptible of rigorous solution. Outside A and B the motion is the same as that previously investigated, when the obstructing plate is infinitely thin; between A and B the flow is uniform. The resistance is therefore on the whole

$$\frac{1}{2R} + \frac{L}{\pi R^2},$$

whence

$$c = \frac{\pi R^2}{L + \frac{1}{2}\pi R} \qquad\qquad (1).$$

If α denote the correction, which must be added to L on account of an open end,

$$\alpha = \tfrac{1}{4}\pi R \qquad\qquad (2).$$

This correction is in general under the mark, but, when L is very small in comparison with R, the assumed motion coincides more and more nearly with the actual motion, and thus the value of α in (2) tends to become correct.

A superior limit to the resistance may be calculated from a hypothetical *motion of the fluid. For this purpose we will suppose* infinitely thin pistons introduced at A and B, the effect of which will be *to make the normal velocity constant at those places.* Within the tube the flow will be uniform as before, but for the external space we have a new problem to consider:—To determine the motion of a fluid bounded by an infinite plane, the normal velocity over a circular area of the plane having a given constant value, and over the remainder of the plane being zero.

The potential may still be regarded as due to matter distributed over the disc, but it is no longer constant over the area; the *density* of the matter, however, being proportional to $d\phi/dn$ is constant.

The kinetic energy of the motion

$$= \tfrac{1}{2}\iint \phi \frac{d\phi}{dn}\, d\sigma = \tfrac{1}{2}\frac{d\phi}{dn}\iint \phi\, d\sigma,$$

the integration going over the area of the circle.

The total current through the plane

$$= \iint \frac{d\phi}{dn}\, d\sigma = \pi R^2 \frac{d\phi}{dn}.$$

Hence

$$\frac{2\ \text{kinetic energy}}{(\text{current})^2} = \frac{\iint \phi\, d\sigma}{\pi^2 R^4 \dfrac{d\phi}{dn}}.$$

If the density of the matter be taken as unity, $d\phi/dn = 2\pi$, and the required ratio is expressed by $P/\pi^3 R^4$, where P denotes the potential on itself of a circular layer of matter of unit density and of radius R.

The simplest method of calculating P depends upon the consideration that it represents the work required to break up the disc into infinitesimal elements and to remove them from each other's influence[1]. If we take polar co-ordinates (ρ, θ), the pole being at the edge of the disc whose radius is a, we have for the potential at the pole, $V = \iint d\theta\, d\rho$, the limits of ρ being 0 and $2a\cos\theta$, and those of θ being $-\tfrac{1}{2}\pi$ and $+\tfrac{1}{2}\pi$.

Thus

$$V = 4a \qquad\qquad (3).$$

Now let us cut off a strip of breadth da from the edge of the disc. The work required to remove this to an infinite distance is $2\pi a\, da \,.\, 4a$. If we gradually pare the disc down to nothing and carry all the parings to infinity[2], we find for the total work by integrating with respect to a from 0 to R,

$$P = \frac{8\pi R^3}{3}.$$

The limit to the resistance (for one side) is thus $8/3\pi^2 R$; we conclude that the resistance of the whole channel is less than

$$\frac{L}{\pi R^2} + \frac{16}{3\pi^2 R} \quad\ldots\ldots\ldots\ldots\ldots\ldots\ldots\ldots (4).$$

Collecting our results, we see that

$$\frac{\pi}{4} R < \alpha < \frac{8}{3\pi} R \quad\ldots\ldots\ldots\ldots\ldots\ldots\ldots\ldots (5),$$

or in decimals,

$$\left.\begin{array}{l} \alpha > \cdot 785\ R \\ \alpha < \cdot 849\ R \end{array}\right\} \quad\ldots\ldots\ldots\ldots\ldots\ldots\ldots\ldots (6).$$

It must be observed that α here denotes the correction for one end. The whole resistance corresponds to a length $L + 2\alpha$ of tube having the section πR^2.

When L is very great in relation to R, we may take simply

$$c = \frac{\pi R^2}{L} \quad\ldots\ldots\ldots\ldots\ldots\ldots\ldots\ldots (7).$$

In this case we have from (6) § 304

$$\lambda = \frac{2\sqrt{\pi} \,.\, \sqrt{(SL)}}{R} \quad\ldots\ldots\ldots\ldots\ldots\ldots\ldots\ldots (8).$$

The correction for an open end (α) is a function of L, coinciding with the lower limit, viz. $\frac{1}{4}\pi R$, when L vanishes. As L increases, α increases with it; but does not, even when L is infinite, attain the superior limit $8R/3\pi$. For consider the motion going on in any middle piece of the tube. The kinetic energy is greater than corresponds merely to the length of the piece. If therefore the piece be removed, and the free ends brought together, the motion otherwise continuing as before, the kinetic energy will be diminished more than corresponds to the length of the piece subtracted. *A fortiori* will this be true of the real motion which would exist in the shortened tube. That, when $L = \infty$, α does not become $8R/3\pi$ is evident, because the normal velocity at the end, far from being constant, as was assumed in the calculation of this result, must increase from the centre outwards and become infinite at the edge.

A further approximation to the value of α may be obtained by assuming a variable velocity at the plane of the mouth. The calculation will be found in Appendix A. It appears that in the case of an infinitely long tube α cannot be so great as $\cdot 82422\ R$. The real value of α is probably not far from $\cdot 82\ R$.

308. Besides the cylinder there are very few forms of channel whose conductivity can be determined mathematically. When however the form is approximately cylindrical we may obtain limits, which are useful as allowing us to estimate the effect of such departures from mathematical accuracy as must occur in practice.

An inferior limit to the resistance of any elongated and approximately straight conductor may be obtained immediately by the imaginary introduction of an infinite number of plane perfectly conducting layers perpendicular to the axis. If σ denote the area of the section at any point x, the resistance between two layers distant dx will be $\sigma^{-1}dx$, and therefore the whole actual resistance is certainly greater than

$$\int \sigma^{-1} dx \quad\ldots\ldots\ldots\ldots\ldots\ldots\ldots\ldots (1),$$

unless indeed the conductor be truly cylindrical.

In order to find a superior limit we may calculate the kinetic energy of the current on the hypothesis that the velocity parallel to the axis is uniform over each section. The hypothetical motion is that which would follow from the introduction of an infinite number of rigid pistons moving freely, and the calculated result is necessarily in excess of the truth, unless the section be absolutely constant. We shall suppose for the sake of simplicity that the channel is symmetrical about an axis, in which case of course the motion of the fluid is symmetrical also.

If U denote the total current, we have *ex hypothesi* for the axial velocity at any point x

$$u = \sigma^{-1} U \quad\ldots\ldots\ldots\ldots\ldots\ldots\ldots\ldots (2),$$

from which the radial velocity v is determined by the equation of

---

[1] A part of § 302 is repeated here for the sake of those who may wish to avoid the difficulties of the more complete investigation.

[2] This method of calculating P was suggested to the author by Professor Clerk Maxwell.

continuity (6 § 238),

$$\frac{d\,(ru)}{dx} + \frac{d\,(rv)}{dr} = 0.$$

Thus $$rv = \text{const.} - \tfrac{1}{2}\,Ur^2\,\frac{d\sigma^{-1}}{dx},$$

or, since there is no source of fluid on the axis,

$$v = -\tfrac{1}{2}\,Ur\,\frac{d\sigma^{-1}}{dx} \;\ldots\ldots\ldots\ldots\ldots\ldots\ldots\ldots\; (3).$$

The kinetic energy may now be calculated by simple integration:—

$$\int u^2\sigma\,dx = U^2\int \sigma^{-1}dx,$$

$$\iint v^2 2\pi r\,dr\,dx = \frac{\pi U^2}{8}\int y^4\left(\frac{d\sigma^{-1}}{dx}\right)^2 dx,$$

if y be the radius of the channel at the point x, so that $\sigma = \pi y^2$.

Thus $$\frac{2\text{ kinetic energy}}{(\text{current})^2} = \int \frac{1}{\pi y^2}\left\{1 + \tfrac{1}{2}\left(\frac{dy}{dx}\right)^2\right\}dx \ldots\ldots\ldots (4).$$

This is the quantity which gives a superior limit to the resistance. The first term, which corresponds to the component velocity u, is the same as that previously obtained for the lower limit, as might have been foreseen. The difference between the two, which gives the utmost error involved in taking either of them as the true value, is

$$\frac{1}{2\pi}\int \frac{1}{y^2}\left(\frac{dy}{dx}\right)^2 dx \;\ldots\ldots\ldots\ldots\ldots\ldots\ldots\ldots\; (5).$$

In a nearly cylindrical channel dy/dx is a small quantity and so the result found in this manner is closely approximate. It is not necessary that the section should be nearly constant, but only that it should vary slowly. The success of the approximation in this and similar cases depends upon the fact that the quantity to be estimated is at a minimum. Any reasonable approximation to the real motion will give a result very near the truth according to the principles of the differential calculus.

By means of the properties of the potential and stream functions (§ 238) the present problem admits of actual approximate solution. If ϕ and ψ denote the values of these functions at any point x, r; u, v denote the axial and transverse velocities,

$$u = \frac{d\phi}{dx} = \frac{1}{r}\frac{d\psi}{dr}, \qquad v = \frac{d\phi}{dr} = -\frac{1}{r}\frac{d\psi}{dx} \;\ldots\ldots\ldots\; (6),$$

whence by elimination

$$\frac{d^2\phi}{dr^2} + \frac{1}{r}\frac{d\phi}{dr} + \frac{d^2\phi}{dx^2} = 0 \;\ldots\ldots\ldots\ldots\ldots\; (7),$$

$$\frac{d^2\psi}{dr^2} - \frac{1}{r}\frac{d\psi}{dr} + \frac{d^2\psi}{dx^2} = 0 \;\ldots\ldots\ldots\ldots\ldots\; (8).$$

If F denote the value of ϕ as a function of x when $r = 0$, the general values of ϕ and ψ may be expressed in terms of F by means of (7) and (8) in the series

$$\left.\begin{aligned} \phi &= F - \frac{r^2F''}{2^2} + \frac{r^4F^{\text{iv}}}{2^2\,.\,4^2} - \frac{r^6F^{\text{vi}}}{2^2\,.\,4^2\,.\,6^2} + \ldots \\ \psi &= \frac{r^2F'}{2} - \frac{r^4F'''}{2^2\,.\,4} + \frac{r^6F^{\text{v}}}{2^2\,.\,4^2\,.\,6} - \frac{r^8F^{\text{vii}}}{2^2\,.\,4^2\,.\,6^2\,.\,8} + \ldots \end{aligned}\right\}\ldots\ldots\ldots (9),$$

where accents denote differentiation with respect to x. At the boundary of the channel where $r = y$, ψ is constant, say ψ_1. Then

$$\psi_1 = \frac{y^2F'}{2} - \frac{y^4F'''}{2^2\,.\,4} + \frac{y^6F^{\text{v}}}{2^2\,.\,4^2\,.\,6} - \;\ldots\ldots\ldots\ldots\ldots\; (10)$$

is the equation connecting y and F. In the present problem y is given, and we have to express F by means of it. By successive approximation we obtain from (10)

$$F' = \frac{2\psi_1}{y^2} + \frac{y^2}{8}\left\{\frac{d^2}{dx^2}\left(\frac{2\psi_1}{y^2}\right) + \frac{1}{8}\frac{d^2}{dx^2}\,y^2\,\frac{d^2}{dx^2}\left(\frac{2\psi_1}{y^2}\right)\right\}$$

$$- \frac{y^4}{12\,.\,4^2}\frac{d^4}{dx^4}\left(\frac{2\psi_1}{y^2}\right) \ldots\ldots\ldots\ldots\ldots\ldots\ldots (11).$$

The total stream is given by the integral

$$\int_0^y \frac{d\phi}{dx}\,2\pi r\,dr = \int_0^y \frac{1}{r}\frac{d\psi}{dr}\,2\pi r\,dr = 2\pi\psi_1;$$

and therefore the resistance between any two equipotential surfaces is represented by

$$\frac{1}{2\pi\psi_1}\int F'dx.$$

The expression for the resistance admits of considerable simplification by integration by parts in the case when the channel is truly cylindrical in the neighbourhood of the limits of integration. In this way we find for the final result,

$$\text{resistance} = \int \frac{dx}{\pi y^2}\left\{1 + \tfrac{1}{2}y'^2 - \frac{(3y'^2 - yy'')^2}{48}\right\} \text{.........}(12)^1,$$

y', y'' denoting the differential coefficients of y with respect to x.

It thus appears that the superior limit of the preceding investigation is in fact the correct result to the second order of approximation. If we regard y as a function of ωx, where ω is a small quantity, (12) is correct as far as terms containing ω^4.

309. Our knowledge of the laws on which the pitch of resonators depends, is due to the labours of several experimenters and mathematicians.

The observation that for a given mouthpiece the pitch of a resonator depends mainly upon the volume S is due to Liscovius, who found that the pitch of a flask partly filled with water was not altered when the flask was inclined. This result was confirmed by Sondhauss[1]. The latter observer found further, that in the case of resonators without necks, the influence of the aperture depended mainly upon its area, although when the shape was very elongated, a certain rise of pitch ensued. He gave the formula

$$N = 52400\frac{\sigma^{\frac{1}{4}}}{S^{\frac{1}{2}}} \text{..........................}(1),$$

the unit of length being the millimetre.

The *theory* of this kind of resonator we owe to Helmholtz[2], whose formula is

$$N = \frac{a\sigma^{\frac{1}{4}}}{2^{\frac{1}{2}}\pi^{\frac{5}{4}}S^{\frac{1}{2}}} \text{..........................}(2),$$

applicable to circular apertures.

For flasks with long necks, Sondhauss[3] found

$$N = 46705\frac{\sigma^{\frac{1}{2}}}{L^{\frac{1}{2}}S^{\frac{1}{2}}} \text{..........................}(3),$$

corresponding to the theoretical

$$N = \frac{a}{2\pi}\frac{\sigma^{\frac{1}{2}}}{L^{\frac{1}{2}}S^{\frac{1}{2}}} \text{..........................}(4).$$

In practice it does not often happen either that the neck is so long that the correction for the open ends can be neglected, as (4) supposes, or, on the other hand, so short that it can itself be neglected, as supposed in (2). Wertheim[4] was the first to shew that the effect of an open end could be represented by an addition (α) to the length, independent, or nearly so, of L and λ.

The approximate theoretical determination of α is due to Helmholtz, who gave $\frac{1}{4}\pi R$ as the correction for an open end fitted with an infinite flange. His method consisted in inventing forms of tube for which the problem was soluble, and selecting that one which agreed most nearly with a cylinder. The correction $\frac{1}{4}\pi R$ is rigorously applicable to a tube whose radius at the open end and at a great distance from it is R, but which in the neighbourhood of the open end bulges slightly.

From the fact that the true cylinder may be derived by introducing an obstruction, we may infer that the result thus obtained is too small.

It is curious that the process followed in this work, which was first given in the memoir on resonance, leads to exactly the same result, though it would be difficult to conceive two methods more unlike each other.

The correction to the length will depend to some extent upon whether the flow of air from the open end is obstructed, or not. When the neck projects into open space, there will be less obstruction than when a backward flow is prevented by a flange as supposed in our approximate calculations. However, the uncertainty introduced in this way is not very important, and we may generally take $\alpha = \frac{1}{4}\pi R$ as a sufficient approximation. In practice, when the necks are short, the hypothesis of the flange agrees pretty well with fact, and when the necks are long, the correction is itself of subordinate importance.

The general formula will then run

$$N = \frac{a}{2\pi}\sqrt{\frac{\sigma}{S\{L + \frac{1}{2}\sqrt{(\pi\sigma)}\}}} \text{.................}(5),$$

where σ is the area of the section of the neck, or in numbers

$$N = \frac{a}{6{\cdot}2832}\frac{\sigma^{\frac{1}{2}}}{S^{\frac{1}{2}}\sqrt{(L + {\cdot}8863\sqrt{\sigma})}} \text{.................}(6).$$

---

[1] *Proceedings of the London Mathematical Society*, Vol. VII. p. 70, 1876.

[1] Ueber den Brummkreisel und das Schwingungsgesetz der cubischen Pfeifen. *Pogg. Ann.* LXXXI. pp. 235, 347. 1850.

[2] Crelle, Bd. LVII. 1—72. 1860.

[3] Ueber die Schallschwingungen der Luft in erhitzten Glasröhren und in gedeckten Pfeifen von ungleicher Weite. *Pogg. Ann.* LXXIX. p. 1. 1850.

[4] Mémoire sur les vibrations sonores de l'air. *Ann. d. Chim.* (3) XXXI. p. 385. 1851.

A formula not differing much from this was given, as the embodiment of the results of his measurements, by Sondhauss[1] who

[1] *Pogg. Ann.* CXL. pp. 53, 219. 1870.

at the same time expressed a conviction that it was no mere empirical formula of interpolation, but the expression of a natural law. The theory of resonators with necks was given about the same time[1] in a memoir 'on Resonance' published in the *Philosophical Transactions* for 1871, from which most of the last few pages is derived.

310. The simple method of calculating the pitch of resonators with which we have been occupied is applicable to the gravest mode of vibration only, the character of which is quite distinct. The overtones of resonators with contracted necks are relatively very high, and the corresponding modes of vibration are by no means independent of the inertia of the air in the interior of the reservoir. The character of these modes will be more evident, when we come to consider the vibrations of air within a completely closed vessel, such as a sphere, but it will rarely happen that the pitch can be calculated theoretically.

There are, however, cases of multiple resonance to which our theory is applicable. These occur when two or more vessels communicate by channels with each other and with the external air; and are readily treated by Lagrange's method, provided of course that the wave-length of the vibration is sufficiently large in comparison with the dimensions of the vessels.

Suppose that there are two reservoirs, S, S', communicating with each other and with the external air by narrow passages or necks. If we were to consider SS' as a single reservoir and apply our previous formula, we should be led to an erroneous result; for that formula is founded on the assumption that within the reservoir the inertia of the air may be left out of account, whereas it is evident that the energy of the motion through the connecting passage may be as great as through the two others. However, an investigation on the same general plan as before meets the case perfectly. Denoting by X_1, X_2, X_3 the total transfers of fluid through the three passages, we have as in (2) § 304 for the kinetic energy the expression

Fig. 60.

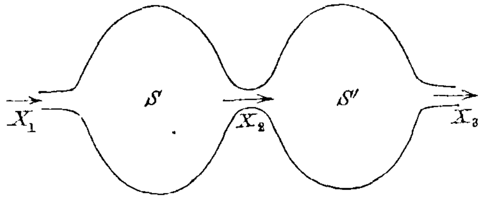

$$T = \tfrac{1}{2}\rho\left\{\frac{\dot{X}_1^2}{c_1} + \frac{\dot{X}_2^2}{c_2} + \frac{\dot{X}_3^2}{c_3}\right\} \text{..................} (1),$$

and for the potential energy,

$$V = \tfrac{1}{2}\rho a^2\left\{\frac{(X_2 - X_1)^2}{S} + \frac{(X_3 - X_2)^2}{S'}\right\} \text{............} (2).$$

An application of Lagrange's method gives as the differential equations of motion,

$$\left.\begin{aligned} \frac{\ddot{X}_1}{c_1} + a^2\frac{X_1 - X_2}{S} &= 0 \\ \frac{\ddot{X}_2}{c_2} + a^2\left\{\frac{X_2 - X_1}{S} + \frac{X_2 - X_3}{S'}\right\} &= 0 \\ \frac{\ddot{X}_3}{c_3} + a^2\frac{X_3 - X_1}{S'} &= 0 \end{aligned}\right\} \text{...............} (3).$$

By addition and integration,

$$\frac{X_1}{c_1} + \frac{X_2}{c_2} + \frac{X_3}{c_3} = 0 \text{.....................} (4).$$

Hence on elimination of X_2,

$$\left.\begin{aligned} \ddot{X}_1 + \frac{a^2}{S}\left\{(c_1 + c_2) X_1 + \frac{c_1 c_2}{c_3} X_3\right\} &= 0 \\ \ddot{X}_3 + \frac{a^2}{S'}\left\{(c_3 + c_2) X_3 + \frac{c_3 c_2}{c_1} X_1\right\} &= 0 \end{aligned}\right\} \text{.........} (5).$$

Assuming $X_1 = Ae^{pt}$, $X_3 = Be^{pt}$, we obtain on substitution and determination of $A : B$,

$$p^4 + p^2 a^2\left\{\frac{c_1 + c_2}{S} + \frac{c_3 + c_2}{S'}\right\} + \frac{a^4}{SS'}\left\{c_1 c_3 + c_2(c_1 + c_3)\right\} = 0 \text{...} (6),$$

as the equation to determine the natural tones. If N be the frequency of vibration, $N^2 = -p^2/4\pi^2$, the two values of p^2 being of course real and negative. The formula simplifies considerably if $c_3 = c_1$, $S' = S$; but it will be more instructive to work out this case from the beginning. Let $c_1 = c_3 = mc_2 = mc$.

---

[1] *Proceedings of the Royal Society*, Nov. 24, 1870.

The differential equations take the form

$$\left.\begin{aligned}\ddot{X}_1+\frac{a^2c}{S}\{(1+m)X_1+X_3\}=0\\ \ddot{X}_3+\frac{a^2c}{S}\{(1+m)X_3+X_1\}=0\end{aligned}\right\}\ldots\ldots\ldots\ldots(7),$$

while from (4) $X_2=-\dfrac{X_1+X_3}{m}$.

Hence

$$\left.\begin{aligned}(\ddot{X}_1+\ddot{X}_3)+\frac{a^2c}{S}(m+2)(X_1+X_3)=0\\ (\ddot{X}_1-\ddot{X}_3)+\frac{a^2c}{S}m(X_1-X_3)=0\end{aligned}\right\}\ldots\ldots\ldots(8).$$

The whole motion may be divided into two parts. For the first of these

$$X_1+X_3=0\ldots\ldots\ldots\ldots\ldots\ldots\ldots\ldots\ldots(9),$$

which requires that $X_2=0$. The motion is therefore the same as might take place were the communication between S and S' cut off, and has its frequency given by

$$N^2=\frac{a^2c_1}{4\pi^2S}=\frac{a^2mc}{4\pi^2S}\ldots\ldots\ldots\ldots\ldots\ldots\ldots(10).$$

The density of the air is the same in both reservoirs.

For the other component part, $X_1-X_3=0$, so that

$$X_2=-\frac{2X_1}{m};\qquad N'^2=\frac{a^2(m+2)c}{4\pi^2S}\ldots\ldots\ldots\ldots(11).$$

The vibrations are thus opposed in phase. The ratio of frequencies is given by $N'^2:N^2=m+2:m$, shewing that the second mode has the shorter period. In this mode of vibration the connecting passage acts in some measure as a second opening to both vessels, and thus raises the pitch. If the passage be contracted, the interval of pitch between the two notes is small.

A particular case of the general formula worthy of notice is obtained by putting $c_3=0$, which amounts to suppressing one of the communications with the external air. We thus obtain

$$p^4+a^2p^2\left(\frac{c_1+c_2}{S}+\frac{c_2}{S'}\right)+\frac{a^4c_1c_2}{SS'}=0\ldots\ldots\ldots\ldots(12),$$

or, if $\qquad S=S',\quad c_1=mc_2=mc,$

$$p^4+a^2p^2\frac{(m+2)c}{S}+\frac{a^4mc^2}{S^2}=0\ldots\ldots\ldots\ldots\ldots(13),$$

whence $\qquad N^2=\dfrac{a^2c}{8\pi^2S}\{m+2\pm\sqrt{(m^2+4)}\}\ldots\ldots\ldots\ldots(14).$

If we further suppose $m=1$, or $c_2=c_1$,

$$N^2=\frac{a^2c}{8\pi^2S}(3\pm\sqrt{5}).$$

If N' be the frequency for a simple resonator (S, c),

$$N'^2=\frac{a^2c}{4\pi^2S},$$

and thus $\qquad N_1^2:N'^2=\dfrac{3+\sqrt{5}}{2}=2{\cdot}618,$

$$N'^2:N_2^2=\frac{2}{3-\sqrt{5}}=2{\cdot}618.$$

It appears that the interval from N_1 to N' is the same as from N' to N_2, namely, $\sqrt{(2{\cdot}618)}=1{\cdot}618$, or rather more than a fifth. It will be found that whatever the value of m may be, the interval between the two tones cannot be less than 2·414, which is about an octave and a minor third. The corresponding value of m is 2.

A similar method is applicable to any combination, however complicated, of reservoirs and connecting passages under the single restriction as to the comparative magnitudes of the reservoirs and wave-lengths; but the example just given is sufficient to illustrate the theory of multiple resonance. A few measurements of the pitch of double resonators are detailed in my memoir on resonance, already referred to.

311. The equations which we have employed hitherto take no account of the escape of energy from a resonator. If there were really no transfer of energy between a resonator and the external atmosphere, the motion would be isolated and of little practical interest: never [illegible] the characteristic of a resonator consists in its vibrations being in great measure independent. Vibrations, once excited, will continue for a considerable number of periods without much loss of energy, and their frequency will be almost entirely independent of the rate of dissipation. The rate of dissipation is, however, an important feature in the character of a resonator, on which its behaviour under certain circumstances materially depends. It will be understood that the dissipation here spoken of means only the escape of energy from the vessel and its neighbourhood, and its diffusion in the surrounding medium, and not the transformation of ordinary energy into heat. Of such transformation our equations take no account, unless special terms be introduced for the purpose of representing the effects of viscosity, and of the conduction and radiation of heat.

[The influence of the conduction of heat has been considered by Koláček[1].]

Fig. 61.

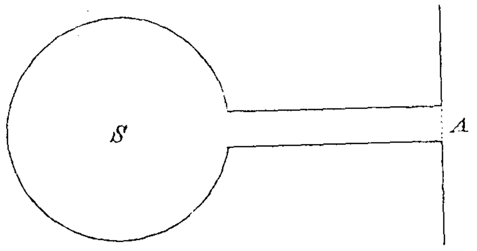

In a previous chapter (§ 278) we saw how to express the motion on the right of the infinite flange (Fig. 61), in terms of the normal velocity of the fluid over the disc A. We found, § 278 (3),

$$\phi = -\frac{1}{2\pi}\iint \frac{d\phi}{dn}\frac{e^{-ikr}}{r}\,d\sigma,$$

where ϕ is proportional to e^{int}.

If r be the distance between any two points of the disc, kr is a small quantity, and $e^{-ikr} = 1 - ikr$ approximately.

Thus $$\phi_A = -\frac{1}{2\pi}\left(\iint \frac{d\phi}{dn}\frac{d\sigma}{r} - ik\iint \frac{d\phi}{dn}\,d\sigma\right) \text{..........} (1).$$

The first term depends upon the distribution of the current. If we suppose that $d\phi/dn$ is constant, we obtain ultimately a term representing an increase of inertia, or a correction to the length, equal to $8R/3\pi$. This we have already considered, under the supposition of a piston at A. The second term, on which the dissipation depends, is independent of the distribution of current, being a function of the total current ($\dot X$) only. Confining our attention to this term, we have

$$\phi_A = \frac{ik\dot X}{2\pi} \text{........................} (2).$$

Assuming now that $\phi \propto e^{int}$, we have for the part of the variation of pressure at A, on which dissipation depends,

$$\delta p = -\rho\dot\phi_A = -i\rho n\phi_A = \frac{\rho nk\dot X}{2\pi} = \frac{\rho n^2\dot X}{2\pi a} \text{.........} (3).$$

The corresponding work done during a transfer of fluid δX is $\frac{\rho n^2\dot X}{2\pi a}\delta X$; and since, as in § 304, the expressions for the potential and kinetic energies are

$$V = \tfrac{1}{2}\rho a^2\frac{X^2}{S}, \qquad T = \tfrac{1}{2}\rho\frac{\dot X^2}{c} \text{..............} (4),$$

the equation of motion (§ 80) is

$$\ddot X + \frac{n^2c}{2\pi a}\dot X + \frac{a^2c}{S}X = 0 \text{................} (5)^1,$$

in place of (3) § 304. In the valuation of c an allowance must be included for the inertia of the fluid on the right-hand side of A, corresponding to the term omitted in the expression for δp.

Equation (5) is of the standard form for the free vibrations of dissipative systems of one degree of freedom (§ 45). The amplitude varies as $e^{-n^2ct/4\pi a}$, being diminished in the ratio $e : 1$ after a time equal to $4\pi a/n^2c$. If the pitch (determined by n) be given, the vibrations have the greatest persistence when c is smallest, that is, when the neck is most contracted.

If S be given, we have on substituting for c its value in terms of S and n,

$$\frac{4\pi a}{n^2c} = \frac{4\pi a^3}{n^4S} \text{.........................} (6),$$

shewing that under these circumstances the duration of the motion increases rapidly as n diminishes.

In the case of similar resonators $c \propto n^{-1}$, and then

$$\frac{4\pi a}{n^2c} \propto \frac{1}{n},$$

which shews that in this case the same proportional loss of amplitude always occurs after the lapse of the same number of periods. This result may be obtained by the method of dimensions, as a consequence of the principle of dynamical similarity.

As an example of (5), I may refer to the case of a globe with a neck, intended for burning phosphorus in oxygen gas, whose capacity is ·251 cubic feet [7100 c.c.]. It was found by experiment that the note of maximum resonance made 120 vibrations per second, so that $n = 120 \times 2\pi$. Taking the velocity of sound (a) at 1120 feet [34200 cent.] per second, we find from these data

$$\frac{4\pi a^3}{n^4S} = \frac{1}{5} \text{ of a second nearly.}$$

---

[1] *Wied. Ann.* t. 12, p. 353, 1881.

[1] Equation (5) is only approximate, inasmuch as the dissipative force is calculated on the supposition that the vibration is permanent; but this will lead to no material error when the dissipation is small.

Judging from the sound produced when the globe is struck, I think that this estimate must be too low; but it should be observed that the absence of the infinite flange assumed in the theory must influence very materially the rate of dissipation.

We will now examine the forced vibrations due to a source of sound external to the resonator. If the pressure δp at the mouth of the resonator due to the source, i.e. calculated on the supposition that the mouth is closed, be $F e^{ikat}$, the equation of motion corresponding to (5), but applicable to the forced vibration only, is

$$\frac{\rho}{c}\ddot{X} + \frac{\rho k^2 a}{2\pi}\dot{X} + \frac{\rho a^2}{S}X = F e^{ikat} \quad \text{..............(7)}.$$

If $X = X_0 e^{i(kat+\epsilon)}$, where X_0 is real,

$$\frac{F^2}{\rho^2 a^4 X_0^2} = \left(\frac{1}{S} - \frac{k^2}{c}\right)^2 + \left(\frac{k^3}{2\pi}\right)^2.$$

The maximum variation of pressure (G) inside the resonator is connected with X_0 by the equation

$$G = \frac{a^2 \rho X_0}{S} \quad \text{..........................(8)},$$

since $X_0 \div S$ is the maximum condensation. Thus

$$\frac{F^2}{G^2} = \left(1 - \frac{k^2 S}{c}\right)^2 + \left(\frac{k^3 S}{2\pi}\right)^2 \quad \text{.................(9)},$$

which agrees with the equation obtained by Helmholtz for the case where the communication with the external air is by a simple aperture (§ 306). The present problem is nearly, but not quite, a case of that treated in § 46, the difference depending upon the fact that the coefficient of dissipation in (7) is itself a function of the period, and not an absolutely constant quantity. If the period, determined by k, and S be given, (9) shews that the internal variation of pressure (G) is a maximum when $c = k^2 S$, that is, when the natural note of the resonator (calculated without allowance for dissipation) is the same as that of the generating sound. The maximum vibration, when the coincidence of periods is perfect, varies inversely as S; but, if S be small, a very slight inequality in the periods is sufficient to cause a marked falling off in the intensity of the resonance (§ 49). In the practical use of resonators it is not advantageous to carry the reduction of S and c very far, probably because the arrangements necessary for connecting the interior with the ear or other sensitive apparatus involve a departure from the suppositions on which the calculations are founded, which becomes more and more important as the dimensions are reduced. When the sensitive apparatus is not in connection with the interior, as in the experiment of reinforcing the sound of a tuning-fork by means of a resonator, other elements enter into the question, and a distinct investigation is necessary (§ 319).

In virtue of the principle of reciprocity the investigation of the preceding paragraph may be applied to calculate the effect of a source of sound situated in the interior of a resonator.

312. We now pass on to the further discussion of the problem of the open pipe. We shall suppose that the open end of the pipe is provided with an infinite flange, and that its diameter is small in comparison with the wave-length of the vibration under consideration.

As an introduction to the question, we will further suppose that the mouth of the pipe is fitted with a freely moving piston without thickness and mass. The preceding problems, from which the present differs in reality but little, have already given us reason to think that the presence of the piston will cause no important modification. Within the tube we suppose (§ 255) that the velocity-potential is

$$\phi = (A\cos kx + B\sin kx)\, e^{int} \text{.................(1)},$$

where, as usual, $k = 2\pi/\lambda = n/a$. At the mouth, where $x = 0$,

$$\phi_0 = A e^{int}; \qquad \left(\frac{d\phi}{dx}\right)_0 = kB\, e^{int} \text{..............(2)}.$$

On the right of the piston the relation between ϕ_0 and $\left(\frac{d\phi}{dx}\right)_0$ is by § 302

$$\iint \phi_0 d\sigma \;:\; \left(\frac{d\phi}{dx}\right)_0 = i\frac{\pi R^2}{k}\left\{1 - \frac{J_1(2kR)}{kR}\right\} - \frac{\pi}{2k^3}K_1(2kR) \text{......(3)},$$

R being the radius of the pipe. From this the solution of the problem may be obtained without any restriction as to the smallness of kR: since, however, it is only when kR is small that the presence of the piston would not materially modify the question, we may as well have the benefit of the simplification at once by taking as in (1) § 311

$$\iint \phi_0\, d\sigma \;:\; \left(\frac{d\phi}{dx}\right)_0 = \frac{i\pi k R^4}{2} - \frac{8R^3}{3} \text{..............(4)}.$$

Now, since the piston occupies no space, the values of $(d\phi/dx)_0$ must be the same on both sides of it; and since there is no mass, the like must be true of the values of $\iint\phi_0 d\sigma$. Thus

$$A\sigma = kB\left\{-\frac{8R^3}{3} + i\frac{k\pi R^4}{2}\right\}$$

or

$$A = B\left\{-\frac{8kR}{3\pi} + i\frac{k^2R^2}{2}\right\} \text{..................(5)}.$$

Substituting in (1), we find on rejecting the imaginary part, and putting for brevity $B = 1$,

$$\phi = \left\{\sin kx - \frac{8kR}{3\pi}\cos kx\right\}\cos nt - \tfrac{1}{2}k^2R^2\cos kx\,\sin nt\,......(6).$$

In this expression the term containing $\sin nt$ depends upon the dissipation, and is the same as if there were no piston, while that involving $8kR/3\pi$ represents the effect of the inertia of the external air in the neighbourhood of the mouth. In order to compare with previous results, let α be such that

$$\sin kx - \frac{8kR}{3\pi}\cos kx = \sin k(x - \alpha);$$

then, the squares of small quantities being neglected,

$$\alpha = \frac{8R}{3\pi}\,.............................(7),$$

and

$$\phi = \sin k(x - \alpha)\,\cos nt - \tfrac{1}{2}k^2R^2\cos kx\,\sin nt\,...........(8).$$

These formulæ shew that, if the dissipation be left out of account, the velocity-potential is the same as if the tube were lengthened by $8/3\pi$ of the radius, and the open end then behaved as a loop. The amount of the correction agrees with what previous investigations would have led us to expect as the result of the introduction of the piston. We have seen reason to know that the true value of α lies between $\frac{1}{4}\pi R$ and $8R/3\pi$, and that the presence of the piston does not affect the term representing the dissipation. But, before discussing our results, it will be advantageous to investigate them afresh by a rather different method, which besides being of somewhat greater generality, will help to throw light on the mechanics of the question.

313. For this purpose it will be convenient to shift the origin in the negative direction to such a distance from the mouth that the waves are there approximately plane, a displacement which according to our suppositions need not amount to more than a small fraction of the wave-length. The difficulty of the question consists in finding the connection between the waves in the pipe, which at a sufficient distance from the mouth are plane, and the diverging waves outside, which at a moderate distance may be treated as spherical. If the transition take place within a space small compared with the wave-length, which it must evidently do, if the diameter be small enough, the problem admits of solution, whatever may be the form of the pipe in the neighbourhood of the mouth.

Fig. 62.

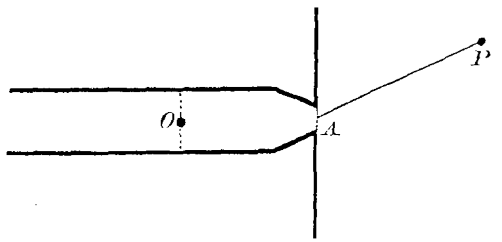

At a point P, whose distance from A is moderate, the velocity-potential is (§ 279)

$$\psi = \frac{A'}{r}e^{-ikr}e^{int}\,.......................(1),$$

whence

$$\frac{d\psi}{dr} = -\frac{A'e^{i(nt-kr)}}{r^2}(1 + ikr)\,.................(2).$$

Let us consider the behaviour of the mass of air included between the plane section at O and a hemispherical surface whose centre is A, and radius r, r being large in comparison with the diameter of the pipe, but small in comparison with the wave-length. Within this space the air must move approximately as an incompressible fluid would do. Now the current across the hemispherical surface

$$= 2\pi r^2\frac{d\psi}{dr} = -2\pi A'(1 + ikr)e^{i(nt-kr)} = -2\pi A'e^{int}\,........(3),$$

if the square of kr be neglected.

If, as before, we take for the velocity-potential within the pipe

$$\phi = (A\cos kx + B\sin kx)\,e^{int}\,....................(4),$$

we have for the current across the section at O,

$$\sigma\left(\frac{d\phi}{dx}\right)_0 = \sigma kB\,e^{int}\,..........................(5);$$

and thus

$$\sigma kB = -2\pi A'\,..........................(6).$$

This is the first condition; the second is to be found from the consideration that the total current (whose two values have just been equated) is proportional to the difference of potential at the terminals. Thus, if c denote the conductivity of the passage between the terminal surfaces,

$$\sigma\left(\frac{d\phi}{dx}\right)_0 = c(\psi_r - \phi_0),$$

or

$$\frac{\sigma kB}{c} = \frac{A'}{r}e^{-ikr} - A\,.......................(7).$$

On substituting for A' its value from (6), we have

$$-A = \sigma k B\left(\frac{1}{c} + \frac{e^{-ikr}}{2\pi r}\right) = \sigma k B\left\{\frac{1}{c} + \frac{1}{2\pi r} - \frac{ik}{2\pi}\right\}.$$

In this expression the second term is negligible in comparison with the first, for c is at most a quantity of the same order as the radius of the tube, and when the mouth is much contracted it is smaller still. Thus we may take

$$A = \sigma k B\left(-\frac{1}{c} + \frac{ik}{2\pi}\right) \text{..........................} (8).$$

Substituting this in (4), we have for the imaginary expression of the velocity-potential within the tube, if B be put equal to unity,

$$\phi = \left\{\sin kx + \sigma k\left(-\frac{1}{c} + \frac{ik}{2\pi}\right)\cos kx\right\} e^{int},$$

or, if only the real part be retained,

$$\phi = \left\{\sin kx - \frac{\sigma k}{c}\cos kx\right\}\cos nt - \frac{k^2\sigma}{2\pi}\cos kx \sin nt \text{.....} (9).$$

Following Helmholtz, we may simplify our results by introducing a quantity α defined by the equation

$$\tan k\alpha = \frac{k\sigma}{c} \text{..............................} (10).$$

Thus

$$\phi = \frac{\sin k(x-\alpha)}{\cos k\alpha}\cos nt - \frac{k^2\sigma}{2\pi}\cos kx \sin nt \text{...........} (11),$$

and the corresponding potential outside the mouth is

$$\psi = -\frac{\sigma k}{2\pi r}\cos(nt - kr) \text{.................} (12).$$

If R be the radius of the tube, we may replace σ by πR^2.

When the tube is a simple cylinder, and the origin lies at a distance ΔL from the mouth, we know that $\sigma c^{-1} = \Delta L + \mu R$, where μ is a number rather greater than $\frac{1}{4}\pi$. In such a case (the origin being taken sufficiently near the mouth) $k\alpha$ is a small quantity, and therefore from (10)

$$\alpha = \frac{\sigma}{c} = \Delta L + \mu R \text{....................} (13).$$

At the same time $\cos k\alpha$ may be identified with unity. The principal term in ϕ, involving $\cos nt$, may then be calculated, as if the tube were prolonged, and there were a loop at a point situated at a distance μR beyond the actual position of the mouth, in accordance with what we found before. These results, approximate for ordinary tubes, become rigorous when the diameter is reduced without limit, friction being neglected.

If there be no flange at A, the value of c is slightly modified by the removal of what acts as an obstruction, but the principal effect is on the term representing the dissipation. If we suppose as an approximation that the waves diverging from A are spherical, we must take for the current $4\pi r^2\, d\psi/dr$ instead of $2\pi r^2\, d\psi/dr$. The ultimate effect of the alteration will be to halve the expression for the velocity-potential outside the mouth, as well as the corresponding second term in ϕ (involving $\sin nt$). The amount of dissipation is thus seen to depend materially on the degree in which the waves are free to diverge, and our analytical expressions must not be regarded as more than rough estimates.

The correct theory of the open organ-pipe, including equations (11) and (12), was discovered by Helmholtz[1], whose method, however, differs considerably from that here adopted. The earliest solutions of the problem by Lagrange, D. Bernoulli, and Euler, were founded on the assumption that at an open end the pressure could not vary from that of the surrounding atmosphere, a principle which may perhaps even now be considered applicable to an end whose openness is ideally perfect. The fact that in all ordinary cases energy escapes is a proof that there is not anywhere in the pipe an absolute loop, and it might have been expected that the inertia of the air just outside the mouth would have the effect of an increase in the length. The positions of the nodes in a sounding pipe were investigated experimentally by Savart[2] and Hopkins[3], with the result that the interval between the mouth and the nearest node is always less than the half of that interval separating consecutive nodes.

[The correction necessary for an open end is the origin of a departure from the simple law of octaves, which according to elementary theory would connect the notes of closed and open pipes of the same length. Thus in the application to an organ-pipe let αR denote the correction for the upper end when open, and l the length of the pipe including the correction for the mouth at the lower end. The whole effective length of the open pipe is then $l + \alpha R$, while the effective length of the pipe if closed at the upper end is l simply. The open pipe is practically the longer, and the interval between the notes is less than the octave of the simple theory[4].

---

[1] Crelle, Bd. 57, p. 1. 1860.

[2] Recherches sur les vibrations de l'air. *Ann. d. Chim.* t. XXIV. 1823.

[3] Aerial vibrations in cylindrical tubes. *Cambridge Transactions*, Vol. v. p. 231. 1833.

[4] Bosanquet, *Phil. Mag.* VI. p. 63, 1878.

It may be worthy of remark that the correction, assumed to be independent of wave-length, does not disturb the harmonic relations between the partial tones, whether a pipe be open or closed.]

314. Experimental determinations of the correction for an open end have generally been made without the use of a flange, and it therefore becomes important to form at any rate a rough estimate of its effect. No theoretical solution of the problem of an unflanged open end has hitherto been given, but it is easy to see (§§ 79, 307) that the removal of the flange will reduce the correction materially below the value ·82 R (Appendix A). In the absence of theory I have attempted to determine the influence of a flange experimentally[1]. Two organ-pipes nearly enough in unison with one another to give countable beats were blown from an organ bellows; the effect of the flange was deduced from the difference in the frequencies of the beats according as one of the pipes was flanged or not. The correction due to the flange was about ·2R. A (probably more trustworthy) repetition of this experiment by Mr Bosanquet gave ·25R. If we subtract ·22R from ·82R, we obtain ·6R, which may be regarded as about the probable value of the correction for an unflanged open end, on the supposition that the wave-length is great in comparison with the diameter of the pipe.

Attempts to determine the correction entirely from experiment have not led hitherto to very precise results. Measurements by Wertheim[2] on doubly open pipes gave as a mean (for each end) ·663 R, while for pipes open at one end only the mean result was ·746 R. In two careful experiments by Bosanquet[3] on doubly open pipes the correction for one end was ·635 R, when $\lambda = 12\,R$, and ·543 R, when $\lambda = 30\,R$. Bosanquet lays it down as a general rule that the correction (expressed as a fraction of R) increases with the ratio of diameter to wave-length; part of this increase may however be due to the mutual reaction of the ends, which causes the plane of symmetry to behave like a rigid wall. When the pipe is only moderately long in proportion to its diameter, a state of things is approached which may be more nearly represented by the presence than by the absence of a flange. The comparison of theory and observation on this subject is a matter of some difficulty, because when the correction is small, its value, as calculated from observation, is affected by uncertainties as to absolute pitch and the velocity of sound, while for the case, when the correction is relatively larger, which experiment is more competent to deal with, there is at present no theory. Probably a more accurate value of the correction could be obtained from a resonator of the kind considered in § 306, where the communication with the outside air is by a simple aperture; the "length" is in that case zero, and the "correction" is everything. Some measurements of this kind, in which, however, no great accuracy was attempted, will be found in my memoir on resonance[1].

[Careful experimental determinations of the correction for an unflanged open end have been made by Blaikley[2], who employed a vertical tube of thin brass 2·08 inches (5·3 cm.) in diameter. The lower part of the t [illegible] immersed in water, the surface of which defined the "closed end," and the experiment consisted in varying the degree of immersion until the resonance to a fork of known pitch was a maximum. If the two shortest distances of the water surface from the open end thus found be l_1 and l_2, $(l_2 - l_1)$ represents the half wave-length, and the "correction for the open end" is $\frac{1}{2}(l_2 - l_1) - l_1$. The following are the results obtained by Blaikley, expressed as a fraction of the radius. They relate to the same tube resounding to forks of various pitch.

c'	253·68	·565
e'	317·46	·595
g'	380·81	·564
$b\flat'$	444·72	·587
c''	507·45	·568

The mean correction is thus ·576 R.]

Various methods have been used to determine the pitch of resonators experimentally. Most frequently, perhaps, the resonators have been made to *speak* after the manner of organ-pipes by a stream of air blown obliquely across their mouths. Although good results have been obtained in this way, our ignorance as to the mode of action of the wind renders the method unsatisfactory. In Bosanquet's experiments the pipes were not actually made to speak, but short discontinuous jets of air were blown across the open end, the pitch being estimated from the free vibrations as the sound died away. A method, similar in principle, that I have sometimes employed with advantage consists in exciting free vibrations by means of a blow. In order to obtain as well defined a note as possible, it is of importance to accommodate the hardness of the substance with which the resonator comes into contact to the pitch, a low pitch requiring a soft blow. Thus the pitch of a test-tube may be determined in a moment by striking it against the bent knee.

---

[1] *Phil. Mag.* (5) III. 456. 1877. [The earliest experiments of the kind are those of Gripon (*Ann. d. Chim.* III. p. 384, 1874) who shewed that the effect of a large flange is proportional to the diameter of the pipe.]

[2] *Ann. d. Chim.* (3) t. XXXI. p. 394, 1851.

[3] *Phil. Mag.* (5) IV. p. 219. 1877.

[1] *Phil. Trans.* 1871. See also Sondhauss, *Pogg. Ann.* t. 140, 53, 219 (1870), and some remarks thereupon by myself (*Phil. Mag.*, Sept. 1870).

[2] *Phil. Mag.* vol. 7, p. 339, 1879.

In using this method we ought not entirely to overlook the fact that the natural pitch of a vibrating body is altered by a term depending upon the square of the dissipation. With the notation of § 45, the frequency is diminished from n to $n(1-\frac{1}{8}k^2n^{-2})$, or if x be the number of vibrations executed while the amplitude falls in the ratio $e : 1$, from n to

$$n\left(1-\frac{1}{8\pi^2x^2}\right).$$

The correction, however, would rarely be worth taking into account.

The measurements given in my memoir on resonance were conducted upon a different principle by estimating the note of maximum resonance. The ear was placed in communication with the interior of the cavity, while the chromatic scale was sounded. In this way it was found possible with a little practice to estimate the pitch of a good resonator to about a quarter of a semitone. In the case of small flasks with long necks, to which the above method would not be applicable, it was found sufficient merely to hold the flask near the vibrating wires of a pianoforte. The resonant note announced itself by a quivering of the body of the flask, easily perceptible by the fingers. In using this method it is important that the mind should be free from bias in subdividing the interval between two consecutive semitones. When the theoretical result is known, it is almost impossible to arrive at an independent opinion by experiment.

315. We will now, following Helmholtz, examine more closely the nature of the motion within the pipe, represented by the formula (11) § 313. We have

$$\phi = L\cos(nt-\theta) \quad\ldots\ldots\ldots\ldots(1),$$

where

$$L^2 = \frac{\sin^2 k(x-\alpha)}{\cos^2 k\alpha} + \frac{k^4\sigma^2}{4\pi^2}\cos^2 kx \ldots\ldots\ldots\ldots(2),$$

$$\tan\theta = -\frac{k^2\sigma\cos k\alpha\cos kx}{2\pi\sin k(x-\alpha)} \ldots\ldots\ldots\ldots(3).$$

In the expression for L^2 the second term is very small, and therefore the maximum values of ϕ occur very nearly when

$$k(x-\alpha) = (-m+\tfrac{1}{2})\pi,$$

or

$$-x = \tfrac{1}{2}m\lambda - \tfrac{1}{4}\lambda - \alpha \ldots\ldots\ldots\ldots(4),$$

where m is a positive integer.

The distance between consecutive maxima is thus $\frac{1}{2}\lambda$, and the value of the maximum is $\sec^2 k\alpha$. The minimum values of L^2 occur approximately when $k(x-\alpha) = -m\pi$,

or

$$-x = \tfrac{1}{2}m\lambda - \alpha \ldots\ldots\ldots\ldots(5),$$

and their magnitude is given by

$$L^2 = \frac{k^4\sigma^2}{4\pi^2}\cos^2 kx = \frac{k^4\sigma^2}{4\pi^2}\cos^2 k\alpha \ldots\ldots\ldots\ldots(6).$$

In like manner,

$$\frac{d\phi}{dx} = J\cos(nt-\chi) \ldots\ldots\ldots\ldots(7),$$

where

$$J^2 = k^2\frac{\cos^2 k(x-\alpha)}{\cos^2 k\alpha} + \frac{k^6\sigma^2}{4\pi^2}\sin^2 kx \ldots\ldots\ldots\ldots(8),$$

$$\tan\chi = \frac{k^2\sigma\cos k\alpha\sin kx}{2\pi\cos k(x-\alpha)} \ldots\ldots\ldots\ldots(9).$$

The maximum values of J^2 occur when

$$-x = \tfrac{1}{2}m\lambda - \alpha \ldots\ldots\ldots\ldots(10),$$

and the minimum values, when

$$-x = \tfrac{1}{2}m\lambda - \tfrac{1}{4}\lambda - \alpha \ldots\ldots\ldots\ldots(11).$$

The approximate magnitude of the maximum is $k^2\sec^2 k\alpha$, and that of the minimum $k^6\sigma^2\cos^2 k\alpha \div 4\pi^2$. It appears that the maxima of velocity occur in the same parts of the tube as the minima of condensation (and rarefaction), and the minima of velocity in the same places as the maxima of condensation. The series of loops and nodes are arranged as if the first loop were at a distance α beyond the mouth.

With regard to the phases, we see that both θ and χ are in general small; and therefore with the exception of the places where L^2 and J^2 are near their minima the whole motion is synchronous, as if there were no dissipation.

Hitherto we have considered the problem of the passage of plane waves along the pipe and their gradual diffusion from the mouth, without regard to the origin of the plane waves themselves. All that we have assumed is that the origin of the motion is somewhere within the pipe. We will now suppose that the motion is due to the known vibration of a piston, situated at $x=-l$, the origin of co-ordinates being at the mouth. Thus, when $x=-l$,

$$\frac{d\phi}{dx}=G\cos nt \text{ ....}(12),$$

and this must be made to correspond with the expression for the plane waves, generalized by the introduction of arbitrary amplitude and phase.

We may take

$$\frac{d\phi}{dx}=B\,J\cos(nt-\epsilon-\chi) \text{ ....}(13),$$

where J and χ have the values given in (8), (9), while B and ϵ are arbitrary. Comparing (12) and (13) we conclude that

$$\tan\epsilon=\frac{k^2\sigma\cos k\alpha\sin kl}{2\pi\cos k(l+\alpha)} \text{ ....}(14),$$

$$G^2=B^2k^2\left\{\frac{\cos^2 k(l+\alpha)}{\cos^2 k\alpha}+\frac{k^4\sigma^2}{4\pi^2}\sin^2 kl\right\} \text{ .... }(15),$$

by which B and ϵ are determined.

In accordance with (12) § 313, the corresponding divergent wave is represented by

$$\psi=-\frac{\sigma kB}{2\pi r}\cos(nt-\epsilon-kr) \text{ ....}(16).$$

If G be given, B is greatest, when $\cos k(l+\alpha)=0$, that is when the piston is situated at an approximate node. In that case

$$B=\frac{2\pi}{k^3\sigma\cos k\alpha}G \text{ ....}(17),$$

shewing that the magnitude of the resulting vibration is very great, though not infinite, since $\cos k\alpha$ cannot vanish. When the mouth is much contracted, $\cos k\alpha$ may become small, but in this case it is necessary that the adjustment of periods be very exact in order that the first term of (15) may be negligible in comparison with the second. In ordinary pipes $\cos k\alpha$ is nearly equal to unity.

The minimum of vibration occurs when l is such that $\cos k(l+\alpha)=\pm 1$, that is, when the piston is situated at a loop. In that case

$$B=\frac{G\cos k\alpha}{k} \text{ ....}(18).$$

The vibration outside the tube is then, according to the value of α, equal to or smaller than the vibration which there would be if there were no tube and the vibrating plate were made part of the yz plane.

316. Our equations may also be applied to the investigation of the motion excited in a tube by external sources of sound. Let us suppose in the first place that the mouth of the tube is closed by a fixed plate forming part of the yz plane, and that the potential due to the external sources (approximately constant over the plate) is under these circumstances

$$\psi=H\cos nt \text{ ....}(1),$$

where ψ is composed of the potential due to each source and its image in the yz plane, as explained in § 278. Inside the tube let the potential be

$$\phi=H\cos kx\cos nt \text{ ....}(2),$$

so that ϕ and its differential coefficient are continuous across the barrier. The physical meaning of this is simple. We imagine within the tube such a motion as is determined by the conditions that the velocity at the mouth is zero, and that the condensation at the mouth is the same as that due to the sources of sound when the mouth is closed. It is obvious that under these circumstances the closing plate may be removed without any alteration in the motion. Now, however there is in general a finite velocity at $x=-l$, and therefore we cannot suppose the pipe to be there stopped. But when there happens to be a node at $x=-l$, that is to say when l is such that $[\sin kl]=0$, all the conditions are satisfied, and the actual motion within the pipe is that expressed by (2). This motion is evidently the same as might obtain if the pipe were closed at both ends; and in external space the potential is the same as if the mouth of the pipe were closed with the rigid plate.

In the general case in order to reduce the air at $x=-l$ to rest, we must superpose on the motion represented by (2) another of the kind investigated in § 313, so determined as to give at $x=-l$ a velocity equal and opposite to that of the first. Thus, if the second motion be given by

$$d\phi/dx=BJ\cos(nt-\epsilon-\chi),$$

we have $\epsilon+\chi=0$, and

$$B^2\left\{\frac{\cos^2 k(l+\alpha)}{\cos^2 k\alpha}+\frac{k^4\sigma^2}{4\pi^2}\sin^2 kl\right\}=H^2\sin^2 kl \text{.........}(3).$$

When $\sin kl=0$, we have, as above explained, $B=0$. The maximum value of B occurs when $\cos k(l+\alpha)=0$, and then

$$B = \frac{2\pi H}{k^2\sigma} \text{ ....(4)}^1.$$

It appears, as might have been expected, that the resonance is greatest when the reduced length is an odd multiple of $\frac{1}{4}\lambda$.

317. From the principle that in the neighbourhood of a node the inertia of the air does not come much into play, we see that in such places the form of a tube is of little consequence, and that only the capacity need be attended to. This consideration allows us to calculate the pitch of a pipe which is cylindrical through most of its length (l), but near the closed end expands into a bulb of small capacity (S). The reduced length is then evidently

$$l + \alpha + S\sigma^{-1} \text{..............................(1)},$$

where α is the correction for the open end, and σ is the area of the transverse section of the cylindrical part. This formula is often useful, and may be applied also when the deviation from the cylindrical form does not take the shape of an enlargement.

When the enlargement represented by S is too large to allow of the above treatment, we may proceed as follows. The dissipation being neglected, the velocity-potential in the tube may be taken to be

$$\phi = \sin k(x - \alpha) \cos nt,$$

the origin being at the mouth, while $\alpha = \frac{1}{4}\pi R$ approximately. At $x = -l$, we have

$$\dot{\phi} = n \sin k(l + \alpha) \sin nt,$$

and

$$\frac{d\phi}{dx} = k \cos k(l + \alpha) \cos nt.$$

Now the condensation is given by $s = -a^{-2}\dot{\phi}$, and the condition to be satisfied at $x = -l$ is

$$S\frac{ds}{dt} = -\sigma\frac{d\phi}{dx} \text{ ....(2)},$$

if it be assumed that the condensation within S is sensibly uniform. Thus

$$Sn^2a^{-2} \sin k(l + \alpha) = \sigma k \cos k(l + \alpha),$$

or, since $n = ak$,

$$\tan k(l + \alpha) = \frac{\sigma}{kS} \text{ ....(3)}$$

is the equation determining the pitch. Numerical examples of

---

[1] Helmholtz, *Crelle*, Bd. 57, 1860.

the application of (3) are given in my memoir on resonance (*Phil. Trans.* 1871, p. 117).

Similar reasoning proves that in any case of stationary vibrations, for which the wave-length is several times as great as the diameter of the bulb, the end of the tube adjoining the bulb behaves approximately as an open end if kS be much greater than σ, and as a stopped end if kS be much less than σ.

318. The action of a resonator when under the influence of a source of sound in unison with itself is a point of considerable delicacy and importance, and one on which there has been a good deal of confusion among acoustical writers, the author not excepted.

There are cases where a resonator absorbs sound, as it were attracting the vibrations to itself and so diverting them from regions where otherwise they would be felt. For example, suppose that there is a simple source of sound B situated in a narrow tube at a distance $\frac{1}{2}\lambda$ (or any odd multiple thereof) from a closed end, and not too near the mouth: then at any distant external point A, its effect is nil. This is an immediate consequence of the principle of reciprocity, because if A were the source, there could be no variation of potential at B. The restriction, precluding too great a proximity to the mouth, may be dispensed with, if we suppose the source B to be diffused uniformly over the cross section, instead of concentrated in one point. Then, whatever may be the size and shape of the section, there is absolutely no disturbance on the further side. This is clear from the theory of vibrations in one dimension; the reciprocal form of the proposition—that whatever sources of disturbance may exist beyond the section, $\iint\psi d\sigma = 0$—may be proved from Helmholtz's formula (2) § 293, by taking for ϕ the velocity potential of the purely axial vibration of the same period.

It is scarcely necessary to say that, whenever no energy is emitted, the source does no work; and this requires, not that there shall be no variation of pressure at the source, for that in the case of a simple source is impossible, but that the variable part of the pressure shall have exactly the phase of the acceleration, and no component with the phase of the velocity.

Other examples of the absorption of sound by resonators are afforded by certain modifications of Herschel's interference tube used by Quincke[1] to stop tones of definite pitch from reaching the ear.

---

[1] Pogg. *Ann.* CXXVIII. 177. 1866.

In the combinations of pipes represented in Fig. 63, the sound enters freely at A; at B it finds itself at the mouth of a resonator of pitch identical with its own. Under these circumstances it is absorbed, and there is no vibration propagated along BD. It is clear that the cylindrical tube BC may be replaced by any other resonator of the same pitch (γ), without prejudice to the action of the apparatus. The ordinary explanation by interference (so called) of direct and reflected waves is then less applicable.

Fig. 63.

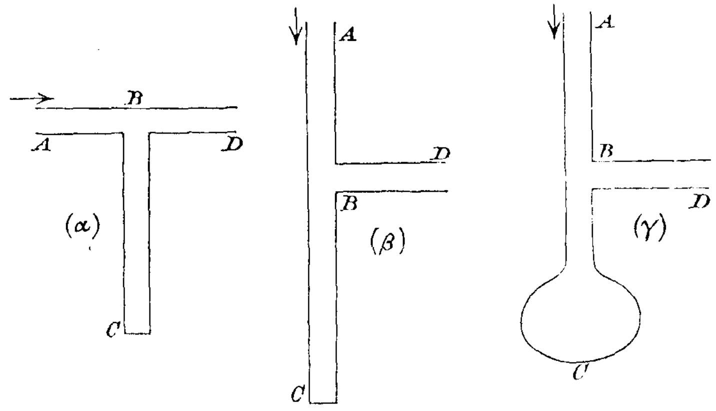

These cases where the source is at the mouth of a resonator must not be confused with others where the source is in the interior. If B be a source at the bottom of a stopped tube whose reduced length is $\frac{1}{4}\lambda$, the intensity at an external point A may be vastly greater than if there had been no tube. In fact the potential at A due to the source at B is the same as it would be at B were the source at A.

319. For a closer examination of the mechanics of resonance, we shall obtain the problem in a form disembarrassed of unnecessary difficulties by supposing the resonator to consist of a small circular plate, backed by a spring, and imbedded in an indefinite rigid plane. It was proved in a previous chapter, (30) § 302, that if M be the mass of the plate, ξ its displacement, $\mu\xi$ the force of restitution, R the radius, and σ the density of the air, the equation of vibration is

$$\left(M+\frac{8\sigma R^3}{3}\right)\ddot{\xi}+\frac{a\sigma\pi k^2R^4}{2}\dot{\xi}+\mu\xi=F \text{ ....(1)},$$

where F and ξ are proportional to e^{ikat}.

If the natural period of vibration (the reaction of external air included) coincide with that imposed, the equation reduces to

$$\tfrac{1}{2}a\sigma\pi k^2R^4\dot{\xi}=F \text{ ....(2)}.$$

Let us now suppose that F is due to an external source of sound, giving when the plate is at rest a potential ψ_0, which will be nearly constant over the area of the plate. Thus

$$F=-\delta p\,.\,\pi R^2=ika\sigma\,.\,\pi R^2\,.\,\psi_0 \text{ ....(3)};$$

so that $$\pi R^2\dot{\xi}=\dot{X}=2i\pi k^{-1}\psi_0=i\lambda\psi_0 \text{ ....(4)},$$

and the potential ϕ due to the motion of the plate at a distance r will be

$$\phi=-\frac{\dot{X}}{2\pi}\frac{e^{-ikr}}{r}=-\frac{i\psi_0}{k}\frac{e^{-ikr}}{r}=\psi_0\frac{e^{-ikr}}{ikr} \text{ ....(5)},$$

independent, it should be observed, of the area of the plate.

Leaving for the present the case of perfect isochronism, let us suppose that

$$-\left(M+\frac{8\sigma R^3}{3}\right)k'^2a^2+\mu=0 \text{ ....(6)},$$

so that $2\pi/k'$ is the wave-length of the natural note of the resonator. If M' be written for $M+\frac{8}{3}\sigma R^3$, the equation corresponding to (5) takes the form

$$\phi=\psi_0\frac{e^{-ikr}}{ikr}\div\left[1-2iM'\frac{k'^2-k^2}{\pi\sigma k^3R^4}\right] \text{ ....(7)},$$

from which we may infer as before that if $k'=k$ the efficiency of the resonator as a source is independent of R. When the adjustment is imperfect, the law of falling off depends upon $M'R^{-4}$. Thus if M' be great and R small, although the maximum efficiency of the resonator is no less, a greater accuracy of adjustment is required in order to approach the maximum (§ 49). In the case of resonators with simple apertures $M'=\frac{16}{3}\sigma R^3$, so that $M'R^{-4}$ varies as R^{-1}. Accordingly resonators with small apertures require the greatest precision of tuning, but the difference is not important. From a comparison of the present investigation with that of § 311 it appears that the conditions of efficiency are different according as internal or external effects are considered.

We will now return to the case of isochronism and suppose further that the external source of sound to which the resonator A responds, is the motion of a similar plate B, whose distance c from A is a quantity large in comparison with the dimensions of the plates. The intensity of B may be supposed to be such that its potential is

$$\psi=\frac{e^{-ikr}}{r} \text{ ....(8)}.$$

Accordingly $\psi_0 = c^{-1} e^{-ikc}$, and therefore by (5)

$$\phi = \psi_0 \frac{e^{-ikr}}{ikr} = \frac{e^{-ikc}}{ikc} \cdot \frac{e^{-ikr}}{r} \quad \ldots\ldots\ldots\ldots\ldots\ldots(9),$$

shewing that at equal distances from their sources

$$\phi : \psi = e^{-ikc} : ikc \quad \ldots\ldots\ldots\ldots\ldots\ldots(10).$$

The relation of phases may be represented by regarding the induced vibration ϕ as proceeding from B by way of A, and as being subject to an additional retardation of $\frac{1}{4}\lambda$, so that the whole retardation between B and A is $c + \frac{1}{4}\lambda$. In respect of amplitude ϕ is greater than ψ in the ratio of $1 : kc$.

Thus when kc is small, the induced vibration is much the greater, and the total sound is much louder than if A were not permitted to operate. In this case the phase is retarded by a quarter of a period.

It is important to have a clear idea of the cause of this augmentation of sound. In a previous chapter (§ 280) we saw that, when A is fixed, B gives out much less sound than might at first have been expected from the pressure developed. The explanation was that the *phase* of the pressure was unfavourable; the larger part of it is concerned only in overcoming the inertia of the surrounding air, and is ineffective towards the performance of work. Now the pressure which sets A in motion is the whole pressure, and not merely the insignificant part that would of itself do work. The motion of A is determined by the condition that that component of the whole pressure upon it, which has the phase of the velocity, shall vanish. But of the pressure that is due to the motion of A, the larger part has the phase of the acceleration; and therefore the prescribed condition requires an equality between the small component of the pressure due to A's motion, and a pressure comparable with the large component of the pressure due to B's motion. The result is that A becomes a much more powerful source than B. Of course no work is done by the piston A; its effect is to augment the work done at B, by modifying the otherwise unfavourable relation between the phases of the pressure and of the velocity.

The infinite plane in the preceding discussion is only required in order that we may find room behind it for our machinery of springs. If we are content with still more highly idealized sources and resonators, we may dispense with it. To each piston must be added a duplicate, vibrating in a similar manner, but in the opposite direction, the effect of which will be to make the normal velocity of the fluid vanish over the plane AB. Under these circumstances the plane is without influence and may be removed. If the size of the plates be reduced without limit they become ultimately equivalent to simple sources of fluid; and we conclude that a simple source B will become more efficient than before in the ratio of $1 : kc$, when at a small distance c from it there is allowed to operate a simple resonator (as we may call it) of like pitch, that is, a source in which the inertia of the immediately surrounding fluid is compensated by some adequate machinery, and which is set in motion by external causes only.

In the present state of our knowledge of the mechanics of vibrating fluids, while the difficulties of deduction are for the most part still to be overcome, any simplification of conditions which allows progress to be made, without wholly destroying the practical character of the question, may be a step of great importance. Such, for example, was the introduction by Helmholtz of the idea of a source concentrated in one point, represented analytically by the violation at that point of the equation of continuity. Perhaps in like manner the idea of a simple resonator may be useful, although the thing would be still more impossible to construct than a simple source.

320. We have seen that there is a great augmentation of sound, when a suitably tuned resonator is close to a simple source. Much more is this the case, when the source of sound is compound. The potential due to a double source is (§§ 294, 324)

$$r\psi = \mu e^{-ikr}\left(1 + \frac{1}{ikr}\right) \ldots\ldots\ldots\ldots\ldots\ldots\ldots(1).$$

If the resonator be at a small distance c,

$$\psi_0 = \mu_0 \frac{e^{-ikc}}{ikc^2},$$

and therefore the potential due to the resonator at a distance r' is

$$\phi = \mu_0 \frac{e^{-ikc}}{ikc^2} \cdot \frac{e^{-ikr'}}{ikr'} = \mu_0 \frac{e^{-ikc}}{i^2k^2c^2} \cdot \frac{e^{-ikr'}}{r'} \ldots\ldots\ldots\ldots\ldots(2).$$

If μ_0 vanish, the resonator is without effect; but when $\mu_0 = \pm 1$, that is, when the resonator lies on the axis of the double source, we have

$$\phi = \mp \frac{e^{-ikc}}{k^2c^2} \cdot \frac{e^{-ikr'}}{r'} \ldots\ldots\ldots\ldots\ldots\ldots\ldots(3).$$

At a distance from the double source its potential is

$$\psi = \mu \frac{e^{-ikr}}{r} \text{ ....(4).}$$

Thus we may consider that the potential due to the resonator is greater than that due to the double source in the ratio $k^2c^2 : 1$, the angular variation being disregarded.

A vibrating rigid sphere gives the *same kind* of motion to the surrounding air as a double source situated at its centre; but the substitution suggested by this fact is only permissible when the radius of the sphere is small in comparison with c: otherwise the presence of the sphere modifies the action of the resonator. Nevertheless the preceding investigation shews how powerful in general the action of a resonator is when placed in a suitable position close to a compound source of sound, whose character is such that it would of itself produce but little effect at a distance.

One of the best examples of this use of a resonator is afforded by a vibrating bar of glass, or metal, held at the nodes. A strip of plate glass about a foot [30 cm.] long and an inch [2·5 cm.] broad, of medium thickness (say $\frac{1}{8}$ inch [·32 cm.]), supported at about 3 inches [7·6 cm.] from the ends by means of string twisted round it, answers the purpose very well. When struck by a hammer it gives but little sound except overtones; and even these may almost be got rid of by choosing a hammer of suitable softness. This deficiency of sound is a consequence of the small dimensions of the bar in comparison with the wave-length, which allows of the easy transference of air from one side to the other. If now the mouth of a resonator of the right pitch[1] be held over one of the free ends, a sound of considerable force and purity may be obtained by a well-managed blow. In this way an improved harmonicon may be constructed, with tones much lower than would be practicable without resonators. In the ordinary instrument the wave-lengths are sufficiently short to permit the bar to communicate vibrations to the air independently.

The reinforcement of the sound of a bell in a well-known experiment due to Savart[2] is an example of the same mode of action; but perhaps the most striking instance is in the arrangement adopted by Helmholtz in his experiments requiring pure tones, which are obtained by holding tuning-forks over the mouths of resonators.

---

[1] To get the best effect, the mouth of the resonator ought to be pretty close to the bar; and then the pitch is decidedly lower than it would be in the open. The final adjustment may be made by varying the amount of obstruction. This use of resonators is of great antiquity.

[2] *Ann. d. Chim.* t. XXIV. 1823.

321. When two simple resonators A_1, A_2, separately in tune with the source, are close together, the effect is less than if there were only one. If the potentials due respectively to A_1, A_2 be ϕ_1, ϕ_2, we may take

$$\phi_1 = A_1 \frac{e^{-ikr_1}}{r_1}, \qquad \phi_2 = A_2 \frac{e^{-ikr_2}}{r_2}.$$

Let R represent the distance A_1A_2, and ψ_1, ψ_2, the potentials that would exist at A_1, A_2, if there were no resonators; then the conditions to determine A_1, A_2 are by (5) § 319

$$\left.\begin{array}{l} \psi_1 + A_2/R = + ikA_1 \\ \psi_2 + A_1/R = + ikA_2 \end{array}\right\} \text{ ....(1).}$$

By hypothesis ψ_1 and ψ_2 are nearly equal, and therefore

$$A_1 = A_2 = \frac{R}{-1 + ikR} \psi \text{ ....(2).}$$

Since ikR is small, the effect is much less than if there were only one resonator. It must be observed however that the diminished effectiveness is due to the resonators putting one another out of tune, and if this tendency be compensated by an alteration in the spring, any number of resonators near together have just the effect of one. This point is illustrated by § 302, where it will be seen (32) that though the resonance does not depend upon the size of the plate, still the inertia of the air, which has to be compensated by a spring, does depend upon it.

322. It will be proper to say a few words in this place on an objection, which has been brought forward by Bosanquet[1] as possibly invalidating the usual calculations of the pitch of resonators and of the correction to the length of organ-pipes. When fluid flows in a steady stream through a hole in a thin plate, the motion on the low pressure side is by no means of the character investigated in § 306. Instead of diverging after passing the hole so as to follow the surface of the plate, the fluid shapes itself into an approximately cylindrical jet, whose form for the case of two dimensions can be calculated[2] from formulæ given by Kirchhoff. On the high pressure side the motion does not deviate so widely from that determined by the electrical law. In like manner fluid passing outwards from a [illegible] continues to move in a cylindrical stream. If the external pressure be the greater, the character of the motion is different. In this case the stream lines converge from all directions to the mouth of the pipe, afterwards gathering themselves into a parallel bundle, whose section is considerably less than that of the pipe. It is clear that, if the formation of jets took place to any considerable extent during the passage of air through the mouths of resonators, our calculations of pitch would have to be seriously modified.

---

[1] *Phil. Mag.* Vol. IV. p. 125, 1877.

[2] *Phil. Mag.* Vol. II. p. 441, 1876.

The precise conditions under which jets are formed is a subject of great delicacy. It may even be doubted whether they would occur at all in frictionless fluid moving with velocities so small that the corresponding pressures, which are proportional to the squares of the velocities, are inconsiderable. But with air, as we actually have it, moving under the action of the pressures to be found in resonators, it must be admitted that jets may sometimes occur. While experimenting about two years ago with one of König's brass resonators of pitch c', I noticed that when the corresponding fork, strongly excited, was held to the mouth, a wind of considerable force issued from the nipple at the opposite side. This effect may rise to such intensity as to blow out a candle upon whose wick the stream is directed. It does not depend upon any peculiar motion of the air near the ends of the fork, as is proved by mounting the fork upon its resonance-box and presenting the open end of the box, instead of the fork itself, to the mouth of the resonator, when the effect is obtained with but slightly diminished intensity. A similar result was obtained with a fork and resonator, of pitch an octave lower (c). Closer examination revealed the fact that at the sides of the nipple the outward flowing stream was replaced by one in the opposite direction, so that a tongue of flame from a suitably placed candle appeared to enter the nipple at the same time that another candle situated immediately in front was blown away. The two effects are of course in reality alternating, and only appear to be simultaneous in consequence of the inability of the eye to follow such rapid changes. The formation of jets must make a serious draft on the energy of the motion, and this is no doubt the reason why it is necessary to close the nipple in order to obtain a powerful sound from a resonator of this form, when a suitably tuned fork is presented to it.

At the same time it does not appear probable that jet formation occurs to any appreciable extent at the mouths of resonators as ordinarily used. The near agreement between the observed and the calculated pitch is almost a sufficient proof of this. Another argument tending to the same conclusion may be drawn from the persistence of the free vibrations of resonators (§ 311), whose duration seems to exclude any important cause of dissipation beyond the communication of motion to the surrounding air.

In the case of organ-pipes, where the vibrations are very powerful, these arguments are less cogent, but I see no reason for thinking that the motion at the upper open end differs greatly from that supposed in Helmholtz's calculation. No conclusion to the contrary can, I think, safely be drawn from the phenomena of steady motion. In the [illegible] extreme case of impulsive motion jets certainly cannot be formed, as follows from Thomson's principle of least energy (§ 79), and it is doubtful to which extreme the case of periodic motion may with greatest plausibility be assimilated. Observation by the method of intermittent illumination (§ 42) might lead to further information upon this subject.

322*a*. As has already been mentioned, the free vibrations of the body of air contained in a resonator may be excited by a suitable blow delivered to the latter. The gas does not at first partake of the sudden movement imposed upon the walls, and the relative motion thus initiated is the origin of free vibrations of the kind considered in preceding sections. When corks are drawn from partially empty bottles, or when the lids are suddenly removed from tubular pasteboard pencil-cases, free vibrations of the resonating air columns are initiated in like manner.

If the vibrations are to be maintained with a view to the emission of a continued sound, the vibrating body must be in communication with a source of energy (§ 68 *a*), and the reaction between the two must be rightly accommodated with respect to phase. The question whether the source of energy or the resonator is to be regarded as the origin of the sound is of no particular significance and will be variously answered according to the point of view of the moment. In the organ the pipe, rather than the compressed air within the bellows or even the escaping wind, is regarded as the parent of the sound, but when a similar pipe is maintained in action by a flame the credit of the joint performance is usually given to the latter.

Up to this point the explanation of maintained vibrations is simple enough: but the complete theory in any particular case demands such an investigation of the reaction as will determine the phase relation. On this depends the whole question whether the reaction is favourable or unfavourable to the continuance of the vibrations, and the determination is often a matter of difficulty.

Before proceeding to discuss the action of the blast it will be desirable to say something further upon the organ-pipe considered simply as a resonator. We have seen (§ 314) how to take account of an upper open end, but according to the rule of Cavaillé-Coll the whole addition which must be made to the measured length of an open pipe in order to bring about agreement with the simple formula (8) § 255 amounts to as much as $3\frac{1}{3}R$, very much greater than the correction ($1{\cdot}2\,R$) necessary for a simple tube of circular section open at both ends. This discrepancy is sometimes attributed to the blast. But it must be remembered that the lower end is very much less open than the upper end, and that if a sensible correction on account of deficient openness is required for the latter, a much more important correction will probably be necessary for the former. Observations by the author[1] have shewn that this is the case. A pipe fitted with a sliding prolongation was tuned to maximum resonance with a given (256) fork as in Blaikley's experiment (§ 314). It was then blown from a well-regulated bellows with measured pressures of wind, and the pitch of the sounds so obtained was referred to that of the fork by the method of beats (§ 30). The results shewed that at practical pressures the pitch of the pipe as sounded by wind was *higher* than its natural note of maximum resonance; so that the considerable correction to the length found by Cavaillé-Coll is not attributable to the blast, but to the contracted character of the lower end treated as open in the elementary theory. In order to estimate the natural note an even larger "correction to the length" would be required.

The rise of pitch due to the wind increases with pressure. Thus in the case referred to above the pipe under a pressure of 1·06 inches (2·7 cm.) of water gave a note about 2 vibrations per second sharper than that of the fork, but when the wind pressure was raised to 4·2 inches (10·7 cm.) the excess was as much as 11 vibrations per second. When the pressure was raised much further, the pipe was "over blown" and gave the octave of its proper pitch. This, of course, corresponds to another mode of vibration of the aerial column.

It remains to consider the maintaining action of the blast. The vibrations of a column of air may be encouraged either by the introduction of fluid at a place where the density varies and at a moment of condensation (and by the similar abstraction of fluid at a moment of rarefaction), or by a suitable acceleration of the parts of the column situated near a loop. Since the blast of an organ acts at an open end of the pipe, it is clear that here we have to do with the latter alternative. The sheet of wind directed across the lip of the pipe is easily deflected. When during the vibration the external air tends to enter the pipe, it carries the jet with it more or less completely. Half a period later when the natural flow is outwards, the jet is deflected in the corresponding direction. In either case the jet encourages the prevailing motion, and thus renders possible the maintenance of the vibration.

For ready speech it is necessary that the sheet of wind be accurately adjusted. But Schneebeli[1] has shewn that when the vibration is once started there is more latitude. In an experimental arrangement the jet was so adjusted as to pass entirely outside the pipe. Under these circumstances there was failure to speak until by a temporary strong blast directed upon it from outside the jet was bent inwards to the proper position. The pipe then spoke and continued in action until by a pressure in the reverse direction the jet was bent back. The motion of the jet may be made apparent with the aid of smoke or by means of a piece of tissue paper held so as to vibrate with it. Both Schneebeli and H. Smith[2] insist upon a comparison between the jet and the tongue of a reed organ-pipe, but the modes of action appear to be essentially different.

The above view of the matter, which is that adopted by v. Helmholtz in the fourth edition of his great work, appears to be satisfactory as a general explanation of the maintenance of a continued vibration, but it cannot be regarded as complete. In matters of this kind practice is usually in advance of theory; and many generations of practical men have brought the organ-pipe to a high degree of excellence.

Another view that has been favourably entertained by many good authorities regards the pipe as merely reinforcing by its resonance a sound primarily due to the friction of the jet playing against the lip, and there seems to be no doubt that sounds may thus originate[3]. Perhaps after all there is less difference than might at first appear between the two views, and the latter may be especially appropriate when the initiation of the sound rather than its maintenance is under consideration. A detailed discussion of the question will be found in an essay by Van Schaik[1]. For a fuller explanation we must probably await a better knowledge of the mechanics of jets.

---

[1] *Phil. Mag.* III. p. 462, 1877; XIII. p. 340, 1882.

[1] *Pogg. Ann.* Bd. 153, p. 301, 1874.

[2] *Nature*, 1873, 1874, 1875.

[3] See for example Melde's *Akustik*, p. 252; Sondhauss *Pogg. Ann.* XCI. p. 126, 1854.

322 *b*. The character of the sound emitted from a pipe depends upon the presence or absence of the various overtones, a matter which requires further consideration. When a system vibrates freely, the overtones may be harmonic or inharmonic according to the nature of the system, and the composition of the sound depends upon the initial circumstances. But in the case of a maintained vibration like that now before us the motion is strictly periodic, and the overtones must be harmonic if present at all. The frequency of the whole vibration will correspond approximately with that natural to the pipe in its gravest mode[2], but the agreement between the pitch of an audible overtone and that of any free vibration may be much less close. The strength of any overtone thus depends upon two things: first upon the extent to which the maintaining forces possess a component of the right kind, and secondly upon the degree of approximation between the overtone and some natural tone of the vibrating body. In organ-pipes the sharpness of the upper lip and the comparative thinness of the sheet of wind are favourable to the production of overtones; so that in narrow open pipes v. Helmholtz was able to hear plainly the first six partial tones. In wider open pipes, on the other hand, the agreement between the overtones and the natural tones is less close. In consequence, pipes of this class, especially if of wood, give a softer quality of sound, in which besides the fundamental only the octave and twelfth are to be detected[3].

When a bottle (§ 26), or a spherical resonator, is blown by wind after the manner of an organ-pipe, there are no natural tones in the neighbourhood of the harmonics, and the resulting sound is almost free from overtones.

322 *c*. When two organ-pipes of the same pitch stand side by side, complications ensue which not unfrequently give trouble in practice. In extreme cases the pipes may almost reduce one another to silence. Even when the mutual influence is more moderate, it may still go so far as to cause the pipes to speak in absolute unison, in spite of inevitable small natural differences. The simplest case that can be considered is that of a pipe, along the median plane of which a thin resisting wall is supposed to be introduced. If this wall occupy the whole plane, the original pipe is divided into two, independent of, and perfectly similar to one another. And the pitch of these segments is the same as that of the original pipe, fluid friction being neglected, since during the vibrations of the latter there is no motion across the median plane of symmetry. But the case is altered if the wall be limited to the part of the plane included within the pipe, for then the two vibrating columns are free to react upon one another. The system as a whole has two degrees of freedom—we are not now regarding overtones—and free vibrations are performed in two distinct periods. The first of these is characterised by synchronism of phase between the vibrations of the component columns, and the pitch is accordingly the same as before the separation into two parts. But in the second mode the phases of vibration of the component columns are opposed, so that the air which escapes from one open end is absorbed by the contiguous open end of the other part. In consequence the "correction for the open ends" is much diminished in amount, and the pitch in this mode is correspondingly raised. So long as the motion is free, temporary vibrations in both modes may co-exist, and would give rise to beats; but it does not follow that both can be maintained by the blast. This would indeed seem improbable beforehand, and experiment shews that after the first moment the vibrations are confined to the second mode. The contiguous open ends act as opposed sources, and but little sound escapes, although within the pipes, and indeed outside in the immediate neighbourhood of their mouths, the vigour of the vibrations is unimpaired. Effects of the same kind are produced when two distinct but similar pipes are mounted side by side, and under the influence of the blast the compound system may vibrate in one mode only, in spite of small differences of pitch between the notes of the pipes when sounding separately[1].

322 *d*. Direct observation of the state of things within a vibrating air column is of course a matter of great difficulty, but

---

[1] *Ueber die Tonerregung in Labialpfeifen.* Rotterdam, 1891.

[2] We are not now speaking of "over blowing."

[3] *Tonempfindungen.* Fourth edition, p. 155, 1877.

[1] *Proceedings of the Musical Association*, Dec. 1878.

interesting results have been obtained by Töpler and Boltzmann[1], calling to their aid the method of optical interference to meet the difficulty arising out of the invisibility of air and the method of stroboscopic vision to meet that arising out of the rapidity of the changes. The upper end of an organ-pipe, closed by a thin plate of metal, was provided with sides of worked glass projecting above beyond the metal plate, and by suitable optical arrangements interference was produced between light which passed above and below. The space above being occupied by air at normal density and that below by air in a state of increased or diminished density according to the phase at the moment, the interference bands undergo displacements synchronous with the aerial vibration. Observed directly these displacements would escape the eye; but by the aid of a fork electrically maintained and provided with suitable slits (§ 42) the light may be rendered intermittent in a period nearly coincident with that of the vibration, and then the sequence of changes becomes apparent. From the observed movement of the bands it is possible to infer not merely the total change of density from maximum to minimum, but the law of the variation of density as a function of time.

When a pipe of large section was but moderately blown, the change of density at the node amounted to ·009 of an atmosphere, and the law was very nearly simple harmonic. Under a greater pressure of wind the simple harmonic law was widely departed from, the bands shifting themselves almost suddenly from one extreme position to the other. In this case the amplitude of the first overtone (the twelfth) was about one quarter of that of the fundamental tone. The whole variation of density was ·019 atmosphere.

322 *e*. In some experimental investigations a form of pipe more completely symmetrical with respect to the axis has been employed[2]. The lip is constituted by the entire circular edge of the pipe as defined by a plane perpendicular to the axis, and upon this an annular sheet of wind is brought to bear. A similar arrangement is adopted in the ordinary steam whistle.

Another way of applying wind to evoke the speech of small pipes has been experimented upon by Sondhauss[3], and the rationale is even less understood. A tube entirely open at one end is partially closed at the other by a plate of wood or metal 2 or 3 mm. thick and pierced by a cylindrical aperture with sharp edges (Fig. 63 *a*).

Fig. 63 *a*.

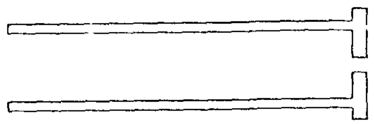

To set the pipe into action it is only necessary to insert the open end into a reservoir of wind. For rough purposes when it is not required to register the pressure nor to preserve a constant temperature, the mouth suffices, and the sound may be evoked either by pressure or by suction. The cylindrical aperture may be replaced by one of conical form, but in that case the wind must flow from the narrower towards the wider end. The sounds tabulated by Sondhauss vary from a' to f^6, corresponding in all cases to proper tones of the tube.

The whistling sounds of the unaided mouth are evidently of this class, the adjustment of pitch (from about c'' to c^5) being effected mainly by varying the internal capacity (§ 304). The formation of sound in whistling is sometimes said to be connected with a vibration of the lips, but this appears to be a mistake. I have found it possible to whistle through a suitable conical aperture in a piece of box-wood held tightly between the lips.

The occurrence of vibration may be taken as evidence that the steady flow of air through the passages in question is unstable. Contrary to what occurs in the organ-pipe and in sensitive flames, the deformations of the jet would seem here to be of the symmetrical sort. There is perhaps a tendency alternately to follow and to depart from the course marked out by the walls.

322 *f*. An important part of our present subject relates to the maintenance of vibrations by means of heat, and it will be possible to give at least a general account of the manner in which the effect takes place. In almost all cases where heat is communicated to a body expansion ensues, and this expansion may be made to do mechanical work. If the phases of the forces thus operative be favourable, a vibration may be maintained.

An instructive example is afforded by Trevelyan's rocker, consisting of a mass of iron or copper, so shaped that during vibration the weight is alternately carried on one or other of two adjacent and parallel ridges. When the instrument is heated and placed upon a block of cold lead, the vibrations persist so long as the heat remains sufficient. "Sir John Leslie first suggested that the cause of these vibrations is to be found in the expansion of the cold block by the heat which flows into it from the hot metal at the points of contact. Faraday[1], Seebeck[2], and Tyndall[3] have adopted this explanation; and they have shewn that most of the facts that they and others have ascertained respecting these vibrations are easily explained upon this view of their cause, supposing only that the expansion is sufficiently great to produce any sensible effect. Forbes[4], on the other hand, after an extensive series of experiments, was led to reject Sir John Leslie's explanation, one of his principal reasons for doing so being the impossibility, as it appeared to him, that the expansion occasioned by so slow a process as the conduction of heat could produce any sensible mechanical effect."

---

[1] *Pogg. Ann.* CXLI. p. 321, 1870.

[2] Gripon, *Ann. d. Chemie*, III. p. 384, 1874.

[3] *Pogg. Ann.* XCI. p. 126, 1854.

Davis, from whom[5] the above sentences are quoted, has examined the question mathematically, and has shewn that the explanation is adequate. It is evidently important that the lower body should possess a high rate of expansibility with temperature. In this respect lead stands high among the metals, and rock salt, which Tyndall found to answer well, is even more expansible.

The objection taken by Forbes may be met by the reply that the conduction of heat is not a slow process when small distances and masses are in question; and the special repulsion invoked by him as the basis of an alternative explanation would be of unsuitable character in respect of phase. It is essential that the phase of the force should be in arrear of the phase of the negative displacement.

In an experiment due to Page[6] the vibrations are made independent of an initial difference of temperature, the local heating at the points of contact being obtained with the aid of an electric current caused to pass from one body to the other. In this arrangement there is no contraction in the upper body to be deducted from the expansion in the lower. On a similar principle Gore[1] has contrived a continuous motion of a copper ball which travels upon circular rails themselves connected with a powerful battery.

322 *g*. But the most interesting examples of vibrations maintained by heat are those which occur when the resonating body is gaseous. "If heat be periodically communicated to, and abstracted from, a mass of air vibrating (for example) in a cylinder bounded by a piston, the effect produced will depend upon the phase of the vibration at which the transfer of heat takes place. If heat be given to the air at the moment of greatest condensation, or be taken from it at the moment of greatest rarefaction, the vibration is encouraged. On the other hand, if heat be given at the moment of greatest rarefaction, or abstracted at the moment of greatest condensation, the vibration is discouraged. The latter effect takes place of itself (§ 247) when the rapidity of alternation is neither very great nor very small in consequence of radiation; for when air is condensed it becomes hotter, and communicates heat to surrounding bodies. The two extreme cases are exceptional, though for different reasons. In the first, which corresponds to the suppositions of Laplace's theory of the propagation of sound, there is not sufficient time for a sensible transfer to be effected. In the second, the temperature remains nearly constant, and the loss of heat occurs during the *p*[illegible] of condensation, and not when the condensation is effected. This case corresponds to Newton's theory of the velocity of sound. When the transfer of heat takes place at the moment of greatest condensation or of greatest rarefaction, the pitch is not affected.

If the air be at its normal density at the moment when the transfer of heat takes place, the vibration is neither encouraged nor discouraged, but the pitch is altered. Thus the pitch is *raised* if heat be communicated to the air a quarter period *before* the phase of greatest condensation; and the pitch is *lowered* if the heat be communicated a quarter period *after* the phase of greatest condensation.

In general both kinds of effects are produced by a periodic transfer of heat. The pitch is altered, and the vibrations are either encouraged or discouraged. But there is no effect of the second kind if the air concerned be at a loop, i.e. a place where the density does not vary, nor if the communication of heat be the same at any stage of rarefaction as at the corresponding stage of condensation[1]."

Thus in any problem which may present itself of the maintenance of a vibration by heat, the principal question to be considered is the *phase* of the communication of heat relatively to that of the vibration.

---

[1] *Proc. of Roy. Inst.* vol. II. p. 119, 1831.

[2] *Pogg. Ann.* vol. LI. p. 1, 1840.

[3] *Phil. Mag.* vol. VIII. p. 1, 1854.

[4] *Phil. Mag.* vol. IV. pp. 15, 182, 1834.

[5] *Phil. Mag.* vol. XLV. p. 296, 1873.

[6] Silliman's *Journal*, vol. IX. p. 105, 1850.

[1] *Phil. Mag.* vol. XV. p. 519, 1858; vol. XVIII. p. 94, 1859.

322 *h*. The sounds emitted by a jet of hydrogen burning in a pipe open at both ends, were noticed soon after the discovery of the gas, and have been the subject of several elaborate inquiries. The fact that the notes are substantially the same as those which may be elicited in other ways, e.g. by blowing, was announced by Chladni. Faraday[2] proved that other gases were competent to take the place of hydrogen, though not without disadvantage. But it is to Sondhauss[3] that we owe the most detailed examination of the circumstances under which the sound is produced. His experiments prove the importance of the part taken by the column of gas in the tube which supplies the jet. For example, sound cannot be got with a supply tube which is plugged with cotton in the neighbourhood of the jet, although no difference can be detected by the eye between the flame thus obtained and others which are competent to excite sound. When the supply tube is unobstructed, the sounds obtainable by varying the resonator are limited as to pitch, often dividing themselves into distinct groups. In the intervals between the groups no coaxing will induce a maintained sound; and it may be added that, for a part of the interval at any rate, the influence of the flame is inimical, so that a vibration started by a blow is damped more rapidly than if the jet were not ignited.

Forms of resonator other than the open pipe may be employed, and sometimes with advantage. Very low notes can be got from spherical resonators, such as the large globes employed for demonstrating the combustion of phosphorus in oxygen gas. A globe of this kind gave in its natural condition a deep and pure tone of 64 vibrations per second. When it was fitted with a longer and narrower neck formed from a pasteboard tube, the calculated frequency fell to 25, and the vibrations, though vigorous enough to extinguish the flame, were hardly audible. When it is desired to excite very deep sounds, the supply tube should be made of considerable length, and the orifice must not be much contracted.

Singing flames may sometimes replace electrically maintained tuning-forks for the production of pure tones, when absolute constancy of pitch is not insisted upon. In order to avoid progressive deterioration of the air, it is advisable to use a resonator open above as well as below. A bulbous chimney, such as are often used with paraffin lamps, meets this requirement, and at the same time emits a pure tone. Or an otherwise cylindrical pipe may be blocked in the middle by a loosely fitting plug[1].

As Wheatstone shewed, the intermittence of a singing flame is easily made manifest by an oscillating, or a revolving, mirror. A more minute examination is best effected by the stroboscopic method, § 42. Drawings of the transformations thus observed have been given by Töpler[2], from which it appears that at one phase the flame may withdraw itself entirely within the supply tube.

Vibrations capable of being maintained are not always self-starting. The initial impulse may be given by a blow administered to the resonator, or by a gentle blast directed across the mouth. In the striking experiments of Schaffgotsch and Tyndall[3] a flame, previously silent, responds to a sound in unison with its own. In some cases the vibrations thus initiated rise to such intensity as to extinguish the flame.

The experiments of Sondhauss shew that a relationship of proportionality subsists between the lengths of the supply tubes and of the sounding columns. When the nature of the gas is varied, the same supply tube being retained, the mean lengths of the speaking columns are approximately as the square roots of the density of the gas. A connection is thus established between the natural note of a supply tube and the notes which can be sounded with its aid.

Partly in consequence of the peculiar and ill understood behaviour of flames, and partly for other reasons, the thorough explanation of the phenomena now under consideration is a matter of some difficulty; but there can be no doubt that they fall under the head of vibrations maintained by heat, the heat being communicated periodically to the mass of air confined in the sounding tube at a place where, in the course of a vibration, the pressure varies. Although some authors have shewn a tendency to lay stress upon the effects of the draught of air through the pipe, the sounds, as we have seen, can be readily produced, not only when there is no through draught, but even when the flame is so situated that there is no sensible periodic motion of the air in its neighbourhood.

---

[1] *Proc. Roy. Inst.* vol. VIII. p. 536, 1878; *Nature*, vol. XVIII. p. 319, 1878.

[2] *Quart. Journ. Sci.* vol. V. p. 274, 1818.

[3] *Pogg. Ann.* vol. CIX. pp. 1, 426, 1860.

[1] *Phil. Mag.* vol. VII. p. 149, 1879.

[2] *Pogg. Ann.* vol. CXXVIII. p. 126, 1866.

[3] *Sound*, 3rd edition, p. 224, 1875.

In consequence of the variable pressure within the resonator, the issue of gas, and therefore the development of heat, varies during the vibration. The question is under what circumstances the variation is of the kind necessary for the maintenance of the vibration. If we were to suppose, as we might at first be inclined to do, that the issue of gas is greatest when the pressure in the resonator is least, and that the phase of greatest development of heat coincides with that of the greatest issue of gas, we should have the condition of things the most unfavourable of all to the persistence of the vibration. It is not difficult, however, to see that both suppositions are incorrect. In the supply tube (supposed to be unplugged, and of not too small bore) stationary, or approximately stationary, vibrations are excited, whose phase is either the same or the opposite of that of the vibration in the resonator. If the length of the supply tube from the burner to the open end in the gas-generating flask be less than a quarter of the wave-length in hydrogen of the actual vibration, the greatest issue of gas *precedes* by a quarter period the phase of greatest condensation; so that, if the development of heat is *retarded* somewhat in comparison with the issue of gas, a state of things exists *favourable* to the maintenance of the sound. Some such retardation is inevitable, because a jet of inflammable gas can burn only at the outside; but in many cases a still more potent cause may be found in the fact that during the retreat of the gas in the supply tube small quantities of air may enter from the interior of the resonator, whose expulsion must be effected before the inflammable gas can again begin to escape.

If the length of the supply tube amounts to exactly one quarter of the wave-length, the stationary vibration within it will be of such a character that a node is formed at the burner, the variable part of the pressure just inside the burner being the same as in the interior of the resonator. Under these circumstances there is nothing to make the flow of gas, or the development of heat, variable, and therefore the vibration cannot be maintained. This particular case is free from some of the difficulties which attach themselves to the general problem, and the conclusion is in accordance with Sondhauss' observations.

When the supply tube is somewhat longer than a quarter of the wave, the motion of the gas is materially different from that first described. Instead of preceding, the greatest outward flow of gas *follows* at a quarter period interval the phase of greatest condensation, and therefore if the development of heat be somewhat retarded, the whole effect is unfavourable. This state of things continues to prevail, as the supply tube is lengthened, until the length of half a wave is reached, after which the motion again changes sign, so as to restore the possibility of maintenance. Although the size of the flame and its position in the tube (or neck of resonator) are not without influence, this sketch of the theory is sufficient to explain the fact, formulated by Sondhauss, that the principal element in the question is the length of the supply tube.

322 *i*. Another phenomenon of the class now under consideration occasionally obtrudes itself upon the notice of glass-blowers. When a bulb about 2 cm. in diameter is blown at the end of a somewhat narrow tube, 12 or 15 cm. long, a sound is sometimes heard proceeding from the heated glass. For experimental purposes it is well to use hard glass, which can afterwards be reheated at pleasure without losing its shape. As was found by De la Rive, the production of sound is facilitated by the presence of vapour, especially of alcohol and ether.

It was proved by Sondhauss[1] that a vibration of the glass itself is no essential part of the phenomenon, and the same indefatigable observer was very successful in discovering the connection (§§ 303, 309) between the pitch of the note and the dimensions of the apparatus. But no adequate explanation of the production of sound was given.

For the sake of simplicity, a simple tube, hot at the closed end and getting gradually cooler towards the open end, may be considered. At a quarter period *before* the phase of greatest condensation (which occurs almost simultaneously at all parts of the column) the air is moving inwards, i.e. towards the closed end, and therefore is passing from colder to hotter parts of the tube; but the heat received at this moment (of normal density) has no effect either in encouraging or discouraging the vibration. The same would be true of the entire operation of the heat, if the adjustment of temperature were instantaneous, so that there was never any sensible difference between the temperatures of the air and of the neighbouring parts of the tube. But in fact the adjustment of temperature takes *time*, and thus the temperature of the air deviates from that of the neighbouring parts of the tube, inclining towards the temperature of that part of the tube *from* which the air has just come. From this it follows that at the phase of greatest condensation heat is received by the air, and at the phase of greatest rarefaction heat is given up from it, and thus there is a tendency to maintain the vibrations. It must not be forgotten, however, that apart from transfer of heat altogether, the condensed air is hotter than the rarefied air, and that in order that the whole effect of heat may be on the side of encouragement, it is necessary that previous to condensation the air should pass not merely towards a hotter part of the tube, but towards a part of the tube which is hotter than the air will be when it arrives there. On this account a great range of temperature is necessary for the maintenance of vibration, and even with a great range the influence of the transfer of heat is necessarily unfavourable at the closed end, where the motion is very small. This is probably the reason of the advantage of a bulb. It is obvious that if the *open* end of the tube were heated, the effect of the transfer of heat would be even more unfavourable than in the case of a temperature uniform throughout.

---

[1] *Pogg. Ann.* vol. LXXIX. p. 1, 1850.

322 *j*. The last example of the production of sound by heat which we shall here consider is a very striking phenomenon discovered by Rijke[1]. When a piece of fine metallic gauze, stretching across the lower part of a tube open at both ends and held vertically, is heated by a gas flame placed under it, a sound of considerable power and lasting for several seconds is observed almost immediately *after* the removal of the flame. Differing in this respect from the case of sonorous flames (§ 322), the generation of sound was found by Rijke to be closely connected with the formation of a through draught impinging upon the heated gauze. In this form of the experiment the heat is soon abstracted, and then the sound ceases; but by keeping the gauze hot by the current from a powerful galvanic battery Rijke was able to obtain the prolongation of the sound for an indefinite period.

These notes may be obtained upon a large scale and form a very effective lecture experiment. For this purpose a cast iron pipe 5 feet (152 cm.) long and $4\frac{3}{4}$ inches (12 cm.) in diameter may be employed. The gauze (iron wire) is of about 32 meshes to the linear inch (2·54 cm.), and may advantageously be used in two thicknesses. It may be moulded with a hammer on a circular wooden block of somewhat smaller diameter than that of the pipe, and will then retain its position in the pipe by friction. When it is desired to produce the sound, the gauze caps are pushed up the pipe to a distance of about a foot (30·5 cm.), and a gas flame from a large rose burner is adjusted underneath, at such a level as to heat the gauze to bright redness. For this purpose the vertical tube of the lamp should be prolonged, if necessary, by an additional length of brass tubing. When a good red heat is attained, the flame is suddenly removed, either by withdrawing the lamp or by stopping the supply of gas. In about a second the sound begins, and presently rises to such intensity as to shake the room, after which it gradually dies away. The whole duration of the sound may be about 10 seconds[2].

In discussing the question of maintenance in accordance with the views already explained, we have to examine the character of the variable communication of heat from the gauze to the air. So far as the communication is affected directly by variations of pressure or density, the influence is unfavourable, inasmuch as the air will receive less heat from the gauze when its own temperature is raised by condensation. The maintenance depends upon the variable transfer of heat due to the varying *motions* of the air through the gauze, this motion being compounded of a uniform motion upwards with a motion, alternately upwards and downwards, due to the vibration. In the lower half of the tube these motions conspire a quarter period *before* the phase of greatest condensation, and oppose one another a quarter period after that phase. The rate of transfer of heat will depend mainly upon the temperature of the air in contact with the gauze, being greatest when that temperature is lowest. Perhaps the easiest way to trace the mode of action is to begin with the case of a simple vibration without a steady current. Under these circumstances the whole of the air which comes in contact with the metal, in the course of a complete period, becomes heated; and after this state of things is established, there is comparatively little further transfer of heat. The effect of superposing a small steady upwards current is now easily recognized. At the limit of the inwards motion, i.e. at the phase of greatest condensation, a small quantity of air comes into contact with the metal, which has not done so before, and is accordingly cool; and the heat communicated to this quantity of air acts in the most favourable manner for the maintenance of the vibration.

A quite different result ensues if the gauze be placed in the *upper* half of the tube. In this case the fresh air will come into the field at the moment of greatest rarefaction, when the communication of heat has an unfavourable instead of a favourable effect. The principal note of the tube therefore cannot be sounded.

---

[1] *Pogg. Ann.* vol. CVII. p. 339, 1859; *Phil. Mag.* vol. XVII. p. 419, 1859.

[2] *Phil. Mag.* vol. VII. p. 155, 1879.

A complementary phenomenon discovered by Bosscha[1] and Riess[2] may be explained upon the same principles. If a current of *hot* air impinge upon *cold* gauze, sound is produced; but in order to obtain the principal note of the tube the gauze must be in the upper, and not as before in the lower, half of the tube. In an experiment due to Riess the sound is maintained indefinitely. The upper part of a brass tube is kept cool by water contained in a surrounding vessel, through the bottom of which the tube passes. In this way the gauze remains comparatively cool, although exposed to the heat of a gas flame situated an inch or two below it. The experiment sometimes succeeds better when the draught is checked by a plate of wood placed somewhat closely over the top of the tube.

Both in Rijke's and Riess' experiments the variable transfer of heat depends upon the motion of vibration, while the effect of the transfer depends upon the variation of pressure. The gauze must therefore be placed where both effects are sensible, i.e. neither near a node nor near a loop. About a quarter of the length of the tube, from the lower or upper end, as the case may be, appears to be the most favourable position[1].

322 *k*. It remains to consider briefly another class of maintained aerial vibrations where the maintenance is provided for by the actual mechanical introduction of fluid, taking effect at a node and near the phase of maximum condensation. Well-known examples are afforded by such reed instruments as the clarinette, and by the various wind instruments actuated directly by the lips. The notes obtained are determined in the main by the aerial columns, modified, it may be, to some extent by the maintaining appliances. The reeds of the harmonium and organ come under a different head. The pitch is there determined almost entirely by the tongues themselves vibrating under their own elasticity, resonating air columns being either altogether absent or playing but a subordinate part.

In the instruments now under discussion the air column and the wind-pipe are connected by a narrow aperture, which is opened and closed periodically by a vibrating tongue. Tongues are distinguished by v. Helmholtz as in-beating and out-beating. In the first case the passage is opened when the tongue moves inwards, i.e. against the wind, as happens in the clarinette. Lip instruments, such as the trombone, belong to the second class, the passage being open when the lips are moved outwards or with the wind.

Let us consider the case of a cylindrical pipe, open at the further end, in which the air vibrates at such a pitch as to make the quarter wave-length equal to the length of the pipe. The end of the column where the tongue is situated thus coincides with an approximate node, and the aerial vibration can be maintained if the passage is open at the moment of greatest condensation, so that air from the wind-pipe is then forcibly injected. The tongue is maintained in motion by the variable pressure within the pipe, and the phase of its motion will depend upon whether it is in-beating or out-beating. In the latter case its phase is nearly the opposite to that of the forces operative upon it, being open when the pressure tending to close it is greatest. This is the state of things in lip instruments, the lips being heavy in relation to the rapidity of the vibrations actually performed, § 46. When the tongue is light and stiff, it must be made in-beating, as in the clarinette, and its phase is then in approximate agreement with the phase of the forces. A slight departure in the proper direction from precise opposition or precise agreement of phase, as the case may be, will allow of the communication of sufficient energy to maintain the motion in spite of dissipative influences. A more complete analytical statement of the circumstances has been given by v. Helmholtz[1], to whom the whole theory is due.

The character of the sounds from the various wind instruments used in music differs greatly. Strongly contrasted qualities are obtained from the trombone and the euphonion, the former brilliant and piercing, and the latter mellow. Blaikley[2] has analysed the sounds from a number of instruments, and has called attention to various circumstances, such as the size of the bell-mouth, and the shape of the cup applied to the lips, upon which the differences probably depend. The pressures used in practice, rising to 40 inches (102 cm.) of water in the case of the euphonion, have been measured by Stone[3].

---

[1] *Pogg. Ann.* vol. CVII. p. 342, 1859.

[2] *Pogg. Ann.* vol. CVIII. p. 653, 1859; CIX. p. 145, 1860.

[1] *Proc. Roy. Inst.* vol. VIII. p. 536, 1879; *Nature*, vol. XVIII. p. 319, 1878.

[1] *Tonempfindungen*, 4th edition, appendix VII.

[2] *Phil. Mag.* vol. VI. p. 119, 1878.

[3] *Phil. Mag.* vol. XLVIII. p. 113, 1874.

PNEUMATIC HANDBOOK, RH WARRING P.97

Compressor Installation

A COMPRESSOR installation may be *centralized* where all the compressors needed are housed in a single compressor plant; or *decentralized* where individual compressors are located near the points of use. A *centralized* installation can show greater cost-effectiveness as well as making it easier to optimize intake conditions and silencing. Modern practice with centralized installations is to install individual compressors with their associated ancillary equipment as completely separate units. It is then possible to shut down a single compressor for maintenance without shutting down the entire installation.

Ideally a compressor should be located where it can induct clean, dry and cool air. Another primary consideration is that a compressor is inherently a noisy machine and, unless specifically designed or treated for noise control, should be located in a 'noisy' area of a factory or workshop. In the case of a centralized installation it is generally desirable (and virtually necessary in the case of larger machines) to have the compressor in a separate well ventilated room or chamber, inducting air from the outside of the building. Each compressor should have a separate air intake, and pressure drop over the intake system should be kept low.

Basic treatment which can be applied is the fitting of an air intake filter of a suitable type and size to ensure that air reaching the compressor is clean; and a separate air intake silencer to reduce 'intake noise', which is usually a predominant noise-generator. Further noise treatment may, or may not, have to be applied to the machine itself and the room (*eg* the provision of adequate ventilation can establish noise-escape paths which may have to be dealt with).

In the case of reciprocating compressors the intake flow is pulsatory. This can aggravate noise problems through resonance with critical lengths of intake piping as well as affecting flow into the compressor. As a general rule the chance of resonance occurring is greatest when the intake pipe length corresponds to a quarter or three-quarters of the pressure pulse wavelength (λ) which for a single-acting compressor is:

$$\lambda = \frac{61.5 \times T^{0.5}}{n}$$

where λ = wavelength in metres

T = absolute temperature, K

n = compressor shaft rev/min

Note: the quantity $(61.5 \times T^{0.5})$ is the velocity of sound in air in m/sec.

---

physics textbook - Rossing
pg 49-57

CHAPTER 4

Resonance

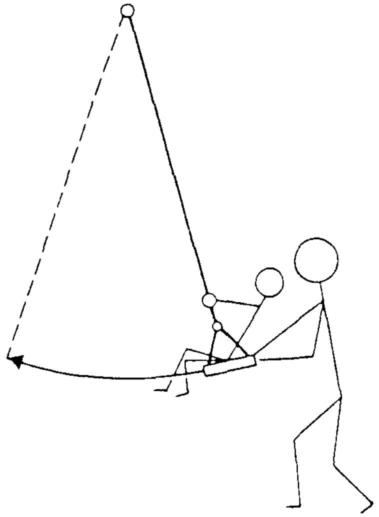

FIG. 4.1
An example of resonance: a child in a swing.

Consider a simple mechanical system: a child in a swing (Fig. 4.1). The swing has a natural frequency that is determined by its length (as the pendulum described in Section 2.3). If the swing is given a small push at the right time in each cycle, its amplitude gradually increases. This is an example of *resonance*. The swing receives only a small amount of energy during each push, but provided this amount is larger than the energy lost due to friction during each cycle, the amplitude of swing increases.

4.1 RESONANCE OF A MASS-SPRING VIBRATOR

Consider a mass-spring system similar to the one discussed in Section 2.1. Suppose that the spring is attached to a crank, as shown in Fig. 4.2. Let the crankshaft revolve at a frequency f and let the natural frequency of the mass-spring system be f_0. If f is varied slowly, the amplitude A of the mass is observed to change, reaching its maximum A_{max} when $f = f_0$. The mass is forced to vibrate at the frequency f of the crank, but when f matches f_0, the natural frequency of the system, resonance occurs. At resonance the maximum transfer of energy occurs, and the amplitude builds up to a value A_{max} determined by the friction in the system. The graph of amplitude A as a function of fre-

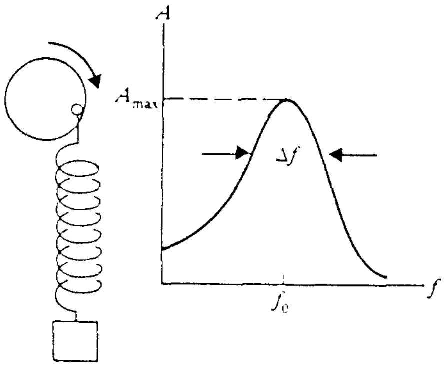

FIG. 4.2
Resonance of mass-spring vibrator driven at a frequency f.

quency f, shown in Fig. 4.2, is a nearly symmetrical curve, with a width Δf often called the *linewidth*. The linewidth is usually measured at an amplitude of 71% of A_{max} ($A_{max}/\sqrt{2}$).

Just as A_{max} depends on the rate of energy loss (due to friction or damping), so Δf also depends on energy loss. For a heavily damped system, Δf is large, and A_{max} is small. For a system with little loss, a "sharp" resonance with small Δf and large A_{max} occurs. Engineers define a quantity $Q = f_0/\Delta f$ to characterize the sharpness of a resonance. (The use of the letter Q comes from the term "quality factor" used to describe electrical circuits.) A high Q circuit is one with a sharp resonance; a low Q circuit has a broad resonance curve.

The linewidth Δf and the Q associated with a resonance are intimately related to the damping constant and the decay curve of a vibrator described in Section 2.2. A vibrator that loses its energy slowly will have a sharp resonance, and a vibrator that loses its energy rapidly will have a broad resonance. If the vibrator is set into motion and left to vibrate freely, its decay time is directly proportional to the Q of its resonance.

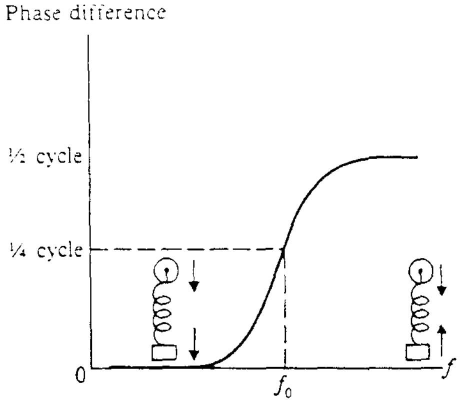

FIG. 4.3
Phase difference between crank and mass in a driven mass-spring system. At resonance they differ in phase by one-fourth of a cycle.

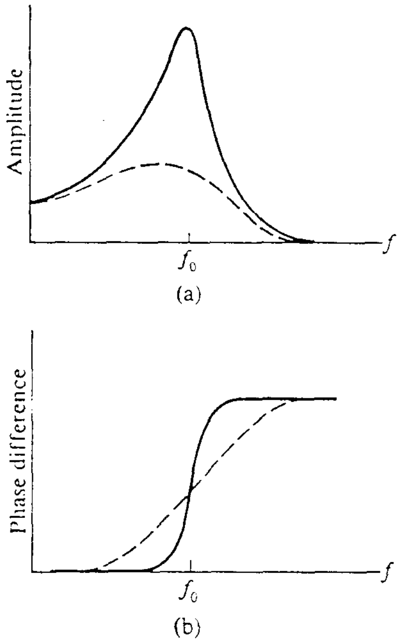

FIG. 4.4
(a) Response and (b) phase difference for vibrators with more (dotted curve) and less (solid curve) damping.

4.2 PHASE OF DRIVEN VIBRATIONS

If we carefully observe the direction of motion of the crank and the mass, we note an interesting phenomenon. At low frequencies, far below resonance, the two move in the same direction. At frequencies far above resonance, however, they move in opposite directions.

We describe this phenomenon by using the term *phase*, which may be thought of as a specification of the "starting point" of a vibration. At low frequencies, the entire system follows the motion of the crank, and the spring hardly stretches at all. As the frequency of the crank increases, however, it is more difficult to move the mass, and thus it begins to lag behind the driving force supplied by the crank. At resonance, the mass is one-fourth cycle behind the crank, although its amplitude builds up to its maximum value. As the crank frequency is increased still further, the phase difference becomes greater until finally the mass is one-half cycle behind the crank; that is, the mass and the crank move in opposite directions, as shown at the right in Fig. 4.3. The higher the Q, the more abrupt is this transition from "in phase" to "opposite phase." A vibrator with a lot of damping, on the other hand, exhibits a gradual change of phase, as shown in Fig. 4.4.

4.3 STANDING WAVES ON A STRING

In Section 3.4, we learned how interference between two waves traveling in opposite directions leads to standing waves. We also learned how reflection occurs when waves or pulses reach the boundary of the medium in which they propagate. We now combine these two ideas, and show how the modes of vibration or resonances of acoustical systems can be interpreted as waves propagating back and forth between the boundaries.

A simple and familiar example of such a system is a string of length L with both ends fixed as shown in Fig. 4.5. In its fundamental mode (that is, the standing wave with the lowest frequency and the longest wavelength), the string vibrates as shown in Fig. 4.5(a). The wavelength λ can be seen to be twice the string length, so the frequency is $f_1 = v/2L$. In the second mode, shown in Fig. 4.5(b), the wavelength λ equals the string length, so $f_2 = v/L = 2f_1$. Continuing to higher modes, we find that they have frequencies $3f_1$, $4f_1$, etc. The frequency of the nth mode will be

$$f_n = n\frac{v}{2L} = nf_1.$$

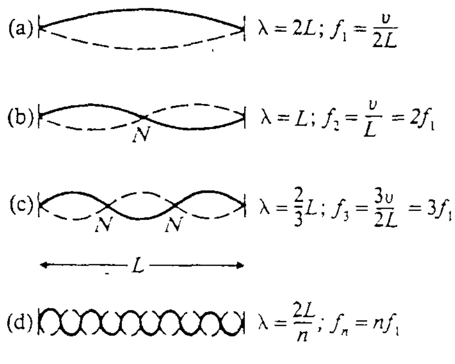
(a)
$\lambda = 2L;\ f_1 = \frac{v}{2L}$
(b)
N
$\lambda = L;\ f_2 = \frac{v}{L} = 2f_1$
(c)
N
N
$\lambda = \frac{2}{3}L;\ f_3 = \frac{3v}{2L} = 3f_1$
L
(d)
$\lambda = \frac{2L}{n};\ f_n = nf_1$

FIG. 4.5
Modes of vibration of resonances of a vibrating string as standing waves. The nodes are denoted by N. Note that the frequencies are harmonics of the fundamental frequency f_1.

Substituting the expression for wave speed given in Section 3.2 gives the following expression for the modes of a vibrating string:

$$f_n = \frac{n}{2L}\sqrt{\frac{T}{\mu}},$$

where T is tension and μ is mass per unit length.

If a string is driven at the frequency of one of its natural modes, resonance can occur. There are many ways in which to apply the driving force, three of which are illustrated in Fig. 4.6. The magnetic drive shown in Fig. 4.6(b) works only for a string of steel or other magnetic material. The moving violin bow applies a rather complicated driving force (to be described in Chapter 10), which has components at several different frequencies. The string may also be driven electromagnetically, even when the string is made of a nonmagnetic metal, by placing a permanent magnet near the string and passing an alternating current of the desired frequency through the string.

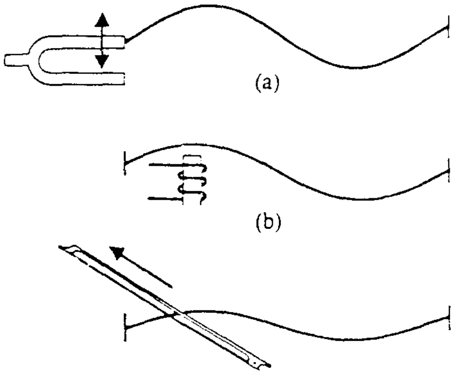

FIG. 4.6
Three ways to drive a string at one of its resonances: (a) a tuning fork; (b) an electromagnet; (c) a violin bow.

4.4 PARTIALS, HARMONICS, AND OVERTONES

It is appropriate at this point to clarify nomenclature in order to avoid confusion. We will use the term *harmonics* to refer to modes of vibration of a system that are whole-number multiples of the fundamental mode, and also to the sounds that they generate. (It is customary to stretch the definition a bit so that it includes modes that are *nearly* whole-number multiples of the fundamental: 2.005 times the fundamental rather than 2, for example.) Thus we say that the modes of an ideal vibrating string are harmonics of the fundamental, but the modes of a real string are usually so close to being whole-number multiples that we also speak of them as harmonics. Note that the term "first harmonic" refers to the fundamental.

Many vibrators do not have modes that are whole-number multiples of the fundamental frequency, however, and the term *overtones* is used to denote their higher modes of vibration. Harmonics are therefore described as overtones whose frequencies are whole-number multiples of the fundamental frequency. Minor confusion arises, however, from the fact that the term harmonics includes the fundamental, but the term overtones does not. Thus the second harmonic is the first overtone, the third harmonic is the second overtone, and so forth.

There is another term in common use that refers to modes of vibration of a system or the components of a sound: *partials*. Partials include all the modes or components, the fundamental plus all the overtones, whether they are harmonics or not. The term *upper partials* excludes the fundamental and thus is a synonym of overtones, but use of the former will be avoided in this book.

The actual motion of a vibrating string is a combination of the various modes of vibration. The way in which these modes or partials combine is given by the *spectrum* of the vibration. A vibration spectrum is like a recipe that specifies the relative amplitudes of the partials. Similarly, the spectrum of a sound specifies the amplitudes of its partials, as we will discuss in Chapter 7.

4.5 OPEN AND CLOSED PIPES

The reflection of sound pulses at open and closed ends of pipes was described in Section 3.5. At an open end, a pulse of positive pressure reflects back as a negative pulse; at a closed end, it reflects as a positive pulse. These two end conditions can be used to arrive at the resonances for open and closed pipes.

The motion of the vibrating air in a pipe is a little harder to visualize than the transverse vibrations of a string, since the motion of the air is longitudinal. The motion of the air is greatest at an *open* end, but the pressure variation is maximum at a *closed* end. A pressure-sensitive microphone inserted into the tube will pick up the most sound at the points where the pressure variations above and below atmospheric pressure are maximum. Thus in Figs. 4.7 and 4.8, both the air motion and the pressure variations are shown.

In an actual pipe, the pressure variations do not drop to zero right at the open end of the pipe, but rather a small distance beyond. Thus the pipe appears to have an acoustic length that is slightly greater than its physical length. For a cylindrical pipe of radius r, the additional length, called the *end correction*, is $0.61r$. Twice this amount should be added to the length of a pipe with two open ends to obtain its acoustic length.

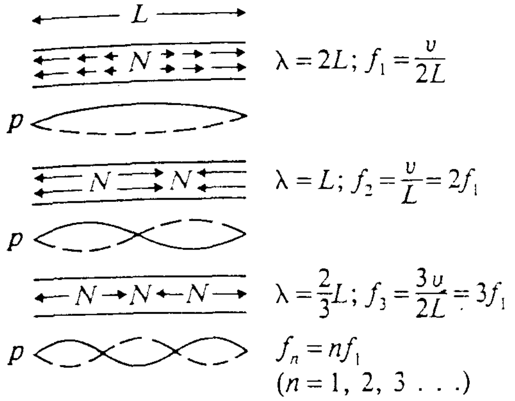
L
N
$\lambda = 2L;\ f_1 = \frac{v}{2L}$
p
N N
$\lambda = L;\ f_2 = \frac{v}{L} = 2f_1$
p
N N N
$\lambda = \frac{2}{3}L;\ f_3 = \frac{3v}{2L} = 3f_1$
p
$f_n = nf_1$
$(n = 1, 2, 3 \ldots)$

FIG. 4.7
Modes of vibration or resonances of an open pipe. At the open ends the pressure is equal to atmospheric pressure. The resulting modes include both odd-numbered and even-numbered harmonics. Minimum motion occurs at the nodes denoted by N.

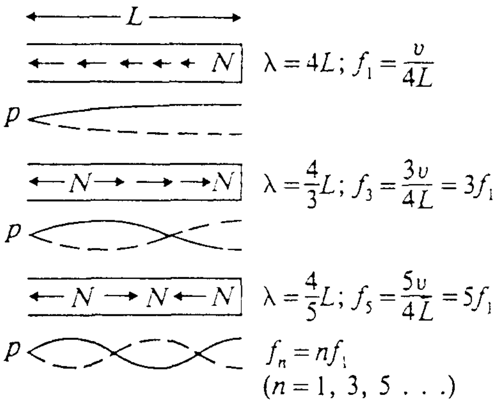
L
N
$\lambda = 4L;\ f_1 = \frac{v}{4L}$
p
N N
$\lambda = \frac{4}{3}L;\ f_3 = \frac{3v}{4L} = 3f_1$
p
N N N
$\lambda = \frac{4}{5}L;\ f_5 = \frac{5v}{4L} = 5f_1$
p
$f_n = nf_1$
$(n = 1, 3, 5 \ldots)$

FIG. 4.8
Modes of vibration or resonances of a closed pipe. At the closed end, the air motion is minimum but the pressure is maximum. The resulting modes include odd-numbered harmonics only. Minimum motion occurs at the nodes denoted by N.

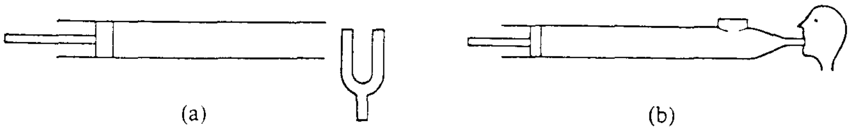
(a) (b)

FIG. 4.9
Resonance of a closed tube demonstrated by (a) holding a tuning fork near one end; (b) blowing on an organ pipe.

Resonance of a tube can be demonstrated by placing a tuning fork near one end of it, as shown in Fig. 4.9(a). A piston at the closed end makes it possible to change the resonance frequency. Blowing through a closed ("stopped") organ pipe may excite several of its resonances. Gentle blowing excites the lowest mode, but blowing much harder causes the pipe to vibrate in its first overtone, which for a closed pipe is the third harmonic ($f_3 = 3f_1$), a musical twelfth above the lowest mode.

In Chapter 15, which deals with speech production, we will be interested in resonances of the human vocal tract that allow us to enunciate various vowel sounds. There, we will consider not only reflections from open and closed ends but from constrictions and changes in pipe diameter as well. At every such discontinuity, a portion of the sound wave is reflected, thus leading to standing waves and resonances. If reflections occur at several places along the pipe, the resonances (in the vocal tract, they are called *formants*) can become rather complex.

4.6 ACOUSTIC IMPEDANCE

A quantity that acoustical engineers find very useful is *acoustic impedance* Z_A. It is defined as the ratio of sound pressure p to volume velocity U and is measured in acoustic ohms:

$$Z_A = p/U.$$

The volume velocity U is the amount of air that flows through a specified area per second due to passage of a sound wave. In the case of sound propagating in a tube, the specified area would be the cross-sectional area of the tube.

In the case of plane waves propagating in a tube, the acoustic impedance can be found by using the formula $Z_A = \rho v/S$, where ρ is the density of the air (1.15 kg/m^3 at room temperature), v the speed of sound, and S the cross-sectional area of the tube. Hence $Z_A \simeq 400/S$, with S measured in square meters. We will find the numerical value of Z_A much less important than the fact that it varies inversely with area S. Thus when there is a constriction, a change in diameter, or a sidebranch in a tube, the impedance change at that point leads to reflection of sound waves.

Acoustic impedance is analogous to electrical impedance, which is the ratio of voltage to electrical current (see Chapter 15). In this case, the voltage is the forcing function that causes current to flow. In the case of a sound wave, sound pressure is the forcing function that causes air flow with volume velocity U. In the chapters on wind instruments, use will be made of acoustic input impedance, which is the ratio of pressure to volume velocity at the input (mouthpiece) of a wind instrument.

4.7 HELMHOLTZ RESONATOR

The Helmholtz resonator was described as a vibrating system in Section 2.3. As a resonator, it has many applications in acoustics. Only a few of them will be described.

1. Before the invention of microphones, amplifiers, and spectrum analyzers, Helmholtz resonators were used to study vibrating objects and analyze complex sounds. In Fig. 4.10(a) the modes of vibration of a bell are being probed by a Helmholtz resonator having a second opening through which resonant sound can be heard by the investigator.
2. The main air resonance of a violin or guitar is essentially a Helmholtz resonance. The frequency can be determined by blowing across the *f*-holes of a violin or the rose hole of a guitar and listening for the pitch of the resonance. A more precise method is to insert a microphone inside the instrument and generate sound outside by means of a loudspeaker and audio generator.
3. Bass reflex loudspeaker cabinets are designed so that radiation from the back of the speaker cone excites the Helmholtz resonance of the cabinet and appears at the reflex port in phase with the front of the speaker.
4. Some automobile mufflers make use of side branches that absorb sound at their resonance frequency, as shown in Fig. 4.10(d).

4.8 SYMPATHETIC VIBRATIONS: SOUNDBOARDS

The amount of sound radiated by a vibrating system depends on the amount of air it displaces as it moves (the volume velocity defined in Section 4.6). A vibrating string or the narrow prongs of a tuning fork displace very little air as they vibrate; thus they radiate a small amount of sound. The moving cone of a loudspeaker and the vibrating membrane of a drum, on the other hand, radiate sound rather efficiently.

It is possible to increase the sound radiation from a tuning fork by pressing its handle against a wood plate or table top, so that the tuning fork forces the large wood area to vibrate. The vibrations of the wood, called sympathetic vibrations, may or may not occur at a frequency near a resonance of the wood plate, but nevertheless they amplify the sound because of the large surface set into vibration.

Violins, guitars, cellos, lutes, and other string instruments depend almost completely on sympathetic vibrations of the wood sounding box for radiation of their sound. Most of the sound radiation in these instruments comes from sympathetic vibrations of the top plate, which is driven by the vibrating strings through the bridge. The top plate has many resonances of its own distributed throughout the playing range, and these resonances, to a large part, determine the quality of the instrument. Sympathetic vibration of the wood also sets the air inside the instrument into vibration, so that sound is radiated from the *f*-holes (violin) or sound hole (guitar). String instruments will be discussed in Chapter 10.

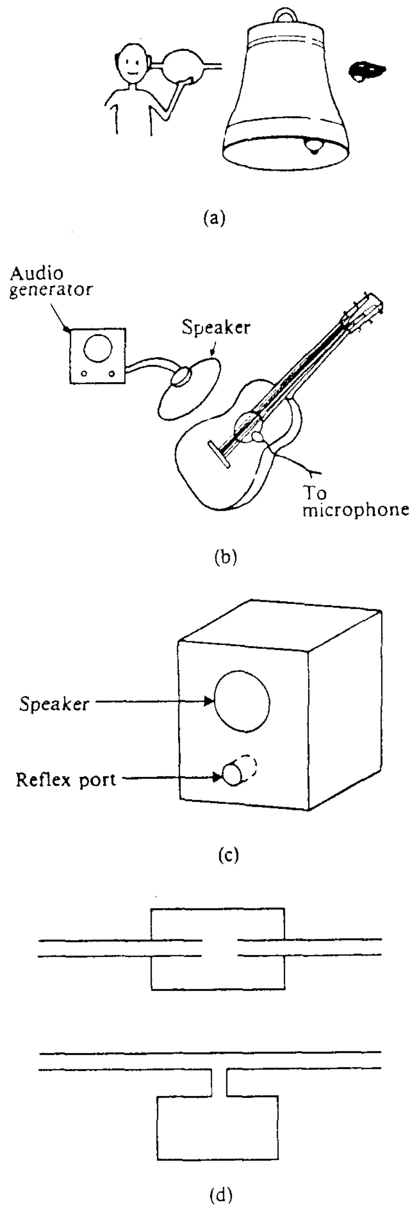

FIG. 4.10
Some examples of Helmholtz resonators: (a) analysis of vibrations of a bell; (b) air resonance of a guitar body; (c) bass reflex loudspeaker cabinet; (d) two types of side-branch mufflers.

Pianos and harpsichords have large soundboards with many resonances of their own closely spaced throughout the playing range. Vibrations are transmitted from the string to the soundboard through the bridge as in the violin or guitar. We will discuss pianos and harpsichords in Chapter 14.

4.9 SUMMARY

Resonance occurs when a force applied to a vibrating system varies with a frequency at or near the natural frequency of the system. Linewidth, Q, and maximum response are ways to describe the sharpness of the resonance, which in turn depends on the amount of damping in the system. The phase difference between the vibrating object and the driving force changes near the frequency resonance.

Normal modes of vibration of strings, pipes, and similar systems may be described as standing waves. Standing waves, which consist of waves propagating back and forth between the boundaries, lead to resonances in vibrating systems. Acoustic impedance, which is the ratio of sound pressure to volume velocity, is a quantity useful in the analysis of acoustical systems. Since sound radiation depends on air displacement, radiation from a vibrating string is greatly enhanced by the sympathetic vibration of a soundboard.

References

Backus, J. (1969). *The Acoustical Foundations of Music.* New York: Norton. (See Chapter 4.)

Benade, A. H. (1976). *Fundamentals of Musical Acoustics.* New York: Oxford. (See Chapter 10.)

French, A. P. (1966). *Vibrations and Waves.* New York: Norton. (See Chapter 4.)

Sears, F. W., and M. W. Zemansky (1980). *College Physics*, 5th ed. Reading, Mass.: Addison-Wesley.

Glossary of Terms

acoustic impedance A measure of the difficulty of generating flow (in a tube, for example); it is the ratio of the sound pressure to the volume velocity due to a sound wave.

amplitude The height of a wave; the maximum displacement of a vibrating system from equilibrium.

damping Energy loss in a system that slows it down or leads to a decrease in amplitude.

electromagnetic force The force that results from the interaction of an alternating electric current with a magnetic field.

fundamental The mode of vibration (or component of sound) with the lowest frequency.

harmonic A mode of vibration (or a component of a sound) whose frequency is a whole-number multiple of the fundamental frequency.

Helmholtz resonator A vibrator consisting of a volume of enclosed air with an open neck or port.

linewidth The width Δf of a resonance curve, usually measured at 71 percent of its maximum height; a measure of the sharpness of a resonance (a sharp resonance is characterized by a small linewidth).

overtone A mode of vibration (or component of a sound) with a frequency greater than the fundamental frequency.

partial A mode of vibration (or component of a sound); includes the fundamental plus the overtones.

phase difference A measure of the relative positions of two vibrating objects at a given time; also the relative positions, in a vibration cycle, of a vibrating object and a driving force.

Q A parameter that denotes the sharpness of a resonance; $Q = f_0/\Delta f$, where f_0 is the resonance frequency and Δf is the linewidth.

resonance When a vibrator is driven by a force that varies at a frequency at or near the natural frequency of the vibrator, a relatively large amplitude results.

soundboard A sheet of wood or other material that radiates a substantial amount of sound when it is driven in sympathetic vibration by a vibrating string or in some other manner.

spectrum A recipe for vibratory motion (or sound) that specifies the relative amplitudes of the partials.

Resonance in Closed-ended Pipes
(written for this work by a retired mechanical engineer)

Considering only pressure changes--that is, compressions, C, and rarefactions, R--in a closed pipe whose length, L, is adjusted to be one-fourth the wavelength of the entering sound (Fig. 1), let us follow successive regions of C and R as they move into the pipe and are reflected from the ends, remembering that change of pressure phase occurs at the open but not at the closed end.

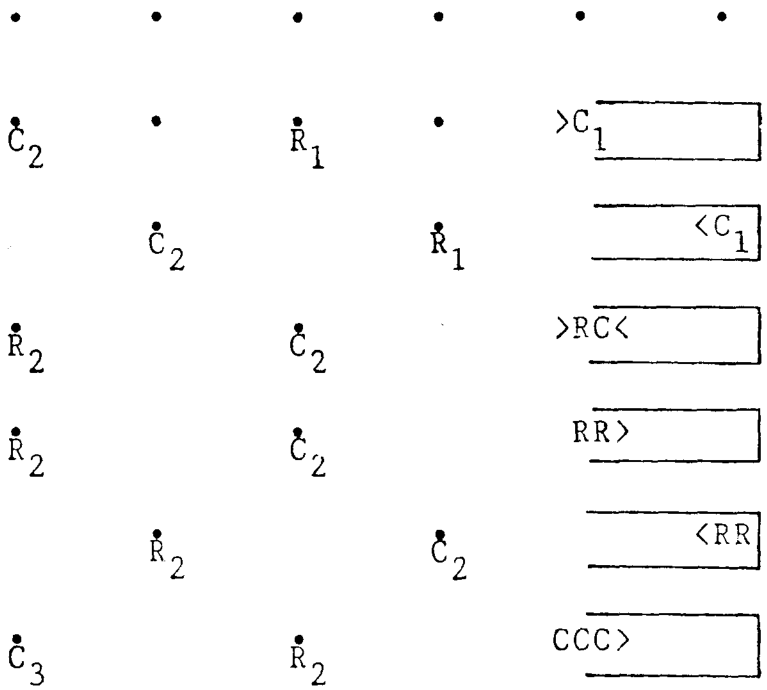

Fig. 1) resonance in 1/4- or 3/4-wave closed-end tubes

The compression wave C_1 enters the pipe, is reflected at the closed end, and reaches the open end just as R_1 is about to enter. As R_1 enters, C_1 is reflected back in the opposite phase as an R, and unites with entering R_1. The now amplified R_1 is reflected at the closed end, and on returning to the open end, is reflected as an amplified C, which is further amplified by uniting with entering C_2.

Thus the pressure disturbance traveling back and forth within the pipe is greatly augmented, and an intensity is built up within the pipe which is very much greater than that in a corresponding length of the incoming wave itself. In this way, a sound of such low intensity as to be inaudible outside the pipe becomes loud and clear on reinforcement be the resonance built up in an air column properly tuned to respond to it.

The same phenomenon occurs likewise if the closed pipe is three-quarters wavelengths of the incoming wave. Compression C_1 then unites with rarefaction R_2, and these again with C_3 and R_4; also, C_3 meets rarefaction R_3 and C_4. Similarly one gets resonance in a closed pipe if the length is any ODD number of quarter-wavelengths (see Fig. 1 again).

Resonance, closed pipe, for $L = 1, 3, 5, 7, \ldots \frac{\lambda}{4}(2n-1)$

or for a given pipe length, response will occur for waves of length

$$\lambda_{1,\ 3,\ 5,\ 7,\ 9,\ldots} = 4L,\ \frac{4L}{3},\ \frac{4L}{5},\ \frac{4L}{7},\ \frac{4L}{9},\ \ldots$$

COMPRESSED AIR AND GAS DATA
INGERSOLL RAND P. 6-49, 50, 51

Resonance in Air Piping

Most air compressors do not use pulsation dampeners on either intake or discharge. Although resonance (systematic vibration of the air column in the pipe as in an organ) is not frequent in these systems, every air compressor has inlet and discharge pipe lengths to be avoided.

Open End Intake Piping

A resonant condition in the open end inlet pipe normally causes supercharging and driver overload, valve breakage, and vibration, often with serious results. Supercharging is the overfilling of the cylinder at the end of the suction stroke, a building up of the pressure in the cylinder at that point to a value considerably higher than atmospheric. Compression starting at this higher value (greater p_1) results in greater horsepower. See formula (3.38), page 3-19.

The predominant resonant inlet pipe lengths can be predicted by the following. Piping should be selected to avoid these lengths.

Within the intake pipe, the air column pulses in accordance with the piston movement at a wave length dependent upon the speed of sound in air and the rpm of the compressor. Strong resonant waves are developed if the total equivalent pipe length is one-quarter or three-quarters of this wave length. These are the total pipe lengths to be avoided by a suitable margin.

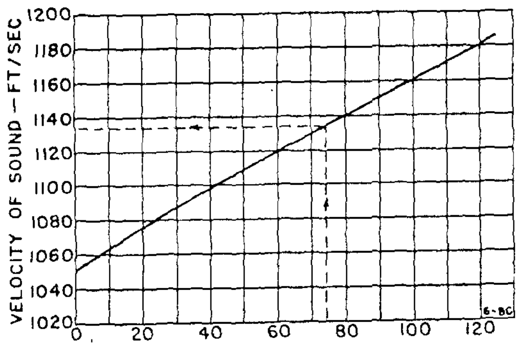

Fig. 6-BC. Velocity of sound in atmospheric air at sea level.

The velocity of sound varies with temperature as in Fig. 6-BC. See formula (5.25) on page 5-15. The value of 1135 ft/sec (75°F) is frequently used as standard although it would be more accurate to figure the lower limits of lengths to be avoided at the lowest expected air temperature and upper limits at the highest temperature. A band either side of the theoretical bad spots is usually avoided.

Total Equivalent Lengths to be Avoided

	Quarter Wave	Three-quarter Wave
Lower limit	0.17 Wave length	0.67 Wave length
Upper limit	0.33 Wave length	0.83 Wave length

The full wave length for a *double-acting* cylinder can be obtained by the following:

$$\lambda = \frac{60a}{2n} \qquad (6.4)$$

or when a is 1135

$$\lambda = \frac{34050}{n} \qquad (6.5)$$

where λ is wave length-ft
a is speed of sound –ft/sec
n is rpm

For a single-acting cylinder (or a double-acting cylinder with one end unloaded), the wave length will be twice as long. It is wise to check resonance for this condition as well as at full load.

This formula is correct only when an intake pipe feeds air to a single cylinder and the pipe is of uniform size throughout.

Equivalent pipe length contained in the cylinder inlet passages and the cylinder end into which the air is flowing must be *subtracted* from the upper and lower limits of length to be avoided. This will give the actual pipe length from the cylinder inlet flange to the end of the inlet pipe. The air filter does not count. All bends must be measured on their centerline.

The equivalent pipe length (L) within the cylinder depends upon the cylinder and passage volume. Formula (6.6) has been empirically developed to estimate this.

$$V = \frac{2.58\,\pi\,D^2S}{4} = 2.03\,d^2S \qquad (6.6)$$

where V is equivalent cylinder and passage volume — cu ft
D is cylinder diameter-ft
S is cylinder stroke-ft

$$L = \frac{\lambda}{360} \times \tan^{-1}\left(\frac{2\,\pi\,V}{A\lambda}\right) \qquad (6.7)$$

where L is equivalent pipe length within cylinder-ft
A is inside area of inlet pipe-sq ft
$\tan^{-1}$ is the angle in degrees whose tanget is the second term.

Discharge Piping

Resonance in the discharge piping can cause driver overload, loss of capacity, objectionable receiver noise, and aftercooler tube damage. Annoying and possible destructive vibration can occur. It is not always simple to predict when this will happen, although a solution can usually be suggested. Supply the manufacturer with a sketch of the piping from compressor to receiver and a complete report.

AIR COMPRESSORS by Eugene Feller
McGraw-Hill 1944, p. 176-178

The piping must be well supported so that it imposes no strain on the compressor cylinder, aftercooler, or receiver. Any shutoff valves installed in the air line should be of gate design to minimize friction loss.

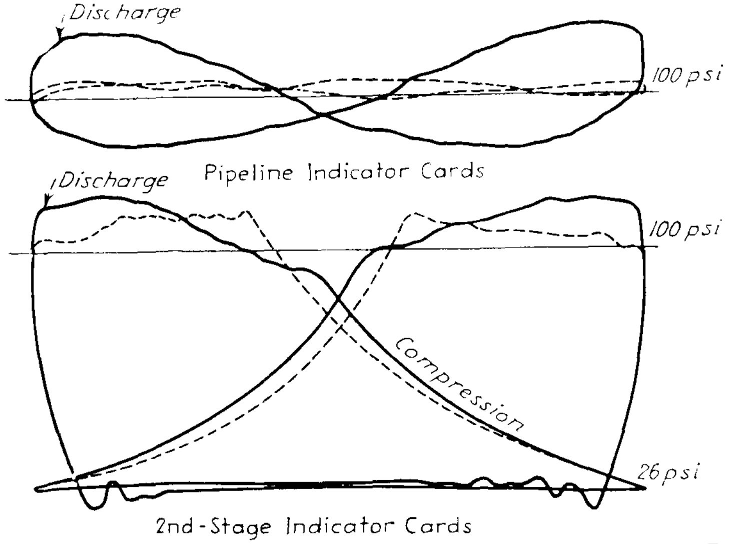

Fig. 178.—Extra power required because of discharge-pipe pulsations. Dotted lines show reduction after installing surge chamber. (*Courtesy of Power.*)

Line losses come from air friction on the inside of pipe and fittings, pulsation of air pressure, and air leakage. Pipe lines that are too small for the air volume handled cause excessive pressure drop and power loss. The size or length of pipe between the compressor and receiver, or between the compressor and a right-angle bend in the discharge, may be such that it will produce surges in resonance with the frequency of the cylinder discharge. When such surges occur, discharge pressure goes higher than normal, with a corresponding power loss. In Fig. 176, curve *A* gives the recommended discharge-pipe sizes for single-stage compressors, and curve *B* for two-stage units.

Indicator diagrams (Fig. 177) show a condition where the line from the compressor to the receiver is so small that it causes an excessive pressure increase each time the compressor discharges. These cards were taken simultaneously on the high-pressure cylinder and on the discharge line, the indicator drive in both cases being connected to the high-pressure crosshead. Normally, this compressor would require 250 hp for continuous operation against 100 psi, but in this case it required 265 hp, which caused the driving motor to overheat. The dotted line shows the cards after a larger pipe was installed.

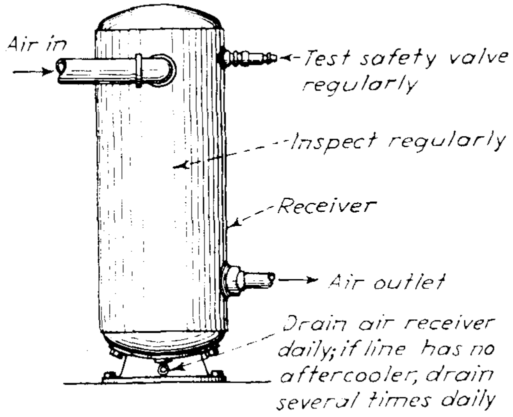
Air in
Test safety valve regularly
Inspect regularly
Receiver
Air outlet
Drain air receiver daily; if line has no aftercooler, drain several times daily

Fig. 179.—Suggested safety measures.

The effects of pipe-line surges are best illustrated by a typical compressor and compressor-discharge pipe-line indicator card (Fig. 178). Pulsations set up in the pipe line were of such frequency that the waves returned to the compressor at the instant of discharge. This caused a build-up in pressure for part of the cycle and increased the work required to deliver air to the line. During the rest of the cycle, pressure fell below normal to give an average of 100 psi, as indicated on a damped gage connected to this line.

The cards show about 30 hp excess load due to pipe-line pulsations, which was corrected by connecting a pipe tee and a short length of pipe, equal to half the cylinder volume, to act as a surge chamber. Pipe-line and compressor indicator diagrams, taken after the change was made, are shown in dotted lines. The lower compression lines were probably caused by the lower temperature of the cylinders as the discharge-air temperature dropped from 240 to 225 F after installing the surge pipe.

Air pulsations may be suspected if the motor is overheating or if power requirements are higher than expected. To determine the existence of these surges, take indicator cards on the line; always take diagrams when a new machine is installed.

Computing Propagation of Sound in Engine Ducts

An updated computer program is easier to use.

Marshall Space Flight Center, Alabama

The Frequency Domain Propagation Model (FREDOM) computer program accounts for acoustic loads applied to components of engines. In particular, the program models the propagation of noise through fluids in ducts between components and through passages within components. It can be used not only to analyze hardware problems, but also for design purposes. FREDOM is an updated version of the FREQPL program, which was first developed in 1959.

These programs were devised specifically for use in analyzing the acoustic loads in rocket engines, where noise generated in pumps, combustion chambers, and duct bends can be so intense as to cause mechanical failures, and where resonances in ducts can amplify the effects of noise. The underlying physical and mathematical concepts implemented in these programs should also be applicable to acoustic propagation in other enclosed spaces; they might be useful, for example, in analyzing process plumbing and ducts in industrial buildings with a view toward reducing noise in work areas.

The older program, FREQPL, is basically a matrix solver with plotting capabilities. Before running FREQPL, the user had to do all the preparatory theoretical and computational work, which included (1) writing the often complicated wave equations, flow equations, and other equations as they apply to the system to be analyzed, (2) putting the equations into matrix•vector form, and (3) entering the matrix elements into the computer by responding to program prompts one element at a time. This preparatory work required an engineer with a high level of sophistication in acoustics and detailed knowledge of the system, consumed much time, and was highly susceptible to theoretical and typing errors. Also, the matrix for FREQPL was set up to solve for a specific variable. Most of the time, results are needed at many locations (different variables) of the system. When using FREQPL, the preparatory work had to be repeated for each new variable.

FREDOM incorporates the matrix solver of FREQPL, but it also automates the preparatory theoretical work, thereby greatly reducing the

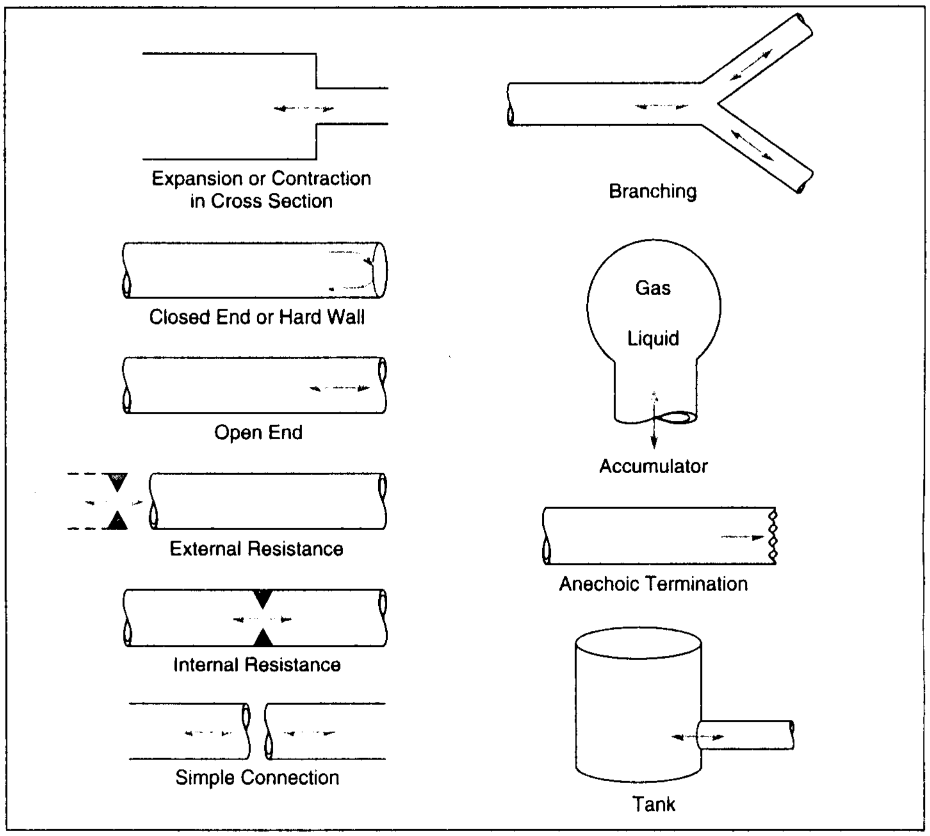

Figure 1. **Various Boundary Conditions** are treated automatically and routinely. FREDOM even provides for small changes in cross-sectional area of a duct due to the distensibility of the duct material.

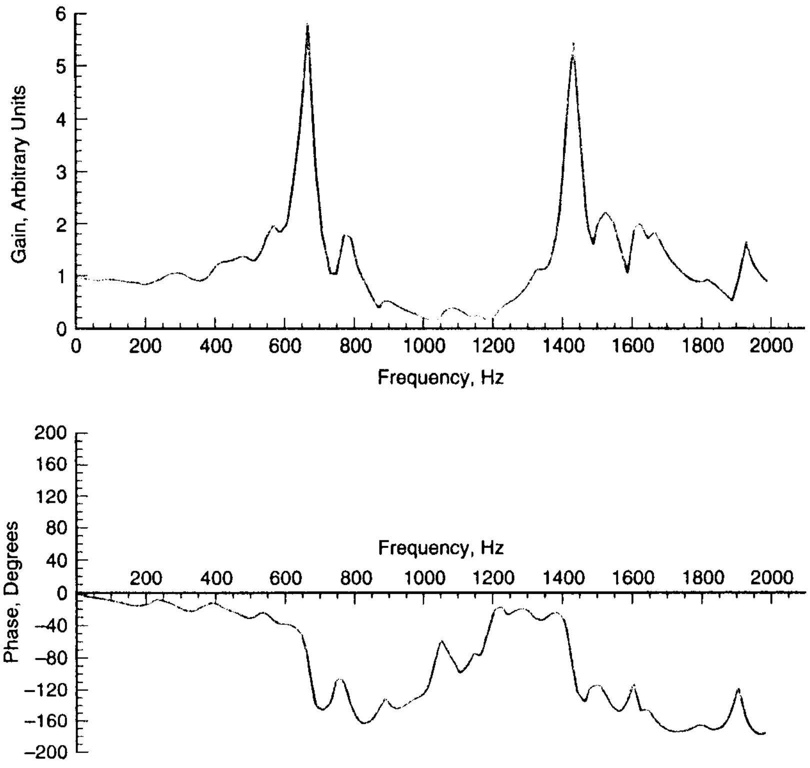

Figure 2. The **Frequency Response** plotted here is a transfer function that represents the acoustic response at one point along a duct to an acoustic excitation at another point along the duct. The peaks in the gain plot indicate the resonances of the duct. Also note a customary phase change in the accompanying phase plot at the resonance peaks.

probability of errors. FREDOM is a user-friendly and menu-driven code. It guides the user step by step through the analysis. The user needs only a good knowledge of acoustics.

The user provides data that describe the duct passage geometry, connections, and properties of the fluid in the system via four input files. FREDOM also accounts for boundary conditions of the system automatically. The user merely states the type(s) of boundary condition(s) and the code incorporates the coefficients of the corresponding equation(s) into the coefficient matrix. Figure 1 shows the variety of boundary conditions handled by FREDOM. For example, if an accumulator is needed, the user need merely specify its location, the type of gas, and initial pressure and volume. For most boundary conditions, it suffices to specify locations only.

FREDOM then constructs the matrix from the data provided by the user — that is, FREDOM automatically does the equivalent of what the user would do in writing the acoustic equations for the system, but does it faster and more accurately. The matrix in FREDOM differs from that in FREQPL: the FREDOM matrix contains the coefficients of the system equations that have been manipulated to put all variables on the left side; that is, the right sides of all the equations are set equal to zero. This matrix, along with the information used to create it, is stored in a "system file". Once the system file is obtained, any of the variables can be set on the right side of the equations for calculation of the applicable frequency response, without having to create a new matrix for each variable. Results can be plotted (see Figure 2) and/or tabulated.

FREDOM works directly in the frequency domain. In this respect, FREDOM offers a great advantage over a time-domain code, the output data of which would have to be postprocessed to convert them into the frequency domain. Postprocessing could add several hours to the overall computational process. In a large iterative analysis (for example, probabilistic analysis of a system), a frequency-domain approach takes several days less than does a time-domain approach.

This work was done by Silvia Saylor of Rockwell International Corp. for **Marshall Space Flight Center**. *For further information,* ***write in 248*** *on the TSP Request Card.*
MFS-29971

How the right switch anatomy can help you avoid an autopsy

Switch failure at the wrong time can have you sorting through the pieces later. That's why Janco makes switches that work every time...even in the most extreme environmental conditions.

Janco rotary switches are designed to resist it all: shock, vibration, thermal variance, moisture, salt, and other contaminates. So if you can't afford the price of failure, contact Janco for more information on our extensive line of miniature, power, push-button, and solenoid operated rotary switches today.

3111 Winona Avenue, Burbank, CA 91504
Phone: (818) 846-1800 • FAX: (818) 842-3396

Janco
AN ESOP CORP.

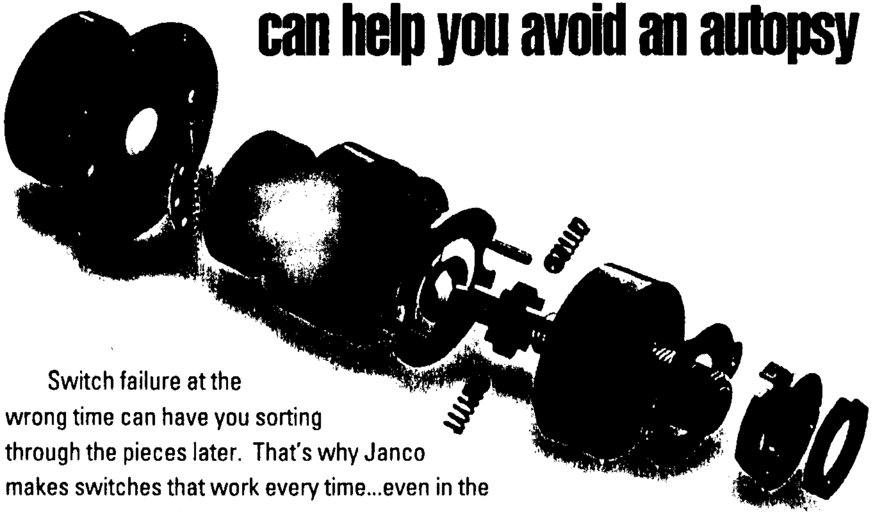

For More Information Write In No. 457

Logistics searching is about to heat up.

New HAYSTACK™ for Windows™ – is the hottest choice for researching government purchases and stocked parts. Work for the U.S. government or a contractor? Support U.S.-made equipment? HAYSTACK for Windows parts research and logistics management systems provide comprehensive data on parts contained in the FSC and related databases. (Product catalogs are available in the IHS™ Vendor service.) Call today and we'll send you a demo diskette. Fire it up to preview new features and functions, better parts selection, savings in time and money, and improved productivity.

Phone: 800-241-7824 Fax: 303-790-0730

Registered to ISO 9001 Certificate No. A8183

HAYSTACK® for Windows™

IHS™ The Information Solution

Available for PCs, online and network configurations.
Windows is a trademark of Microsoft Corporation. Haystack is a trademark of IHS

A537

For More Information Write In No. 433

27. TRANSMISSION THROUGH TUBES

Many important acoustic problems involve the transmission of sound through tubes; for example, speaking tubes, horns for the production and amplification of sound as well as for its reception, stethoscopes, special types of acoustic filters, and apparatus for the measurement of acoustical intensity and impedance.

Effect of Length. If a plane sound wave produced by a diaphragm or other source is led into a cylindrical tube, the wave form will depend in the first place on the length of the tube. If the tube is short, the reflected wave from the end of the tube away from the source will combine with the direct wave to form a more or less complicated pattern; if the tube is very long the reflected wave may be largely damped out and a wave traveling effectively in one direction results.

Change in Cross-section. Consider a wave traveling in one direction and note what happens to it when the size of the tube is altered.* At A, in Fig. 4a, the wave coming from the left encounters an abrupt increase in cross section. In Art. 21 it was noted that reflection ensues so that to the left of A there are waves in both directions. The wave that goes across A is therefore weakened in intensity and indeed by an amount which depends on the ratio of the cross sections (formula 15). The ratio of the total energy flow (watts) in the transmitted wave to the right of the boundary to that in the incident wave may be called the power transmission ratio and will be denoted by P_r. There is no change in phase of the transmitted wave. Incidentally P_r is the same in either direction. The loss in intensity can be very much mitigated by the use of a connector joining the two tubes so as to make the change in dimensions less abrupt; the longer the connector the greater is P_r.

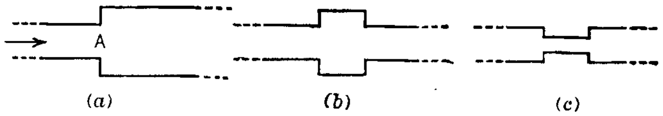

FIG. 4.

In Fig. 4b, again, a plane wave coming from the left meets an expansion of finite length which joins the main line. In Fig. 4c the analogous case of a constriction is illustrated. Calculation and experiment indicate that P_r in both examples is a function of the frequency, being fairly close to unity for low frequencies but becoming very small for a considerable range of high frequencies, then rising and falling again in a series of alternate peaks and hollows, as in Fig. 5. Such a structure is said to be *selective*. Change in phase of the transmitted wave is also involved. This has important application to the pinching of a sound tube in order to control intensity.

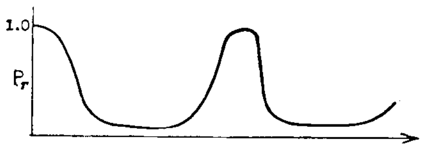

FIG. 5.

Orifices or Side Openings. Another important case of transmission is that through a tube containing one or more orifices in the side. The physical effect of the openings is to cut down the transmission by producing reflection due to the inertia of the air in the orifices; each one is a boundary between the confined air in the tube and the much larger mass of unconfined air outside. Of course there is some actual radiation of sound from the openings, but contrary to what might at first be supposed this is less than the inertia effect. Viscous damping in the openings also plays an insignificant rôle unless they are very narrow. Calculation and experiment indicate that P_r is small for low frequencies and rises as the frequency increases. If more than one hole is used, as their number (they are assumed to be evenly spaced) increases, P_r for low frequency decreases until finally no sound passes through the tube up to a certain frequency: it acts as a high-frequency-pass acoustic filter (see the schematic diagram in Fig. 6a.)†

(a) High-pass Filter (b) Low-pass Filter

FIG. 6.

---

* See bibliography, reference 11.

† See bibliography, references 3, 7, and 11.

Handbook of Eng'g Fundamentals
Ovid W. Eshbach 2nd ed Wiley NY
1952

It is seen that all the transmission problems discussed so far in this section involve acoustic filtration to a certain extent. The same is true of a Helmholtz resonator placed over an orifice in the side of a tube. Here, as might be expected, P_r is reduced materially only in the neighborhood of the resonance frequency of the resonator. If, however, one attaches a whole series of resonators to evenly spaced openings (Fig. 6b), the resulting structure is found to act as a low-pass filter; i.e., P_r is different from zero up to a certain frequency dependent on the dimensions of the various parts; it then falls to zero and stays so for a considerable frequency interval. It then rises again and transmission and attenuation bands succeed each other in a way which can be predicted theoretically. The use of more elaborate side branch attachments permits the construction of filters having transmission bands at any desired frequency and of any desired frequency range.

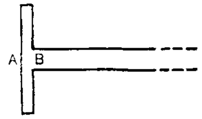

FIG. 7.

The Stethoscope. Another important instrument which is essentially an acoustic filter is one form of the stethoscope (see Fig. 7) consisting of a thin air chamber with a broad base of hard rubber or other solid substance.* Sound is incident on A from the left; some of it passes through the base (which may vibrate as a whole if it is thin, or act as a genuine transmitting medium if it is thick) and then through the air chamber to B where more reflection takes place and a final transmitted wave progresses up the narrow tube. The theory is too complicated for presentation here. An illustration will suffice. Consider the stethoscope immersed in water. Assume that the ratio of the area of cross section at A to that at B = 225 and that the thickness of the chamber is 0.3 mm; then at $\nu = 750$ cycles per sec $P_r = 0.13$. This contrasts with $P_r = 0.0012$ for the ordinary power-transmission ratio going directly from water to air without change in tube cross section. It must be emphasized that this type of stethoscope is highly selective. For medical purposes, small conical horns are now being used extensively (see Art. 28).

28. HORNS

The horn occupies a significant place in the discussion of acoustic transmission.† Strictly speaking, any tube of finite length may be a horn. However, it is usual to restrict the term to tubes of varying cross section.

The Principal Types are shown diagrammatically in Fig. 8, where (a) represents a *conical* horn in which the area of cross section $S = S_0x^2$ (x denoting the coordinate distance along the horn axis from some chosen origin and S_0 the cross-sectional area for unit x); (b) represents an *exponential* horn with $S = S_0e^{mx}$, where m is a parameter governing the flare (this horn has the property that the area S is the geometric mean of the areas at the same distance on either side of S); (c) represents a *parabolic* horn in which $S = S_0x$. There are other types of flaring horns but their properties are very similar to the exponential variety.

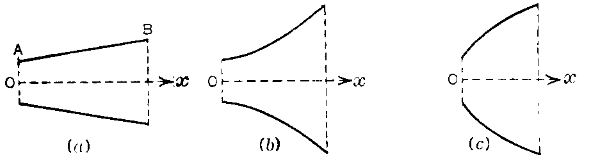

FIG. 8.

The Horn as a Receiver of Sound. If the horn were not there, little difference in the intensity of the sound would be noted at the points A and B. However, with the horn in place, and sound directed toward the large end, there is considerable increase in the intensity at the throat (i.e., the small end) over the intensity at B with no horn present. The ratio of these intensities is the *intensity amplification* (I.A.) of the horn and a measure of the horn's utility as a receiver. The mathematical theory by which this quantity is computed is complicated, and it must be made clear that the qualitative idea of the horn's "concentrating" the sound by reflection from the walls, etc., is quite inadequate except at high frequencies. The action of a horn like that of any air column is mainly dependent on *resonance* characteristics. This is clearly shown in the fact that when I.A. for a conical horn, for example, is plotted as a function of frequency, it shows a number of peaks and hollows, the peaks corresponding to the resonance frequencies of the horn considered as a vibrating air column.

This selectivity is most marked in the conical horn. The parabolic horn gives a much more uniform response and is being widely used in connection with sound-motion pictures.

---

* See bibliography, reference 11.

† See bibliography, references 3, 7, and 11.

ASME 1933
Symposium of Water Hammer
p. 25-27

Simplified Derivation of Water-Hammer Formula

By Lewis F. Moody,[1] Philadelphia, Pa.

As an introduction to the extension of the principles of water hammer to various problems arising in hydraulic practice, it is thought that it may be useful to review and to rederive the basic relations on which this branch of hydraulics rests. Moreover, the author must admit that he has found many of the conventional methods of derivation somewhat difficult to follow and not fully convincing, with their complete acceptance depending mainly on the knowledge that the results have been verified by experience, rather than on the logic of the derivation itself. For example, some authors of well-known textbooks[2] base the proof of the Joukowsky law on the assumption that there is no loss of energy in impact or otherwise in the action which takes place during sudden closure of a conduit outlet. Such a premise is not convincing as it is certainly not axiomatic. The method which will be used here is based on the principle of impulse and reaction, or balance of forces, and rests directly on Newton's second law of motion, thus leading at once to exact relations not dependent on assumptions as to energy losses. It may be useful briefly to review the broader field of varying flow before considering the elastic actions of water hammer specifically.

1. Accelerated or Retarded Flow in Closed Conduits. Consider the case of flow which is uniform along the conduit, that is, constant from point to point, but varying with respect to time. The conditions of steady or unvarying flow are given by writing the Bernoulli formula between sections 1 and 2 for the pipe shown in the sketch, Fig. 1, using the customary notation,

$$h_{p1} + z_1 + \frac{v_1^2}{2g} - h_L = h_{p2} + z_2 + \frac{v_2^2}{2g}$$

This is the condition for equilibrium; that is, the body of water between 1 and 2 is not being accelerated or retarded and no work is being stored in it or withdrawn from its store of inertia. But if h_{p2} is suddenly reduced to h'_{p2} below the value required by the equation, as by partially opening the valve shown, equilibrium is destroyed, and we have an unbalanced force acting on the mass of water tending to accelerate it. This force is

$$P_1 - P_2 = wA\,(h'_{p1} - h_{p1}) - wA\,(h'_{p2} - h_{p2})$$

and is equal to the mass times the acceleration M (dv/dt) or to (wAL/g) (dv/dt), A being the cross-sectional area of the pipe. Hence $(h'_{p1} - h_{p1}) - (h'_{p2} - h_{p2}) = (L/g)\,(dv/dt)$, and substituting the value of $h_{p1} - h_{p2}$ from the first equation, we have

$$h'_{p1} - h'_{p2} = h_{p1} - h_{p2} + \frac{L}{g}\frac{dv}{dt} = \left(z_2 + \frac{v_2^2}{2g}\right) - \left(z_1 + \frac{v_1^2}{2g} - h_L\right) + \frac{L}{g}\frac{dv}{dt}$$

or: $h'_{p1} + z_1 + \frac{v_1^2}{2g} - h_L - \frac{L}{g}\frac{dv}{dt} = h'_{p2} + z_2 + \frac{v_2^2}{2g}$; that is: (pressure head + elevation head + velocity head) at section 1 - lost head - acceleration head = (pressure head + elevation head + velocity head) at section 2. This is the Bernoulli formula generalized to cover varying flow. Evidently, for retarded flow the sign of the acceleration head is reversed. If the conduit is uniform, v_1 and v_2 are identical· if of varying section, a mean value of v must be used in dv/dt, and the formula may be readily extended to cover this more general case. The foregoing relation holds for slowly varying flow, when the "continuity of flow" relation $A_1 v_1 = A_2 v_2$ applies throughout. But if the change of velocity is sudden, as when a valve is quickly closed in a pipe line, the elastic properties of the water and pipe walls affect the conditions and all of the water will not be uniformly retarded. Only the portions of the flow near the valve will immediately feel the effect of the closure; these portions will be compressed and the adjacent walls expanded by the pressure caused by the closure, and the increased pressure will require time to travel along the pipe before the distant portions of the flow feel the effect. Hence some of the elements of the water column will be brought to rest, and other elements will continue at their original velocity until the region of compression has reached them; and we shall have different velocities at different portions of the pipe at the same instant. The region of compression will extend itself progressively upstream at a uniform rate, since the pipe is assumed to be uniform, and this rate is the "velocity of the pressure wave."

2. Sudden Closure--Water Hammer. Consider the long uniform pipe shown in the same figure, flowing full with uniform velocity V. Then imagine the valve at its end to be instantaneously closed. After a time t, the conditions will be as shown in the sketch, Fig. 2. A portion of the column of length x will have had its velocity reduced to zero, the column thus being divided into two regions, one having the original uniform velocity and the other being at rest. Before closure and at the instant of closure the momentum of the entire mass of water is MV. After the closure the entire mass is no longer moving with velocity V, but only a portion of it having a mass m. The increase F in the force on the end of the column caused by the closed gate is equal to the time rate of change of momentum of the column (Newton's second law), or the rate at which momentum is destroyed; that is: F = d (mV) /dt. The rate of change of momentum will be the rate at which the amount of the mass moving with velocity V is reduced, or

---

[1] Professor of Hydraulic Engineering, Princeton University; and Consulting Engineer, Baldwin-Southwark Corporation, I. P. Morris Division. Mem. A.S.M.E.

[2] For example, Mansfield Merriman's "Treatise on Hydraulics," which for many years was a standard work on hydraulics, and to which the author was indebted for his initiation in the subject.

$F = d(mV)/dt = V(dm/dt)$ = product of velocity and rate at which mass is brought to rest

Hence

$$F = (VA\,w/g)(dx/dt)$$

Now dx/dt is the rate at which the pressure wave travels along the pipe, or the velocity of the pressure wave. This is the same as the velocity of sound in the water within the pipe. Call this velocity of propagation of the pressure wave a.

Then $F = aVAW/g = wAy$, y being the rise of pressure head due to the closure. Hence the rise of pressure head due to complete instantaneous closure is $y = aV/g$. This is Joukowsky's law.

Since the pressure wave is traveling up the pipe with uniform velocity, momentum is being destroyed at a uniform rate, and the pressure at the valve remains constant until the wave reaches the open end of the pipe. At any instant all the water between the valve and the wave front will be in a state of uniform compression under a rise in pressure head y and at zero velocity, and all the water from the wave front to the open end will be uncompressed and under its original pressure and moving with constant velocity V. When the wave front reaches the open end, we shall have the pipe completely filled with water at rest, under a uniform pressure head y feet above its initial value, and therefore y feet above the pressure in the reservoir.

The water in the pipe will then expand through the open end, creating a velocity - V, or V in the opposite direction, and relieving the pressure rise. The pressure at the open end thus drops to its normal or original value, and this pressure drop travels backward from the open end to the valve. The time required for the round trip will be 2L/a. When the return wave or wave of unloading has reached the valve, the whole column will be again under normal pressure, but with a velocity - V, discharging water into the reservoir. The original action then begins again, but with reversed sign, since we now have sudden stoppage of flow with velocity - V instead of + V as at first. A wave of rarefaction or of subnormal pressure - y now starts at the valve and makes the round trip, restoring the original velocity + V. At the end of the foregoing cycle everything is again in the same condition as when the valve was initially closed, so that the cycle begins again and repeats itself continuously until the original kinetic energy is dissipated in friction, energy rejected into reservoir, etc. If the valve should be periodically opened and closed in synchronism with the cycle, additional pressure waves could be superposed until the pressure is increased indefinitely. Fig. 3 shows three diagrams of pressures plotted against time for three different points along the length of the pipe line, the closure in this being instantaneous.

If the valve is only partially closed (but instantaneously) so that the velocity in the region near the gate is not completely destroyed but reduced to v, the change in velocity will be V - v instead of V as in the previous case; and the rate of change in momentum will now be $F = (V - v)(dm/dt)$, and the rise in pressure head will be $y = a(V-v)/g$. This pressure rise will as before be maintained at constant value at the valve until the wave front reaches the open end and returns to the valve. If the valve closes only enough to reduce the velocity an infinitesimal amount dv_1, the corresponding pressure rise will be $dy_1 = (a\,dv_1/g)$. If, before the wave front completes the round trip, the valve is closed another similar amount, a second increment of pressure rise dy_2 is superposed on the first. The picture of the situation is indicated in Fig. 4. Here A - A is the wave front due to the first increment of closure, and B - B is the second wave front due to the second increment of closure. Hence, after any gate movement, the total rise in pressure head will be

$$y = \int_{V_1}^{V} \frac{a\,dv}{g} = \frac{a}{g}(V - V_1)$$

This will be true so long as the first pressure wave has not had time to make the circuit and to add (algebraically) a pressure drop to the foregoing values. If therefore the valve is not instantaneously closed, but is partially closed within a time of 2L/a seconds, the total rise of pressure head will be $y = a(V - V_1)/g$, as before; and the amount of total pressure rise is therefore independent of the time or manner of closing so long as the closure takes place within the time 2L/a. If the closure occupies a longer time than 2L/a, the pressure rise will in general be not so great; and its computation becomes more complex. (See, for example, N. R. Gibson, "Pressures in Penstocks," Trans. A.S.C.E., Vol. 83, 1920; R. S. Quick, "Comparisons and Limitations of Various Water-Hammer Theories," Mech. Eng., Mid-May issue, 1927, p. 524.) For non-instantaneous closure in a time less than 2L/a the situation may be visualized by referring to Fig. 5. This sketch indicates the conditions when sufficient time has elapsed after the beginning of valve movement for the initial pressure wave to have traveled upstream as far as A - A. The effect of the completion of the valve closure has traveled as far as B - B. These two wave fronts are traveling upstream at the same rate, the space between them thus remaining of constant length and representing a transition region in which the velocity varies from V at A - A to zero at B - B, and in which the pressure head is increasing from normal at A - A to normal plus y at B - B. All of the water upstream from A - A still has its original velocity V and original pressure, and all the water between the valve and B - B has been brought to rest and is compressed and under the same pressure head, y feet above normal. As the region A - A, B - B moves uniformly upstream, that part of the column having the velocity V is being continuously and uniformly replaced by an equal portion having zero velocity, so that momentum is being extinguished at the same rate as in the case of instantaneous closure, and the pressure rise is the same, as just deduced.

Velocity of the Pressure Wave. In the previous derivation we utilized the equation of forces, or principle of impulse and reaction. We have not yet found the value of a, the velocity of propagation of the pressure wave in the pipe. To find this we shall now apply the equation for volume, or quantity of flow. After the instantaneous closure of the valve, a region of compressed fluid is created in the end of the pipe, extending upstream a distance x at any time t seconds after closure. In this region the water is under excess pressure and the pipe walls are expanded as shown to an exaggerated degree in the sketch (Fig. 6). If A - A is a fixed cross-section of the pipe, which has at the instant considered been just reached by the wave front or boundary of the region of compression, then the volume of water which has passed through the section A - A during the time t, with the constant velocity V, is AVt cubic feet. Since during this time there has been no outlet, this volume must have been accommodated by compression of the water and by the stretching of the pipe walls, so that

$$AVt = A\,x\,\frac{d\,(\text{Volume})}{\text{Volume}} + \frac{x\pi}{4}(d_1^{\,2} - d^2)$$

Here d (Volume)/Volume is the proportional decrease in volume, or the ratio of a small change in volume to the volume of the water; that is, the voluminal "strain" due to compression. Now the "bulk modulus" k of a fluid or solid is the ratio of unit compressive stress or pressure intensity, to the unit strain, or $k = p/[d\ (\mathrm{Vol.})\ /\mathrm{Vol.}]$; so that in the equation d (Vol.)/Vol. may be replaced on p/k, k being the bulk modulus of water.

Also the linear extension of the pipe walls depends on the tensile modulus E of the pipe material, and E = unit stress/unit strain = $S/(d_1 - d)/d$. But for a pipe $2\,e\,S = pd$, so that $E = pd^2/2e(d_1 - d)$ and $d_1 - d = pd^2/2eE$. In the equation, $d_1^2 - d^2$ may be written $(d_1 - d)\ (d_1 + d)$, and since the difference between d_1 and d is small in comparison with d, we can put $d_1 + d = 2d$; hence the last term of the equation becomes

$$x\frac{\pi}{4}(d_1^2 - d^2) = x\frac{\pi}{4}(d_1 - d)\ 2d = x\frac{\pi}{4}\frac{pd^2\ 2d}{2eE} = x\left(\frac{\pi d^2}{4}\right)\frac{pd}{eE} = \frac{xApd}{eE}$$

(putting A for $\pi\ d^2/4$. Our equation now takes the form:

$$AVt = A\ x\frac{p}{k} + \frac{xApd}{e};\quad \text{or}\quad Vt = xp\left(\frac{1}{k} + \frac{d}{eE}\right)$$

Since the elastic moduli k and E are customarily stated in pounds per square inch, and p may be taken in pounds per square inch, the foregoing equation will be dimensionally correct if all of its quantities are expressed in inch units of length. From the last equation we can obtain at once the velocity of the pressure wave

$$a = \frac{x}{t} = \frac{V}{p}\cdot\frac{1}{\left(\frac{1}{k} + \frac{d}{eE}\right)}$$

As just pointed out, V is in inches per second and a is consequently in inches per second, but by dividing both sides by 12, the same expression is correct if both a and V are expressed in feet per second. But, expressing p in terms of pressure head; $p = wy/144$, w being in pounds per cubic foot and y in feet, and from the Joukowsky formula previously derived $p = (w/144)\ (aV/g)$, so that

$$a = \frac{12}{\sqrt{\frac{w}{g}\left(\frac{1}{k} + \frac{d}{eE}\right)}}\quad \text{or}\quad a = \frac{4720}{\sqrt{1 + \frac{kd}{Ee}}}$$

Here a is in feet per second, w is in pounds per cubic feet, g is in feet per second²; e and d may both be in feet or both in inches; and k and E are in pounds per square inch, k usually equals 300,000.

If, finally, we now apply the principle of energy to the problem, and compare the original kinetic energy of the moving water column and the work done in compressing the water and stretching the pipe walls, it may easily be shown that this work is equal to the original energy; so that during the action the kinetic energy of flow is merely transformed into elastic energy of strain, and none is "lost" or converted into heat. This, of course, assumes the pipe to be perfectly elastic, which is very nearly true for stresses less than the elastic limit. It also neglects the friction loss of the flow in the pipe, and neglects the variation of velocity across the pipe. Actually the original kinetic energy is finally dissipated in pipe friction, loss of velocity head due to non-uniformity of velocity over a section, and velocity head rejected into the reservoir; but the dissipation is slow, and the pressure waves may continue for a long period, being gradually damped. This damping affects but little, however, the pressure curve for a single cycle or several cycles, under usual conditions.

Proceedings of the Institution of
Mechanical Engineers, Vol. 202, 1988
No. A4, P. 249-256

On the optimum utilization of water hammer

P H Azoury, DIC, BSc, PhD and **M Baasiri**, BSc, PhD
American University of Beirut, Lebanon

H Najm, BE, MSc
Massachusetts Institute of Technology, Cambridge, Massachusetts, USA

The computerized method of characteristics was used to analyse, for a single pipeline discharging into the atmosphere, the effects of valve-closure schedule and pipe length on optimum water-hammer strength. It was found that the criteria of optimum water-hammer utilization are a non-linear inherent valve schedule in which the bulk of the pressure surge occurs near the beginning or towards the end of valve closure, together with as small a value of dimensionless valve-closure time and as high a value of wide-open valve area as is consistent with cavitation-free operation. Also, a comparison of the results with hydraulic ram test data suggests that optimum drive pipe length may be based solely on optimum water-hammer strength, in the light of the relative effects of pipe friction and dimensionless valve-closure time. In general, optimum pipe length is not highly sensitive to inherent valve-closure schedule, water-hammer strength, pipe size or reservoir head.

NOTATION

a	wave speed
A_p	cross-sectional pipe area
A_v	theoretical valve flow area
C_d	discharge coefficient
D	inside pipe diameter
f	friction coefficient
g	gravitational acceleration
h	static head
h_o	drop in static head across the valve under steady state flow conditions
h_{del}	static delivery head in the hydraulic ram
h_{res}	static reservoir head measured above the valve
H	dimensionless static head $= h/h_{res}$
H_f	dimensionless friction-head loss $= fLu_o^2/2gDh_{res}$
L	pipe length
Q_o	volumetric flowrate under steady state flow conditions
t	time
t_{cl}	time to close the valve
T	dimensionless time $= at/L$
T_{cl}	dimensionless time to close the valve $= at_{cl}/L$
u	flow velocity
u_o	flow velocity under steady state flow conditions
U	dimensionless flow velocity $= u/u_o$
y	exponent
α	pipeline constant $= au_o/gh_{res}$
β	relative valve loss parameter $= H_f/H_o$
τ	dimensionless valve opening $= C_d A_v/(C_d A_v)_o$
ϕ	dimensionless steady-flow valve area or installed valve constant $= (C_d A_v)_o/A_p$

Subscripts

max	maximum
min	minimum
o	steady state flow conditions with the valve wide open ($\tau = 1$)
opt	optimum

1 INTRODUCTION

In any type of unsteady duct flow, the mode and duration of the duct opening and closing processes exert a governing influence on the flow. This is so because pressure waves are generated by the opening and closing operations, and the manner of these is directly related to the resulting wave strengths. In the transient compressible frictionless flow of pressure wave machines (1), for example, it has been found that, with linear opening and closing (where the change in the relevant flow area is a linear function of time), pressure waves are fully utilized if the ratio of the time taken to open or close a duct to the time taken for a sound wave to travel the duct length at the thermodynamic stagnation state of the port gas is of the order of or less than 0.5.

The only engineering application of unsteady incompressible duct flow is that of the hydraulic ram (2–4). This ingenious, two-centuries-old pump that operates without the need of any external source of power has lately been paid renewed attention in the current quest for energy-saving devices. In comparison with the vast technological attention that the device received since the discovery of its underlying principle of operation in 1772, rigorous treatment of the relevant transient flow phenomena is meagre. While applications of unsteady gas flow, such as pressure wave scavenging and supercharging of reciprocating internal combustion engines, have greatly benefited in their analyses from the computerized approach, the only computer simulation of the hydraulic ram known to the authors is a rather simplified model by Chiang and Seireg (5).

Figure 1 illustrates a typical hydraulic ram installation. The essential components consist of a supply reservoir, a 'drive' (or supply) pipe connecting the supply reservoir to the hydraulic ram, the hydraulic ram with its impulse (or 'waste') valve, discharge valve and air chamber to dampen the pressure fluctuations on the discharge side and a discharge pipe connecting the ram to the delivery reservoir. Associated with the air chamber is an air (or snifting) valve through which a small amount of atmospheric air is drawn into the chamber during the low-pressure part of the cycle upon closure of the discharge valve (see below). This quantity of air compensates for that absorbed by the water.

The cycle of ram operation may be divided into the following sequence of events:

1. With the discharge valve fully closed, the impulse valve begins to open under the effect of its own

The MS was received on 9 September 1987 and was accepted for publication on 14 June 1988.

98/88 © IMechE 1988

p 249-256

weight (or spring load) and by virtue of a pressure drop in the valve box generated in the previous cycle. Water starts to escape through the impulse valve.

2. With the impulse valve fully open, the flow through the drive pipe continues to accelerate until the drag force overcomes the weight of the valve.
3. The impulse valve starts closing and thereby generates a 'hammer' (or compression) wave until its fully closed position.
4. The hammer wave is immediately felt by the discharge valve which starts opening, allowing water to flow into the air chamber, through the discharge pipe and into the delivery reservoir.
5. When the momentum in the discharge flow is expended, flow reversal takes place in the discharge pipe until the discharge valve is fully closed. This closure sets up an expansion wave which actuates the air valve and relieves the pressure on the underside of the impulse valve. This valve then starts to open under its own weight, and the cycle recommences.

In contrast with water-hammer *control* that is the common concern of the hydraulics engineer, it is maximum water-hammer *utilization* that should be aimed at in the hydraulic ram. This, however, should be consistent with cavitation-free operation. It is evident from the above description of the hydraulic ram that it is the water hammer generated by the closing of the impulse valve that provides the unit with the main motive power needed for its continuous operation. In this paper, the results of some basic studies regarding optimum water-hammer utilization are reported with particular reference to the hydraulic ram. Specifically, the effect of valve-closure schedule on maximum water-hammer strength is analysed to determine the criteria of optimum water-hammer utilization. In the analysis, use is made of an assumed functional relation that yields a wide variety of inherent valve schedules (6). Also, the effect of pipe length on optimum water-hammer strength is investigated for a definite valve-closure time in an attempt to establish the criterion of optimum length. The effects of pipe size and reservoir head on optimum length are then determined. It is well known that the drive pipe length is an important parameter in hydraulic ram performance. This length has so far been based mostly on empirical grounds. Calvert (7), for example, recommends a length–diameter ratio within the range of 150–1000. According to Krol (2), the American and European experience favours the limits $6 \leqslant L/h_{res} \leqslant 12$, where L is the drive pipe length and h_{res} is the supply reservoir head above the waste valve. Krol (8) developed theoretical expressions for ram performance, based on a single-cycle analysis, in terms of L, but did not verify them experimentally.

2 ANALYSIS

The system considered in the analysis is a single horizontal pipeline connected to a constant-head reservoir at its upstream end and discharging into the atmosphere through a valve at its downstream end (Fig. 2). (This system can be considered essentially as that of a hydraulic ram with the delivery valve fully closed, corresponding to the maximum possible delivery head that the ram can develop for given conditions of supply head, drive pipe and waste valve.) Initially, it is assumed that the valve is wide open, with the flow velocity in the pipe at the steady state value u_o. The steady state volumetric flowrate equation can be written in terms of the drop in static head across the valve (h_o) as follows:

$$Q_o = (C_d A_v)_o (2gh_o)^{1/2} = u_o A_p \quad (1)$$

so that

$$u_o = \phi(2gh_o)^{1/2} \quad (2)$$

where

$$\phi = \frac{(C_d A_v)_o}{A_p} \quad (3)$$

In equation (1), C_d is the valve discharge coefficient, A_v the geometric (theoretical) valve flow area and A_p the pipe cross-sectional area. ϕ, which may be regarded as the installed valve constant, is an important parameter because it not only reflects the valve flow characteristics but also the pipe flow losses (6). Application of the energy relation between ① and ② in Fig. 2 leads to

$$H_o = \frac{h_o}{h_{res}} = \frac{1}{1 + (1 + K_e + fL/D)\phi^2} \quad (4)$$

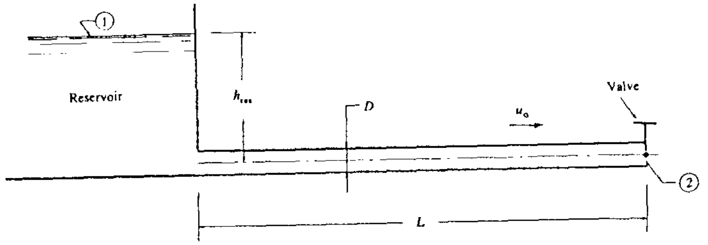

Fig. 2 Single pipeline system used in analysis

where h_{res} is the height of the reservoir water surface above the valve, K_e the pipe entrance loss coefficient, f the pipe friction coefficient, L the pipe length and D the inside pipe diameter. Substituting the expression for h_o from equation (4) into equation (2) then yields

$$\phi = \left\{\frac{1}{(2gh_{res}/u_o^2) - K_e - fL/D - 1}\right\}^{1/2} \quad (5)$$

Thus, ϕ relates to the flow losses in the pipe system.

For the purpose of analysing the effect of valve-closure schedule on optimum water-hammer strength, it is assumed that valve schedule in the closing process is a simple continuous power function of the fraction of the closing time, *viz.*

$$\tau = \left\{1 - \left(\frac{t}{t_{cl}}\right)\right\}^y \quad (6)$$

where τ is the dimensionless valve opening $[= C_d A_v/(C_d A_v)_o]$ and t_{cl} is the time of closure. A large variety of practical valve schedules is provided by this function, depending on the chosen value of y, as shown in Fig. 3. For example, for $y = 0.5$, the valve schedule corresponds approximately to that of a quick-closing valve, which is basically the type of valve used as impulse and discharge valves in hydraulic rams. The valve flow characteristics shown in Fig. 3 are assumed to be under a constant pressure drop, in which case the change in flow depends on the change in area and hence on the shape of the valve plug and seat. When the valve forms part of a pipe system, it no longer operates at constant pressure drop and the *installed* valve schedule then differs from the inherent one. Thus, for a given inherent schedule, there can be different installed schedules. As a measure of the relative importance of pipe friction loss as compared to valve loss, the dimensionless parameter $\beta = H_f/H_o = fL\phi^2/D$ is used, where H_o is defined by equation (4) and the dimensionless friction-head loss $H_f = fLu_o^2/2gDh_{res}$ is the initial steady state head loss in the pipe.

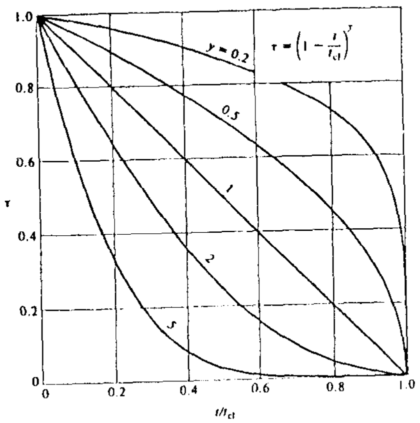

Fig. 3 Inherent valve-closure schedules

The valve-closure time is represented by the dimensionless parameter T_{cl}, defined as the ratio of the time taken to close the valve to the time taken for a sound wave to travel the pipe length, that is $T_{cl} = at_{cl}/L$, where a is the wave speed.

The criterion of water-hammer strength is taken as the maximum dimensionless head H_{max} $(= h_{max}/h_{res})$ attained at the valve end due to closure. Now, it can be shown (9–11) that the compatibility equations for unsteady, one-dimensional frictional flow of an incompressible fluid can be written in finite-difference form as

$$\alpha \frac{\Delta U}{\Delta T} \pm \frac{\Delta H}{\Delta T} + H_f U|U| = 0 \quad (7)$$

where U is the dimensionless flow velocity $(= u/u_o)$ and α $(= au_o/gh_{res})$ may be regarded as the pipeline constant. The optional + and − signs refer to right-running and left-running waves respectively. Thus, H_{max} due to valve closure is a function of the relevant velocity profile at the valve end. In turn, for a given reservoir head and initial flow conditions, this profile depends partly on the associated inherent valve schedule and partly on pipe friction. In the analysis, the value of H was scanned over a sufficiently large interval of time at the valve end to locate H_{max}.

The computerized method of characteristics, based on a first-order finite-difference technique, was used to analyse the transient conditions in the pipe system under consideration. Details of this standard procedure can be found in the literature (9–10). The computer program was implemented on a Data General Eclipse Model S 130 computer.

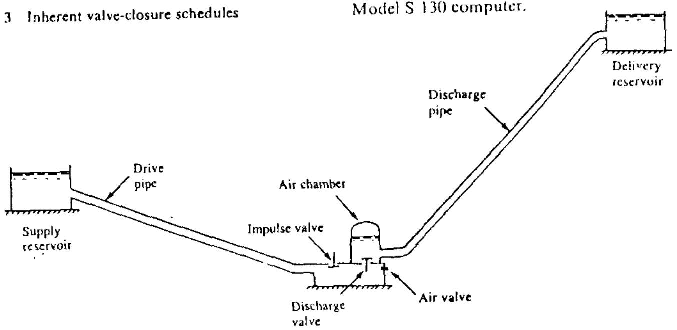

Fig. 1 Diagrammatic layout of hydraulic ram installation

3 RESULTS AND DISCUSSION

3.1 The effect of valve-closure schedule on water-hammer strength

The analysis in the pipeline system was made for the following conditions: $h_{res} = 4$ m, $L = 20$ m, $D = 50.8$ mm, $a = 1324$ m/s, $f = 0.018$ and $K_e = 0.05$. Eight values of ϕ were employed, *viz.* 0.01, 0.02, 0.04, 0.06, 0.08, 0.10, 0.15 and 0.20. These yield the following corresponding values of α and β: $\alpha = 2.988$, 5.970, 11.88, 17.68, 23.32, 28.74, 41.22, 51.94 and $\beta = 0.001$, 0.003, 0.011, 0.026, 0.047, 0.072, 0.159, 0.279. The values of T_{cl} and y were as follows: $T_{cl} = 1$, 3, 5, 7, 10, 15 and $y = 0.5$, 0.7, 1.0, 2.0, 5.0, 10, 20, 30.

Figure 4 shows plots of H_{max} versus y, with curves of constant values of T_{cl}, for the eight sets of conditions employed. Included in the plots are the boundary curves of incipient cavitation at the valve end. Cavitation, which results from the reflected expansion wave at the reservoir end, occurs whenever the head in the pipe reaches a value of $h \cong -10$ m (-32.8 ft), which corresponds to the saturation water vapour pressure under ordinary atmospheric conditions.

The boundary curves were obtained by locating, for a particular value of y, the value of H_{max} that is associated with $H_{min} = -2.5$, H_{min} occurring later than H_{max}. The boundaries of incipient cavitation displayed are not as restrictive as they may appear. In the hydraulic ram, the discharge valve usually starts to open before the waste valve is fully closed. By this means, cavitation effects associated with the reflected expansion wave arriving from the reservoir end tend to be suppressed or cancelled. In general, values of ϕ (> 0.2) in excess of those relevant to water-hammer control can be used in the ram due to this feature. However, there is obviously an upper limit on the value of ϕ at which a hydraulic ram would operate; for a given delivery head, under cavitation-free conditions. Such a limit would imply a maximum practical value of h_{res} for a given drive pipe and ram unit. Also, since high delivery head ratios (h_{del}/h_{res}) would require relatively low discharge valve openings (thus increasing the tendency towards incipient cavitation), and vice versa, it may be expected that the acceptable value of h_{res} would decrease with increasing delivery head ratio. In support of this, one manufacturer's catalogue quotes a maximum value of h_{res} of 20 m and the highest delivery head ratio ($\cong 42$) at $h_{res} = 3$ m. Such limits can be determined analytically only through a computerized study of the complete transient phenomena in the unit, taking the effect of cycling into account.

As regards maximum water-hammer utilization, it is apparent from Fig. 4 that the criteria are a non-linear inherent valve schedule having a value of y appreciably smaller or larger than 1, coupled with as small a value of T_{cl} and as large a value of ϕ as is consistent with cavitation-free operation.

3.2 The effect of pipe length on water-hammer strength

In analysing the effect of pipe length on optimum water-hammer strength, the valve-closure time t_{cl} was held constant, implying a given valve stroke and average travel speed. The existence of an optimum pipe length in the light of the relative effects of friction and valve-

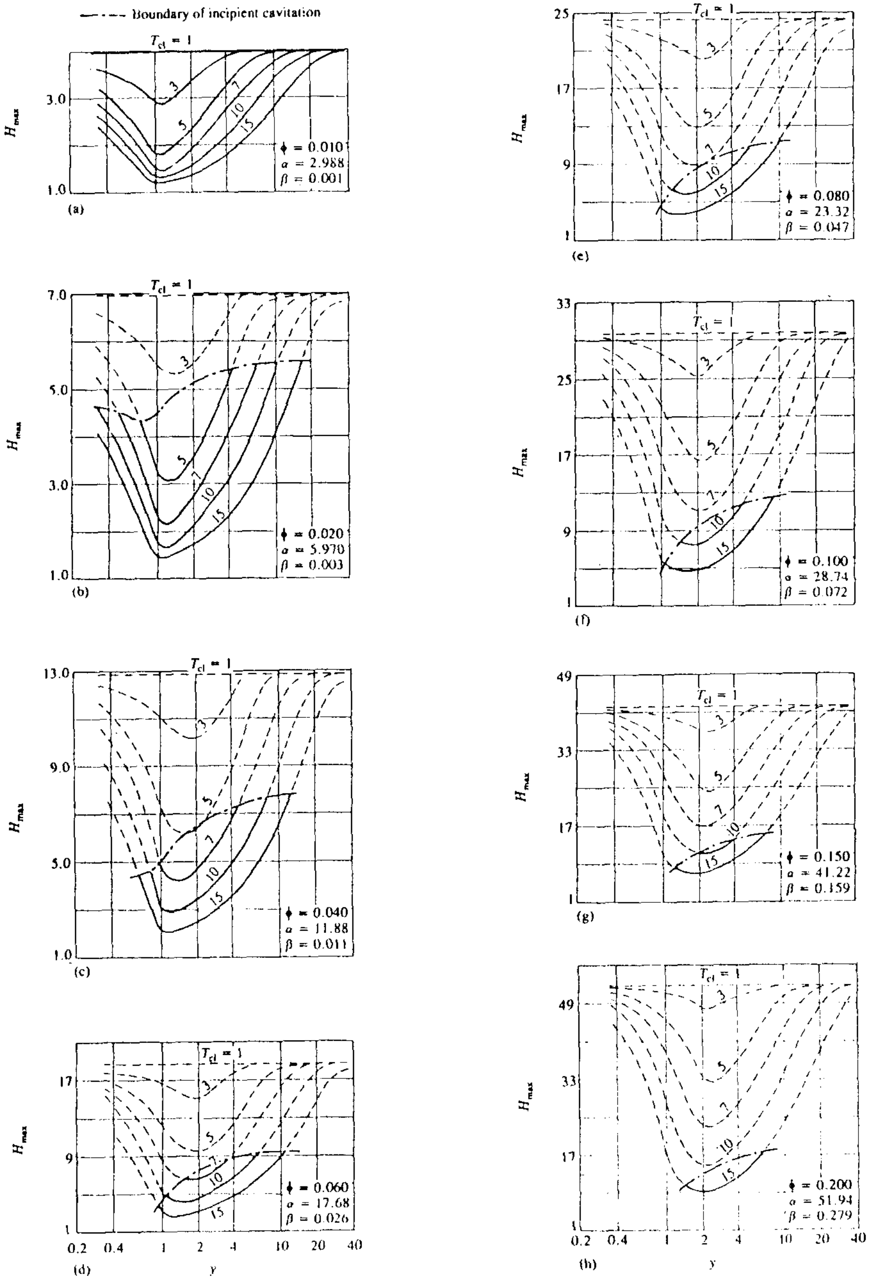

Fig. 4 Water-hammer strength

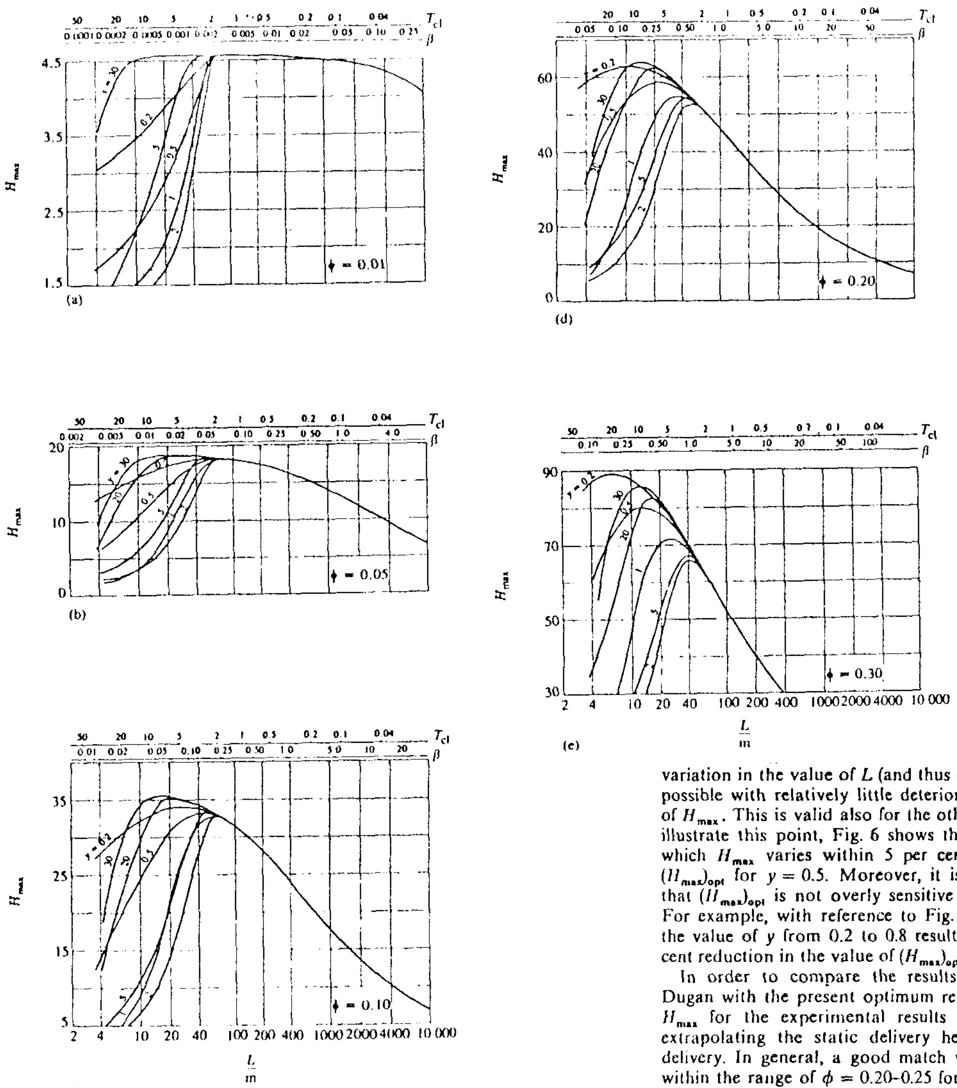

Fig. 5 Optimum pipe length

closure time can then be deduced qualitatively as follows. For a given pipe size, a given value of t_{cl} and a selected valve schedule, increasing the pipe length increases frictional effects (leading to a drop in H_{max}) but decreases the value of T_{cl} (tending to increase H_{max}). Since the reverse also holds, there is obviously a best pipe length (L_{opt}) at which H_{max} optimizes [at $(H_{max})_{opt}$]. This approach is incomplete in the sense that the effects of the discharge valve and related air chamber are not considered, that is the full ram cycle is not taken into account. This is at least partly justified by the fact that the hammer wave is the single most important phenomenon in the hydraulic ram. Further justification is given later when reported test results on an experimental hydraulic ram are compared with the results of this study.

The pipe diameter and reservoir static head used in the optimum length analysis were selected to be the same as those relevant to the 2 inch experimental hydraulic ram employed by Lansford and Dugan (12), *viz.* $D = 52.5$ mm (2.067 in) and $h_{res} = 2.8$ m (9.2 ft). It is assumed that $K_e = 0.5$ and $f = 0.019$, the latter value conforming with the assumption of turbulent friction and commercial steel piping. The valve-closure time t_{cl} was taken as 0.1 s, this being approximately the average measured value reported by Lansford and Dugan. Five values of ϕ were used in the analysis, *viz.* 0.01, 0.05, 0.10, 0.20 and 0.30. Pipe lengths were as follows: 5, 10, 20, 30, 40, 50, 60, 70, 80, 90, 100, 200, 400, 600, 800, 1000, 5000 and 10 000 m. The values of y used were 0.2, 0.5, 1.0, 2.0, 5.0, 20 and 30.

Figure 5 shows plots of H_{max} versus L (as well as β and T_{cl}), with curves of constant values of y. It is seen that, for $\phi = 0.01$, L_{opt} ranges from about 70 m to about 300 m for almost *all* the valve schedules. For $L < L_{opt}$, H_{max} is governed essentially by valve loss, since $\beta \cong 0$, and can be highly sensitive to relatively short pipe lengths. For $L > L_{opt}$, the drop in H_{max} becomes significant only for $\beta \gtrsim 0.25$ when $L \gtrsim 5000$ m. With increasing values of ϕ, the effect of valve schedule on L_{opt} becomes more distinct. Thus, for $\phi = 0.2$ and $y = 0.5$, $L_{opt} = 21$ m. It is significant to note here that, because the valve schedule curve is fairly flat, an appreciable variation in the value of L (and thus of T_{cl}) about L_{opt} is possible with relatively little deterioration in the value of H_{max}. This is valid also for the other values of ϕ. To illustrate this point, Fig. 6 shows the range of L over which H_{max} varies within 5 per cent of the value of $(H_{max})_{opt}$ for $y = 0.5$. Moreover, it is seen from Fig. 5 that $(H_{max})_{opt}$ is not overly sensitive to valve schedule. For example, with reference to Fig. 5d, an increase in the value of y from 0.2 to 0.8 results in only a 10 per cent reduction in the value of $(H_{max})_{opt}$.

In order to compare the results of Lansford and Dugan with the present optimum results, the values of H_{max} for the experimental results were obtained by extrapolating the static delivery head down to zero delivery. In general, a good match was found to exist within the range of $\phi = 0.20$–0.25 for $y = 0.5$, the latter value being typical of quick-opening disc valves. For example, for the test ram, $L = 54.8$ ft (16.7 m), and for $\phi = 0.22$, $H_{max} = 56$, $\beta = 0.28$ and $T_{cl} = 14$. At $\phi = 0.22$ and $y = 0.5$, the analytical results gave $(H_{max})_{opt} = 62$, $L_{opt} = 18.5$ m (60.7 ft), $\beta = 0.32$ and $T_{cl} = 7$. (The apparently large discrepancy in the value of T_{cl} is not serious because, as noted above, this corresponds to a relatively small change in the value of H_{max}. Nevertheless, it should be noted here that difficulty was encountered by Lansford and Dugan in the precise determination of the point on the autographic record where the valve began to move. Their *calculated* value of T_{cl}, using an analytical expression for t_{cl} based on the assumption of constant acceleration of the valve, amounted to 9.4.) Such a satisfactory agreement suggests that, for a given value of t_{cl}, the optimum drive pipe length may be based solely on optimum water-hammer strength in the light of the relative effects of T_{cl} and β.

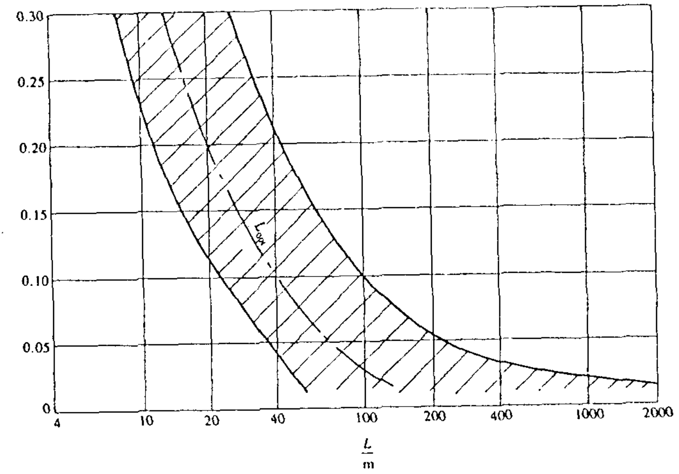

Fig. 6 Range of L over which H_{max} varies within 5 per cent of $(H_{max})_{opt}$ for $y = 0.5$

3.3 The effects of pipe size and reservoir head on optimum pipe length

To investigate the effects of pipe size and reservoir head on optimum pipe length, the following additional values of D (together with the corresponding values of a and f) and h_{res} were used in the analysis: $D = 9.25$ mm, $a = 1375$ m/s, $f = 0.030$; $D = 26.6$ mm, $a = 1356$ m/s, $f = 0.023$; $D = 102.3$ mm, $a = 1302$ m/s, $f = 0.016$; $h_{res} = 1.5$, 5 and 10 m. The values of pipe length, t_{cl}, and y were the same as those quoted in the preceding section, but the values of ϕ were restricted to 0.2 and 0.3 since it is believed that the range of ϕ that is most relevant to the design point values of hydraulic rams lies approximately within these two values. Only the optimum values of L and H_{max} at $y = 0.5$ are reported here, this value of y being considered as typical in practice.

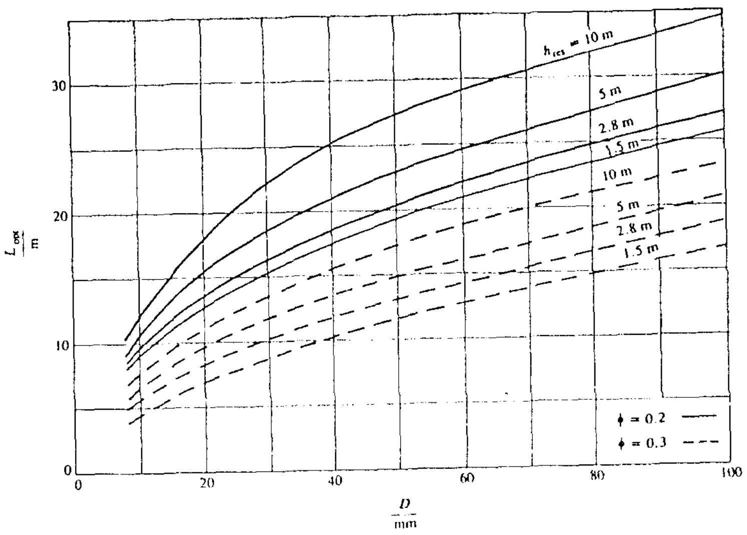

Fig. 7 Effect of pipe size on optimum pipe length for $y = 0.5$

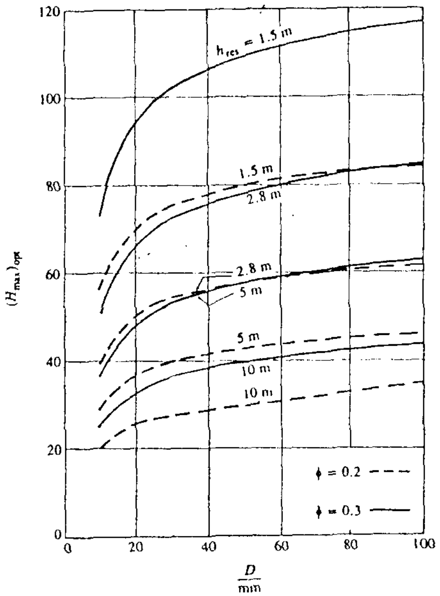

Fig. 8 Effect of pipe size on optimum water-hammer strength for $y = 0.5$

Figure 7 shows a plot of D versus L_{opt} for the various values of h_{res} and ϕ used. Bearing in mind the fact, noted above and illustrated in Fig. 6, that an appreciable variation in pipe length about L_{opt} is possible with relatively little variation in maximum water-hammer strength, it can be concluded from Fig. 7 that, for a given value of ϕ, the effects of D and h_{res} on L_{opt} are inappreciable. However, there is a minimum value of D (D_{min}) below which $(H_{max})_{opt}$ deteriorates rapidly. This is evident from Fig. 8, in which it can [illegible] that $D_{min} \cong 25$ mm (1 in), which is suggested as the minimum practical standard commercial pipe size for hydraulic rams.

4 SUMMARY AND CONCLUSIONS

In this investigation, the computerized method of characteristics was used to analyse, for a single pipeline discharging into the atmosphere, the effects of valve-closure schedule and pipe length on optimum water-hammer strength. For this purpose, the inherent valve-closure schedule was assumed to be a simple continuous power function of the fraction of the closing time. The following conclusions may be drawn:

1. The criteria of maximum water-hammer utilization are a non-linear inherent valve schedule having a value of y appreciably smaller or larger than unity, together with as small a value of T_{cl} and as large a value of ϕ as is consistent with cavitation-free operation.
2. A comparison of the results with hydraulic ram test data suggests that optimum drive pipe length may be based solely on optimum water-hammer strength in the light of the relative effects of T_{cl} and β. In general, optimum length is not highly sensitive to inherent valve schedule, and an appreciable variation in pipe length about this optimum is possible with relatively little variation in water-hammer strength.
3. For a given value of ϕ, the effects of D and h_{res} on L_{opt} are inappreciable. It is suggested that 25 mm (1 in) nominal size be considered as the minimum drive pipe size for efficient water-hammer utilization in hydraulic rams.

ACKNOWLEDGEMENT

The authors wish to thank the American University of Beirut for the provision of financial support to Mr H. Najm and for the use of their computer facilities. They also wish to express their appreciation to Mr M. Rifai for his assistance in the computer work.

REFERENCES

1 **Azoury, P. H.** An introduction to the dynamic pressure exchanger. *Proc. Instn Mech. Engrs*, 1965–6, 180, Part I(18), 451–480.
2 **Krol, J.** The automatic hydraulic ram. *Proc. Instn Mech. Engrs*, 1951, 165, 53–73.
3 **Rennie, L. C.** and **Bunt, E. A.** The automatic hydraulic ram. *S. Afr. Mech. Engr*, 1981, Part I, 31, 258–273; Part II, 31, 286–311.
4 **Starmer, C.** Blake's Hydram or the rise and fall of the hydraulic ram. *Chart. Mech. Engr*, 1981, **28**, 19–21.
5 **Chiang, Y. C.** and **Seireg, A. A.** Hydraulic rams—computer simulation and optimum design. *Computers in Mech. Engng*, 1985, 3(4), 65–68.
6 **Azoury, P. H., Baasiri, M.** and **Najm, H.** Effect of valve-closure schedule on water hammer. *ASCE J. Hydraul. Engng*, 1986, 112(10), 890–903.
7 **Calvert, N. G.** Drive pipe of hydraulic ram. *The Engineer*, 1958, 206(5370), 1001.
8 **Krol, J.** The automatic hydraulic ram: its theory and design. ASME paper 76-DE-17, 1976.
9 **Chaudhry, M. H.** *Applied hydraulic transients*, 1979 (Van Nostrand Reinhold Company, New York).
10 **Watters, G. Z.** *Modern analysis and control of unsteady flow in pipelines*, 1979 (Ann Arbor Science Publishers, Inc., The Butterworth Group, Ann Arbor, Mich.).
11 **Wylie, E. B.** and **Streeter, V. L.** *Fluid transients*, 1978 (McGraw-Hill Book Company, New York).
12 **Lansford, W. M.** and **Dugan, W. G.** An analytical and experimental study of the hydraulic ram. *University of Illinois Bull.*, 1941, 38(326).

Handbook of Hydraulics
Ernest F. Brater, p. 11-12 to 11-24

Water Hammer

Assume a pipe with a valve at its outlet discharging from a reservoir. If the valve is suddenly closed, a dynamic pressure, in addition to the normal static pressure, is created within the pipe. This dynamic pressure is commonly called *water hammer*. It is caused by the sudden transformation of kinetic energy to pressure energy. If P is the pressure due to water hammer and M is the mass of water in the pipe whose velocity is reduced the amount dV in the time interval dt, then

$$P = M\frac{dV}{dt} \tag{11-52}$$

If $dt = 0$, the pressure becomes infinite. Instantaneous change in velocity is not, however, possible. In the following nomenclature, all units are expressed in feet and seconds except as noted:

b = thickness of pipe walls
d = inside diameter of pipe
a = cross-sectional area of pipe, sq ft
e = modulus of elasticity of pipe walls, lb per sq ft
e' = modulus of elasticity of water, lb per sq ft
E = modulus of elasticity of pipe walls, lb per sq in.
E' = modulus of elasticity of water, lb per sq in.
g = acceleration of gravity
ΔH = head due to water hammer (in excess of static head)
H = total head producing discharge through valve
H_0 = original head in pipe
L = length of pipeline
T = time of closing valve
V_0 = mean velocity of water in pipe before closure of valve
v_w = velocity of pressure wave along pipe

Let l_1, l_2, l_3, . . . , l_n represent successive infinitesimally short sections of pipe beginning at the outlet. The instant the valve is closed, the water in section l_1 is brought to rest, its kinetic energy is transformed into pressure energy, the water is somewhat compressed, and the pipe wall with which it is in contact expands slightly. Because of the enlarged cross-sectional area of l_1 and the compressed condition of the water within it, a greater mass of water is contained within this section than before the closure. A small volume of water has flowed into l_1 after the valve was closed. An instant later, a similar procedure takes place in l_2 and then in l_3, causing a wave of increased pressure to travel up the pipe. The instant this wave reaches the reservoir, the entire pipe is expanded and the water within it is compressed. There is now no moving mass of water to maintain this high pressure, and the pipe begins to contract and the water to expand, with a consequent return to normal static pressure. This process starts at the reservoir and travels as a wave to the lower end. During this second period some of the water stored within the pipe flows back into the reservoir, but on account of the inertia of this moving mass, an amount flows back greater than the excess amount stored at the end of the first period, so that the instant this second wave reaches the valve, the pressure at that point drops, not only to the normal static pressure, but also below it.[5] A third period now follows during which a wave of pressure less than normal static pressure passes up the pipe to the[6] reservoir. When it reaches the reservoir the entire pipe is under less than static pressure, but since all the water is again at rest, the pressure in l_n immediately returns to the normal static pressure due to the head of water in the reservoir. This starts a fourth period marked by a wave of normal static pressure moving down the pipe. When the valve is reached, the pressure there is normal, and for an instant the conditions throughout the pipe are similar to what they were when the valve was first closed. The velocity of the water (and the resultant water hammer) is now, however, somewhat less than it was at the time of closure because of friction and the imperfect elasticity of the pipe and the water.

Instantly another cycle begins similar to the one above described, and then another, and so on, each set of waves successively diminishing, until the waves finally die out.

Equation (11-52) shows that, for instantaneous closure of valve, the pressure created would be infinite if the water were incompressible and the pipe inelastic. It is impossible to close a valve instantaneously, but if the valve is completely closed before the first pressure wave has time to return to the valve as a wave of low pressure, or in other words, if T is less than $2L/v_w$, the pressure will continue to increase up to the time of complete closure, and the resulting pressure is just the same as if the valve had been instantaneously closed. If T is greater than $2L/v_w$, the earlier pressure waves return as waves of low pressure and tend to reduce the rise of pressure resulting from the final stages of valve closure.

Hence, if T is equal to or less than $2L/v_w$, h will be the same as for instantaneous closure, but if T is greater than $2L/v_w$, h will be diminished as T increases.

The kinetic energy contained in the moving mns of water within the pipe is

$$\text{KE} = \frac{MV_0^2}{2} = waL\frac{V_0^2}{2g} \tag{11-53}$$

This energy is used in the work of compressing the water and stretching the pipe walls. If the increase in pressure head is ΔH ft, the compression of the water column absorbs $(w\,\Delta H)^2aL/2e'$ ft-lb of energy because the average pressure force of the water is $w\,\Delta Ha/2$ and the distance through which this force moves is $w\,\Delta HL/e'$.

In a similar manner the work done in stretching the pipe walls is $(w\,\Delta H)^2LaD/2eb$. Then, relating the energy of the water to the work done in stopping it,

$$waL\frac{V_0^2}{2g} = \frac{(w\,\Delta H)^2aL}{2e'} + \frac{(w\,\Delta H)^2LaD}{2eb} \tag{11-54}$$

or

$$H = \frac{V_0}{g}\sqrt{\frac{1}{w/g(1/e' + D/eb)}} \tag{11-55}$$

As this pressure wave moves along the pipe with a velocity v_w, the force may be equated to the rate of change in momentum as follows:

$$w\,\Delta Ha = \frac{w}{g}v_waV_0 \tag{11-56}$$

or

$$\Delta H = \frac{v_w}{g}V_0 \tag{11-57}$$

and

$$v_w = \sqrt{\frac{1}{w/g(1/e' + D/eb)}} \tag{11-58}$$

This derivation is approximate in that the stress in the longitudinal direction is neglected. When this is included Eq. (11-57) becomes[1]

$$v_w = \sqrt{\frac{1}{w/g(1/e' + Dc/eb)}} \tag{11-59}$$

where c is related to Poisson's ratio and the manner in which the pipe is held in place. Values of c are somewhat less than unity;[2] however, it is on the safe side to use Eq. (11-57), in which c is assumed to be unity. The analysis presented here is credited to Professor N. Jankovsky of Moscow.[3] The analysis may also be carried out by writing the basic dynamic and continuity equations in a manner similar to the derivation presented for open channels in the first part of this section.[4,5]

---

[1] John Parmakian, "Water Hammer Analysis," Prentice-Hall, Inc., Englewood Cliffs, N.J., 1955.

[2] *Ibid.*

[3] O. Simin, Water Hammer, with Special Reference to Researches of Professor N. Jankovsky, *Proc. Am. Water Works Assoc.*, vol. 24, 1904.

[4] *Ibid.*

[5] George R. Rich, "Hydraulic Transients," McGraw-Hill Book Company, Inc., New York, 1951.

[6] N. R. Gibson, Pressures in Penstocks Caused by the Gradual Closing of Turbine Gates, *Trans. ASCE*, vol. 83, 1919.

Pressure When $T < 2L/v_w$. For this case ΔH may be computed directly from Eq. (11-55) or from Eq. (11-57) after v_w is determined from Eq. (11-58).

If, for example, v_w is 4,680 ft per sec and V_0 is 11.75 ft per sec, closure of a valve in a time $T \lesseqgtr 2L/v_w$ will create an additional pressure head of the gate of

$$\Delta H = \frac{v_w V_0}{g} = 1{,}770 \text{ ft}$$

Pressure When $T \gtreqless 2L/v_w$. For slow gate closure the computations may be carried out in steps by a method suggested by Gibson[6] or by means of a graphical solution. Both methods will be described and illustrated by means of a numerical example. In the step solution Eq. (11-57) is written as follows:

$$\Delta H = \frac{v_w}{g} \Delta V \qquad (11\text{-}60)$$

where ΔH is the increase in pressure head resulting from one step in the valve closure, which reduces the velocity in the pipe by the amount ΔV. It is convenient to write Eq. (11-60) in terms of the initial condition as follows:

$$\frac{\Delta H}{H_0} = \frac{v_w V_0}{g H_0} \frac{\Delta V}{V_0} \qquad (11\text{-}61)$$

Relations between head and pipe velocity for various gate openings must next be developed. It is assumed that this relationship can be expressed as follows:

$$Q = aV = C_d A_g \sqrt{2gH} \qquad (11\text{-}62)$$

where a is the area of the pipe, V is the average velocity in the pipe, $C_d A_g$ is the product of the coefficients of discharge and the area of the gate, and H is the head at the gate. Then, for full gate opening,

$$Q = aV_0 = (C_d A_g)_0 \sqrt{2gH_0} \qquad (11\text{-}63)$$

and, in general,

$$\frac{V}{V_0} = \frac{C_d A_g}{(C_d A_g)_0} \sqrt{\frac{H}{H_0}} \qquad (11\text{-}64)$$

or, for simplicity,

$$\frac{V}{V_0} = \tau \sqrt{\frac{H}{H_0}} \qquad (11\text{-}65)$$

where τ is $C_d A_g/(C_d A_g)_0$. Values of τ vary from 1.0 for a fully open gate to zero when the gate is closed. Solutions of slow closure problems consist of the step-by-step simultaneous solution of Eqs. (11-61) and (11-65), as will be illustrated by the following example.

Example 11-2. Determine the rise in pressure in a penstock leading to a power plant if the turbine gates are closed in 2.1 sec. $H_0 = 165$ ft, $L = 820$ ft, $V_0 = 11.75$ ft per sec, and $v_w = 4{,}680$ ft per sec. The solution of the problem will be carried forward in six time increments of $2.1/6 = 0.35$ sec, arbitrarily chosen equal to the travel time of the pressure wave from the gate to reservoir and back to the gate

$$\frac{2L}{v_w} = 0.35 \text{ sec}$$

A sketch of the penstock is shown in Fig. 11-5. The gate is closed in such a manner that six uniform decrements of area occur during each of the six time intervals. Then τ has the values shown in column 2 of the accompanying table. In solving the problem it helps to visualize that the head at the gate is increasing linearly during the time of uniform closure. Then, at $t = 0.167$ sec, the front of the pressure wave has just reached the reservoir and the pressure in the pipe is as shown by line 1-2 in Fig. 11-5. At $t = 0.35$ sec, the pressure is the sum of the positive pressures indicated by the line 3-4 and the negative pressures indicated by the line 5-6. Thus, at $t = 0.35$ sec, the pressure wave has just returned to the gate G but has zero value at that point. Therefore, at time $t = 0.35$ sec, there is only an increase in pressure at G computed as follows, noting first that $V_1 = V_0 - \Delta V_1$, $H_1 = H_0 + \Delta H_1$, and $\tau = 0.833$, the subscripts indicating values at the end of the first time interval. Equation (11-65) becomes

	(1)	(2)	(3)	(4)	(5)	(6)	(7)	(8)
Time interval	t, sec	τ	$\frac{\Delta V}{V_0}$	$\frac{\Delta H}{H_0}$	$\frac{V}{V_0}$	V, ft per sec	$\frac{H}{H_0}$	H, ft
0	0	1.00	0	0	1	11.75	1	165
1	0.35	0.833	0.033	0.34	0.967	11.35	1.34	221
2	0.70	0.667	0.067	0.69	0.867	10.18	1.69	279
3	1.05	0.500	0.095	0.98	0.705	8.28	1.98	327
4	1.40	0.333	0.117	1.19	0.493	5.79	2.19	362
5	1.75	0.167	0.123	1.29	0.253	2.97	2.29	378
6	2.10	0	0.130	1.32	0	0	2.32	382

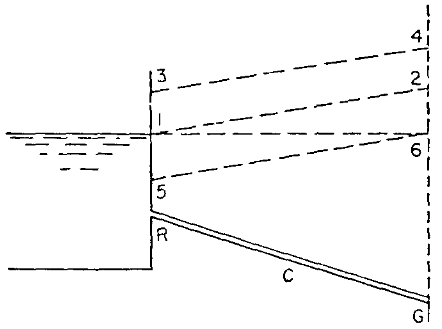

FIG. 11-5. Definition sketch, water hammer.

$$\frac{V_1}{V_0} = 1 - \frac{\Delta V_1}{V_0} = \tau \sqrt{\frac{H_1}{H_0}} = 0.833 \sqrt{1 + \frac{\Delta H_1}{H_0}} \qquad (11\text{-}65a)$$

Also, Eq. (11-61) becomes

$$\frac{\Delta H_1}{H_0} = \frac{v_w V_0}{g H_0} \frac{\Delta V_1}{V_0} = \frac{4{,}680 \times 11.75}{32.2 \times 165} \frac{\Delta V_1}{V_0} = 10.36 \frac{\Delta V_1}{V_0} \qquad (11\text{-}61a)$$

These two equations are then solved by successive approximations. As a first trial assume $\Delta V_1/V_0 = 0.10$. Then, from Eq. (11-61a),

$$\frac{\Delta H_1}{H_0} = 10.36 \times 0.10 = 1.04$$

and Eq. (11-65a) becomes

$$1 - \frac{\Delta V_1}{V_0} = 0.833 \sqrt{1 + \frac{\Delta H_1}{H_0}}$$

$$1 - 0.10 = 0.833 \sqrt{1 + 1.04}$$

$$0.90 \neq 1.19$$

Because this is not an equality, further trials must be carried out. The final solution for this time interval gave values of

$$\Delta V_1/V_0 = 0.033$$

and $\Delta H/H_0 = 0.34$. Then $V_1/V_0 = 0.967$ and

$$V_1 = 0.967 \times 11.75 = 11.35 \text{ ft per sec}$$

Similarly, $H_1/H_0 = 1.34$ and $H_1 = 1.34 \times 165 = 221$ ft. These values are recorded in the table.

During the second time interval the solution of Eq. (11-61a) is carried out as before, except for the subscripts, because this equation deals only with the pressure increment resulting from another reduction in velocity.

$$\frac{\Delta H_2}{H_0} = 10.36 \frac{\Delta V_2}{V_0} \qquad (11\text{-}61a)$$

However, Eq. (11-65a) must be revised because there is superimposed upon the positive pressure wave the negative wave returning from the reservoir. At $T = 0.70$ sec this negative wave will cause a reduction in velocity equal to the increment from the first interval denoted here as ΔV_1 ($\Delta V_1/V_0 = 0.033$) and a reduction in pressure ΔH_0 ($\Delta H_1/H_0 = 0.34$). These values must be included in the discharge relationship at the gate as given by Eq. (11-65*a*) as follows:

$$\frac{V_2}{V_0} = \frac{V_1}{V_0} - \frac{\Delta V_1}{V_0} - \frac{\Delta V_2}{V_0} = \tau\sqrt{\frac{H_2}{H_0}}$$

$$\doteq \tau\sqrt{\frac{H_1}{H_0} - \frac{\Delta H_1}{H_0} + \frac{\Delta H_2}{H_0}} \qquad (11\text{-}65a)$$

Inserting numerical values,

$$0.967 - 0.033 - \frac{\Delta V_2}{V_0} = 0.667\sqrt{1.34 - 0.34 + \frac{\Delta H_2}{H_0}}$$

or

$$0.934 - \frac{\Delta V_2}{V_0} = 0.667\sqrt{1 + \frac{\Delta H_2}{H_0}} \qquad (11\text{-}65a)$$

Solution yields $\Delta V_2/V_0 = 0.067$ and $\Delta H_2/H_0 = 0.693$. Then $V_2/V_0 = 0.867$ and $H_2/H_0 = 1.693$. Corresponding values of V_2 and H_2 are shown in the table. Computations were continued in this manner, and the results are tabulated.

Much less tedious than the step computations described above is a *graphical method*[1] of solving slow-closure problems. The equations upon which this method is based are obtained by solving the differential equations for dynamic equilibrium and continuity.[2] For any two points in a pipeline such as R and G in Fig. 11-5, the following equations can be written:

$$h_{Gt_1} - h_{Rt_2} = \frac{v_w V_0}{gH_0}(v_{Gt_1} - v_{Rt_2}) \qquad (11\text{-}66)$$

$$h_{Rt_2} - h_{Gt_3} = -\frac{v_w V_0}{gH_0}(v_{Rt_2} - v_{Gt_3}) \qquad (11\text{-}67)$$

In these equations $h = H/H_0$ and $v = V/V_0$ and t_1, t_2, and t_3 are successive times separated by uniform time intervals. Furthermore, h_{Gt_1}, v_{Gt_1} and h_{Rt_2}, v_{Rt_2} are coordinates of points on a graph such as that shown in Fig. 11-6, and Eq. (11-66) represents a straight line having a slope v_wV_0/gH_0 connecting these two points. The points are designated in Fig. 11-6 by the subscripts only. A similar line is represented by Eq. (11-67), except that it has a negative slope. These two equations are derived from the dynamic relationship resulting from the water hammer and thus correspond to Eq. (11-61). The discharge relationship at the gate is taken care of in the graphical solution by plotting the parabolas represented by Eqs. (11-64) and (11-65) for various values of τ as shown in Fig. 11-6. The use of these equations in making a graphical solution will be illustrated by applying them to the same problem solved in the previous example by the step method.

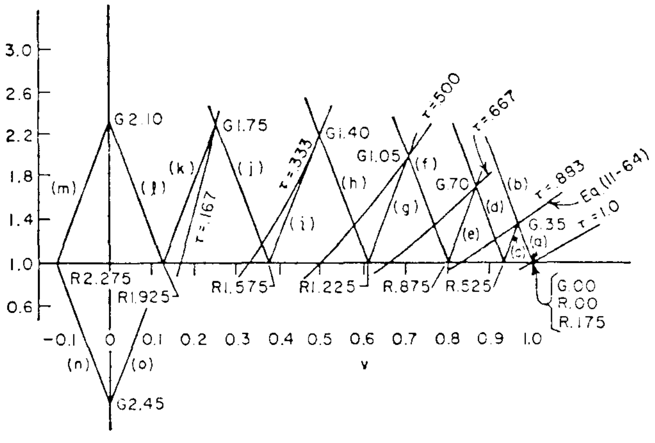

Fig. 11-6. Graphical solution, Example 11-3.

Example 11-3. The graphical solution is conveniently made by writing the equations for time intervals equal to half the round-trip travel time of the wave, or $L/v_w = 0.175$ sec. Then the first four required forms of Eqs. (11-66) and (11-67) are:

$$h_{G.0} - h_{R.175} = 10.36(v_{G.0} - v_{R.175}) \qquad (a)$$

$$h_{R.175} - h_{G.35} = -10.36(v_{R.175} - v_{G.35}) \qquad (b)$$

$$h_{G.35} - h_{R.525} = 10.36(v_{G.35} - v_{R.525}) \qquad (c)$$

$$h_{R.525} - h_{G.667} = -10.36(v_{R.525} - v_{G.667}) \qquad (d)$$

Once the pattern of the equations is envisioned, they can be represented diagrammatically[1] as shown in Fig. 11-7, in which the four equations shown above are represented by lines a to d. It need only be remembered that equations showing a time sequence from G to R have a positive slope, and those proceeding in the opposite direction have a negative slope.

At zero time $V = V_0$ and $H = H_0$; therefore $h_{G.0}$ and $v_{G.0}$ both have the value 1.0 and the point $G.0$ is plotted at that location in Fig. 11-6. Furthermore, at the reservoir, the original conditions exist at time $t = 0$ and $t = 0.175$ sec, so that points $R.0$ and $R.175$ are also plotted at $v = 1$, $h = 1$. Because both ends of the line a, as represented by Eq. (a), occur at the same point, Eq. (a) is also represented by the same point as shown in the figure. The gate-discharge relationship also is satisfied by this point because, with $\tau = 1.0$, Eq. (11-65) passes through $h = 1$, $v = 1$. However, at time $t = 0.35$ sec, the conditions at the gate are represented by Eq. (b) as well as by Eq. (11-65), with τ equal to 0.833. This value of τ may be read from the table shown in Example 11-2. Equation (11-65), with $\tau = 0.833$, and Eq. (b) are plotted, and their intersection locates point $G.35$. Values of $h = H_{.35}/H_0$ and $v = V_{.35}/V_0$ may be read from this point and compared with the tabulated values computed by the step method in Example 11-2.

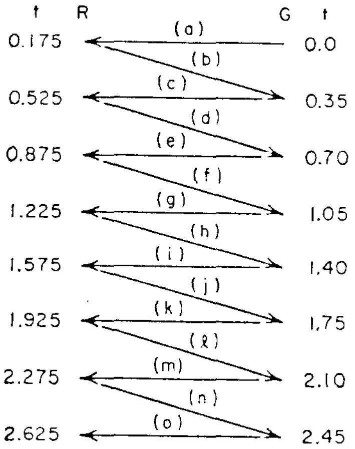

Fig. 11-7. Diagrammatic representation of equations, Example 11-3.

Equation (c) is plotted through $G.35$ with a positive slope, and the location of $R.525$ is found at $h = 1.0$ because the head at the reservoir must remain constant at the original value H_0. Point $G.70$ is then located by extending Eq. (d) with a negative slope from point $R.525$ to its intersection with Eq. (11-65) with $\tau = 0.667$. The solution is then continued in the same manner until the valve is completely closed, after which, because friction has been neglected, the pressure continues to fluctuate from a maximum positive to a maximum negative value as shown by the loop at the left end of the figure. It may be noted that the graphical solution gives results identical with the step solution shown in the previous example.

The graphical solution is much faster than the step solution, which usually involves a considerable number of trials for each step. An additional advantage of the graphical solution is that it can be readily set up to find the pressure at other locations in the pipe. This is illustrated by means of the following example.

Example 11-4. For the same penstock used in Examples 11-2 and 11-3, find the variations in the pressure at mid-length (point c in Fig. 11-5) as well as at the gate during valve closure. In this problem Eqs. (11-66) and (11-67) are written between G and C and also between C and R. The first few equations are given below, and the simpler scheme of representing the equations described in the previous example is shown in Fig.

---

[1] Parmakian, *op. cit.*

[2] R. W. Angus, Simple Graphical Solution for Pressure Rise in Pipes and Pump Discharge Lines, *J. Eng. Inst. Canada*, February, 1935, p. 72.

[1] This scheme is patterned after one shown by Parmakian, *op. cit.*

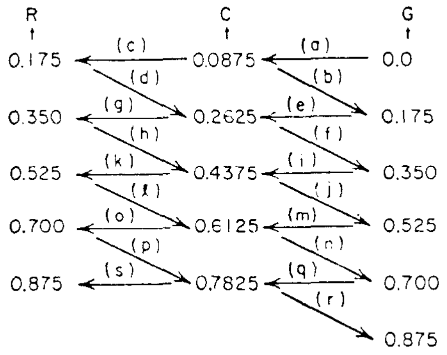

Fig. 11-8. Diagrammatic representation of equations, Example 11-4.

11-8. For this example the equations are written for time intervals of $L/2v_w = 0.0875$ sec.

$$h_{G.0} - h_{C.0875} = 10.36(v_{G.0} - v_{C.0875}) \tag{a}$$

$$h_{C.0875} - h_{G.175} = -10.36(v_{C.0875} - v_{G.175}) \tag{b}$$

$$h_{C.0875} - h_{R.175} = 10.36(v_{C.0875} - v_{R.175}) \tag{c}$$

$$h_{R.175} - h_{C.2625} = -10.36(v_{R.175} - v_{C.2625}) \tag{d}$$

$$h_{G.175} - h_{C.2625} = 10.36(v_{G.175} - v_{C.2625}) \tag{e}$$

$$h_{C.2625} - h_{G.35} = -10.36(v_{C.2625} - v_{G.35}) \tag{f}$$

Several steps in the graphical solution are shown in Fig. 11-9. The reasoning is the same as that of Example 11-3, except that points at the center of the pipe are located by the intersection of two of the straight lines. For example, *C*.4375 is at the intersection of lines *h* and *i*. The location of line *h* is established by its starting point at *R*.35 and its negative slope, and the location of *i* is determined by its starting point at *G*.35 and its positive slope. It may be noted that points such as *G*.35, *G*.70, *R*.525, and *R*.70 have the same coordinates as determined in Example 11-3 and shown in Fig. 11-6.

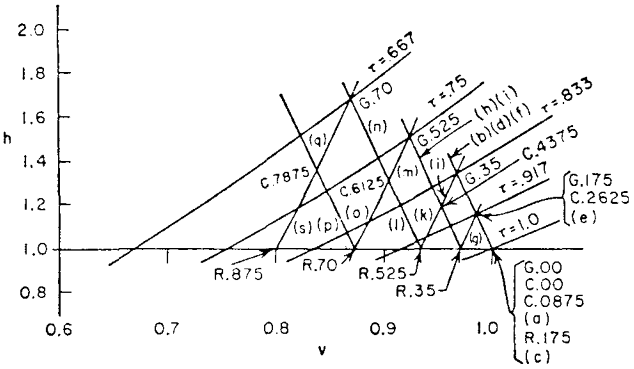

Fig. 11-9. Graphical solution, Example 11-4.

Although the graphical solution is much quicker and easier than the analytical solution previously described, it also becomes cumbersome when very complicated conditions are encountered. Under such conditions water-hammer problems can probably be solved most expeditiously by means of the digital computer.[1,2] A convenient method of applying the computer to water-hammer problems is the method of characteristics.[2,3] The procedure is carried forward in steps in a manner similar to that described in the first portion of this section, in which the method characteristics were applied to flow with a free surface.

---

[1] F. D. Ezekiel and H. M. Paynter, "Computer Representations of Engineering Systems Involving Fluid Transients," *Trans. ASME*, vol. 79, p. 1840, 1957.

[2] V. L. Streeter and Chintu Lai, Water-hammer Analysis Including Fluid Friction, *Proc. ASCE, J. Hydraulics Div.*, May, 1962, p. 79.

[3] C. A. M. Gray, Analysis of Water Hammer by Characteristics, *Trans. ASCE*, vol. 119, p. 1176, 1954.

The Institution of Mechanical Engineers, Proceedings Vol. 165
1951, p. 43-52

Water Hammer in a Pumping Main and its Prevention

By A. M. Binnie, M.A., M.I.Mech.E.*, and D. G. Thackrah, M.A., Ph.D.†

An earlier investigation has been continued on the protection of a rising water main against the consequences of a sudden interruption in the supply. In place of the air bottle previously tried, an automatic air-inlet valve was placed at the lower end of the pipe-line. Experiments on a laboratory scale showed that the cushion of air thus introduced brought the returning water column to rest without sound or shock. Theoretical calculations of maximum pressure and of air drawn in were verified. The lift of the pipe-line being small compared with its length, it was found that, over the range of velocity usually employed, the maximum pressure set up by the returning column diminished as the initial velocity of the interrupted supply was increased.

With no protective device in use, a series of violent impacts took place owing to the column striking and rebounding from the closed valve at the lower end of the pipe-line. An electronic gauge, having a very high natural frequency, was used to measure the magnitude and duration of the shock pressures. Its indications were generally in accord with an analysis based on the usual theory of pressure waves, but the maximum pressures actually recorded somewhat exceeded the theoretical estimates, owing to the existence of additional pressure fluctuations caused by reflections from bends, sockets, and other discontinuities in the pipe-line. The insertion of a spring-loaded relief valve only slightly reduced the shock pressures.

INTRODUCTION

In a long rising main there is a risk that damage may be caused by a sudden stoppage of the pump. The stoppage may be accidental, due to a failure of the electric supply, or it may be designed, as when the pump motor is arranged to be switched directly on and off by means of a float in the suction well or the reservoir. In either case the pressure in the main may be so greatly reduced that collapse may ensue. A more serious danger is that the column in the main may break; the upper portion, after first coming to rest, will then return and fill up the cavity with a heavy and possibly disastrous impact. Six methods of avoiding these troubles are available:—

(1) Automatic air-inlet valves may be fitted at the positions where the column is expected to break. The valves admit air to the main as long as the pressure in the pipe falls below atmospheric, and this air serves as a cushion to break the force of the returning water. This method is of particular value in low-head installations in which the water contains solid matter. It was shown by Binnie (1945)‡ how the positions where the column is most likely to break may be calculated. The column will break at the instant of stoppage if at all.

(2) Non-return valves may be placed in the pipe. The merits of this method were explained by Angus (1945).

(3) An air-vessel may be attached to the main as investigated by Binnie (1945) and by Blair (1945).

(4) Massive flywheels may be added to the pumps in order that the stoppage should be very gradual, but this plan is undesirable if the pump motor is started by direct connexion to the electric supply through simple control gear.

(5) A relief valve may be fitted to the main and designed to lift when the internal pressure becomes excessive.

(6) The pump may be by-passed by a short length of pipe.

All these devices are capable of influencing the surges which result from a shut-down, but only methods (3), (4), (5), and (6) can be effective in reducing the pressure rise due to a sudden start.

The first part of this paper is concerned with method (1); its purpose is to show how an estimate may be made of the volume of air sucked in when the pump stops, the time taken for the column to come to rest, and the maximum pressure developed when the returning column first comes to rest under the influence of the air cushion. Of these quantities the first is required in order that a sufficiently large release valve may be fitted nearby to permit the escape of the air from the main. The second is wanted for comparison with the probable lapse of time before the pump is restarted by means of the float-operated switch, while the third is of value for comparison with the normal pumping pressure. The necessary theory has been derived and compared with the results of experiments with water on a laboratory scale.

The consequences of omitting a protective device are next examined. Under these conditions water hammer of great intensity is set up, in contrast to the relatively gentle surges mentioned in the preceding paragraph. A fairly complete theory of shock waves in pipes has long been known, and numerous experiments have been performed on them, but many of these tests leave much to be desired because the mechanical pressure gauges employed were incapable of following accurately the very high rates of pressure change which occur. As O'Brien and Hickox (1937) remarked, measurements of water hammer when compared with theory are in good agreement, which might even be improved if more reliable instruments were available. The development of electronic apparatus has now made satisfactory observations of this kind possible, and tests were carried out on the same laboratory pipe-line with the aid of a capacity pressure gauge having a natural frequency of over 30,000 cycles per sec.

Finally, with the same apparatus, trials were made of the performance of a relief valve in reducing the shock pressure (method (5)). Both theory and experiment revealed that when exposed to violent pressure rises this device is relatively ineffective.

THE USE OF AN AIR INLET VALVE

Theoretical Calculations. The profile of the main having uniform cross-section A sq. ft. and static lift H feet is shown diagrammatically in Fig. 1. An air inlet valve is fitted at B, where the column is expected to break. After time t seconds from the instant of stoppage, the length x feet of main from B to C is filled with air of volume V cu. ft. at absolute pressure p feet of water. The length L feet of the main from B to the outlet D is taken to be large compared with the maximum value of x. It is not to be expected that the shape of the air bubble will be precisely as indicated in Fig. 1. In a large pipe it will tend to be

---

The MS. of this paper was first received at the Institution on 15th November 1949. For the Minutes of the meeting in London on 12th January 1951, at which this paper was presented, see Proc. I.Mech.E., 1951, vol. 164, p. 103.

* Fellow of Trinity College and University Lecturer in Engineering, Cambridge.

† Mechanical Engineer, I.C.I., Ltd., General Chemicals Division, lately research scholar, Trinity College, Cambridge.

‡ An alphabetical list of references is given in Appendix II, p. 52.

elongated, and it will ascend the main faster than the water if the slope is sufficient. However, in mains of small gradient the upward movement will be slight, while if the main is relatively steeply inclined the water will come to rest quickly before the bubble can travel far. Thus in an approximate calculation it seems sufficiently accurate to assume that the bubble remains close to B throughout the motion, and that x is given by V/A. How long the pump takes to come to rest, and its frictional resistance (when stopping) to the passage of water through it, are matters on which information is usually lacking. It will, therefore, be assumed that the water in the main below B is instantly brought to rest at the moment of stoppage, and remains stationary during the motion of the portion CD, being prevented from falling back by the non-return valve which is almost invariably fitted close to the pump. This assumption will lead to an over-estimate of the volume of air drawn in.

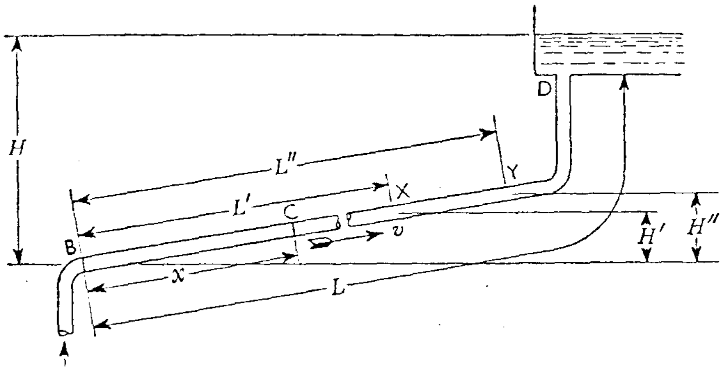

Fig. 1. Profile of Pipe-line

On these suppositions the equation of motion for the broken column is

$$H+P-p+kv^2 = -\frac{Lv}{g}\frac{dv}{dx} \quad . \quad . \quad . \quad . \quad (1)$$

in which g ft. per sec. per sec. is the acceleration due to gravity, v ft. per sec. is the mean velocity of the column, regarded as positive in the direction BD, and P feet of water is the atmospheric pressure, assumed to be the same at B and at the reservoir; for simplicity the friction loss of head in the main is taken to be kv^2 feet of water, where k is a constant.

The calculations can be pushed to a quick conclusion if the valve at B is so large and light that during the process of air admission, p may be regarded as a constant, say p_0, the magnitude of which is controlled by a weight or spring; again this hypothesis will result in an over-estimate of V. Equation (1) is then easily integrated and shows that the total volume V_1 of air drawn in, measured at pressure p_0, is

$$V_1 = Ax_1 = \frac{AL}{2gk}\log_e\left(1+\frac{kv_0^2}{H+P-p_0}\right) \quad . \quad . \quad (2)$$

where v_0 is the initial velocity, and x_1 is the value of x where the column comes to rest. To find the corresponding time t_1 it is necessary to replace vdv/dx in equation (1) by dv/dt. The integration is again simple and yields

$$t_1 = \frac{L}{g}\{k(H+P-p_0)\}^{-\frac{1}{2}}\tan^{-1}\frac{k^{\frac{1}{2}}v_0}{(H+P-p_0)^{\frac{1}{2}}} \quad . \quad (3)$$

After momentarily coming to rest in its extreme position the column falls back under the action of gravity. It will be supposed that the valve at B instantly closes, so that an air bubble of volume V_1, calculated from equation (2), is trapped at pressure p_0 in the neighbourhood of B. This bubble acts as a spring, and the column will oscillate to and fro until brought finally to rest by friction. The maximum air pressure p_2 developed in the course of these oscillations is required, and this will occur when the column reaches its lowest position for the first time. On the assumption that the pressure-volume changes of the air are isothermal, p_2 can be determined by an adaptation of the method employed by Binnie (1943) for calculating the pressure changes in closed surge tanks. Equation (1) holds good, but dv/dt must be substituted for vdv/dx, and the sign of k reversed because the column is moving in the opposite direction. Thus, by means of the equation of continuity

$$Av = \frac{dV}{dt} \quad . \quad . \quad . \quad . \quad . \quad . \quad (4)$$

equation (1) transforms to

$$p = H+P-\frac{k}{A^2}\left(\frac{dV}{dt}\right)^2+\frac{L}{Ag}\frac{d^2V}{dt^2} \quad . \quad . \quad . \quad (5)$$

At the start of the return motion the product of air pressure and volume is p_0V_1, hence the left-hand side of equation (5) is equal to p_0V_1/V. As shown in Appendix I the resulting equation can be treated to yield V_2, the air volume when the column is in its lowest position. The expression for V_2 is

$$Ei(-rV_1)-Ei(-rV_2) = \frac{1}{qr}\{\exp(-rV_2)-\exp(-rV_1)\} \quad (6)$$

where $$r = \frac{2kg}{AL} \text{ and } q = \frac{p_0V_1}{H+P} \quad . \quad . \quad . \quad . \quad (7)$$

This equation for V_2 is readily solved by trial, the calculations being greatly facilitated by the tables of the exponential function $\exp(x)$ and of the exponential integral $Ei(x)$ published by the Federal Works Agency (1939 and 1940). Finally, p_2 is found from the relation $p_2 = p_0V_1/V_2$. If required, the corresponding time can be determined by the method explained in the paper already referred to.

Experimental Apparatus. A diagrammatic elevation of the apparatus used to check the theory is shown in Fig. 2. The uniform pipe-line JL, which had a nominal internal diameter of 2 inches, was provided with water from an elevated tank or, for velocities exceeding 6 ft. per sec., from a centrifugal pump. The supply passed through the orifice plate G and the control valve H to the disk valve J, which could be suddenly shut by means of a lever in order to simulate the abrupt stoppage of a pump. The air bottle K protected the supply pipe at the instant of closure. The length of the pipe-line JL was 164¼ feet. The first 46 feet was straight and almost horizontal; this was followed by a 180 deg. bend, a horizontal length of 85 feet, a 90 deg. bend and a further horizontal length of 21 feet, after which the pipe-line rose vertically to the reservoir M. This tank, which was 37 × 18 inches in plan and 24 inches deep, was fitted with a long overflow weir, so that the level in it remained nearly constant whatever the velocity in the pipe-line might be. The difference in height between the sill of the weir and the centre of the valve J was 11·7 feet. The orifice-plate G was calibrated in position by leading the overflow from the weir to a measuring tank. The sluice valve W was inserted to isolate the reservoir when necessary, and a drain valve was attached to the horizontal part of the pipe-line.

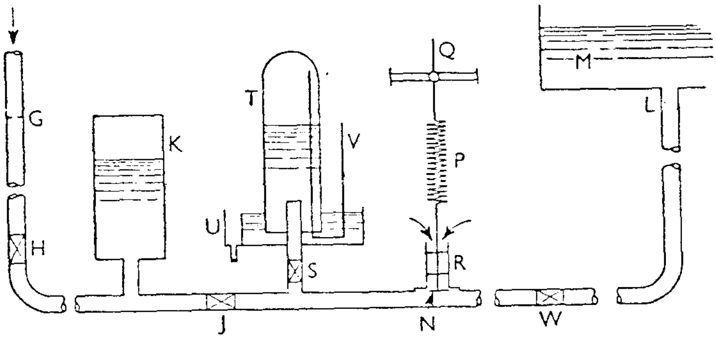

Fig. 2. Arrangement of Air Valve and Air Measurement Apparatus

To admit air when the pressure in the pipe-line fell below a predetermined value, the mushroom valve N, which was 2·5 inches in diameter and weighed only 0·42 lb., was fitted close to J. A stop limited its travel to 1 inch; in this extreme position, the area of the opening was two and a half times the cross-section of the pipe-line. In order that the entry of air through the tube R should be obstructed to the least possible extent, the valve guide consisted merely of two sets of four light horizontal rods attached radially to the valve stem, their outer ends sliding on the inner surface of the tube. The valve was controlled by the light spring P, which was so long that the force it exerted was virtually independent of the valve opening. Two alternative springs were used, having tensions up to 0·8 lb. and 16 lb. respectively, and they could be adjusted by means of the rod Q, supported on a fixed horizontal bar. Thus, the valve was so designed as to conform as closely as possible to the assumptions which were found necessary in the derivation of the theory.

To remove and measure the air admitted to the pipe-line, the valve S was opened and thereupon the water in the reservoir vigorously expelled the air into the graduated glass bell jar T, which was fixed in the shallow water tank U. The process was assisted by a slight fall in the pipe-line from J onwards, which also ensured that no air travelled up the pipe-line to escape at the reservoir. Before an observation was made, most of the air in the jar was sucked out by a water ejector connected to the tube V. The scale was calibrated by inverting the jar and pouring in known volumes of water.

The pressure variations in the pipe-line, being slow, were satisfactorily measured by a calibrated steam-engine indicator (not shown in Fig. 2), which was attached close to the valve J. Its drum was rotated uniformly by an electric motor. From time to time the frictional loss of head was ascertained from readings on an open stand-pipe carried up from the lower end of the pipe-line to a position near the reservoir. To this pipe a mercury-water gauge was connected when the velocity, and hence the accompanying loss, was large.

Experimental Results. A typical indicator diagram is shown in Fig. 3. When the disk valve was closed, the air valve instantly opened and the pressure fell abruptly to the suction value. This part of the diagram was obscured by instrumental vibrations but, being quickly damped out, they were of no importance. Thereafter the suction pressure was sensibly constant, as the theory requires; when the air valve had shut, the pressure performed damped oscillations with the static head as mean.

Experimental and theoretical values of the volumes (at atmospheric pressure) of admitted air are given in Fig. 4 for spring tensions of 0·8, 8, and 16 lb., which correspond to pressures, required to open the valve, of 0·2, 3·5, and 7·3 feet of water. It was found that the latter pressures never differed from the suction pressures by more than 0·7 foot of water, an amount which itself is not far from the limit of accuracy of the diagrams. Equation (2) yields the theoretical volume at the suction pressure, and for the purpose of determining it at atmospheric pressure the passage of air into the pipe-line has been taken as isothermal. The agreement between the observed and calculated volumes is good; even at the highest velocity in the pipe-line the discrepancies are slight.

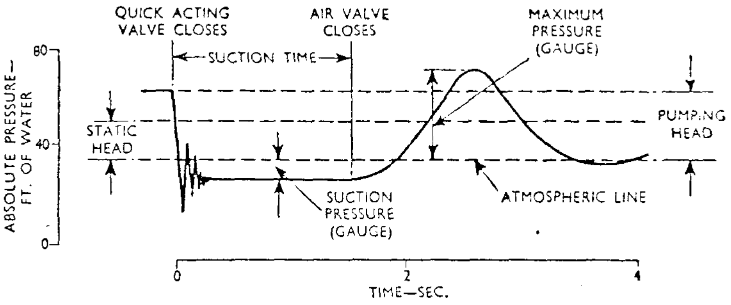

Fig. 3. Typical Indicator Diagram

Air valve loaded to lift at pressure 7·3 feet of water. $v_0 = 6$ ft. per sec.

The maximum pressures developed at the first return of the water column are displayed in Fig. 5, to which the observed pumping head has been added for comparison. Again the results

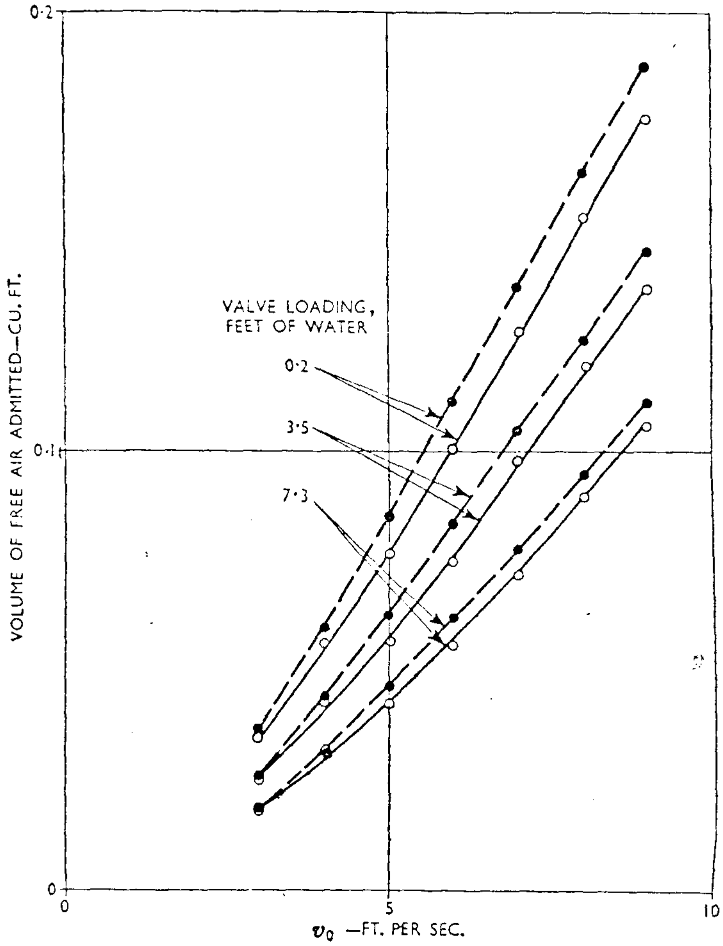

Fig. 4. Volume of Air Admitted

○——○ Observed. ●- - - -● Calculated.

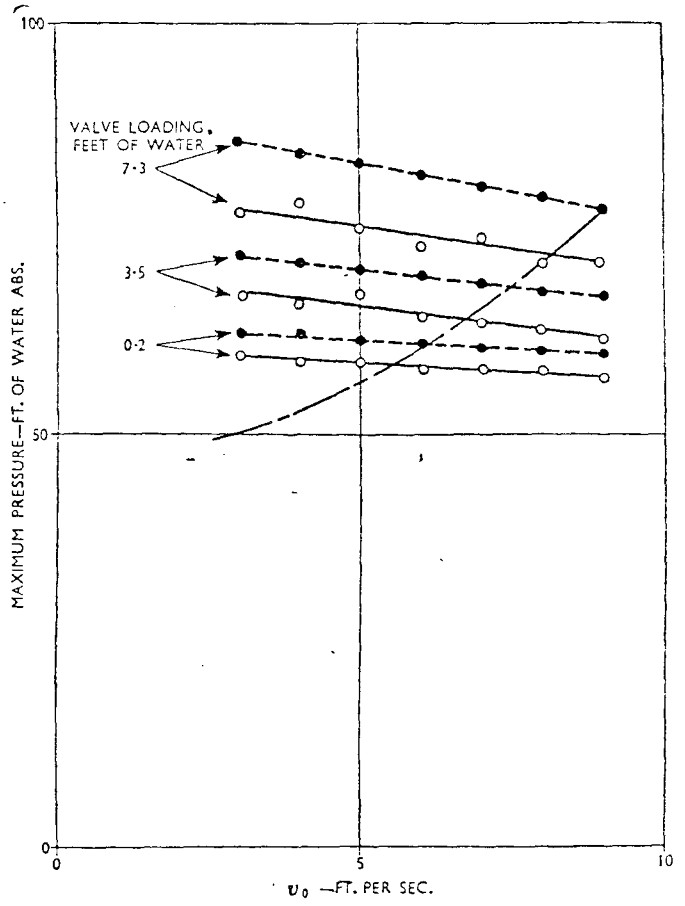

Fig. 5. Maximum Pressure in Pipe-line

○——○ Observed. ●- - - -● Calculated.

— — — Pumping head.

are satisfactory, and the important point emerges, both from experiment and theory, that the rebound pressure decreases as v_0 is raised. If employed on a long pipe-line with a small static lift, the air valve is a device the efficacy of which actually improves when the conditions of working are made more onerous. At high rates of flow the rebound pressure fell below the pumping pressure, and if this pipe-line were always operated at 9 ft. per sec. there would be no point in reducing the spring tension below 16 lb. Indeed, it would be undesirable to do so, for no more air than is necessary should be admitted to the pipe-line because of the difficulty of removing it.

The compression of the admitted air by the returning column being taken to follow the relation $pV^n =$ constant, n was found from the observations of pressure and volume to lie in the range 1·11–1·13; hence the original assumption of isothermal compression was not seriously in error. A few of the measured suction times were compared with those calculated from equation (3); the latter were consistently smaller by amounts varying from 10 to 23 per cent.

The pipe-line was made up of new steam tubing, and the friction loss of head h increased perceptibly as the experiments described in this paper proceeded. After allowance had been made for the bends and fittings, the coefficient λ in the formula $h = \lambda Lv^2/(2gD)$ rose, over the range 5–9 ft. per sec., from 0·021 after 29 days to 0·024 after 911 days.

THE UNPROTECTED PIPE-LINE

After the air valve and the air measuring apparatus had been removed, it was found that, when the disk valve was suddenly closed, a quiet interval of the order of a second ensued, followed by a succession of loud shocks. At the instant of closure a vacuous space was evidently formed near the valve while the water column in the pipe-line continued onwards. The water returned under gravity, refilling the space and striking the valve with great violence; it then rebounded, again leaving a space, and the cycle of events was repeated until the water was brought to rest owing to the loss of its energy by friction and the transfer of vibrations to the surroundings. A detailed account of these effects will now be given.

Theoretical Calculations. Equation (1) defines the motion of the water column up the pipe-line until it comes to rest for the first time. An experiment to be described showed that during this process the absolute pressure p in the cavity near the disk valve possessed a constant value p_0, therefore V_1 and t_1 can be determined from equations (2) and (3). Usually p_0 is so small that it can be neglected in comparison with $(H+P)$. For the return motion, equation (1) holds good when the sign of k is reversed and p is taken to be the same constant p_0; and the velocity v_2, with which the column strikes the valve, is required. The equation analogous to (2) is

$$Ax_1 = -\frac{AL}{2gk}\log_e\left(1-\frac{kv_2{}^2}{H+P-p_0}\right) \quad . \quad . \quad (8)$$

and with the aid of equation (2) the result is

$$v_2 = -v_0\left(1+\frac{kv_0{}^2}{H+P-p_0}\right)^{-\frac{1}{2}}, \quad . \quad . \quad . \quad (9)$$

the first minus sign arising from the convention that v is measured positively in the direction of pumping. The corresponding time is found by integration to be given by the logarithmic expression

$$\frac{L}{2g}\{k(H+P-p_0)\}^{-\frac{1}{2}}\log_e\frac{1+\dfrac{k^{\frac{1}{2}}v_2}{(H+P-p_0)^{\frac{1}{2}}}}{1-\dfrac{k^{\frac{1}{2}}v_2}{(H+P-p_0)^{\frac{1}{2}}}} \quad . \quad . \quad (10)$$

Next the variation in the absolute pressure, say, p' feet of water, must be determined at an intermediate section X (Fig. 1), which is H' feet above B and distant L' feet from it, measured along the pipe-line. If L' is large compared with the length of the cavitation bubble, then, during the first upward movement of the column, the equation of motion of the portion BX is

$$H'+p'-p_0+kv^2 = -\frac{L'v}{g}\frac{dv}{dx} \quad . \quad . \quad (11)$$

But the acceleration is given by equation (1), hence

$$p' = \frac{L'}{L}(H+P)-H'+\left(1-\frac{L'}{L}\right)p_0 \quad . \quad . \quad (12)$$

Thus, p' is independent of t and of k, and for a pipe-line of constant gradient it varies linearly from p_0 at the lower end to P at the upper. In a similar way it can be proved that equation (12) is true also for the return motion.

At the instant when the cavity is filled up and the lower end of the column suddenly brought to rest, a shock wave is produced which travels up the pipe-line, leaving each part in succession at rest and abruptly increasing its pressure by a constant amount, say p_2 feet of water. The wave reaches the open end at the reservoir after a lapse of time L/a seconds, a ft. per sec. being the steady velocity of the wave, and there it is reflected as a wave of tension p_2, relieving each section in turn of pressure and giving it velocity v_2. After a further interval of time L/a the wave arrives at the lower end of the pipe, and at this moment the entire column possesses velocity v_2. At the disk valve, which may be regarded as forming a closed end to the pipe-line, the tension wave is reflected unaltered in sign, and, if $(H+P)$ exceeds p_2, it is able to travel up the pipe-line in this form. But in the present circumstances $(H+P)$ is smaller than p_2, and the water column, being incapable of withstanding tensile stress, bounces clear of the disk, again leaving a cavity behind it. Under the ideal conditions which are assumed in this account, the process may be summarized by stating that the column, after an interval $2L/a$, rebounds with unimpaired velocity. The whole sequence of events described above in this section is then repeated with the reduced velocity v_2.

It is shown in text-books that the relation between p_2 and v_2 is

$$p_2 = -v_2\left(\frac{K'}{g\rho}\right)^{\frac{1}{2}} \quad . \quad . \quad . \quad . \quad . \quad (13)$$

where the apparent bulk modulus K' of the water in the elastic pipe-line is

$$K' = \frac{K}{1+\dfrac{DK}{SE}\dfrac{(5-4\sigma)}{4}} \quad . \quad . \quad . \quad . \quad (14)$$

if the pipe-line is subjected to longitudinal as well as to hoop stress, or is

$$K' = \frac{K}{1+\dfrac{DK}{SE}(1-\sigma^2)} \quad . \quad . \quad . \quad . \quad (15)$$

if longitudinal strain is prevented. Here ρ lb. per cu. ft. and K lb. per sq. ft. denote the density and the true bulk modulus of water, E lb. per sq. ft. and σ Young's modulus and Poisson's ratio for the material of the pipe-line, and D inches and S inches the diameter and wall thickness of the pipe-line. It is also well-known that the velocity of the shock wave is given by

$$a = \left(\frac{K'g}{\rho}\right)^{\frac{1}{2}} \quad . \quad . \quad . \quad . \quad . \quad (16)$$

which, when combined with equation (13), yields

$$p_2 = -\frac{av_2}{g} \quad . \quad . \quad . \quad . \quad . \quad (17)$$

Equation (13) can be obtained from considerations of energy or of momentum, and the tacit supposition is made that no energy is lost within the system, or finds its way out in the form of vibrations. Among possible sources of internal loss are the imperfect elasticity of the water and the pipe-line wall, and also the friction associated with the longitudinal movement, due to compression of each cross-section of the water. In a long pipe-line this last effect can be considerable; for example, the reduction in length of a column of water filling a rigid pipe 100 miles long when stressed to 100 lb. per sq. in. is about 165 feet. We must also expect the wave to suffer partial reflection at any points such as bends, branches, and open valves, where the uniformity of the pipe-line is interrupted.

It is now possible to follow the pressure changes due to the shock wave at the intermediate section X, and it is convenient for purposes of explanation to consider also another section Y (lying between X and the reservoir), the quantities associated with this being distinguished by double dashes. The pressure at X remains at the value given by equation (12) until the wave arrives after a lapse of time L'/a from the moment of impact, and it is then abruptly increased by an amount p_2. After an additional passage of time $(L''-L')/a$ the wave reaches Y. Immediately ahead of it the pressure is still given by equation (12) with L'' and H'' substituted for L' and H', and the pressure difference across the wave remains p_2; between X and Y the column is at rest. These effects do not completely reach X until a further time interval $(L''-L')/a$, and at that instant the pressure p' there is given by their sum

$$\left\{\frac{L''}{L}(H+P)-H''+\left(1-\frac{L''}{L}\right)p_0\right\}+p_2+(H''-H') \quad . \quad (18)$$

When Y is taken to be at the open end of the pipe-line, the expression (18) shows that

$$p' = H+P-H'+p_2 \quad . \quad . \quad . \quad . \quad (19)$$

and at the moment this pressure is attained, the return wave passes X, leaving behind it only the static pressure $(H+P-H')$. The pressure change at X, which occurs between the transits of the upward and downward waves, is linear if the gradient of the pipe-line is uniform. When the wave reaches the valve, it is reflected as a tension wave into a region where the pressure is $(H+P)$, and the column breaks in circumstances akin to the separation of the two parts of the pressure bar used by Hopkinson (1914) in his researches on the pressures caused by the detonation of high explosives and the impact of bullets. In the ideal case in which the wave has a vertical front, the nose of the wave cannot penetrate into the column before fracture occurs. Thus, the sudden reduction in pressure which takes place at the foot of the rebounding column is from $(H+P)$ to p_0, and this is propagated as a tension wave of magnitude $(H+P-p_0)$. The experimental pipe-line was almost horizontal for most of its length, and in this portion the wave will not reduce the pressure below zero, but in the part close to the reservoir, where the pipe-line rose steeply, the column may be expected to disintegrate. At a point near the valve and continuously in contact with the column the pressure changes are relatively simple; they are indicated in Fig. 6.

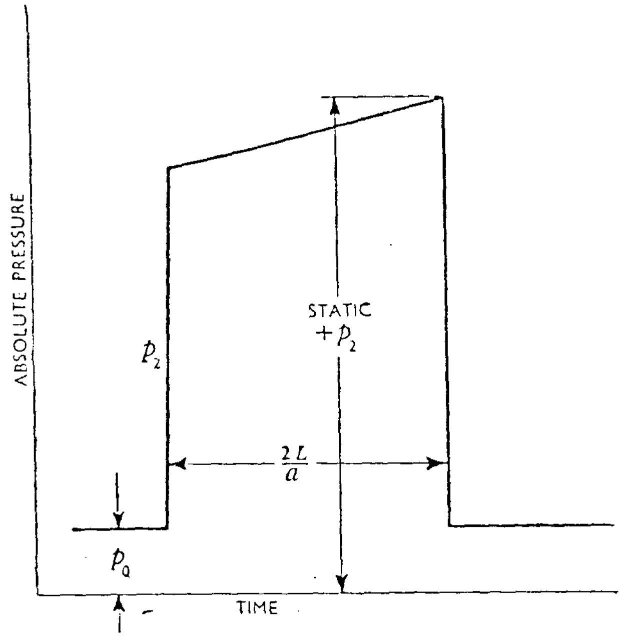

Fig. 6. Theoretical Pressure Changes in the Column Close to the Valve

The final theoretical discussion, which is required, concerns the partial reflection which the shock wave undergoes at a section where the uniformity of the pipe-line is interrupted. Consider a wave of pressure P travelling with velocity a in the pipe-line, the cross-sectional area of which is A, and encountering a length from 1 to 2 (Fig. 7), where the area is A' and the velocity of propagation a'. On the assumption that conditions over each cross-section are uniform, text-book writers, for example O'Brien and Hickox (1937), showed that at 1 the transmitted wave is

$$\frac{2M}{M+1}\mathrm{P} \quad . \quad . \quad . \quad . \quad . \quad . \quad . \quad (20)$$

and the reflected wave is

$$\frac{M-1}{M+1}\mathrm{P} \quad . \quad . \quad . \quad . \quad . \quad . \quad (21)$$

in which

$$M = \frac{A}{A'}\frac{a'}{a} \quad . \quad . \quad . \quad . \quad . \quad . \quad (22)$$

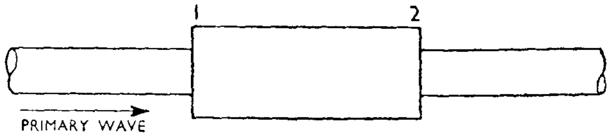

Fig. 7. Change of Cross-section and Rigidity of the Pipe-line

Where the portion 1–2 is a fitting, such as a socket, giving this length greater rigidity than the rest of the pipe-line, M may be expected to exceed unity, and in these circumstances the sign of the reflected wave is the same as that of the transmitted and the original waves. If, for convenience, the transmitted wave is denoted by $(1+\alpha)\mathrm{P}$, it follows from expressions (20) and (21) that the reflected wave is $\alpha\mathrm{P}$. The transmitted wave continues its course until it is partially reflected at 2, where the above equations hold good after M has been replaced by its reciprocal. Thus, the wave which passes onward along the pipe-line is

$$\frac{2/M}{1/M+1}(1+\alpha)\mathrm{P} = (1-\alpha^2)\mathrm{P} \quad . \quad . \quad . \quad . \quad (23)$$

A wave

$$\frac{1/M-1}{1/M+1}(1+\alpha)\mathrm{P} = -\alpha(1+\alpha)\mathrm{P} \quad . \quad . \quad . \quad (24)$$

is reflected back to 1, where the consequences of the discontinuity are that a wave

$$-\frac{2/M}{1/M+1}\alpha(1+\alpha)\mathrm{P} = -\alpha(1-\alpha^2)\mathrm{P} \quad . \quad . \quad (25)$$

returns towards the origin of the original disturbance, and at the same time a wave

$$-\frac{1/M-1}{1/M+1}\alpha(1+\alpha)\mathrm{P} = \alpha^2(1+\alpha)\mathrm{P} \quad . \quad . \quad (26)$$

is reflected towards 2. In the absence of losses the passage of waves to and fro in 1–2 could continue indefinitely, but we see that, if α is so small that its square can be neglected in comparison with unity, the entire process may be epitomized in the statement that a single pressure wave P is transmitted, while two reflected waves $\alpha\mathrm{P}$ return towards the origin, the first being of pressure and the second of tension.

Experimental Apparatus and Results. The pipe-line had been assembled with as few joints as possible, and any that showed weakness were welded up to withstand the high pressures now developed. Near its lower end the pipe-line passed close to two roof stanchions, and it was fixed to these with connexions of great rigidity in order to reduce the escape of energy in the form of vibration. Under the intense water hammer the disk valve at first gave much trouble, and many trials, including its replacement by a heavy plug cock, were required before its performance became reliable. Ultimately the original valve was found satisfactory when its bronze disk had been exchanged for one of stainless steel, which passed water-tightness tests at 650 lb. per sq. in. without distortion.

(*1*) *Tests on the Cavitation Bubble.* The pressure changes which occurred in the pipe-line near the disk valve were relatively small until the first impact occurred, therefore the engine indicator, previously mentioned, was employed in the same manner to measure them. The experiments required care because it was obviously of vital importance that the indicator cock should be shut before the shock pressure developed. However, all these hazardous tests, twenty-one in number, were performed without accident. After the initial instrumental vibrations had died down the cavitation pressure was found to be sensibly constant, and with values of $v_0 = 3, 4, \ldots 9$ ft. per sec. it varied inconsistently from 1·2 to 1·9 feet of water absolute. But these figures are not very accurate for, although the gauge pressure could be estimated to 1 per cent, the equivalent absolute pressure, being very low, was correct only to about 25 per cent. Nevertheless, the mean result, 1·6 feet, may be taken as being substantially true, and this appreciably exceeded the vapour pressure of 0·5 foot of water at the temperature of the tests. The difference must be attributed to the liberation of dissolved air from the water.

(2) *Measurements of Shock Pressure.* To determine the shock pressures developed in the pipe-line, an electronic gauge of the capacity type was employed, its indications being displayed on a cathode-ray tube. The pressure head or "pick-up", which was described by Wolfe, Martin, and Judge (1946), was screwed into a boss welded to the pipe-line near the disk valve; it is shown sectioned in Fig. 8. Essentially the head was a parallel-plate air condenser, the upper plate being rigid and the lower plate consisting of a diaphragm exposed to the pressure in the pipe-line; thus the application of pressure deflected the diaphragm and increased the capacity of the condenser. A mica disk was introduced between the plates, and this, having a high dielectric constant, raised the sensitivity by reducing the virtual air gap and at the same time excluded the danger of the plates touching. The diaphragm A of thickness 0·0546 inch and effective area 0·1901 sq. in. rested on an annular seating, and the space below it was connected to the pipe-line by several small perforations, rather than by one large hole in which resonance might more easily be maintained. They were packed with vaseline which, while allowing transmission of pressure, removed the possibility of water penetrating into the interior of the head. On top of the diaphragm the spacing ring B was inserted, and above this a sub-assembly, consisting of the inner electrode C (or fixed plate of the condenser) to which the mica disk D was stuck, the centralizing ring E, and the three Corundite washers F; all were fixed in position by the retaining sleeve G. The setting of the air gap H was a delicate operation. Before fitting, the sub-assembly and the spacing ring were held together and lapped until their faces were level and truly perpendicular to their common axis. The sub-assembly was further lapped until 0·0015 inch had been removed from the face of the inner electrode, and in the gap thus formed a mica disk 0·00075 inch thick was used. To ensure stability of calibration it was found important that the tightening down should be done evenly with a box spanner and should be absolutely solid so that the diaphragm returned after the application of pressure always to the same position. This process necessarily involved distortion, and to obtain a linear calibration a trial and error procedure was required. The gauge was calibrated in position with the aid of a hydraulic accumulator connected to the pipe-line through the drain. If plotted with capacity vertically and pressure horizontally, the calibration curve at a first trial could be convex upwards, showing that at high pressures the mica was being compressed by the diaphragm and that more metal must be removed from the inner electrode. Alternatively, the curve was convex downwards, indicating too large an air gap, and this could be put right by lapping the spacing ring. Thus, after a few attempts the typical straight calibration shown in Fig. 9 was obtained. It was found necessary to recalibrate at intervals of a week, because the sensitivity slowly increased, probably owing to the components bedding down and reducing the air gap.

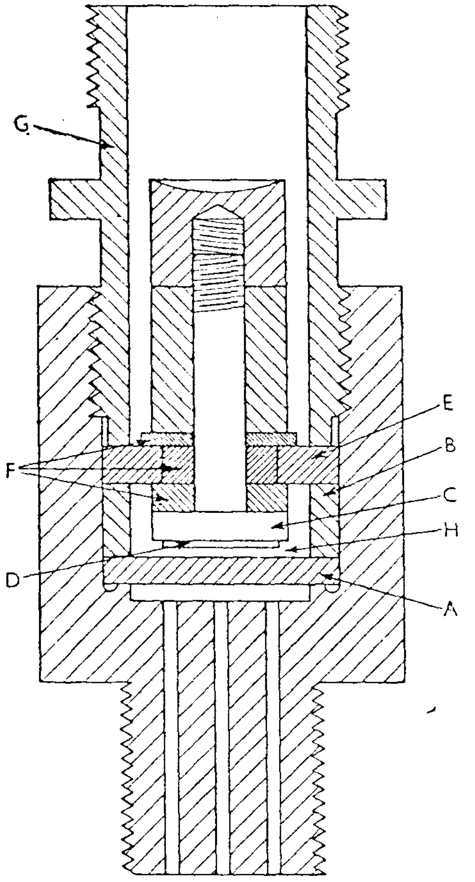

Fig. 8. Pressure Head

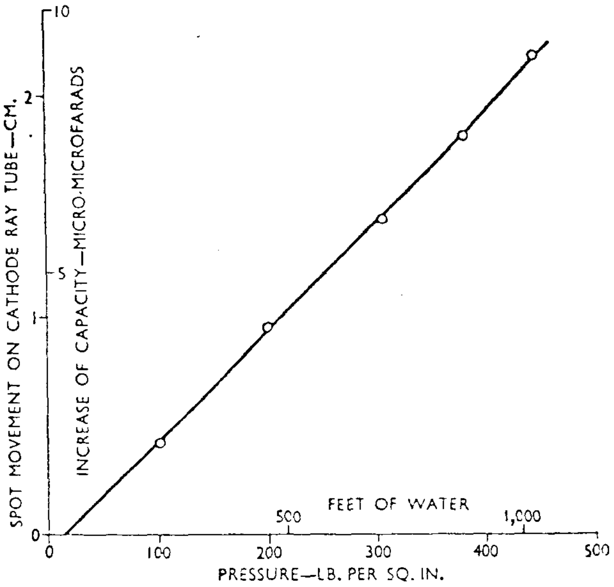

Fig. 9. Typical Pressure Gauge Calibration

With the aid of the analysis due to Lamb (1921) it was estimated that the natural frequency of the diaphragm, if clamped round its periphery, would be 88,000 cycles per sec. in vacuo and 75,000 cycles per sec. when water was present on one side. The nature of the edge fixing is in doubt, but even if the disk were simply supported, the formula given by Prescott (1924) shows that the gravest frequency in vacuo would fall only by one half. It therefore appears probable that the gravest frequency of the diaphragm as used was not below about 37,500 cycles per sec. Now the highest harmonic component of the pressure, which is to be measured, should have a frequency considerably less than that of the diaphragm if a response independent of frequency is to be obtained; Wolfe, Martin, and Judge (1946) and Wolfe (1949) stated that a ratio 0·3 between the two is suitable for design purposes. It appears, therefore, that the pressure head should accurately follow pressures fluctuating at 12,500 cycles per sec.

A block diagram of the electrical apparatus is shown in Fig. 10. It was necessary to change the capacity variations in the pressure head into voltage variations suitable after amplification for display by the cathode-ray tube, and this was achieved by means of an oscillator and detector unit employing A.C. polarization and amplitude modulation. A circuit diagram of the unit appears in Fig. 11 and a list of components in Table 1. The valve V_1, chosen because of its freedom from microphony, was connected as an electron coupled oscillator, its screen grid, control grid, and cathode being joined to a Colpitts oscillator circuit with a frequency of 1 megacycle per sec. The anode, in conjunction with its load R_1 and coupling condenser C_4, formed a buffer amplifier for the oscillator. The output from the buffer amplifier was modulated by a tuned circuit, comprising the inductance L_2 (thirty-six turns of 22 S.W.G. enamelled copper wire on a 1-inch former), the pressure head in series with a padder condenser C_{16}, the capacity of the coaxal cable linking the pressure head to the oscillator and detector unit, and a variable capacity. Coarse variation was achieved by S_1 and the condensers C_5 to C_{14}, fine variation by C_{15}. After modulation the wave was fed to the grid of V_2, selected for its high mutual conductance, 3·6 milliamp per volt; and constancy of bias potential was achieved by connecting the cathode to the potentiometer R_4R_5 across the high-tension supply. The filament required 4 volts, obtained by dropping the general 6·3-volt filament supply through the series resistor R_{10}. The anode of V_2 was supplied from an unearthed 120-volt dry battery, the anode load R_6 being connected between its negative end and earth, and the voltmeter and push-button switch S_2 were used to check the battery and give warning of its failure. The output terminal was joined to a tapping on the battery; thus the output potential, indicated by means of a centre zero micro-ammeter, was backed off so that zero output voltage corresponded to zero pressure on the pressure head. The shunt R_9 served to protect the meter while the unit was warming up, and was disconnected when the output voltage had fallen to a safe amount.

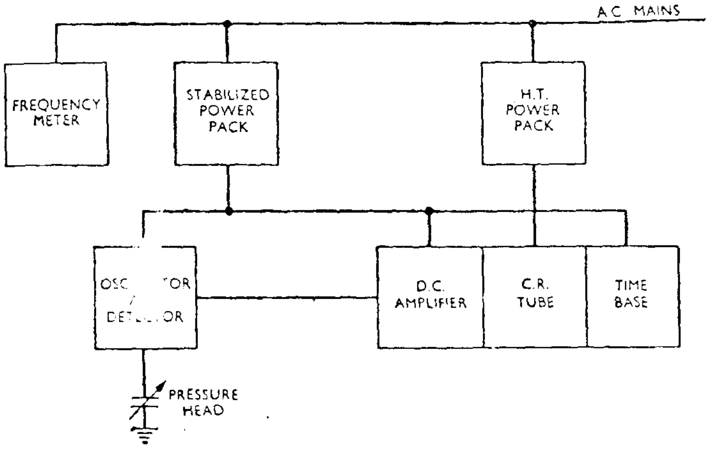

Fig. 10. Block Diagram of Electronic Apparatus

TABLE 1. OSCILLATOR AND DETECTOR UNIT COMPONENTS

R_1	32 kΩ	C_1	0·002 μf
R_2	110 kΩ	C_2	0·002 μf
R_3	43 kΩ	C_3	500 μμf
R_4	13·2 kΩ	C_4	100 μμf
R_5	100 Ω	C_5 to C_{14}	100–950 μμf in stages of 50
R_6	43 kΩ		
R_7	11 kΩ		
R_8	110 kΩ	C_{15}	100 μμf
R_9	10 Ω	C_{16}	0·005 μf
R_{10}	2·5 Ω	C_{17}	0·001 μf
		C_{18}	0·001 μf
L_1	22 μH		
L_2	22 μH	V_1	6SJ7
		V_2	MH4

The D.C. amplifier had a gain of about 120. It included two valves connected in push-pull and matched in order to minimize drift. Nevertheless the drift, as measured over times of the order of minutes, was found to be considerable. It was of no importance during the experiments on shock pressure which were necessarily brief, and care was taken to apply each calibration pressure only for a short time and to obtain the zero immediately before and after this operation, which was carried out as quickly as possible. During visual examination of the trace on the cathode-ray tube the time base was used, triggered by the lever of the disk valve. For the production of records the X plates of the tube were tied by a switch to the earthy focusing electrodes so that the spot could move in the Y direction only, and the screen was photographed with a moving film camera. In this work the afterglow, which was useful for visual observation, proved somewhat disadvantageous since it led to the production of "shadows" on the photographs. Measurements were confined to the central 2 inches

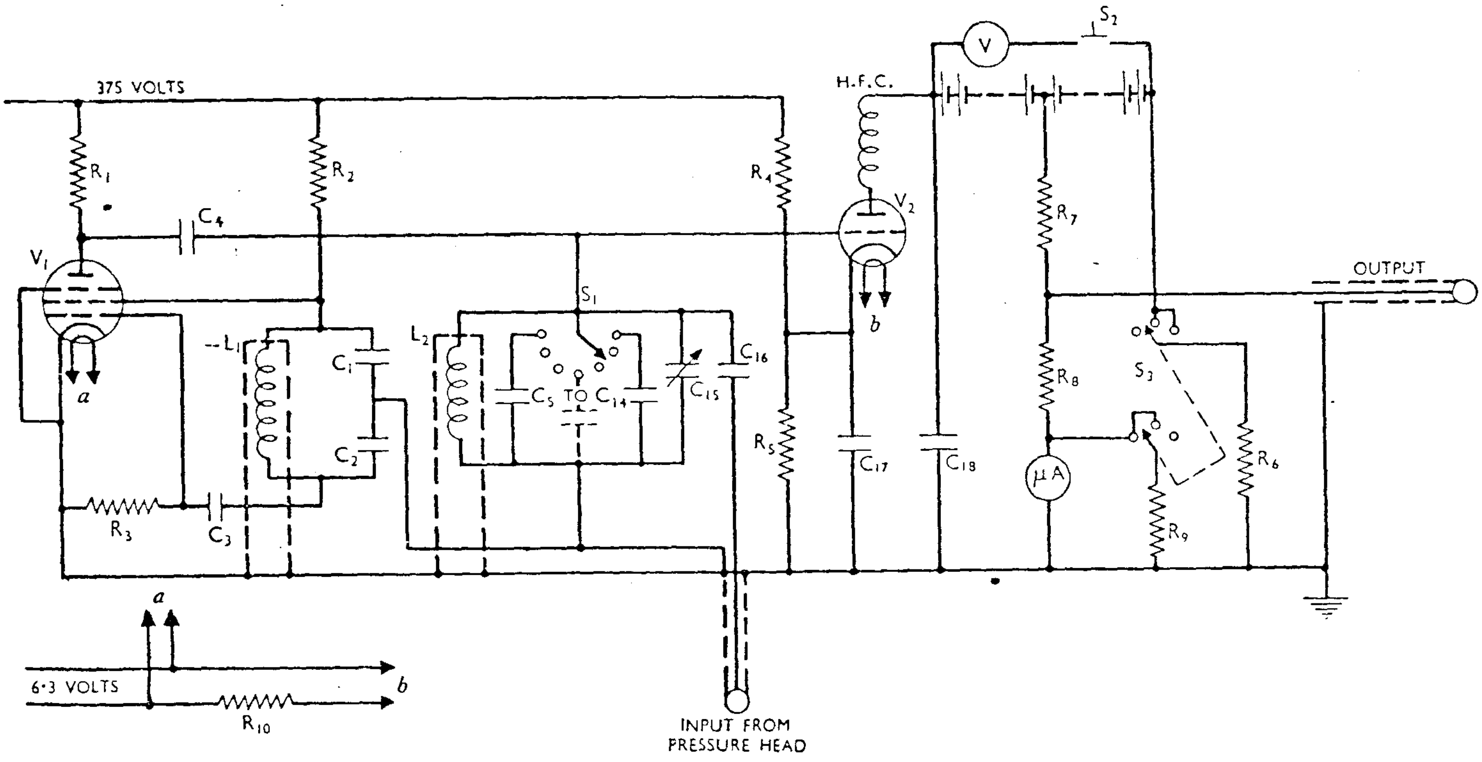

Fig. 11. Oscillator and Detector Unit

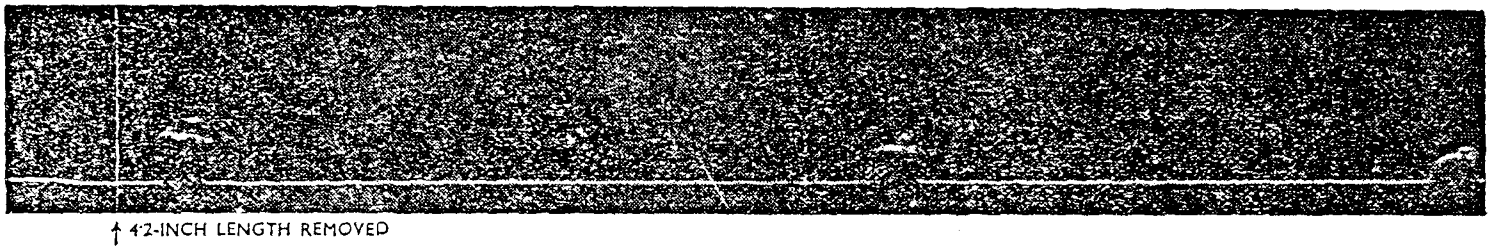

a Without relief valve.

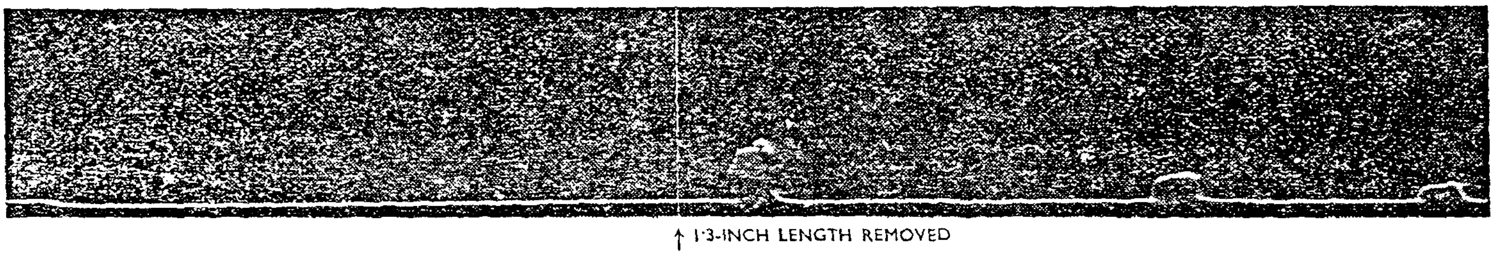

b With relief valve B set to lift at 265 feet of water (abs.).

Fig. 12. Typical Record showing the First Three Impacts

$v_0 = 9$ ft. per sec.

of the 5-inch screen in order to avoid errors due to distortion. Movement of the disk valve was indicated by means of two contacts on its lever, which momentarily increased the spot brightness when the valve started to shut and again when closure was complete. To measure the film speed, which was usually about 4 in. per sec., a small 50 cycles per sec. voltage, checked by the frequency meter, was applied to the amplifier.

The initial part of a typical diagram obtained with this apparatus is given in Fig. 12*a*, which shows the two bright spots indicating valve movement, the slight fall from the pumping to the cavitation pressure, and the succession, at decreasing time intervals, of impacts of diminishing intensity. Fig. 13*a*, which shows the first impact in detail, is an ordinary photographic enlargement, but for examination and measurement the films were placed in a Hilger projector having a linear magnification of 10. The start of the pressure rise was slightly rounded off, owing probably to the nose of the column not occupying the entire cross-section of the pipe; at the top the trace turned to the horizontal direction without overshooting, therefore the gauge was considered satisfactory, and it was not thought necessary to measure its natural period. The summit of the diagram was disturbed by waves, and nothing could be discerned of the changes shown in Fig. 6 which theory suggests; in this pipe-line, however, in which the shock pressures enormously exceeded the pumping pressures, these changes were in any event small.

Ideally, the velocity of the shock wave should be obtained by measuring the time interval from the start of the pressure rise to the start of the pressure fall. But here the latter point was obscured, and consequently the ends of the rise and the fall have been used. In this way the mean velocity of travel was found to be 4,450 ft. per sec., which is the average of twenty-eight observations of the first impact. The theoretical values, 4,600 and 4,620 ft. per sec., obtained from equations (14) and (15) were so close together that the way in which the pipe-line was held was a matter of no significance. The fact that they were higher than the measured value showed that the wall of the pipe-line was slightly less rigid than expected.

At least four records were obtained at each of the values of $v_0 = 3, 4, \ldots 9$ ft. per sec. At all velocities the irregularities in the traces of the impacts followed the same basic pattern, and they were evidently due to the peculiarities of the pipe-line. In an attempt to account for the existence of these waves, the

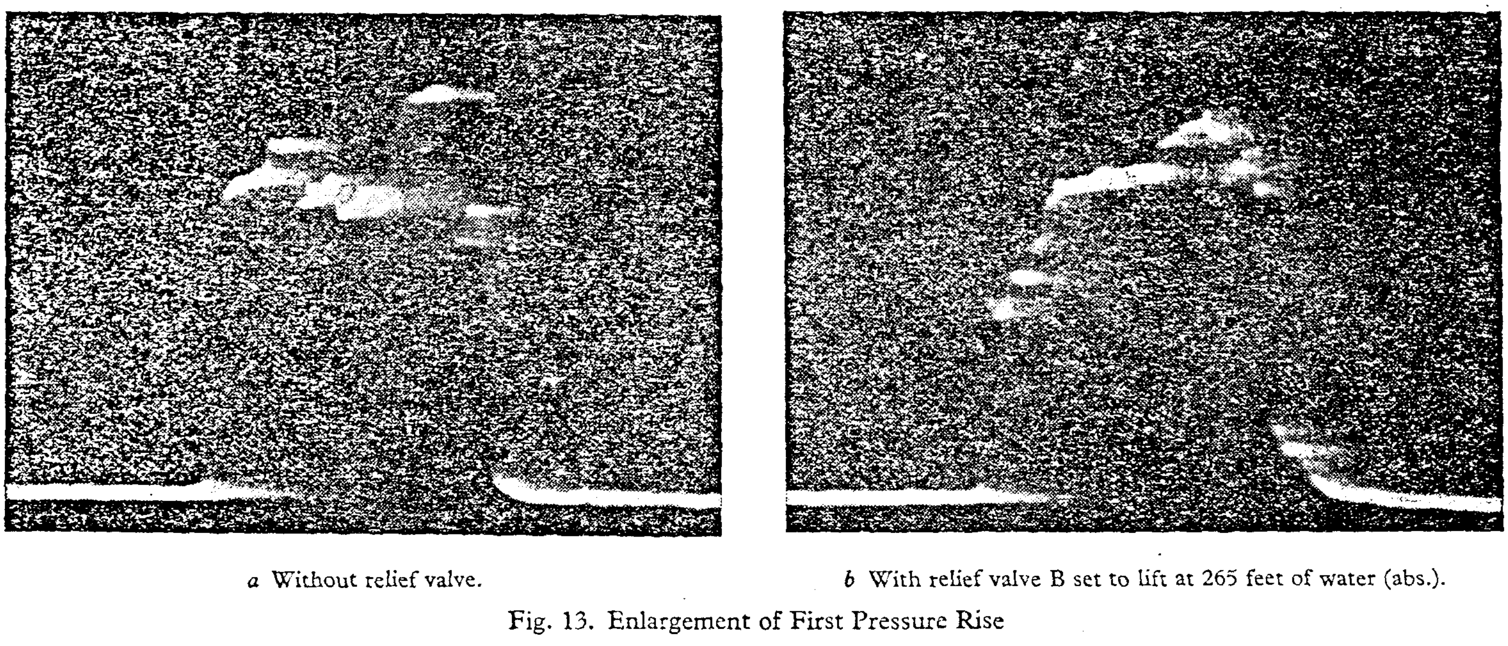

a Without relief valve.

b With relief valve B set to lift at 265 feet of water (abs.).

Fig. 13. Enlargement of First Pressure Rise

$v_0 = 9$ ft. per sec.

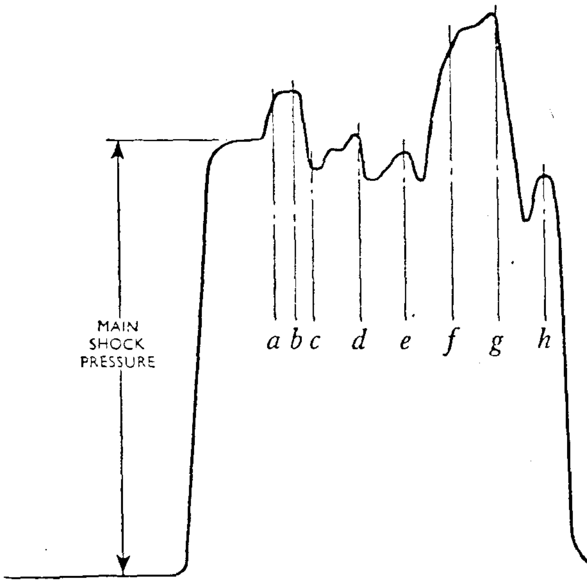

Fig. 14. Tracing of First Pressure Rise without Relief Valve $v_0 = 9$ ft. per sec.

positions of all the various fittings have been added to scale in Fig. 14, which shows a tracing made on the Hilger projector. Their order is:—

(*a*) At 37·8 feet from the disk valve, a small set of 4 inches occupying a length of 11 inches.

(*b*) At 46·0 feet, the 180 deg. bend made up of three sockets and two 90 deg. bends.

(*c*) At 53·6 feet, the drain consisting of a tee and 18 inches of $\frac{1}{4}$-inch piping closed by a valve; this being a branch, the principal reflected wave should be one of tension.

(*d*) At 73·5 feet, a socket.

(*e*) At 93·2 feet, the sluice valve.

(*f*) At 110·9 feet, a socket.

(*g*) At 130·7 feet, the horizontal 90 deg. bend.

(*h*) At 151·6 feet, the vertical 90 deg. bend.

It will be seen that the agreement between these positions and those of the waves is on the whole good, thus the waves can be explained as being due to reflection from the interruptions in the uniformity of the pipe-line. Their period is surprisingly long, perhaps because the fittings were of no great length and hence the assumption on which expressions (20) and (21) are based was to some extent violated. Moreover, each reflected wave, except that due to (*a*), had to pass on its return through at least one fitting, and no account has been taken of the complicated higher-order effects caused by the reflection of reflected waves. The maximum pressure, seen on the right in Fig. 13*a*, was due to the superposition of the waves set up by (*f*) and (*g*).

The means of the observed shock pressure at the first five impacts are shown in Fig. 15*a*. For this purpose the height of the trace at the shoulder on the left was measured because there the diagram was undisturbed by reflected waves. For the first impacts the results agreed well among themselves, the largest departure from the mean being 2 per cent, but this figure increased to 11 per cent for the fifth impacts. Loud intermediate shocks were heard during the later impacts, suggesting that the column was disintegrating as theory predicts, and the decay of repeatability may have been caused by the critical nature of these effects. For the first and second impacts the theoretical shock pressures, obtained from equation (17) and the observed value of *a*, are also given in Fig. 15*a*. For the first the agreement is satisfactory, but for the second the theoretical values were too high, probably owing to the loss of energy at the first impact which was not allowed for in the calculation. The shock pressure rose with increase of v_0, but was not linearly proportional to it because of the effects of friction on the moving column.

The time interval between complete closure of the valve and the arrival of the shock wave was found to vary in a repeatable manner from 0·65 second at $v_0 = 3$ ft. per sec. to 1·64 seconds at $v_0 = 9$ ft. per sec. These times were about 7 per cent lower than the theoretical values; they were, of course, large compared with the time 0·0739 second required for a shock wave to travel up and down the pipe-line, and with the time of closing the valve which ranged in a random way from 0·050 to 0·068 second.

Tests were carried out with gradually decreasing values of v_0 to determine the minimum velocity at which water hammer took place. A faint click could still be heard at a velocity of 0·38 ft. per sec., but at 0·36 ft. per sec. no sound was audible. Sir Geoffrey Taylor has since pointed out that, as the time for the valve to close was less than that taken for a wave to pass to the reservoir and back, a theoretical estimate of the minimum velocity can be obtained by means of equation (17). This velocity was very low, therefore the friction head was negligible, and the limiting pressure change to be considered is from the static absolute head 45·6 feet to the cavitation pressure 1·6 feet. It then follows from equation (17) that the required velocity is 0·32 ft. per sec., which is in good agreement with the observations.

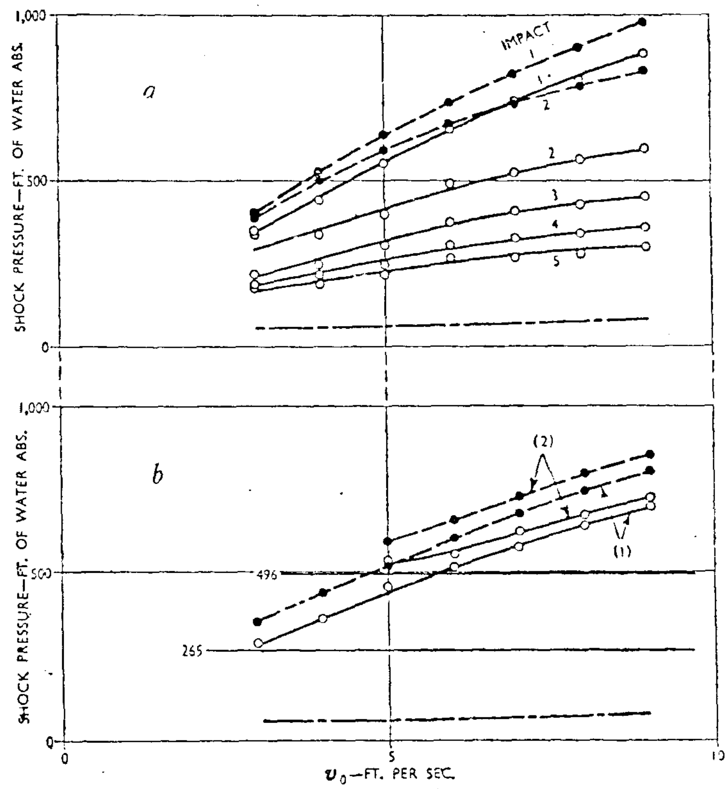

Fig. 15. Shock Pressures

a Without relief valve.

○——○ Observed. ●- - - -● Calculated.

—— - —— Pumping head.

b At first impact with relief valve B.

(1) Valve lifting at 265 feet of water (abs.).

(2) Valve lifting at 496 feet of water (abs.).

○——○ Observed. ●- - - -● Calculated.

—— - —— Pumping head.

THE REDUCTION OF SHOCK PRESSURE DUE TO A SPRING-CONTROLLED RELIEF VALVE

Theoretical Calculations. The required modifications in the theory can be derived on the assumption that the shock pressure at the disk and the relief valves, which were placed near together, is of constant intensity (p_2) while it lasts. The wave as it passes up the pipe-line alters the velocity of flow from v_2 not to zero but to some value, say u_2, therefore the appropriate form of equation (13) is

$$p_2 = -(v_2-u_2)\left(\frac{K'}{gp}\right)^{\frac{1}{2}} \quad . \quad . \quad . \quad . \quad (27)$$

A calibration curve for the relief valve can be experimentally obtained, connecting the pressure difference across the valve with the discharge Q under steady conditions. This curve will approximately hold good under shock conditions also, provided that the valve possesses sufficient damping and a natural period which is high compared with the duration of the shock pressure. Now

$$Q = -u_2 A \quad . \quad . \quad . \quad . \quad . \quad (28)$$

where A is the cross-section of the pipe-line, hence there is another relation between the unknowns p_2 and u_2. The magnitude of both can then be determined; a convenient method is to plot on the calibration curve the relation (27), which is a straight line when v_2 is specified. Since the shock pressure lasts for a time $2L/a$, the total volume of water emitted by the valve is $2LQ/a$. The shock wave while returning from the open end continues to change the velocity of each section by $(v_2 - u_2)$, therefore the column will rebound with velocity $(v_2 - 2u_2)$.

Experimental Apparatus and Results. The electronic gauge already described was again employed, and a relief valve was screwed into a boss welded on the pipe-line near the disk valve. Two commercial safety valves ½ inch in diameter were tried in turn. Valve A, which had been previously used for other purposes, possessed a flat seating, and it was set to lift at 100 lb. per sq. in. gauge (231 feet of water absolute). Valve B with a conical seating was new; it was provided with two alternative springs which lifted at 100 and 200 lb. per sq. in. The valves were calibrated in position under steady pressure with the aid of the hydraulic accumulator connected to the drain. A graduated glass cylinder was used to measure the water ejected from the orifice in the body of the valve, the weir action of the orifice being made as definite as possible by blocking its lower part with a thin plate fixed with its top edge horizontal.

A typical result appears in Fig. 12*b*, which was obtained with valve B lifting at 265 feet of water absolute, the other conditions of the test being identical with Fig. 12*a*. An enlargement of the first pressure rise is shown in Fig. 13*b*. It will be noticed that the series of impacts was not greatly modified by the relief valve. The sharpness of each pressure rise was, however, diminished, but on the right the superposition of two reflected waves again occurred, causing the maximum pressure in the pipe-line. It was not easy to decide which part of the diagrams should be measured for comparison with the pressure rises calculated from equations (27) and (28). The point at the right-hand end of the relatively horizontal portion, immediately preceding the well-marked reflected waves, was chosen, and the results for the first impact with valve B lifting at 265 and 496 feet of water absolute are displayed in Fig. 15*b*; those obtained with valve A were almost identical. The curve obtained at the higher lifting pressure does not extend below $v_0 = 5$ ft. per sec. because at lower velocities the valve failed to move. The theoretical pressures are seen to be somewhat in excess of the experimental, but the discrepancy is nowhere serious. Comparison with Fig. 15*a* reveals that the relief valve, when it lifted, caused only a small reduction in shock pressure. This device must therefore be regarded as almost useless when inserted in a pipe-line to mitigate the effect of water hammer.

As the shock pressures followed in quick succession, it was impossible to isolate the discharges of water caused by the separate impacts. The total volumes actually ejected were found to be considerably less than the theoretical quantities. The difference cannot be attributed to the inertia of the relief-valves, for both were light, and von Freudenreich (1948) showed that the presence of a liquid in contact with a relief valve greatly increases its natural frequency. The discrepancy may be due partly to the lowness and partly to the variation of the observed shock pressure, which in the theory was assumed to be constant; when the discharge was calculated from actual pressure diagrams, much better agreement was obtained.

ACKNOWLEDGEMENT

The authors are greatly indebted to Mr. M. O. W. Wolfe, who assisted in many ways with the electronic apparatus.

APPENDIX I

DERIVATION OF EQUATION (6)

Equation (5) may be rearranged in the form

$$\frac{d^2V}{dt^2} - \frac{r}{2}\left(\frac{dV}{dt}\right)^2 - \frac{s}{V} = -\frac{s}{q}, \quad . \quad . \quad . \quad . \quad . \quad (29)$$

where

$$s = \frac{Ag}{L} p_0 V_1 \quad . \quad . \quad . \quad . \quad . \quad . \quad . \quad (30)$$

and q and r are given by equation (7). With the substitution $dV/dt = y^{\frac{1}{2}}$, equation (29) becomes

$$\frac{dy}{dV} - ry = 2s\left(\frac{1}{V} - \frac{1}{q}\right) \quad . \quad . \quad . \quad . \quad (31)$$

of which the integral is

$$y \, . \exp(-rV) = 2s\int \exp(-rV)\frac{dV}{V} + \frac{2s}{qr}\exp(-rV) + C \quad . \quad (32)$$

where C is a constant. The limits of V are V_1 and V_2, at both of which the left-hand side of equation (32) is zero. Hence, by subtraction, equation (6) is obtained.

APPENDIX II

REFERENCES

Angus, R. W. 1945 Proc. I.Mech.E., vol. 153, p. 20, contribution on Binnie's paper (see below).

Binnie, A. M. 1943 Jl. App. Mech., vol. 10, p. A183, "Oscillations in Closed Surge Tanks".

1945 Proc. I.Mech.E., vol. 153, p. 15, "Protective Air Vessels for Rising Pipe-lines".

Blair, J. S. 1945 Proc. I.Mech.E., vol. 153, p. 1, "Controlling Pipe-line Surges by means of Air Vessels".

Federal Works Agency 1939 "Tables of the Exponential Function".

1940 "Tables of the Sine, Cosine and Exponential Integrals", vols. 1 and 2 (London Agents: Scientific Computing Service, 23 Bedford Square, W.C.1).

Hopkinson, B. 1914 Phil. Trans. Roy. Soc., Series A, vol. 213, p. 437 (Papers, 440), "A Method of Measuring the Pressure Produced in the Detonation of High Explosives or by the Impact of Bullets".

Lamb, Sir H. 1921 Proc. Roy. Soc., Series A, vol. 98, p. 205, "On the Vibrations of an Elastic Plate in Contact with Water".

O'Brien, M. P., and Hickox, G. H. 1937 "Applied Fluid Mechanics", pp. 251 and 246 (McGraw-Hill, New York and London).

Prescott, J. 1924 "Applied Elasticity", p. 598 (Longmans, Green, London).

von Freudenreich, J. 1948 *Brown Boveri Review*, vol. 35, p. 147, "The Chattering of Safety Valves and Similar Mechanisms".

Wolfe, M. O. W., Martin, S., and Judge, J. A. 1946 R.A.E. Report No. S.M.E. 3371.

Wolfe, M. O. W. 1949 Proc. Seventh International Congress for Applied Mechanics, vol. 3, p. 304 (summary only); full text in *Aircraft Engineering*, vol. 21, p. 368, "The Measurement of Fluctuating Fluid Pressures".

[For the discussion and communications on this paper see pp. 65 and 69 respectively.]

length of the pipe is 143 feet. These values for the maximum head rise are plotted on the profile of the pipe line and a smooth curve is drawn through these points as shown in Figure 23. Such a curve is useful in determining the required pipe thickness to withstand safely the maximum head. For example, the maximum head in the pipe adjacent to the gate is 772 feet and the maximum head at the mid-length of the pipe is 563 feet. It is noted that the maximum head rises at these two points in the pipe line do not occur at the same time.

VII

Theory of Graphical Waterhammer Analysis for Gate Operation

27. Conjugate waterhammer equations[1]

The analytical waterhammer solution shown in the preceding chapter gives an indication of the extent of the computations involved in obtaining a solution by that method. In general, the necessity of calculating the term V accurately from Equation (29) makes the method a tedious one. A considerable increase in computations also results when there are physical discontinuities in the pipe line. In order to obtain the waterhammer solution more readily, a graphical method of analysis is used. The method is derived as follows: The fundamental waterhammer equations are

$$H - H_0 = F\left(t - \frac{x}{a}\right) + f\left(t + \frac{x}{a}\right); \qquad (15)$$

$$V - V_0 = -\frac{g}{a}\left[F\left(t - \frac{x}{a}\right) - f\left(t + \frac{x}{a}\right)\right]. \qquad (16)$$

Subtracting Equation (16) from (15) gives

$$H - H_0 = \frac{a}{g}(V - V_0) + 2F\left(t - \frac{x}{a}\right). \qquad (33)$$

The addition of Equations (15) and (16) gives

$$H - H_0 = -\frac{a}{g}(V - V_0) + 2f\left(t + \frac{x}{a}\right). \qquad (34)$$

Since Equation (33) contains only the F wave term, this equation defines the velocity and head relations in the pipe line in terms of F waves. Similarly, Equation (34) defines the velocity and head relations in terms of f waves.

---

[1] See Reference 3.

Consider the pipe line shown in Figure 27. The lower section of pipe is of uniform diameter and thickness and has a wave velocity of a_1 while the upper section of pipe has a wave velocity of a_2 feet per second. Suppose that there is an F_1 wave at B_1 at time t_1. This wave moves up the pipe with a velocity of a_1 feet per second and reaches C_1 at $t_2 = t_1 + L_1/a_1$ seconds. Similarly, suppose that there is an f_2 wave at C_2 at time t_3. This wave moves down the pipe with a velocity of a_2 feet per second and reaches B_2 at $t_4 = t_3 + L_2/a_2$ seconds. Equation (33) is now applied at B_1 and C_1 while Equation (34) is applied at B_2 and C_2 as follows:

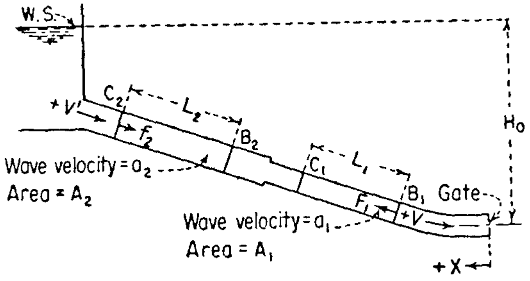

Figure 27

$$H_{B_1t_1} - H_{B_1t_0} = \frac{a_1}{g}(V_{B_1t_1} - V_{B_1t_0}) + 2F_1;$$

$$H_{C_1t_2} - H_{C_1t_0} = \frac{a_1}{g}(V_{C_1t_2} - V_{C_1t_0}) + 2F_1;$$

$$H_{C_2t_3} - H_{C_2t_0} = -\frac{a_2}{g}(V'_{C_2t_3} - V'_{C_2t_0}) + 2f_2;$$

$$H_{B_2t_4} - H_{B_2t_0} = -\frac{a_2}{g}(V'_{B_2t_4} - V'_{B_2t_0}) + 2f_2.$$

After eliminating F_1 and f_2 from these equations and using the relations

$$H_{B_1t_0} = H_{C_1t_0}, \qquad H_{C_2t_0} = H_{B_2t_0},$$
$$V_{B_1t_0} = V_{C_1t_0}, \qquad V'_{B_2t_0} = V'_{C_2t_0},$$

the following equations are obtained:

$$H_{B_1t_1} - H_{C_1t_2} = \frac{a_1}{g}(V_{B_1t_1} - V_{C_1t_2}); \tag{35}$$

$$H_{C_2t_3} - H_{B_2t_4} = -\frac{a_2}{g}(V'_{C_2t_3} - V'_{B_2t_4}). \tag{36}$$

In the derivation of Equations (35) and (36), B_1 and C_1 are arbitrary points on the lower section of uniform pipe, while B_2 and C_2 are arbitrary points on the upper section of uniform pipe. Hence these equations are applicable between any two points, including the end points, of any section of uniform pipe in the pipe line.

These equations are rewritten in another form involving the following ratios:

$$h = \frac{H}{H_0};$$
$$v = \frac{V}{V_0} = \frac{V'}{V'_0} \quad \text{for gate closing movements;}$$
$$v = \frac{V}{V_e} = \frac{V'}{V'_e} \quad \text{for gate opening movements,}$$

where V_0 and V'_0 are the initial steady velocities of water in the pipe sections prior to gate closure, and V_e and V'_e are the final steady velocities of water after gate opening has been completed. Then

$$h_{B_1t_1} - h_{C_1t_2} = 2\rho_1(v_{B_1t_1} - v_{C_1t_2}); \tag{37}$$
$$h_{C_2t_3} - h_{B_2t_4} = -2\rho_2(v_{C_2t_3} - v_{B_2t_4}), \tag{38}$$

where for gate closure,

$$\rho_1 = \frac{a_1V_0}{2gH_0} \quad \text{and} \quad \rho_2 = \frac{a_2V'_0}{2gH_0},$$

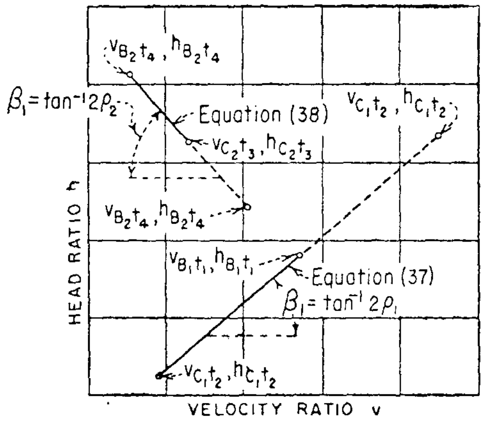

Figure 28

and for gate opening,

$$\rho_1 = \frac{a_1 V_e}{2gH_0} \quad \text{and} \quad \rho_2 = \frac{a_2 V_e'}{2gH_0}.$$

Equations (37) and (38) are the conjugate waterhammer equations, while ρ_1 and ρ_2 are the pipe line constants. On a rectangular coordinate system of h and v the conjugate equations are represented by straight lines which have a slope of $\pm 2\rho$ and pass through known points as shown in Figure 28.

28. Gate discharge equations

Each conjugate waterhammer equation defines the relation between h and v at a point in a uniform pipe line in terms of h and v at another point in the pipe under the action of the waterhammer wave phenomena. In order to determine h and v explicitly, a second independent relation is required. For gate operations this relation is determined from the discharge at the gate. The initial discharge through the gate under steady conditions is

$$V_{A_0} = B_0 \sqrt{H_{A_0}};$$

and the discharge at any gate opening and head as defined by Equation (28) is

$$V_{\text{A}} = B\sqrt{H_{\text{A}}}.$$

Then

$$v_{\text{A}} = \tau \sqrt{h_{\text{A}}}, \tag{39}$$

where

$$v_{\text{A}} = \frac{V_{\text{A}}}{V_{A_0}}, \quad h_{\text{A}} = \frac{H_{\text{A}}}{H_{A_0}}, \quad \text{and} \quad \tau = \frac{B}{B_0}.$$

Although Equation (39) has been derived for gate closure, an identical equation results for gate opening by letting $\tau = B/B_e$, where B_e is the gate opening factor at the end of the gate movement.

29. Graphical solution for gate closure

Consider the pipe line and the gate closure relation shown in Figures 29a and b. This problem is identical to that solved by analytical methods in the previous chapter. In order to illustrate the solution in its simplest form, the head rise at the gate is determined for 2-second time intervals. Since the wave travel time from A to E is 1 second, the necessary conjugate waterhammer equations for the end points of the pipe line are as follows:

$$\left.\begin{aligned}
h_{A_0} - h_{E_1} &= +2(v_{A_0} - v_{E_1}); &\text{(a)}\\
h_{E_1} - h_{A_2} &= -2(v_{E_1} - v_{A_2}); &\text{(b)}\\
h_{A_2} - h_{E_3} &= +2(v_{A_2} - v_{E_3}); &\text{(c)}\\
h_{E_3} - h_{A_4} &= -2(v_{E_3} - v_{A_4}); &\text{(d)}\\
h_{A_4} - h_{E_5} &= +2(v_{A_4} - v_{E_5}); &\text{(e)}\\
h_{E_5} - h_{A_6} &= -2(v_{E_5} - v_{A_6}), &\text{(f)}\\
&\text{etc.}
\end{aligned}\right\} \tag{40}$$

In these equations the head and velocity ratios h and v at the gate are indicated at $t = 0$, 2, 4, and 6 seconds. Hence only the discharge relation at the gate at these specific times will be required in the waterhammer solution. These are as follows:

$$\left.\begin{aligned}
v_{A_0} &= 1.0\sqrt{h_{A_0}}; &\text{(m)}\\
v_{A_2} &= 0.7\sqrt{h_{A_2}}; &\text{(n)}\\
v_{A_4} &= 0.3\sqrt{h_{A_4}}; &\text{(o)}\\
v_{A_6} &= 0; &\text{(p)}\\
v_{A_t} &= 0 \text{ when } t > 6 \text{ seconds.}
\end{aligned}\right\} \tag{41}$$

Equations (40) and (41) are now solved simultaneously by graphical methods as follows: On a set of coordinate axes of v and h, parabolas m, n, o, and p are drawn for values of $\tau = 1.0$, 0.7, 0.3, and 0, as shown in Figure 29c. The parabola $\tau = 0$ coincides with the vertical axis at $v = 0$. The point A_0 prior to the gate movement is located at the coordinates $h = 1$, $v = 1$. Since the effect of a gate movement does not reach the reservoir end of the pipe until after the wave travel time of 1 second, E_1 is also located at the same point as A_0. Equation (40a) is then represented as a point on the diagram at $h = 1$, $v = 1$. Equation (40b) is the equation of a straight line with a slope of -2ρ which passes through the point E_1. Since the point corresponding to A_2 is concurrently located on the parabola n and the sloping line b, it must be located at the intersection of these two lines as shown in the figure. Equation (40c) is the equation of a straight line of slope 2ρ which passes through the point A_2. For a constant reservoir level E_3 is located on the horizontal axis at $h = 1$. The

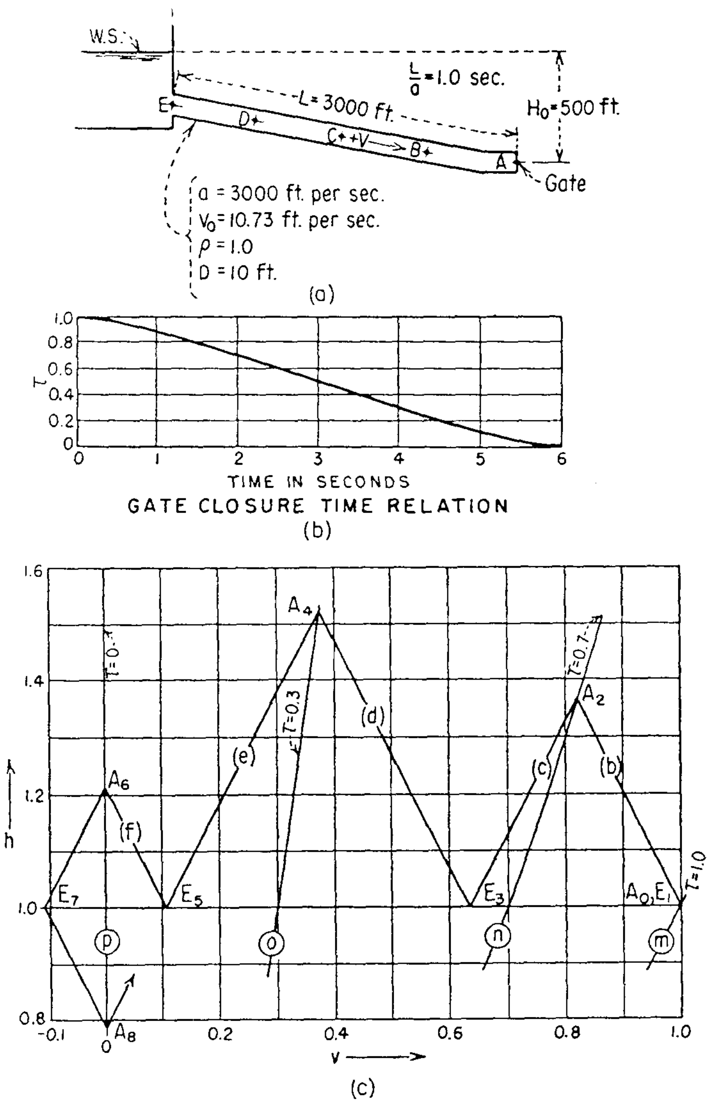

Figure 29

points corresponding to A_4, E_5, A_6, E_7, A_8, etc., are then determined in the manner shown in the figure.

A comparison of the results of this solution with those of the analytical method given in the preceding chapter shows that the results obtained from the two methods are identical. The graphical method of waterhammer analysis is seen to consist essentially of the graphical solution of simultaneous equations. One group

of equations depends upon the values of τ, the effective gate opening, which is specified. These gate relations are represented by parabolas on the h-v diagram. A second group of equations is obtained from the conjugate waterhammer equations. These equations are represented on the h-v diagram by straight lines of slope $\pm 2\rho$. The intersections of the sloping lines and parabolas determine the head and velocity ratios at the gate and the intersections of the sloping lines with the horizontal line $h = 1$ determines these ratios at the reservoir end of the pipe.

VIII

Waterhammer Produced by Gate Closure

30. At the mid-length of pipe

The graphical method of waterhammer analysis is extended to determine the head changes at the mid-length of the pipe for the example used in the preceding section. Time intervals of 1 second are used in the computations, and parabolas corresponding to values of τ for these time intervals are shown on the h-v diagram in Figure 30. Conjugate waterhammer equations at 1-second time intervals are now required for the pipe sections AC and CE. Instead of writing these equations formally as in the preceding chapter, a tabular representation of the equations can be used as shown in Table 3. In this table $t = 0, 1, 2, 3, 4$, etc., are shown in the column directly below the gate at A. The times recorded in the center column at C, the mid-length of the pipe, are equal to times recorded at the gate plus one-half second, the wave travel time between the gate and the mid-length of the pipe. Similarly, the times recorded under E, at the reservoir end of the pipe, are the times recorded at the mid-length plus one-half second. The lines with arrows represent conjugate waterhammer equations and the direction of travel of the pressure waves.

From a consideration of the action of the initial direct and reflected waves, A_0, $C_{0.5}$, and $E_{1.0}$ are located at a common point at $h = 1$, $v = 1$. Then $A_{1.0}$ and $C_{1.5}$ are located at the intersec-

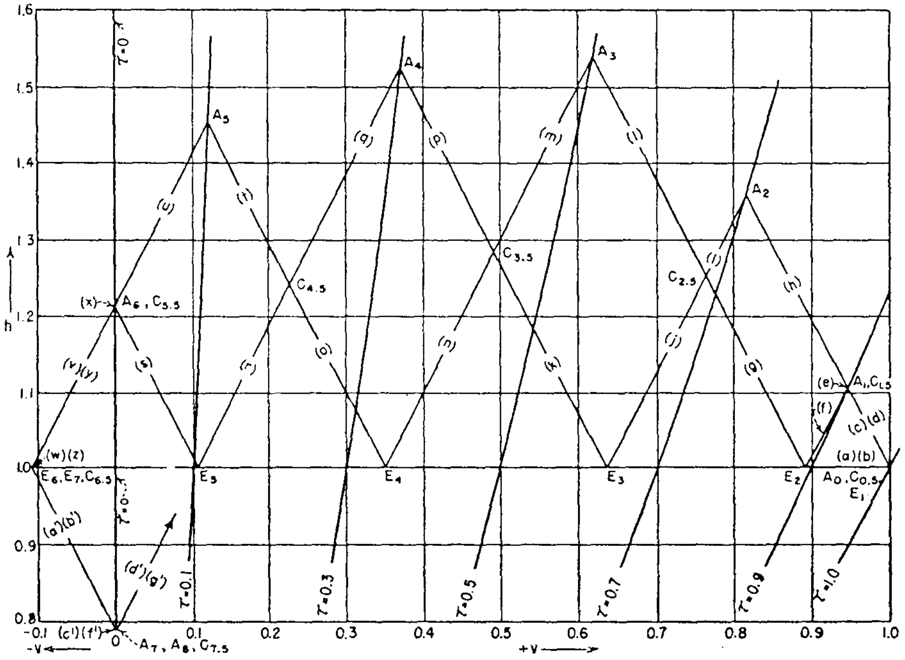

Figure 30

TABLE 3

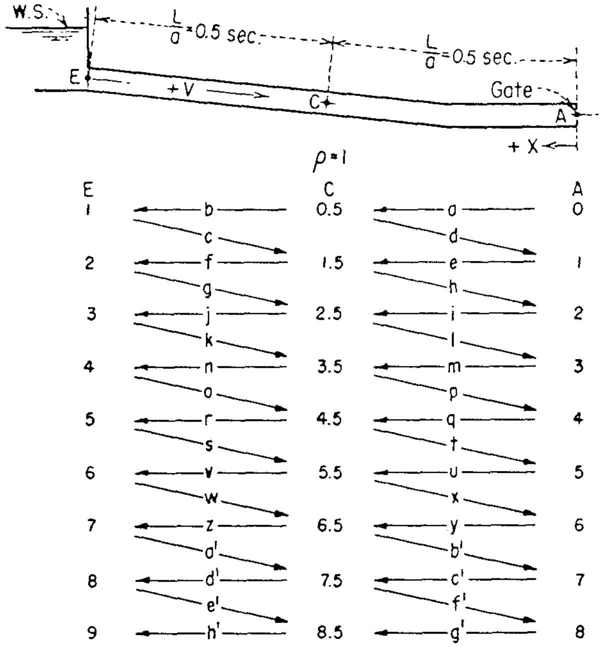

etc.

The numbers in the table indicate the time in seconds after the start of gate closure of the points A, C or E.

tion of the line of slope -2ρ and the parabola corresponding to $\tau = 0.9$. The graphical representation of the remaining conjugate equations is shown in Figure 30 with the segments of the sloping lines marked according to the designation shown in Table 3. The maximum head rise at the gate as obtained from these computations is $0.54H_0$ and occurs at $t = 3$ seconds, while the maximum head rise at the mid-length is $0.28H_0$ and occurs at $t = 3.5$ seconds.

31. At the quarter points of the pipe line

The graphical method of analysis is now extended to determine the pressure changes at other points in the pipe line. In general it is necessary to select points on the pipe line which divide it into an integral number of pipe sections of equal wave travel time. The maximum time interval used in the computations is then the round trip wave travel time for any pipe section. For example, in order to determine the pressure changes at the quarter points in the pipe line shown in Figure 29a, one-half second time

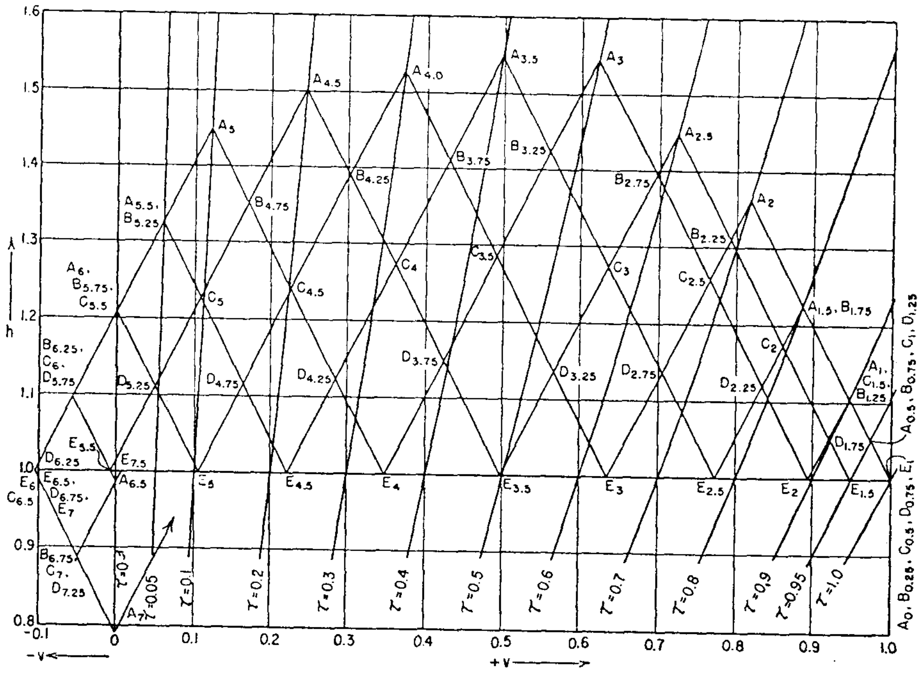

Figure 31

intervals are used. The solution then determines simultaneously the pressure changes at the gate, the one-quarter point, the midpoint, and the three-quarter point of the pipe line for one-half second time intervals as shown in Figure 31.

32. Pipe line with a stepwise change in diameter

In using the conjugate equations in the waterhammer solution the factors which are considered are ρ, the pipe line constant, and the wave travel time between two points in a uniform section of the pipe line. For a pipe line which has a stepwise change in the cross-sectional area or wave velocity, these conjugate equa-

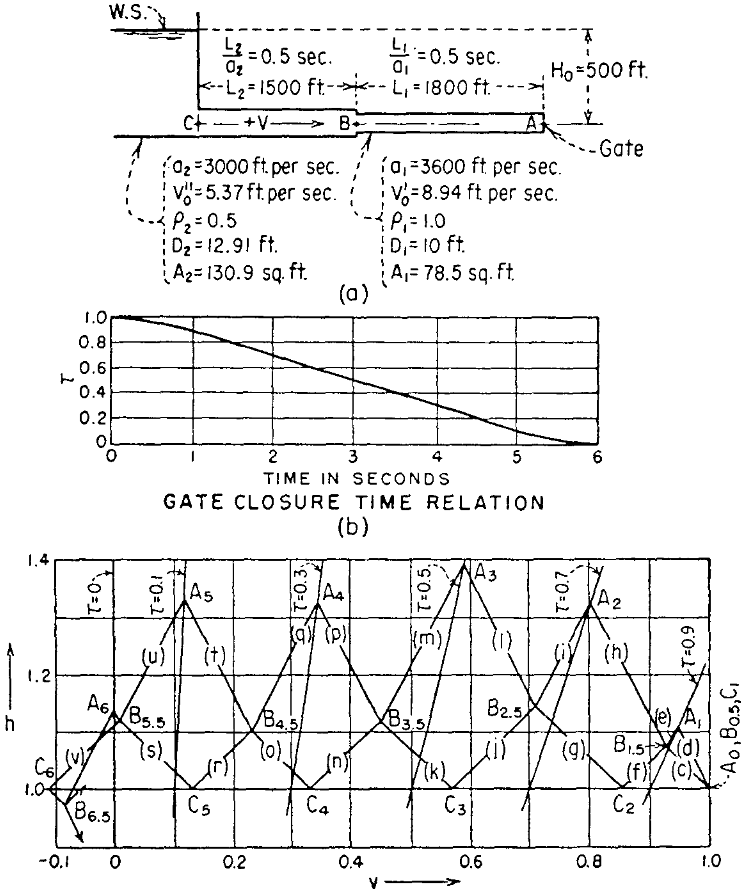

Figure 32

tions are also applicable at the end points of each section of uniform pipe. On the *h*-*v* diagram the graphical representation of these equations is similar to that shown in the preceding section with the exception that one set of the conjugate equations is represented by lines of slope $\pm 2\rho_1$, while the other set has a slope of $\pm 2\rho_2$. For example, consider the pipe line shown in Figure 32a and the gate closure time relation shown in Figure 32b. The round trip wave travel time in pipe sections *AB* and *BC* is 1 second. Therefore the largest time interval which can be used in the computations is 1 second. Parabolas corresponding to the values of τ for 1-second time intervals are shown on the *h*-*v* diagram in Figure 32c. The applicable conjugate equations for 1-second time intervals for the pipe sections *AB* and *BC* are indicated in Table 4. This tabulation differs from Table 3 only in the respect that the value of ρ is different in the two sections of pipe. The graphical representation of these conjugate equations is shown in Figure 32c.

TABLE 4

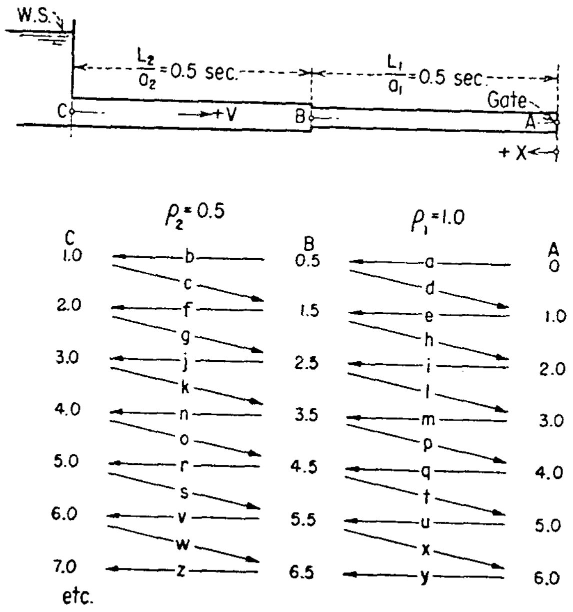

There is no particular difficulty in obtaining a waterhammer solution when the round trip wave travel times in each of the two sections are different as shown for the pipe line in Figure 33. The method is also applicable when there are more than two stepwise changes in the diameter or wave velocity in the pipe line. However, when there are many stepwise changes in the pipe line this method becomes too tedious. In such cases the approximate method given in Chapter XV is useful and of sufficient accuracy for most purposes.

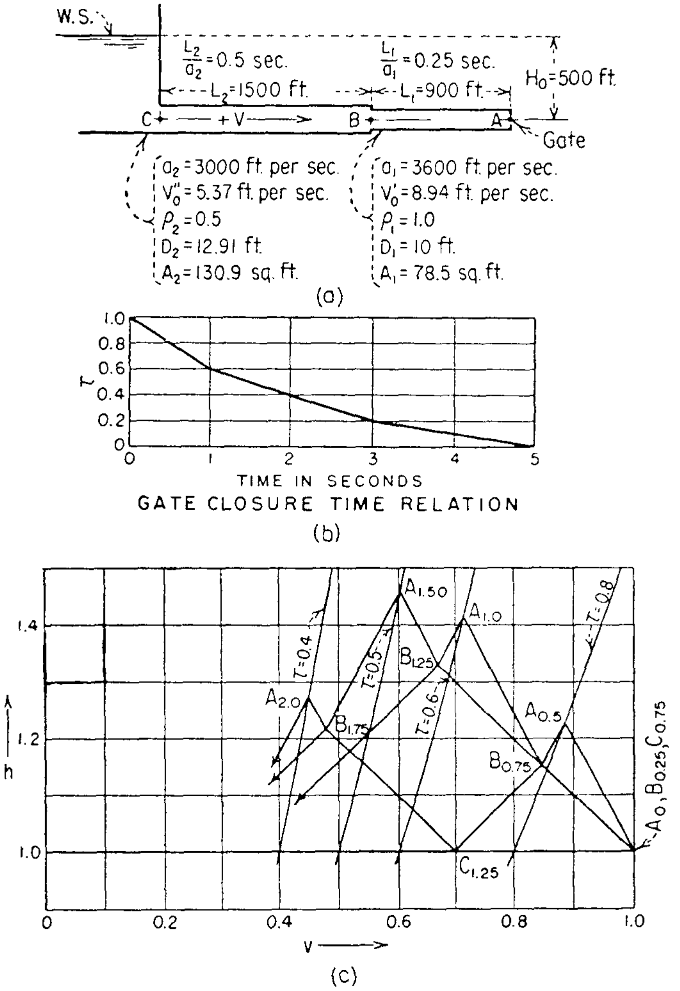

Figure 33

33. Partial gate closure

When the control gate is closed only part way and held there, the waterhammer solution is as shown in Figure 34. This solution shows that although pipe line friction has been neglected, the partial reflections which occur at the open gate cause the pressure and velocity in the pipe to return quickly to a steady value.

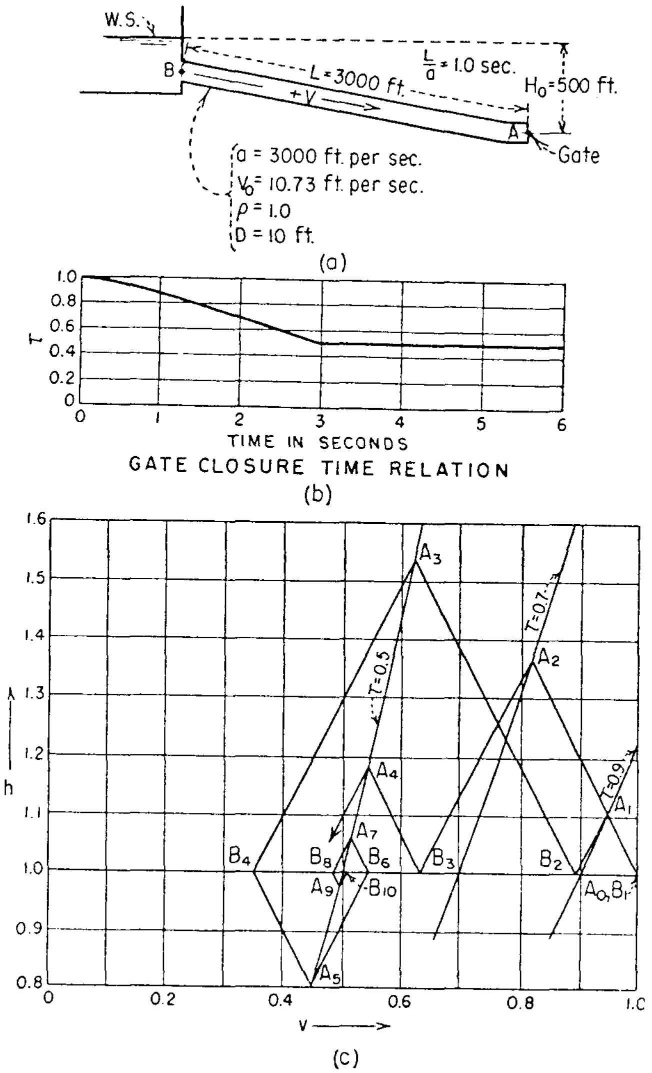

Figure 34

34. Gate closure with a relief valve[1]

Consider a pipe line which has a relief valve near the control gate as shown in Figure 35a. The type of relief valve which is considered is often used in turbine penstock installations for the control of waterhammer, and is operated in such a manner that the relief valve opens as the turbine gates are closing. A short time later the relief valve closes at a much slower rate with a negligible rise in pressure. The assumed combined effective gate

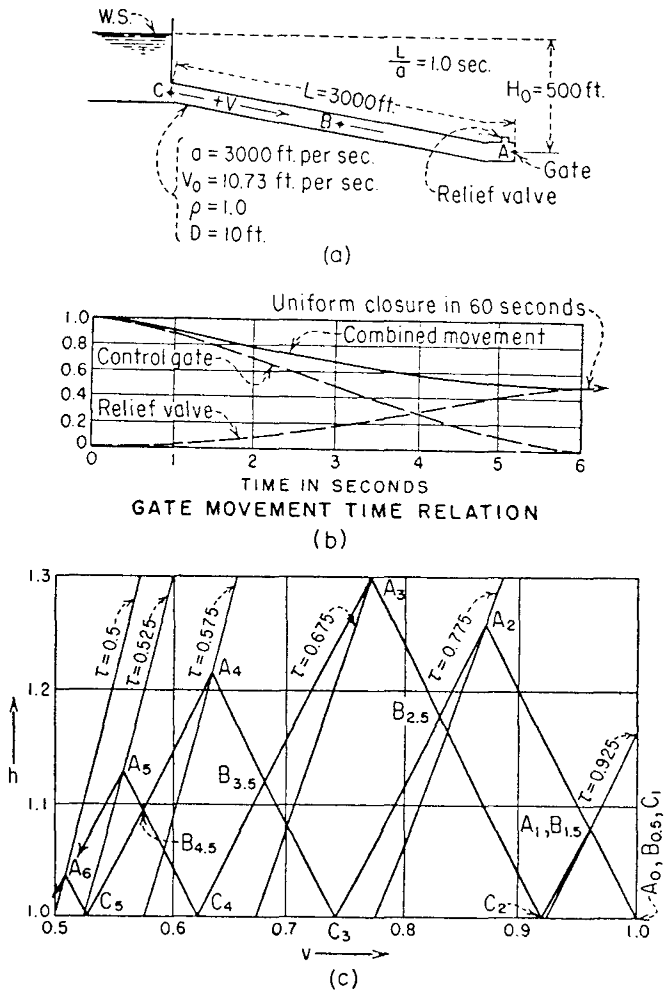

Figure 35

---

[1] See Reference 40.

opening of the control gate and relief valve is shown in Figure 35b. Since the waterhammer effects depend only upon the changes in velocity of water in the penstock, the waterhammer solution is obtained from the combined effective gate opening as shown in Figure 35c.

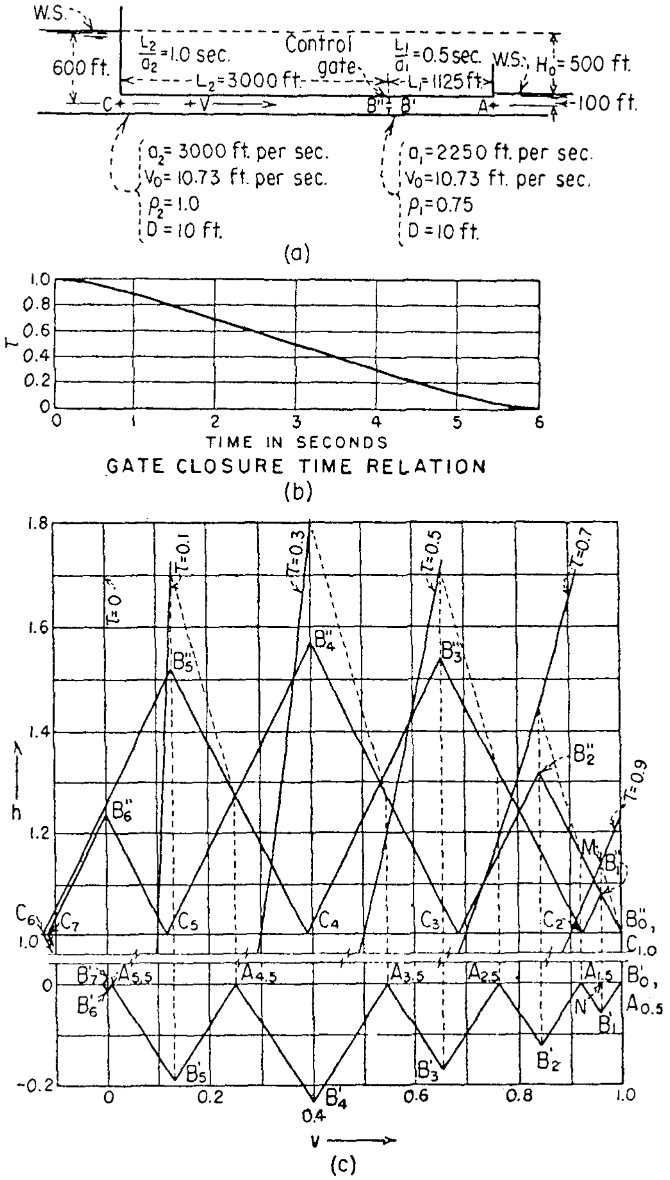

Figure 36

35. Control gate located away from outlet end of pipe

Consider the pipe line shown in Figure 36a and the gate closure shown in Figure 36b. Since the largest common round trip wave travel time which occurs in both sections of the pipe is 1 second, this time interval is used in the waterhammer computations. The discharge through the gate varies with $\sqrt{h_{B''_t} - h_{B'_t}}$. As the gate is closed, pressure waves form at B' and B'', which move toward A and C. In the waterhammer solution B''_0 and C_1 are located at $h = 1$, $v = 1$, while B'_0 and $A_{0.5}$ are located at $h = 0$, $v = 1$ as shown in Figure 36c. A line is now drawn from $C_{0.5}$ (this is the same point as C_1) which has a slope of $-2\rho_2 = -2$ on which B''_1 is to be located. Similarly, a line is drawn from $A_{0.5}$ which has a slope of $+2\rho_1 = 1.5$ on which B'_1 is to be located. Since the flow on both sides of the control valve are equal, B''_1 and B'_1 are located on the same vertical line. Moreover, these two points are located in such a manner that the vertical distance from the point B''_1 to the parabola corresponding to $\tau = 0.9$ is the same as the vertical distance from the horizontal line $h = 0$ to $B'_{1.0}$, that is, $B'_1N = B''_1M$. The reason for this is that at $t = 1.0$ second, the flow through the gate is

$$v_{B'_1} = v_{B''_1} = 0.9\sqrt{h_{B''_1} - h_{B'_1}}.$$

A simple method for locating the points $B'_{1.0}$ and $B''_{1.0}$ is illustrated by the dotted lines in Figure 36c. Starting from B''_0 draw a dotted line of slope $-2(\rho_1 + \rho_2)$ which intersects the parabola corresponding to $\tau = 0.9$ at the point M. Then $B'_{1.0}$ and $B''_{1.0}$ are located on the vertical line which passes through the point M. Other points which are required in the solution are determined in a similar manner as shown in the figure.

36. Control gate located at upper end of pipe

Consider the pipe line installation shown in Figure 37a and the gate closure time relation in Figure 37b. For this installation $h_{B''_t} = 1.0$. Hence, the waterhammer solution shown in Figure 37c is obtained by locating the points B'_2, B'_4, B'_6, etc., so that on the same vertical line the distance $B''M$ above the horizontal line

$h = 1$ to the parabola for each gate opening is equal to $B''B'$ below the line $h = 1$. The solution indicates that the maximum drop in head at the gate is $0.53H_0$ and the maximum head rise is $0.22H_0$.

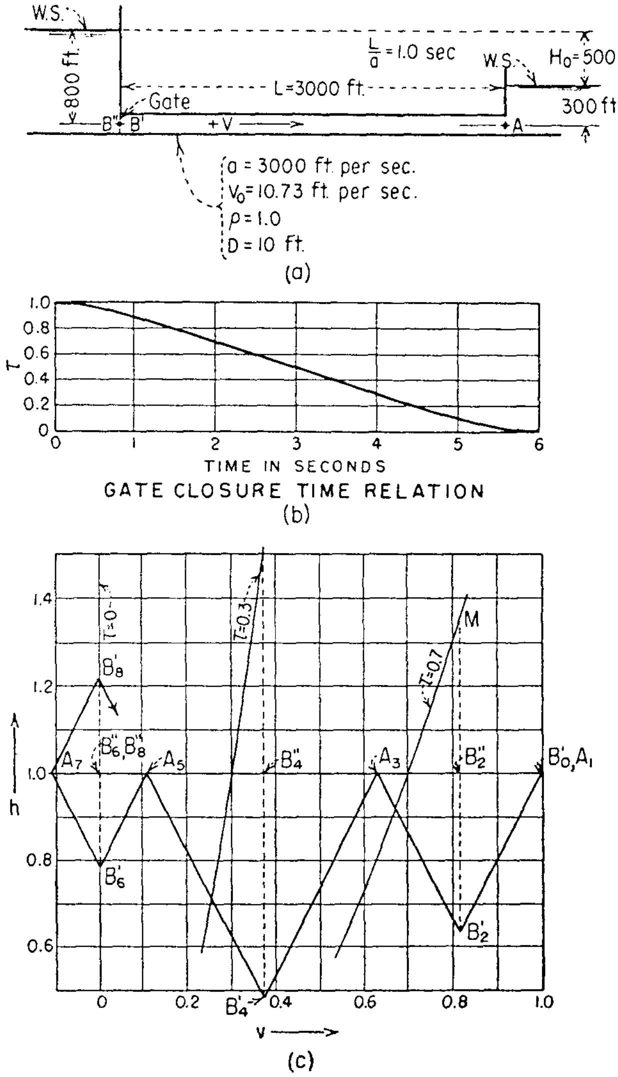

Figure 37

IX

Waterhammer Produced by Gate Opening

37. Fall in pressure produced by gate opening[1]

When the flow of water in a pressure conduit is retarded, the kinetic energy of the water is converted into potential energy as evidenced by an increase in the hydrostatic pressure. Conversely, when the flow of water in a closed conduit is increased, energy is supplied to set the water in motion, with a consequent reduction in the hydrostatic pressure. For example, consider the pipe line shown in Figure 38a and the effective gate opening shown in Figure 38b. Parabolas corresponding to the values of τ for 1-second time intervals are shown in Figure 38c. The initial velocity of water in the pipe is zero and hence the starting point of the graphical solution on the h-v diagram is at the point $h = 1$, $v = 0$. This locates the point for A_0, $B_{0.5}$, and $C_{1.0}$. The graphical waterhammer solution is then completed as shown in the figure.

38. Pressure rise produced by gate opening

After the initial drop in pressure due to a gate opening, a pressure rise above normal occurs because of the reflected waterhammer waves which return from the reservoir. For example, consider the pipe line shown in Figure 39a and the gate opening shown in Figure 39b. The waterhammer solution for the pressure changes at the gate is shown in Figure 39c from which it is seen that at $t = 6$ seconds the pressure rise is $0.10H_0$.

The maximum head rise due to a gate opening occurs when an initially closed gate is opened to its final position in $2L/a$ seconds or less and held there. To illustrate this, consider the pipe line shown in Figure 40a and the gate movement shown in Figure 40b, for which the graphical waterhammer solution is shown in Figure 40c. The maximum head rise at the gate due to the return of the reflected waves from the reservoir is $0.23H_0$ and occurs at $t = 4$ seconds. For this type of gate opening the head rise depends only upon the pipe line constant ρ_e. Hence the results of waterhammer solutions of this type can be indicated on a chart as shown in Figure 41. From this figure it is seen that the maximum head rise produced by a gate opening from zero gate is $0.23H_0$.

---

[1] See References 1 and 25.

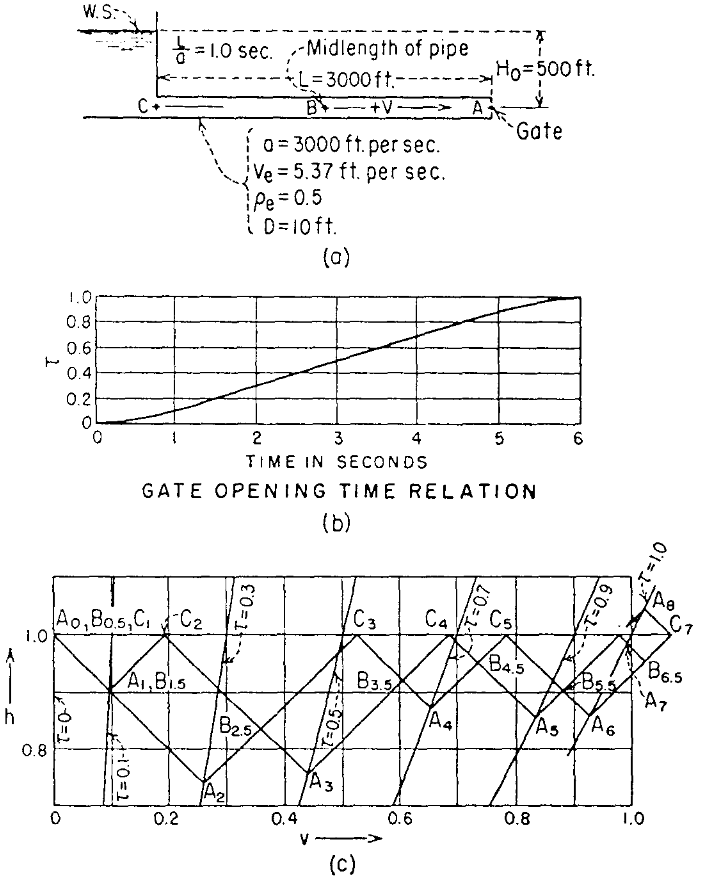

Figure 38

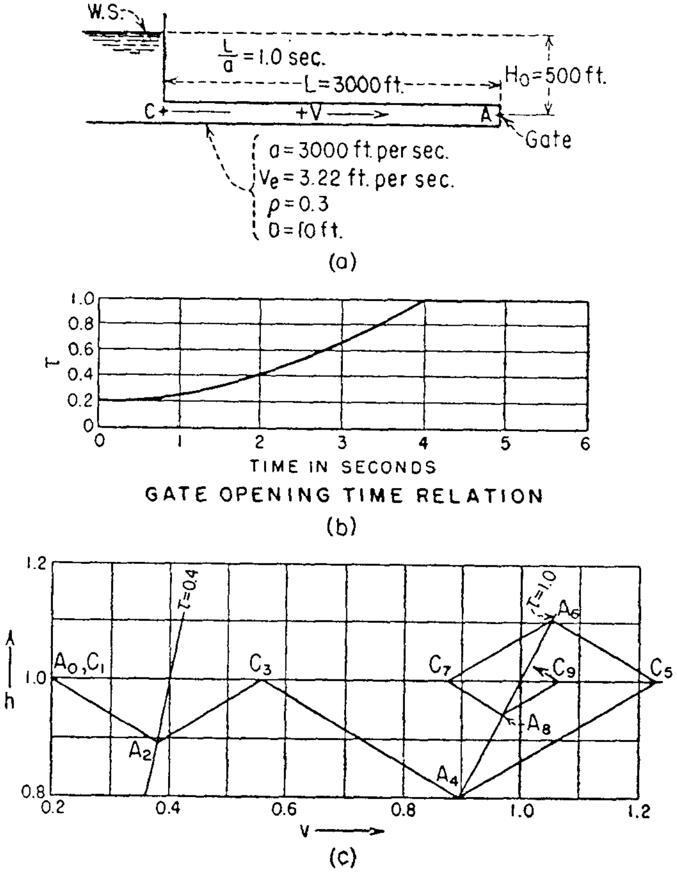

Figure 39

39. Rhythmic opening and closure of control gate[2]

Under certain conditions of gate operation, it is possible to obtain a rhythmic opening and closure of the regulating gate. Such conditions have been observed, for example, in hydraulic turbine installations due to governor action. If the gate motion is in phase with the motion of the waterhammer waves in the pipe line an appreciable head rise can occur. For example, consider the pipe line shown in Figure 42a and the gate movement time history shown in Figure 42b, for which the waterhammer solution is shown in Figure 42c. This solution indicates a maximum head rise of $1.24H_0$ at the gate when a complete cycle of gate operation

---

[2] See References 1 and 21.

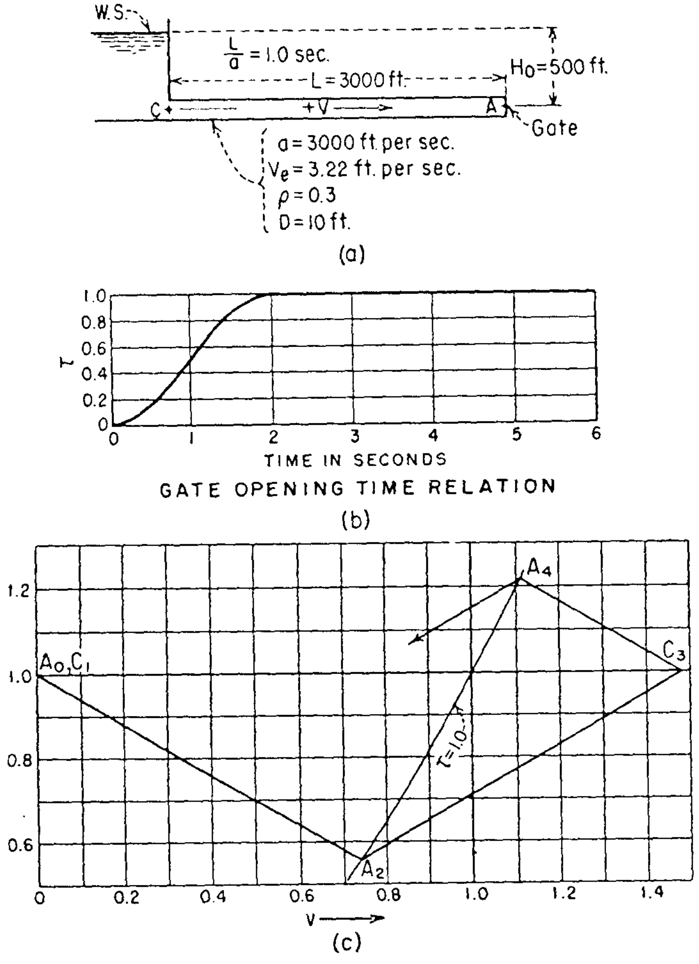

Figure 40

is performed in $4L/a$ seconds. Since the head rise due to this type of gate movement depends only upon the parameter ρ_e, the results of all possible solutions are indicated on a chart as shown in Figure 43. From this figure it is seen that as ρ_e increases, the maximum head rise approaches $2H_0$ as a limit.

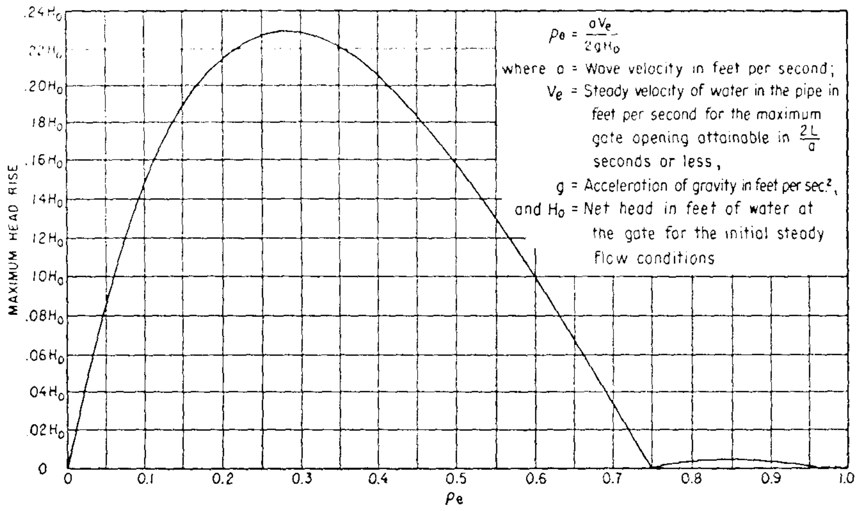

$\rho_e = \frac{aV_e}{2gH_0}$

where a = Wave velocity in feet per second;

V_e = Steady velocity of water in the pipe in feet per second for the maximum gate opening attainable in $\frac{2L}{a}$ seconds or less,

g = Acceleration of gravity in feet per sec.^{2},

and H_0 = Net head in feet of water at the gate for the initial steady flow conditions

MAXIMUM HEAD RISE AT GATE
DUE TO GATE OPENING

Figure 41

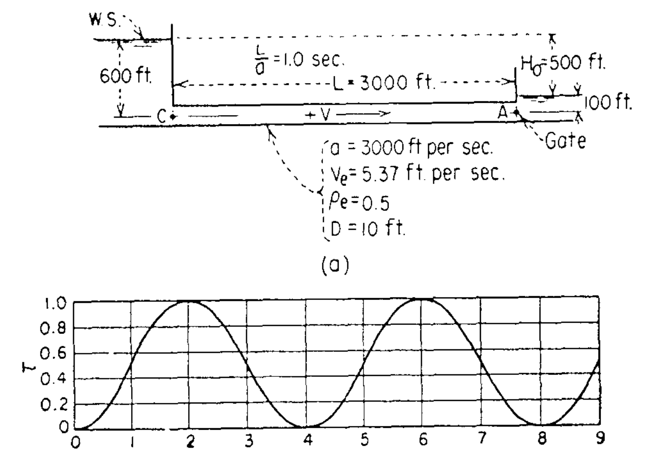

GATE MOVEMENT TIME RELATION

(b)

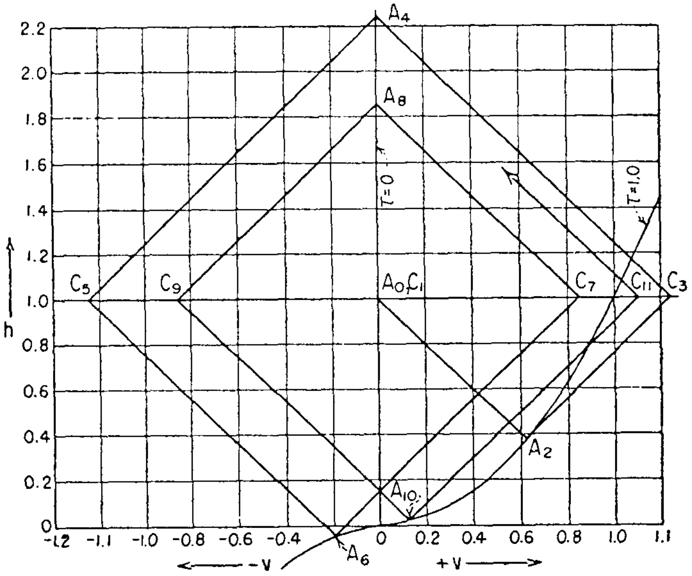

(c)

Figure 42

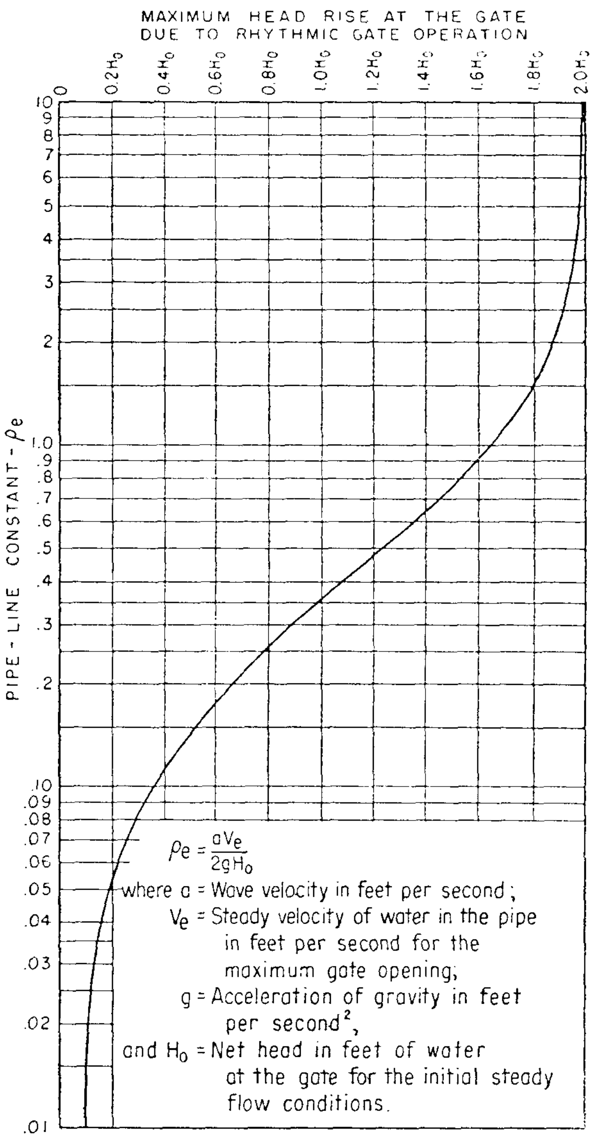

$\rho_e = \frac{aV_e}{2gH_0}$

where a = Wave velocity in feet per second;
V_e = Steady velocity of water in the pipe in feet per second for the maximum gate opening;
g = Acceleration of gravity in feet per second^2,
and H_0 = Net head in feet of water at the gate for the initial steady flow conditions.

MAXIMUM HEAD RISE AT GATE DUE TO RHYTHMIC GATE OPERATION

Figure 43

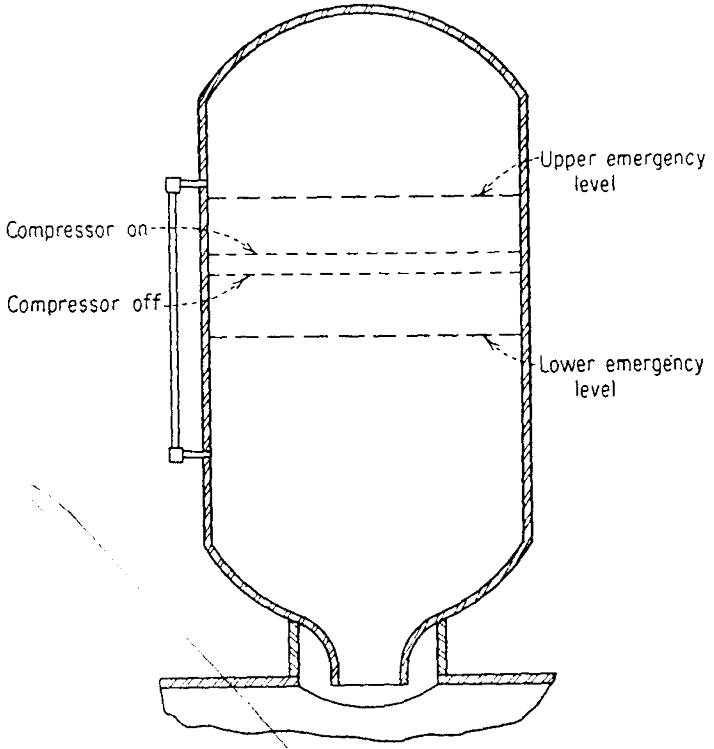

AIR CHAMBER CONTROL LEVELS

Figure 84

volume of the air chamber for these conditions, C_0 is computed from the charts in Figure 83 as before and is then increased by an amount equal to the volume of the chamber between the upper and lower emergency levels. A new value of $H^*_{\min}$ at the base of the chamber is then obtained from the charts. The total volume of the chamber C' is then determined from Equation (78), using the new values of $H^*_{\min}$ and C_0.

References

1. Allievi, L., *Theory of Waterhammer*, translated by E. E. Halmos, printed by Riccardo Garoni, Rome, Italy, 1925.
2. Allievi, L., "Air Chambers for Discharge Pipes," *Transactions ASME*, Vol. 59, Paper Hyd-59-7, November 1937, pp. 651–659.
3. Angus, R. W., "Simple Graphical Solution for Pressure Rise in Pipes and Pump Discharge Lines," *The Journal of the Engineering Institute of Canada*, February, 1935, pp. 72–81.
4. Angus, R. W., "Waterhammer in Pipes, Including Those Supplied by Centrifugal Pumps: Graphical Treatment," *Bulletin 152*, University of Toronto Press, 1938.
5. Angus, R. W., "Waterhammer Pressures in Compound and Branched Pipes," *Proceedings ASCE*, No. 2024, January 1938, pp. 340–401.
6. Angus, R. W., "Air Chambers and Valves in Relation to Waterhammer," *Transactions ASME*, Vol. 59, Paper Hyd-59-8, November, 1937, pp. 661–668.
7. Bergeron, L., "Etude des variations de regime dans les conduites d'eau: Solution graphique generale," *Revue generale de l'hydraulique*, Paris, Vol. 1, 1935, pp. 12–69.
8. Bergeron, L., *Du coup de belier en hydraulique au coup de foudre en electricite*, Dunod, Paris, 1950.
9. Bergeron, L., Discussion of L. Allievi's paper, "Air Chambers for Discharge Pipes," *Transactions ASME*, Vol. 61, July, 1939, pp. 441–445.
10. Billings, A. W. K., Dodkin, O. H., Knapp, F., and Santos, A., Jr., "High-Head Penstock Design," *Symposium on Waterhammer, ASME—ASCE*, 1933, pp. 29–61.
11. Calame, J., and Gaden, D., *Theorie des chambres d'equilibre*, Gauthur-Villars, Paris, 1926.
12. Crawford, C. C., "Curves for the Quick Estimation of Transient Hydraulic Conditions Following Failure of Electric Power to a Pumping Plant," *Thesis for M.S. Degree*, University of Colorado, 1948.
13. Dawson, F. M., and Kalinske, A. A., "Methods of Calculating Waterhammer Pressures," *Journal of the American Water Works Association*, Vol. 31, No. 11, November, 1939, pp. 1835–1864.
14. Durand, W. F., *Hydraulics of Pipe Lines*, D. Van Nostrand Company, Inc., New York, 1921.

15. Evans, W. E., and Crawford, C. C., "Design Charts for Air Chambers on Pump Lines," *Transactions ASME*, Vol. 119, No. 2710, 1954, pp. 1025–1045.

16. Gibson, N. R., "Pressures in Penstocks Caused by the Gradual Closing of Turbine Gates," *Transactions ASCE*, Vol. 83, 1919–1920, pp. 707–775.

17. Glover, R. E., "Computation of Waterhammer Pressures in Compound Pipes," *Symposium on Waterhammer, ASME—ASCE*, 1933, pp. 64–69.

18. Halmos, E. E., "Effects of Surge Tanks on the Magnitude of Waterhammer in Pipe Lines," *Symposium on Waterhammer, ASME—ASCE*, 1933, pp. 72–80.

19. Jacobson, R. S., "Charts for Analysis of Surge Tanks in Turbine or Pump Installations," *Special Report 104*, Bureau of Reclamation, Denver, Colorado, February, 1952.

20. Jaeger, C., "Waterhammer Effects in Power Conduits," *Civil Engineering and Public Works Review*, 1948.

21. Jaeger, C., "Theory of Resonance in Pressure Conduits," *Transactions ASME*, Vol. 61, February, 1939, pp. 109–115.

22. Johnson, R. D., "The Differential Surge Tank," *Transactions ASCE*, Vol. 78, 1915, pp. 760–805.

23. Johnson, R. D., "The Surge Tank in Water Power Plants," *Transactions ASME*, Vol. 30, No. 1204, 1908, pp. 443–501.

24. Joukowsky, N., "Waterhammer," Translated by Miss O. Simin, *Proceedings AWWA*, Vol. 24, 1904, pp. 341–424.

25. Kerr, S. L., "Fall in Pressure in Hydraulic Turbine Penstocks Due to Acceleration of Flow," *Power*, Vol. 60, No. 7, August, 1924, pp. 266–268.

26. Kerr, S. L., "New Aspects of Maximum Pressure Rise in Closed Conduits," *Transactions ASME*, Vol. 51 (1), Paper Hyd-51-3, 1929, pp. 13–30.

27. Kerr, S. L., and Strowger, E. B., "Resumé of Theory of Waterhammer in Simple Conduits," *Symposium on Waterhammer, ASME—ASCE*, 1933, pp. 15–24.

28. Kessler, L. H., "Speed of Waterhammer Pressure Waves in Transite Pipe," *Transactions ASME*, Vol. 61, January, 1939, pp. 11–15.

29. Knapp, R. T., "Complete Characteristics of Centrifugal Pumps and Their Use in the Prediction of Transient Behavior," *Transactions ASME*, Vol. 59, Paper Hyd-59-11, November, 1937, pp. 683–689.

30. Kruse, O. V., Discussion of N. R. Gibson's paper, "Pressures in Penstocks Caused by the Gradual Closing of Turbine Gates," *Transactions ASCE*, Vol. 83, 1919–1920, pp. 741–747.

31. Le Conte, J. N., "Experiments and Calculations on the Resurge Phase of Waterhammer," *Transactions ASME*, Vol. 59, Paper Hyd-59-12, November, 1937, pp. 691–694.

32. Moody, L. F., "Simplified Derivation of Waterhammer Formula," *Symposium on Waterhammer, ASME—ASCE*, 1933, pp. 25–28.

33. Parmakian, J., "Pressure Surges at Large Pump Installations," *Transactions ASME*, Vol. 75, August, 1953, pp. 995–1006.

34. Parmakian, J., "Pressure Surge Control at Tracy Pumping Plant," *Proceedings ASCE*, Vol. 79, Separate No. 361, December, 1953.

35. Peabody, R. M., "Typical Analysis of Waterhammer in a Pumping Plant of the Colorado River Aqueduct," *Transactions ASME*, Vol. 61, February, 1939, pp. 117–124.

36. Quick, R. S., "Comparison and Limitations of Various Waterhammer Theories," *Transactions ASME*, Vol. 49, No. 5a, May, 1927, pp. 524–530.

37. Rich, G. R., *Hydraulic Transients*, 1st ed., Engineering Societies Monographs, McGraw-Hill Book Co., Inc., New York, 1951.

38. Schnyder, O., "Comparisons Between Calculated and Test Results on Waterhammer in Pumping Plant," *Transactions ASME*, Vol. 59, Paper Hyd-59-13, November, 1937, pp. 695–700.

39. Stepanoff, A. J., *Centrifugal and Axial Flow Pumps*, John Wiley & Sons, Inc., New York, 1948.

40. Strowger, E. B., "Relation of Relief-Valve and Turbine Characteristics in the Determination of Waterhammer," *Transactions ASME*, Vol. 59, Paper Hyd-59-14, November, 1937, pp. 701–705.

41. Strowger, E. B., "Waterhammer Problems in Connection with the Design of Hydroelectric Plants," *Transactions ASME*, Vol. 67, July, 1945, pp. 377–392.

42. Strowger, E. B., and Kerr, S. L., "Speed Changes of Hydraulic Turbines for Sudden Changes of Load," *Transactions ASME*, Vol. 48, No. 2009, 1926, pp. 209–262.

43. *Symposium on Waterhammer, ASME—ASCE*, 1933.

44. Thoma, D., *Beitrage zur Theorie des Wasserschlosses bei selbsttatig geregelten Turbinenanlagen*, Oldenburg, Munchen, 1910.

45. Timoshenko, S., *Strength of Materials*, 2d ed., Part 2, D. Van Nostrand Company, Inc., New York, 1941.

46. Warren, M. M., "Penstock and Surge Tank Problems," *Transactions ASCE*, Vol. 79, 1915, pp. 238–305.

47. Wood, F. M., "The Application of Heavisides Operational Calculus to the Solutions of Problems in Waterhammer," *Transactions ASME*, Vol. 59, Paper Hyd-59-15, November, 1937, pp. 707–713.

Chapter VIII

18. A pipe line has the following characteristics: $L = 2400$ feet, $a = 3200$ feet per second, $H_0 = 325$ feet and $V_0 = 5.5$ feet per second.

(a) Compute the maximum head rise at the control gate and one-third points in the pipe line for uniform gate closure to the half open gate position in 3 seconds.

(b) Construct a pressure time history diagram for the pressure changes at the control gate from $t = 0$ to $t = 6$ seconds. *Ans.* (a) 85 feet, 60 feet, and 30 feet.

19. Compute the maximum head at the control gate and the junction B for the pipe line shown in Figure 90 for the following gate closure:

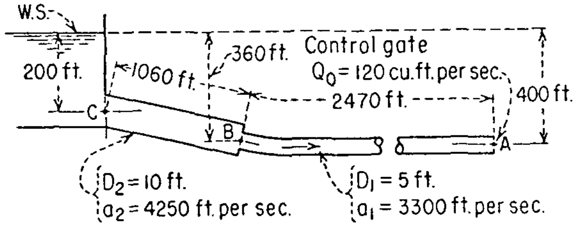

Figure 90

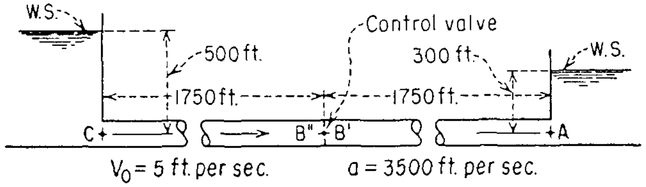

Figure 91

t (seconds),	0	0.5	1.0	1.5	2.0	2.5	3.0	3.5	4.0	4.5	5.0
τ,	1.00	0.77	0.60	0.46	0.36	0.28	0.20	0.15	0.10	0.05	0

Ans. 655 feet and 405 feet.

20. Compute the maximum head rise at B'' for the pipe line shown in Figure 91 for a uniform gate closure in 5 seconds. *Ans.* 75 feet.

21. Compute the maximum head at the gate and mid-length for the pipe line shown in Figure 92 for the following control gate and relief valve operation:

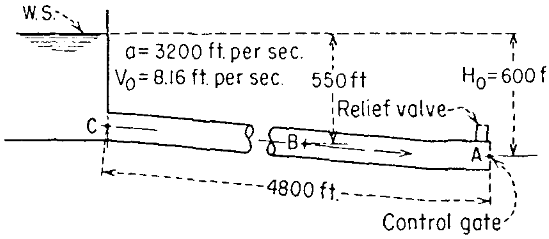

Figure 92

t (seconds),	0	1.5	3.0	4.5	6.0
τ (control gate),	1.00	0.58	0.30	0.13	0
τ (relief valve),	0	0.14	0.40	0.65	0.8

Ans. 770 feet and 705 feet.

22. Compute the minimum head at B' for the pipe line shown in Figure 93 for the following gate closure:

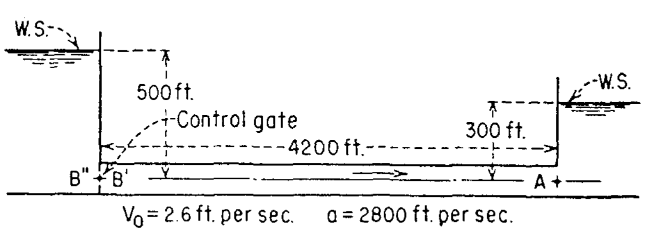

Figure 93

t (seconds),	0	1.5	3.0	4.5	6.0	7.5
τ,	1.00	0.90	0.70	0.50	0.30	0

Ans. 235 feet.

Chapter IX

23. A pipe line has the following characteristics: $L = 4800$ feet, $H_0 = 400$ feet, $a = 3200$ feet per second and $V_e = 4$ feet per second. Determine the minimum and maximum head at the control gate for the following gate opening:

t (seconds),	0	1.5	3.0	4.5	6.0
τ,	0	0.49	0.77	0.93	1.0

Ans. 190 feet and 415 feet.

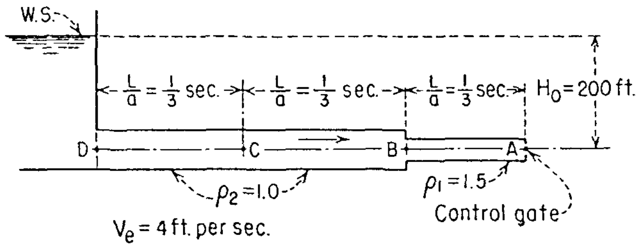
W.S.
$\frac{L}{a} = \frac{1}{3}$ sec.
$\frac{L}{a} = \frac{1}{3}$ sec.
$\frac{L}{a} = \frac{1}{3}$ sec.
H_0 = 200 ft.
D
C
B
A
ρ_2 = 1.0
ρ_1 = 1.5
Control gate
V_e = 4 ft. per sec.

Figure 94

24. Compute the minimum head at the points A, B, and C for the pipe line shown in Figure 94 for a uniform gate opening in $5\frac{1}{3}$ seconds. *Ans.* 90 feet, 120 feet, and 150 feet.

Rossing p. 17-23

Vibrating Systems

Nature provides many examples of vibrating systems: trees swaying in the wind, atoms in a molecule of water, the motion of the tides, electric current in a flash of lightning, and so on. Although the motion is vastly different in each of these systems, they have several things in common: For one thing, the motion repeats in each regular time interval, which we call the *period* of the vibration; second, some type of *force* constantly acts to restore the system toward its point of equilibrium.

2.1 SIMPLE HARMONIC MOTION

Consider the very simple vibrating system in Fig. 2.1 consisting of a mass m attached to the end of a spring. We assume that the amount of stretch in the spring is proportional to the stretching force (which is true of most springs if they are not stretched too far), so that in order to stretch it a length l a force Kl is required. The symbol K is the *spring constant* or "stiffness" of the spring.

Since the spring is vertical, the force of gravity on the mass stretches the spring by an amount that remains constant. In the equilibrium position shown in Fig. 2.1(b), the downward force of gravity on the mass (its weight) is just balanced by the upward force exerted by the spring; therefore the system is in equilibrium. The description of the motion is simplified if we specify the displacement of y of the mass from the equilibrium position and the net force F that acts on the mass. The relationship between F and y is easily shown to be

$$F = -Ky. \tag{2.1}$$

The minus sign in the above equation reminds us that when the mass is below its equilibrium position (y is negative), the net force will be upward (F is positive) as shown in Fig. 2.1(a). Thus the force F could be called a *restoring force*, which always acts in a direction to restore m to its equilibrium position. When the restoring force is proportional to the displacement, as it is in most vibrating systems we study, the motion is given a special name: *simple harmonic motion*. For a system in simple harmonic motion, the period is independent of the amplitude (size) of the vibration. The *frequency* f of vibration is the number of oscillations per second, which is obviously the reciprocal of the period T of one vibration:

$$f = 1/T. \tag{2.2}$$

It is customary to use a unit called the *hertz* (abbreviated Hz) to denote cycles per second. In the case of the vibrating mass-spring system, the frequency of vibration is given by the formula

$$f = \frac{1}{2\pi}\sqrt{\frac{K}{m}}. \tag{2.3}$$

Note that to double the frequency of vibration, the mass m may be reduced to one-fourth its original size, or the spring constant K may be made four times larger.

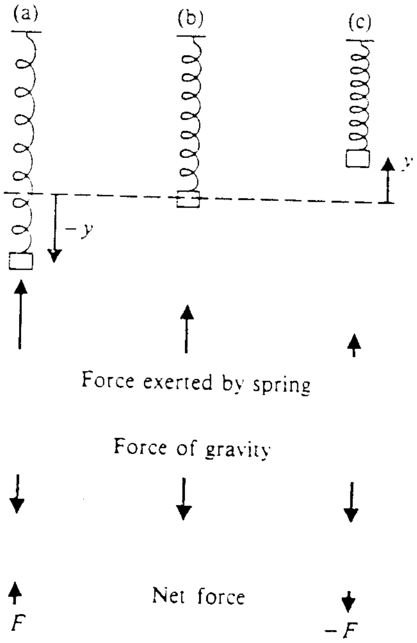

FIG. 2.1
A simple vibrator consisting of mass and spring. In (b) the upward force exerted by the spring and the force of gravity balance each other, and the net force F on the mass is zero.

Numerical Example

Suppose a certain spring stretches 0.10 m when loaded with 2 kg. What is its spring constant? At what frequency will it vibrate when loaded with 2 kg? 0.5 kg?

Solution: At rest $Kl=mg$, so

$$K=\frac{mg}{l}=\frac{2(9.8)}{0.10}=196 \text{ N/m (newtons per meter).}$$

Its frequency of vibration when $m=2$ kg is

$$f=\frac{1}{2\pi}\sqrt{\frac{K}{m}}=\frac{1}{(2)(3.14)}\sqrt{\frac{196}{2}}=\frac{\sqrt{98}}{6.28}=1.6 \text{ Hz.}$$

When loaded with 0.5 kg, the frequency is

$$f=\frac{1}{2\pi}\sqrt{\frac{K}{m}}=\frac{1}{(2)(3.14)}\sqrt{\frac{196}{0.5}}=\frac{\sqrt{392}}{6.28}=3.2 \text{ Hz.}$$

A strobe photograph of a mass-spring system was shown in Fig. 1.9. Also shown was a graph of position y as a function of time. A graph of speed v versus time can be made by taking the slope of that graph at every time t. Graphs of y and v as functions of time are shown in Fig. 2.2. Mathematicians refer to curves shaped like these as *sinusoidal* or *sine* curves. The maximum value of y is called the *amplitude*.

2.2 ENERGY AND DAMPING

The formula for the kinetic energy KE of a moving mass was given in Section 1.7:

$$\text{KE}=\tfrac{1}{2}mv^2, \tag{2.4}$$

where m is mass and v is speed. Similarly, the potential energy PE of a spring, stretched or compressed a distance y from its equilibrium length, was given as

$$\text{PE}=\tfrac{1}{2}Ky^2. \tag{2.5}$$

From the graphs in Fig. 2.2, it is clear that v^2 reaches its maximum value when y^2 is zero and vice versa. Thus, the total mechanical energy is constantly changing from kinetic to potential to kinetic. At times t_1 and t_3, potential energy is a maximum, and at t_2 and t_4, kinetic energy is a maximum.

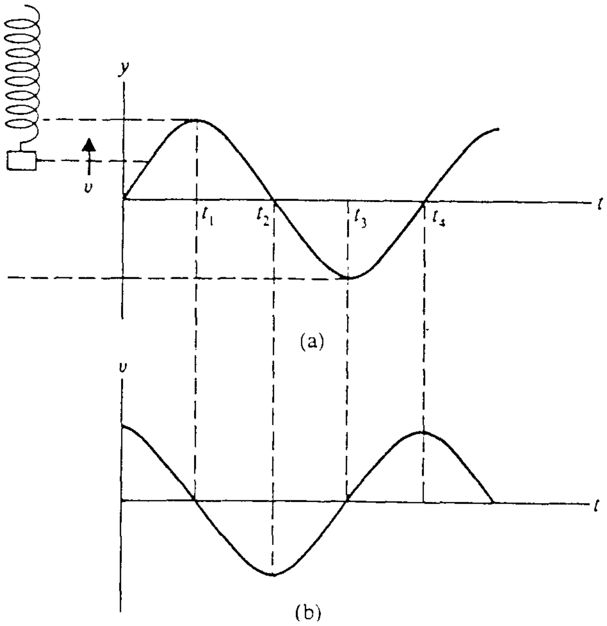

FIG. 2.2
Graphs of simple harmonic motion: (a) displacement vs. time; (b) speed vs. time. Note that speed reaches its maximum when displacement is zero and vice versa.

Any real vibrating system tends to lose mechanical energy as a result of friction and other loss mechanisms. Unless the energy is renewed in some way, the amplitude of the vibrations will decrease with time, as shown in Fig. 2.3. In many vibrating systems, a certain fraction (usually small) of the energy is lost during each cycle of vibration; the result is a curve that decreases in amplitude in the manner shown in Fig. 2.3. The dotted curve, which indicates the change in amplitude with time, is called the *envelope*, or decay curve. A vibrating system whose amplitude decreases in this way is said to be *damped*, and the rate of decrease is the *damping constant*.

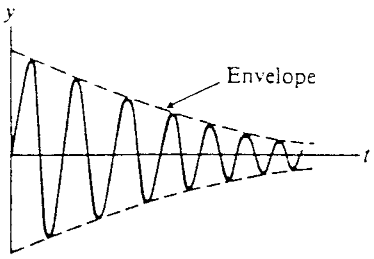

FIG. 2.3
Displacement of a damped vibrator whose amplitude decreases with time.

2.3 SIMPLE VIBRATING SYSTEMS

Besides the mass-spring system already described, the following are examples of systems that vibrate in simple harmonic motion:

1. *Pendulum (small angle)*. A simple pendulum, consisting of a mass m attached to a string of length l (see Fig. 2.4), vibrates in simple harmonic motion, provided that $x \ll l$. Assuming that the mass of the string is much less than m, the frequency of vibration is

$$f = \frac{1}{2\pi}\sqrt{\frac{g}{l}}, \tag{2.6}$$

where g is the acceleration due to gravity. Note that the frequency does not depend on the mass.

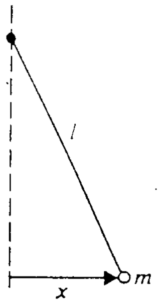

FIG. 2.4
A simple pendulum.

2. *A "spring" of air*. A piston of mass m, free to move in a cylinder of area A and length l, vibrates in much the same manner as a mass attached to a spring (see Fig. 2.5). The spring constant of the air in the cylinder is determined by its compressibility and turns out to be $K = \gamma pA/l$, so the frequency is

$$f = \frac{1}{2\pi}\sqrt{\frac{\gamma pA}{ml}}, \tag{2.7}$$

where p is the gas pressure, A is the area, m is the mass of the piston, and γ is a constant that is 1.4 for air.

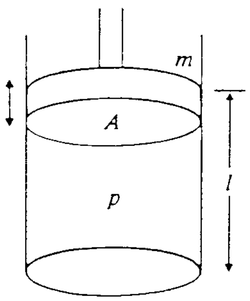

FIG. 2.5
A piston free to vibrate in a cylinder.

3. *A Helmholtz resonator*. Another common type of air vibrator, illustrated in Fig. 2.6, is often called a Helmholtz resonator, after H. von Helmholtz (1821–1894), who used it to analyze musical sounds. The mass of air in the neck now serves as the "piston," and the air in the larger volume V as the "spring." The frequency of vibration is

$$f = \frac{v}{2\pi}\sqrt{\frac{a}{Vl}}, \tag{2.8}$$

where a is the area of the neck, l is its length, V is the volume of the resonator, and v is the speed of sound ($v \simeq 344$ m/s).

In Fig. 1.7(a), the speed remains unchanged in time; in Fig. 1.7(b) it increases at a steady rate. The acceleration in Fig. 1.7(a) is therefore zero; in Fig. 1.7(b) it is

$$a = \frac{35\ \text{cm/s}}{0.5\ \text{s}} = 70\ \text{cm/s}^2.$$

Note the units for acceleration; the unit cm appears to the first power, but the unit s appears squared.

An object in *free fall* in the gravitational field of the earth ex-

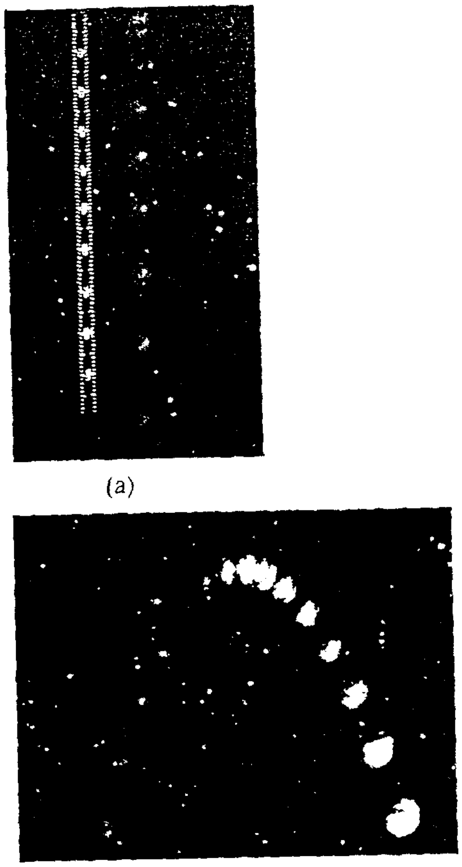
(a)

(b)

FIG. 1.8
Stroboscopic photographs of two objects in free fall: (a) object dropped from rest; (b) object thrown upward. (Photographs by Christopher Chiaverina.)

periences a constant acceleration of 9.8 meters/second². Thus if it begins with no initial speed (up or down), at the end of the first second it will have a speed of 9.8 m/s; at the end of 2 seconds its speed will be 19.6 m/s, and so on.

Note that acceleration does not always increase speed. If an object is thrown upward, the acceleration due to gravity acts to slow it down (sometimes this is called "deceleration"). Figure 1.8 shows stroboscopic photographs of two objects in free fall. In Fig. 1.8(a), the object is dropped from rest; in Fig. 1.8(b), it is thrown upward, slows down, and then begins its descent.

Figure 1.9 shows a stroboscopic photograph of an object with an acceleration that changes its direction with time. The object, a mass attached to a spring, is executing a type of vibratory motion called "simple harmonic" motion, which will be discussed in Chapter 2. The camera has been turned during the exposure, so that multiple images of the object create a photographic record of position as a function of time. Note that position y, speed v, and acceleration a all change with time.

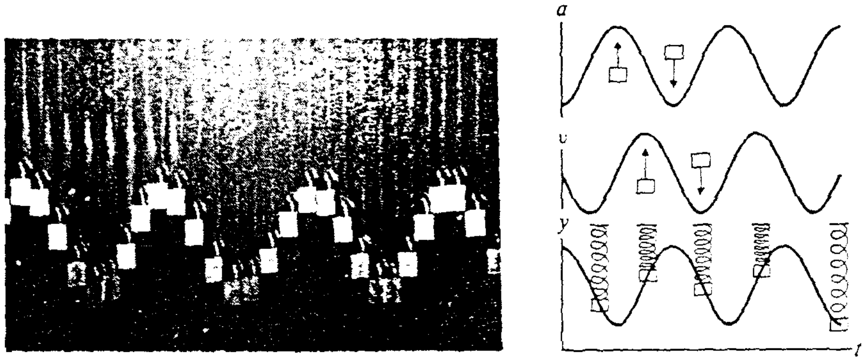

(a)

(b)

FIG. 1.9
Vibratory motion in which y, v, and a all change with time.

1.5 FORCE, MASS, AND NEWTON'S LAWS

Force is a quantity with which we are all familiar; it can be described as a "push" or a "pull." Practically all human activity involves forces: running, lifting, eating, writing, even standing.

The Helmholtz resonator can be thought of as having a mass m and a spring constant K that are:

$$m = \rho a l \quad \text{and} \quad K = \frac{\rho a^2 v^2}{V}, \tag{2.9}$$

where ρ is the density of air.

Helmholtz resonators can have a variety of shapes and sizes. For example, blowing air across an empty pop bottle causes the air in its neck to vibrate at a fairly low frequency. Note that the smaller the neck diameter a, the lower the frequency of vibration, which may seem a little surprising at first glance.

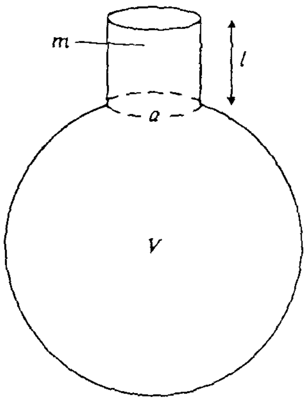

FIG 2.6
A Helmholtz resonator.

2.4 SYSTEMS WITH TWO OR THREE MASSES

The vibrating systems considered in the preceding section have one thing in common: A single coordinate is sufficient to describe their motion. In other words, they have one *degree of freedom*. In this section, we will consider vibrators with two or more degrees of freedom.

Such systems have more than one *mode* of vibration, and the different modes will generally have different frequencies.

Consider the system consisting of two masses and three springs shown in Fig. 2.7. The system has two "normal" or independent modes, as shown in Figs. 2.7(a) and 2.7(b). In one mode, the masses move in the same direction; in the other, they move in opposite directions. Assuming equal masses and springs with the same stiffness K, the frequencies of the two modes are

$$f_a = \frac{1}{2\pi}\sqrt{\frac{K}{m}}, \qquad f_b = \frac{1}{2\pi}\sqrt{\frac{3K}{m}}\,. \tag{2.10}$$

Note that mode (a) has the same frequency as the simple mass-spring system shown in Fig. 2.1, whereas mode (b) has a frequency that is 1.7 times that of mode (a).

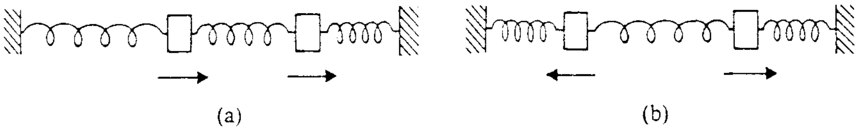

FIG. 2.7
Modes of vibration of a two-mass vibrator. The mode shown in (a), in which the masses move in the same direction, will have the lower frequency.

Modes (a) and (b) are virtually independent of each other. That is, the system can vibrate in mode (a) with minimal excitation of mode (b), and vice versa. If one sets the system into oscillation by giving the two masses a push or pull, the resulting motion will nearly always be a combination of modes (a) and (b). There are many recipes for combining these two modes in different proportions, and thus many ways in which the system can vibrate.

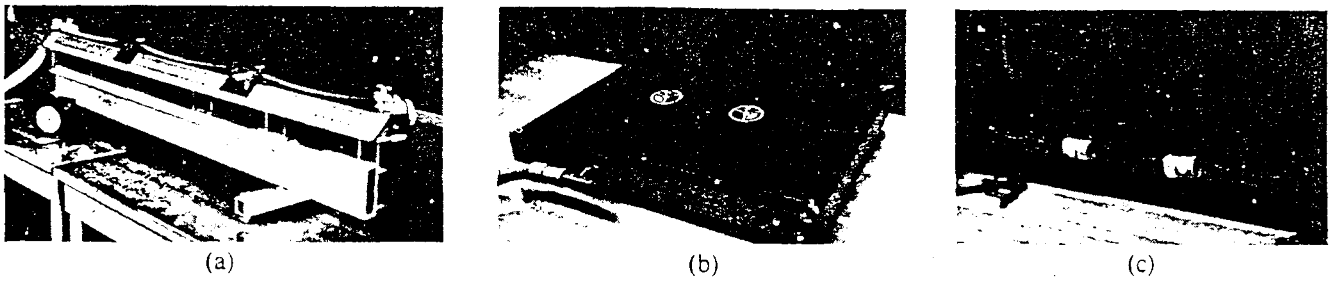

FIG. 2.8
Two-mass vibrators using (a) a linear air track; (b) an air table; (c) masses and springs hung from an overhead rod.

A great deal about the physics of vibration can be learned from watching the motion of a two-mass vibrator. Many physics laboratories have linear air tracks or air tables, on which objects move on a film of air with negligible friction. These are ideal for studying two-mass oscillators. Another convenient arrangement is to hang the masses on long cords from the ceiling or an overhead rod. The cords must be as long as possible to minimize the tendency of the masses to swing like pendulums. These three arrangements are shown in Fig. 2.8.

On the linear air track shown in Fig. 2.8(a), the masses are constrained to move in one direction only. In the systems shown in Figs. 2.8(b) and 2.8(c), however, the masses can move at right angles to the springs as well. Vibrations in this direction are called *transverse* vibrations, whereas vibrations in the direction of the springs are called *longitudinal* vibrations. Some systems vibrate only in transverse modes, some only in longitudinal. The air column of a musical wind instrument, for example, vibrates longitudinally, whereas the membrane of a drum vibrates transversely. A violin string normally vibrates transversely, although longitudinal vibrations (which sound like squeeks or squeals) are occasionally excited by the bowing of unskilled players.

In addition to their two modes of longitudinal vibration, the two-mass systems shown in Figs. 2.8(b) and 2.8(c) have two modes of transverse vibration, which are shown in Fig. 2.9. In the mode of lower frequency, the masses move in the same direction; in the mode of higher frequency, they move in opposite directions; this is similar to the longitudinal modes shown in Fig. 2.7.

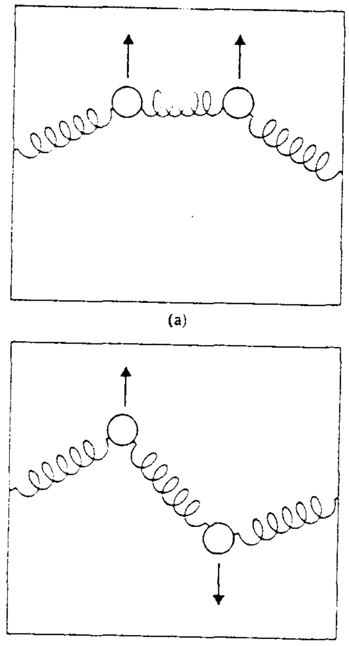

FIG. 2.9
Modes of transverse vibration of a two-mass system. (a) In the mode of lower frequency, masses move in the same direction; (b) in the mode of higher frequency, masses move in opposite directions.

Adding a third mass to the systems of Fig. 2.7 adds additional modes of vibration. In the case of the linear vibrator in Fig. 2.7(a), which vibrates only longitudinally, a third mode of longitudinal vibration appears. The three independent modes of vibration are those shown in Fig. 2.9. The systems in Figs. 2.7(b) and 2.7(c) can vibrate transversely as well; in addition to the three modes of longitudinal vibration in Fig. 2.10, they will have the three independent modes of transverse vibration shown in Fig. 2.11.

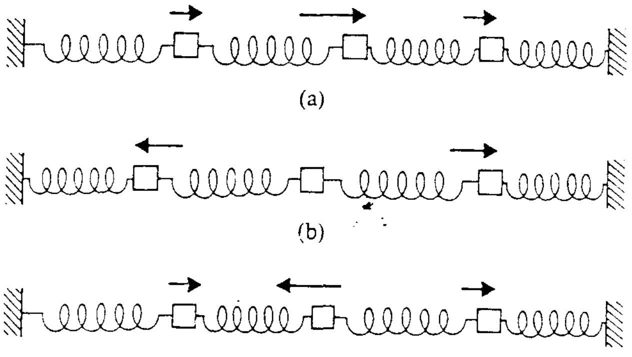

FIG. 2.10
Independent modes of longitudinal vibrations of a three-mass vibrator.

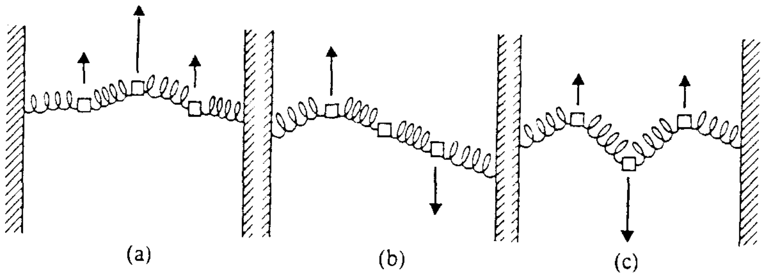

FIG. 2.11
Independent modes of transverse vibration of a three-mass oscillator.

The independent modes shown in Figs. 2.7, 2.9, 2.10 and 2.11 are often called the *normal* modes of the vibrating systems. Getting the system to vibrate in a single normal mode requires special care. It is perhaps best done by driving the system at the frequency of the desired mode (this phenomenon, called *resonance*, will be discussed in Chapter 4). Carefully displacing the masses by the proper amounts and releasing them will also cause the system to vibrate in a single mode.

Compressible-Fluid Dynamics
Philip A. Thompson
McGraw-Hill 1972, p. 392-402

8.6 Piston-induced motion of a perfect gas

As a further application of the theory of simple waves we take up the motion of an initially stationary gas confined within a cylinder closed by a piston. The cases of piston *withdrawal* and piston *advance* will be treated separately.

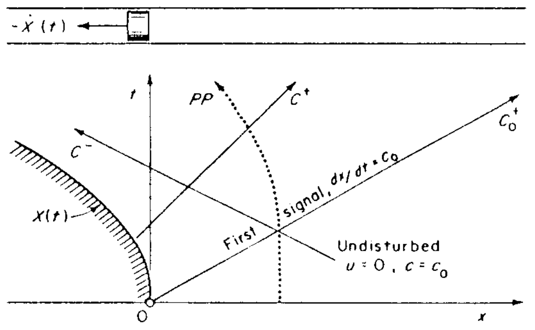

Figure 8.17
Wave diagram for continuous piston withdrawal.

Continuous Piston Withdrawal

At time zero a tube contains gas at uniform state $u = 0$, $c = c_0$. Piston withdrawal is initiated at this time, with finite acceleration (Fig. 8.17). The tube is assumed to be sufficiently long to ensure that no reflected disturbances from the right-hand end appear during the time of interest; i.e., the wave motion remains simple.[1]

This problem can be solved analytically. Let the piston position be given by the known function $X(t)$, with $\dot X < 0$. At $t = 0$ a sound wave leaves the piston and travels into undisturbed fluid; this is the *first signal*, and below this characteristic is necessarily an *undisturbed region*. We then have simple waves with the characteristics C^- originating in this region. We assume, subject to future verification, that every C^- characteristic reaches the piston path line $X(t)$. Then with $J^- = $ const everywhere, with (8.15),

$$u - \frac{2}{\gamma - 1} c = -\frac{2}{\gamma - 1} c_0 \qquad \text{everywhere} \tag{8.26}$$

This equation reduces the number of unknowns to one; the specified piston motion then determines the problem. A typical (straight) characteristic C^+ carries constant c and constant u; the value of u is thus necessarily just the piston velocity $\dot X$ where C^+ intersects $X(t)$, assuming that the gas does not separate from the piston. Then on C^+

$$u = \dot X \qquad c = c_0 + \frac{\gamma - 1}{2} \dot X \tag{8.27}$$

the latter relation following from (8.26). Note that $c \le c_0$ because $\dot X < 0$; then $P \le P_0$ from the isentropic relation, as one would intuitively expect.

The (inverse) slope of the C^+ characteristic is $dx/dt = u + c$, which is from (8.26) and (8.27)

$$u + c = c_0 + \frac{\gamma + 1}{2} \dot X \tag{8.28}$$

For sufficiently large piston speeds this goes to zero (so that C^+ is vertical) when $u = -c$, corresponding to a sonic flow to the left, with conditions necessarily *constant* in time at the corresponding value of x. This sonic value of u, from (8.28) set to zero, is $u = \dot X = -[2/(\gamma + 1)]c_0$ or

$$|u|_{\text{sonic}} = \frac{2}{\gamma + 1} c_0 \tag{8.29}$$

This may be compared with the sonic flow speed for *steady* isentropic acceleration, which is, from (5.56),

$$|u|_{\text{sonic}} = \sqrt{\frac{2}{\gamma + 1}}\, c_0 \tag{8.30}$$

At very large piston speed, the sound speed given by (8.27) goes to *zero* (with the corresponding values of pressure, density, and temperature also formally zero from the isentropic relations). This occurs at $\dot X = -[2/(\gamma - 1)]c_0$ or

$$|u|_{\text{escape}} = \frac{2}{\gamma - 1} c_0 \tag{8.31}$$

which is the *escape speed*, as will be explained. With $c = 0$, the slopes of the particle path and characteristics C^+ and C^- ($dx/dt = u$, $u + c$, and $u - c$, respectively) are necessarily identical, so that these three lines are congruent (see the characteristic labeled $C^\pm$ in Fig. 8.18). Even though the piston may accelerate to still higher speed, the gas cannot physically expand to lower sound speed, so that the gas must *separate* from the piston, as illustrated in the wave diagram. The rather large flow speed given by (8.31), on the order of a few kilometers per second, is called the escape speed because it is just the limiting speed of gas which is allowed to expand suddenly into a vacuum. It may be compared to the limiting speed of a perfect gas expanded into a vacuum in *steady* isentropic flow,

---

[1] Physical examples of piston-withdrawal (rarefaction) flows include the internal flows associated with the popping of a champagne cork and the discharge of a cannon.

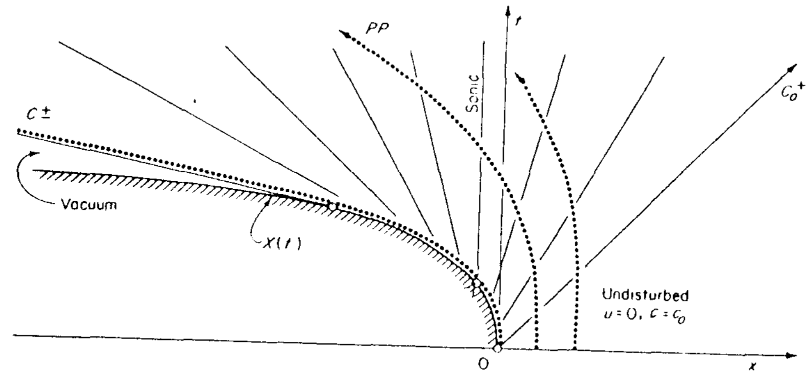

Figure 8.18
Wave diagram illustrating separation of the gas from the piston at the escape speed.

which is, from Eq. (5.61),

$$|u|_{\max} = \sqrt{\frac{2}{\gamma - 1}}\, c_0 \qquad (8.32)$$

where c_0 is the stagnation sound speed.

The physical attainment of the escape speed (8.31) is doubtful because the requisite piston speed would be difficult to attain and because the *equilibrium* isentropic expansion of a gas would eventually result in condensation of liquid or solid. Even if condensation did not set in, by virtue of the very rapid expansion, the gas would eventually become so dilute ($\Lambda \to \infty$ as $\rho \to 0$) that the continuum theory of gasdynamics would no longer be tenable.

The problem of putting the preceding results for piston withdrawal (which are that u and c have known values along the straight C^+ characteristics of known slope) into analytical form is an exercise in elementary analytic geometry which we will not pursue.

Impulsive Piston Withdrawal

The simplest possible piston withdrawal is the impulsive motion

$$\dot{X} = \begin{cases} 0 & t < 0 \\ \text{const} < 0 & t > 0 \end{cases}$$

That is, the piston instantaneously acquires some constant velocity $\dot{X} < 0$. As before, the gas is initially at rest with uniform conditions $u = 0$, $c = c_0$, as shown in Fig. 8.19.

In this problem the origin is a singular point where the velocity takes on all possible values between zero and $\dot{X}$; this can be accomplished only by the intersection of C^+ characteristics at the origin, giving multiple values for u and c at that point. This is superficially like a shock discontinuity; the difference is that this discontinuity does not persist in time but immediately decays, following the rule that *rarefaction waves spread out*.

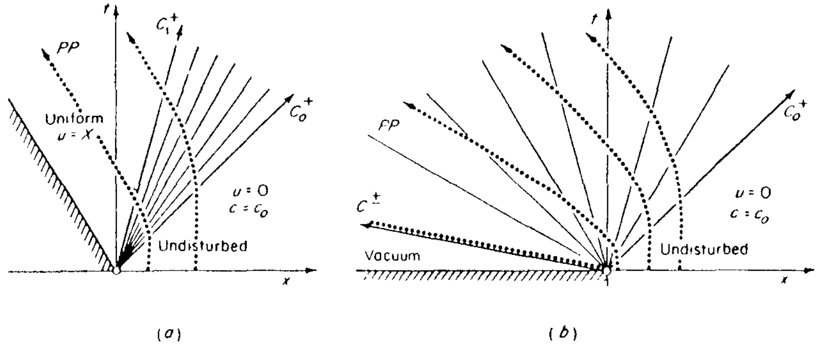

Figure 8.19
Wave diagram for impulsive piston withdrawal: (*a*) finite piston speed; (*b*) infinite piston speed.

The radiation of C^+ characteristics from the origin may be thought of as the limit for increasing piston ac[illegible]ion to constant velocity. In the finite-acceleration case considered previously, the C^+ characteristics spread out from the curved piston path. As the curvature (acceleration) of the path is increased, these characteristics crowd together, until finally in the limit they radiate from a single point, i.e., the origin.

The region of radiating characteristics is called the *fan* or *expansion fan* or *centered rarefaction*. The xt field is then divided into three regions, viz., the undisturbed region, the fan, and the uniform region where $u = \dot{X}$. Consider the fan region of Fig. 8.19*a*; because the wave is simple, with $J^- =$ const everywhere, we have, from Eq. (8.27),

$$c = c_0 + \frac{\gamma - 1}{2} u$$

and from geometry the C^+ characteristics are straight lines given by

$$\frac{x}{t} = u + c = c_0 + \frac{\gamma + 1}{2} u \qquad 0 \geq u \geq \dot{X}$$

Solving this for u and c in terms of x/t gives the dimensionless forms (with the conditions in the undisturbed region listed also, for completeness)

$$\left.\begin{aligned} \frac{u}{c_0} &= 0 \\ \frac{c}{c_0} &= 1 \end{aligned}\right\} \quad \infty > \frac{x}{c_0 t} \geq 1 \qquad (8.33)$$

$$\left.\begin{aligned} \frac{u}{c_0} &= -\frac{2}{\gamma + 1}\left(1 - \frac{x}{c_0 t}\right) \\ \frac{c}{c_0} &= 1 - \frac{\gamma - 1}{\gamma + 1}\left(1 - \frac{x}{c_0 t}\right) \end{aligned}\right\} \quad 1 \geq \frac{x}{c_0 t} \geq 1 + \frac{\gamma + 1}{2}\frac{\dot{X}}{c_0} \qquad (8.34)$$

so that in this case we have simple explicit formulas for u and c in terms of the independent variables.

The expansion process is terminated on the C^+ characteristic where u reaches its final value $\dot{X}$. The properties in the uniform region are then found to be

$$\left.\begin{aligned}\frac{u}{c_0} &= \frac{\dot{X}}{c_0}\\ \frac{c}{c_0} &= 1 + \frac{\gamma - 1}{2}\frac{\dot{X}}{c_0}\end{aligned}\right\} \quad 1 + \frac{\gamma + 1}{2}\frac{\dot{X}}{c_0} \geq \frac{x}{c_0 t} \geq \frac{\dot{X}}{c_0} \tag{8.35}$$

It is a remarkable feature of some unsteady flows that such regions of (temporarily) *steady* flow exist.

Just as before, the sound speed (and therefore the pressure and density) is zero at the escape speed, $u = -2c_0/(\gamma - 1)$. For piston speeds greater than this, the above formulas are invalid, as they would imply negative pressures; the expansion process is then terminated at $c = 0$ (Fig. 8.19*b*). We may conveniently call this the case of *infinite piston speed* [although the flow field is the same for all piston speeds greater than $2c_0/(\gamma - 1)$]. Physically, such a flow is approximated by sudden expansion into a vacuum, as when a barrier at $x = 0$ is instantaneously removed, e.g., by the rapid rupture of a diaphragm. The gas then escapes into the vacuum region.

The distribution of pressure, density, and sound speed, determined from (8.34) and the isentropic relations, is shown in Fig. 8.20 for the case of expansion to zero pressure (infinite piston speed or expansion into a vacuum) and expansion to finite pressure. These figures illustrate a property of characteristics which has not been mentioned, that *discontinuities in the derivatives of the independent variables*, for example in $\partial c/\partial x$, *may occur on characteristics*. In the problem at hand, the derivatives of u and c are discontinuous across C_0^+ and C_1^+ (Fig. 8.19*a*). Certain characteristics thus represent second-order surfaces of discontinuity in physical space and are somewhat analogous to shock waves. (A further discussion of these points appears in Sec. 9.4.)

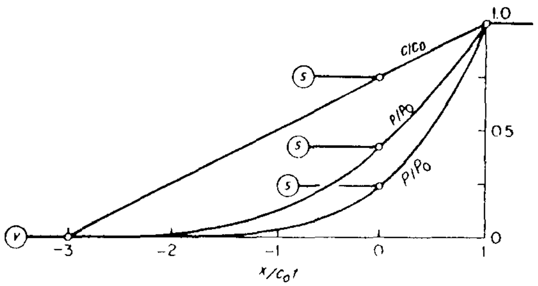

Figure 8.20
Variation of properties across a centered rarefaction terminating at vacuum v and sonic s conditions (calculated for $\gamma = 5/3$).

The *particle paths* (PP) in the centered rarefaction can be found from (8.34). They have the (inverse) slope

$$u = \frac{dx}{dt} = -\frac{2}{\gamma + 1}c_0 + \frac{2}{\gamma + 1}\frac{x}{t}$$

This is a first-order ordinary differential equation for the fluid-particle position $x(t)$. Standard solution techniques give

$$x = -\frac{2}{\gamma - 1}c_0 t + At^{2/(\gamma+1)}$$

Let x_0 be the initial position of the fluid particle. Then the expansion starts at $t_0 = x_0/c_0$ (along C_0^+ in Fig. 8.19); for $t < t_0$ we are in the undisturbed region, and the above solution is inapplicable; that is, $x = x_0 = \text{const}$ in the undisturbed region. With $u = 0$ at $t = t_0$, evaluation of the constant A gives

$$x = -\frac{2}{\gamma - 1}c_0 t + \frac{\gamma + 1}{\gamma - 1}x_0\left(\frac{c_0 t}{x_0}\right)^{2/(\gamma+1)} \tag{8.36}$$

One final comment: we have found that the dependent variables u/c_0 and c/c_0 depend only on the *similarity variable* $x/c_0 t$. This variable can be deduced from dimensional arguments, as discussed in Sec. 3.6. The self-similar quality of the motion is manifested in the wave diagram of Fig. 8.19, which is indifferent to changes in scale; i.e., we see exactly the same figure after photographic enlargement (the reader can verify that an equivalent statement cannot be made about Fig. 8.18, for example).

Continuous Piston Advance

This is just the case $\dot{X} > 0$ (see Fig. 8.21). The equations already developed for continuous withdrawal are applicable; an important difference, however, is the inevitable formation of one or more shocks, leading to possible invalidation of the homentropic model.

A C^+ characteristic coming from the piston path at a point where the piston velocity is $\dot{X}$ has (inverse) slope given by (8.27)

$$u + c = c_0 + \frac{\gamma + 1}{2}\dot{X}$$

This value increases monotonically in moving up the path of the accelerating piston (physically the sound speed increases with the motion-induced compression), so that characteristics are progressively bent over and eventually converge to form a shock.

A shock first forms at point a, where two C^+ characteristics intersect (this point does not necessarily lie on the first-signal characteristic, however). In the region to the left of the C^- characteristic shown we have simple homentropic waves; i.e., the method of characteristics already given is still applicable. In the region to the right of this, however, the shock conditions appear, and our simple calculation scheme will require modification. If the shock is *weak*, it can be fitted into the calculation with very little difficulty, as will be shown in Sec. 8.7; if it is strong, a new calculation procedure is in general required, as will be discussed in Sec. 8.10.

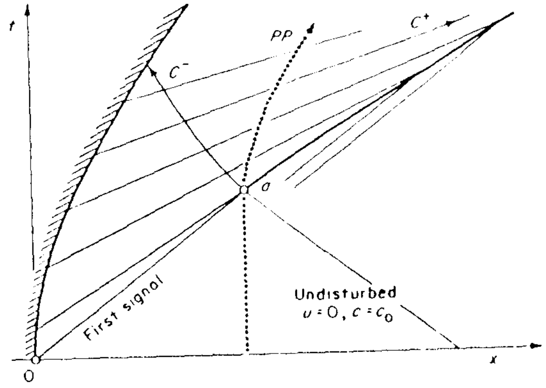

Figure 8.21
Wave diagram for continuous piston advance.

EXAMPLE 8.1 TIME OF SHOCK FORMATION

Find the time t_* at which a shock first forms under a given continuous piston advance $X(t)$ (see Fig. 8.22).

This is similar to the calculation leading to Eq. (8.23), except that the boundary conditions are differently put. From some arbitrary point t on the piston path characteristics will intersect in a time

$$t_* - t = \frac{\delta x}{d(u + c)}$$

[compare Eq. (8.23)]. It is now required to find the differential distance δx. From (8.28),

$$u + c = c_0 + \frac{\gamma + 1}{2} \dot{X}$$

From geometry, $\delta x + dx = (u + c)\, dt$ and $dx = \dot{X}\, dt$; then

$$\delta x = (c_0 + \frac{\gamma - 1}{2} \dot{X})\, dt$$

and the time interval is

$$t_* - t = \frac{\delta x}{d(u + c)} = \frac{(c_0 + \frac{\gamma - 1}{2} \dot{X})\, dt}{\frac{\gamma + 1}{2} \ddot{X}\, dt}$$

where $d(u + c)$ was found from the expression above for $u + c$. This rearranges to

$$t_* = t + \frac{1}{\ddot{X}} \left(\frac{2}{\gamma + 1} c_0 + \frac{\gamma - 1}{\gamma + 1} \dot{X} \right)$$

This is a minimum where $dt_*/dt = 0$. Performing the differentiation and setting to zero gives

$$(\ddot{X})^2 = \frac{1}{\gamma} \left(c_0 + \frac{\gamma - 1}{2} \dot{X} \right) \dddot{X}$$

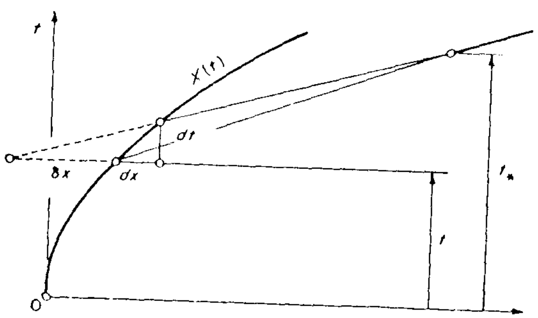

Figure 8.22

which is an implicit relation for $t^*_{\min}$. For the special case of a power-law advance, $X = At^n$, this gives

$$\left(\frac{n - 1}{n - 2} - \frac{\gamma - 1}{2\gamma} \right) nAt^{n-1} = \frac{c_0}{\gamma}$$

For $n = 2$ (parabolic piston path) this in turn gives $t = 0$; hence,

$$t^*_{\min} = \frac{c_0}{(\gamma + 1)A}$$

The corresponding position x_* at which the shock first forms is $X(t) + (u + c) \times (t_* - t)$, which works out to be, for the parabolic case,

$$x^*_{\min} = \frac{c_0^{\,2}}{(\gamma + 1)A}$$

(Strictly, it should be remarked that t_* is a linear increasing function of t in the parabolic case; thus, there is a sharp and obvious minimum at $t = 0$, and the minimum condition is actually satisfied at a discontinuity.)

Impulsive Piston Advance

If the piston instantaneously acquires velocity $\dot{X} > 0$, a shock must form at the origin of motion (see Fig. 8.23). Just as in the withdrawal motions already discussed, the impulsive case may be considered as the limit of

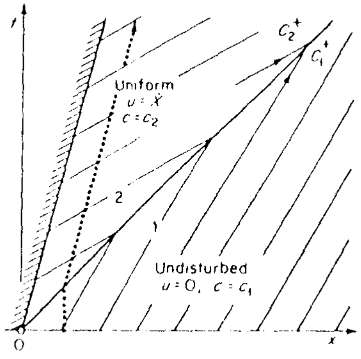

Figure 8.23
Wave diagram for impulsive piston advance.

continuous piston motion with increasing acceleration; the point of shock formation moves closer to the origin and in the limit occurs there.

Let the undisturbed region be denoted by subscript 1 and the region behind the shock by subscript 2 so that the notation is consistent with that of the shock conditions. With $[w] = \mp \dot{X}$, (7.33) gives

$$\frac{\dot{X}}{c_1} = \frac{2}{\gamma + 1}\left(M_{1n} - \frac{1}{M_{1n}}\right) \tag{8.37}$$

This gives the shock Mach number M_{1n} in terms of $\dot{X}/c_1$, and all quantities of interest (P_2/P_1, T_2/T_1, etc.) can then be calculated.

The rightward-traveling shock shown in Fig. 8.23 is called a C^+ shock because it travels at a speed intermediate between that of the upstream and downstream C^+ waves, as shown in Chap. 7 (in the limit of vanishing strength, the shock path becomes of course a characteristic). The motion shown in Fig. 8.23 is divided into two uniform regions by the shock path. The flow is then *piecewise homentropic*. The motion is also self-similar, depending only on x/c_0t, like impulsive withdrawal.

Each of the motions in this section and in the previous one was discussed in terms of C^+ waves. The results for simple C^- waves (e.g., with the piston at the *right-hand* end of the tube in Fig. 8.17 and x still positive to the right—the piston is withdrawn for piston velocities $\dot{X} > 0$) are entirely analogous; it is only necessary to change the sign of u (and $\dot{X}$) in each of the solutions. This reflects the fact that simple C^+ waves and simple C^- waves differ only in direction of travel, i.e., the sense in which x is chosen positive.

Journal of Basic Engineering - Transactions of the ASME
march 1959, p. 24-28

On the Necessity of Unsteady Flow in Fluid Machines

ROBERT C. DEAN, JR.

Head, Advanced Engineering Department,
Ingersoll-Rand Company, Phillipsburg,
N. J. Assoc. Mem. ASME

It is shown that work can be done on, or by, a fluid in a frictionless flow process only if the flow is unsteady. The implications of this conclusion in the analysis of fluid machinery, and provisions which must be made in analysis to account for unsteady flow, are discussed.

The purpose of this paper is to demonstrate that the flow in frictionless fluid machines must be unsteady if work is done on or by the fluid. This fact has great significance in any analysis of these devices, since unsteady terms must be included in the momentum, continuity, and energy expressions applied through the impeller, rotor, or cylinder of the machine. The unsteadiness governs the limits reached in certain idealizations of these devices. Also, in measurement, the recognition of the flow unsteadiness is important in selection of instruments and interpretation of data; utilization of unsteady properties also might offer new measuring techniques.

The analysis leading to equation (30) in this paper is not original. It may be found in German in "Technische Stromungslehre" by B. Eck.[1] However, as far as the author knows, the analysis is not available in English and its implications have never been discussed in the literature.

In order to illustrate the importance of transient effects an apparent paradox will be described first. Then the resolution of this paradox will be given through a development of the relevant general theory of unsteady flow.

Consider the flow of water through a steadily operating, hydraulic turbine as shown in Fig. 1.

This machine may be imagined to be a frictionless, reversible, adiabatic device without compromising the conclusions. Now, for the control volume shown a common result from the steady-flow-energy equation of thermodynamics may be written

$$W_x = -\Delta(g/g_0 H) \tag{1}$$

This equation states that the shaft work per pound of water, W_x, is equal to the decrease in head, $g/g_0 H$, as the water flows through the turbine. The head of the fluid is defined as

$$g/g_0 \equiv \frac{p}{\rho} + \frac{C^2}{2g_0} + g/g_0 z \tag{2}$$

where

H = head (in length units)
p = static pressure
ρ = density
C = velocity (in Newtonian space[2])
z = elevation above a datum plane
g = acceleration of gravity
g_0 = proportionality constant in Newton's law

Inserting (2) into (1) gives

$$W_x = -\Delta\left(\frac{p}{\rho} + \frac{C^2}{2g_0} + g/g_0 z\right) \tag{3}$$

In order to combine the variables p, C, ρ, and z in (3), Bernoulli's equation is utilized for this frictionless, incompressible flow; it states that

$$\Delta\left(\frac{p}{\rho} + \frac{C^2}{2g_0} + g/g_0 z\right) = \Delta g/g_0 H = 0 \tag{4}$$

Upon substitution of (4) into (3) it is discovered that

$$W_x = 0 \tag{5}$$

In other words, *the turbine can produce no shaft work.*

Experience indicates that this conclusion is wrong. Where is the error in analysis?

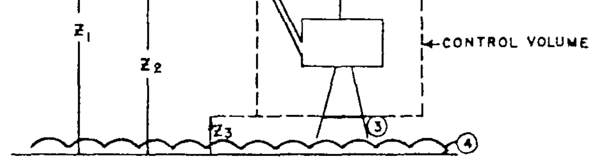

Fig. 1 Schematic of a water turbine

Fundamentals

It must be concluded from this conflict that either the steady-flow-energy equation (1) for the control volume or Bernoulli's equation (4) is wrong or misapplied. Both equations will be re-examined starting from their restrictions of derivation

Restrictions	Applied through this machine
Steady flow energy equation	
1 Incompressible	yes
2 Steady	?
3 Frictionless	yes
4 Adiabatic	yes
Bernoulli	
1 Incompressible	yes
2 Steady	?
3 Along a streamline	? (what happens as the blades chop up the streamlines?)
4 Frictionless	yes

---

[1] Julius Springer, Verlag, Berlin, Germany, 1957, p. 50.

Contributed by the Fluid Mechanics and Compressor Subcommittees of the Hydraulic Division and presented at the Semi-Annual Meeting, Detroit, Mich., June 15–19, 1958, of THE AMERICAN SOCIETY OF MECHANICAL ENGINEERS.

NOTE: Statements and opinions advanced in papers are to be understood as individual expressions of their authors and not those of the Society. Manuscript received at ASME Headquarters, April 24, 1958. This paper was not preprinted.

[2] Any space where: $F \propto Ma$.

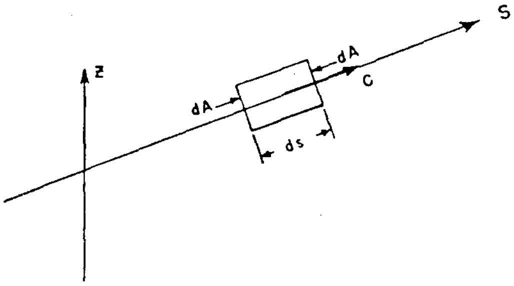

Fig. 2

From this examination, the question of flow steadiness arises with both equations.

In the sense of the flow-energy equation, the flow is steady, for no energy is accumulating inside the control volume $\left(\text{i.e., } \frac{\Delta E_{cv}}{\Delta t} = 0\right)$ over measuring times of several revolutions. Therefore, restriction 2 of the steady-flow-energy-equation tabulation can be answered "yes," clearing that equation and its result, that the shaft work is finite.

But, in the sense of the Bernoulli equation, is the flow steady? The Bernoulli equation will be rederived in an attempt to answer this question.

Consider a particle of fluid dA in cross-section area, ds in length, and of unit depth as shown in Fig. 2. Newton's law states that the sum of all the forces acting thereon in the s or streamline direction must be proportional to the particle's mass times its acceleration in that direction or

$$\Sigma F_s = \frac{1}{g_0} M a_s \tag{6}$$

The sum of the forces in the absence of shear is

$$\Sigma F_s = \underset{\text{net pressure force}}{-\frac{\partial p}{\partial s} ds dA} - \underset{\text{gravity force}}{g/g_0 \frac{\partial z}{\partial s} (\rho ds dA)} \tag{7}$$

The mass of the particle is

$$M = \rho ds dA \tag{8}$$

The acceleration is equal to the particle's time rate of change of velocity *as we follow the particle*, for Newton's law applies only to a particle of fixed identity. A special derivative sign D called the "substantial derivative" is used to indicate that the particle is being followed or

$$a_s = \frac{DC}{Dt} \tag{9}$$

Since the particle velocity C is in the s direction, the acceleration in the s direction a_s is equal to the time derivative of C. Then combining (7), (8), and (9)

$$\frac{1}{g_0} \frac{DC}{Dt} = -\frac{1}{\rho} \frac{\partial p}{\partial s} - g/g_0 \frac{\partial z}{\partial s} \tag{10}$$

Now, the particle's velocity can be thought of in terms of a velocity field at each point of which the velocity is different at any instant and is changing with time. The particle is visualized moving across this field; over a length of time Δt the particle moves from point a to point b. The difference in the particle's velocity when at point b, as compared to its velocity when at point a, can be thought of, approximately, as the difference in the velocity of the field between b and a, at the instant of time when the particle is at point a, plus the change in field velocity of point b during the time it takes the particle to travel from a to b. In other words, indicating the particle velocities by C and the field velocities by C',

$$C_b - C_a = C'_{b_{t=\Delta t}} - C'_{b_{t=0}} + (C_b' - C_a')_{=0} \tag{11}$$

Dividing by the time Δt and replacing the second term on the right-hand side by $\frac{\Delta C'_{b-a} \Delta s}{\Delta s}$ where Δs is the distance between a and b

$$\frac{\Delta C_{b-a}}{\Delta t} = \frac{\Delta C_b'}{\Delta t} + \frac{\Delta s}{\Delta t} \frac{\Delta C'_{b-a}}{\Delta s} \tag{12}$$

Then letting $\Delta t \rightarrow 0$ which causes a and b to be separated by an infinitesimal distance (for finite velocities) and, therefore, $\Delta s \rightarrow 0$ and $\frac{\Delta s}{\Delta t} \rightarrow C$, there is in the limit an exact expression for the particle's acceleration

$$\frac{dC}{dt} = \frac{dC'}{dt} + C \frac{dC'}{ds} \tag{13}$$

But, since the first term on the right was the time rate of change of velocity *at one point in space*, b, the partial derivative $\frac{\partial C'}{\partial t}$ should be written instead of $\frac{dC'}{dt}$ to indicate this fact. Likewise, since the second term on the right was written for a given instant in time ($t = 0$) this term should be written $C' \frac{\partial C'}{\partial s}$ rather than $C \frac{dC'}{ds}$ to indicate this fact. Also the term on the left $\frac{dC}{dt}$ is *for the particle* which is given the special symbol $\frac{DC}{Dt}$ as mentioned before. Since the special derivative D has been adopted, all other derivative symbols can be stated to refer to the field and the primes on C can be dropped without much confusion.

$$\underset{\text{For particle}}{\frac{DC}{Dt}} = \overbrace{\underbrace{\frac{\partial C}{\partial t}}_{\text{at a point}} + \underbrace{C \frac{\partial C}{\partial s}}_{\text{at an instant in time}}}^{\text{For field}} \tag{14}$$

Combining (14) with (10) gives an equation relating changes in velocity C, density ρ, pressure p, and elevation z to position along the streamline s and the time t

$$\frac{1}{g_0} \left(\frac{\partial C}{\partial t} + C \frac{\partial C}{\partial s} \right) + \frac{1}{\rho} \frac{\partial p}{\partial s} + g/g_0 \frac{\partial z}{\partial s} = 0 \tag{15}$$

Now, to obtain a closed-form relation between pressure, elevation, velocity, and density, these properties must be made dependent on only one variable. In general, the properties depend on three space co-ordinates and time. First, time will be eliminated, which makes $\partial C/\partial t = 0$, and all other properties independent of time. If, in addition, there is integration only along streamlines so that changes normal thereto do not appear, two space variables can be eliminated reducing the properties to dependence on only one variable, s. In this condition, the partial derivatives can be replaced by total derivatives or

$$\frac{1}{g_0} C \frac{dC}{ds} + \frac{1}{\rho} \frac{dp}{ds} + g/g_0 \frac{dz}{ds} = 0 \tag{16}$$

Canceling ds, simplifying, and rearranging into familiar order

$$\frac{dp}{\rho} + \frac{dC^2}{2g_0} + g/g_0 \, dz = 0 \tag{17}$$

Euler's Equation is obtained. If the density is constant, it is possible to integrate along the streamline immediately giving

$$\Delta(p/\rho + C^2/2g_0 + g/g_0 z) = 0 \qquad (18)$$

which is *Bernoulli's Equation.*

From this derivation we learn that both Euler's and Bernoulli's equations are limited to applications where: (*a*) *They are applied only along streamlines,* (*b*) *the fluid properties and velocity in Newtonian space at any point in the field are invariable* $\left(i.e., \frac{\partial p}{\partial t} = \frac{\partial \rho}{\partial t} = \frac{\partial C}{\partial t} = 0\right)$. The latter restriction *defines steady flow* as far as Euler's and Bernoulli's equations are concerned.

Now returning to the water turbine or any other fluid machine that does not depend upon friction forces to do its work, our experience tells us that, if we stand and observe the rotor or piston at a point stationary relative to us in Newtonian space, the fluid properties and velocity will not be constant in time. As the blades of a turbine move past the stationary point, first the high-velocity low-pressure region on the blade's suction surface passes, then the relatively lower velocity and higher pressure on the blade's pressure surface. At a point on the casing above the tip of the rotor blades, the velocity and pressure violently fluctuate in time. So, too, do the velocity and pressure at a stationary point in a reciprocating compressor or internal-combustion engine, or in any other fluid machine that does not depend upon friction forces to do its work.

Experience and the restrictions on Euler's and Bernoulli's equations lead to the conclusion that *those equations cannot be applied through a fluid machine in which shaft work is done on or by the fluid.* The generality of this statement will be proved, thus resolving the paradox discussed in the introduction.

Analysis of the Flow in a Fluid Machine

Since steady flow, in the sense that the fluid properties and velocity at each point are invariable, is not a tenable assumption for analysis of fluid machines, particularly since it would lead to the embarrassing conclusion that the shaft work is zero, the unsteadiness of the flow must be included in the analysis. Accordingly, relations between the work done on the fluid and the unsteadiness of the flow will be constructed.

Stagnation enthalpy h_0 is defined in Newtonian space as

$$h_0 \equiv h + \frac{C^2}{2g_0} + g/g_0 z \equiv u + \frac{p}{\rho} + \frac{C^2}{2g_0} + \frac{g}{g_0} z \qquad (19)$$

where

u = internal energy of the matter in the absence of the effects of motion, gravity, capillarity, electricity, and magnetism.

There may also be written for any kind of process in a pure substance[3]

$$Tds = du + pdv \qquad (20)$$

where

T = temperature, absolute
s = entropy
$v = \frac{1}{\rho}$

and for a reversible (implies frictionless) process[4]

$$Tds = dQ \qquad (21)$$

where Q = heat. If in addition, the process is adiabatic

$$dQ = 0 = du + pdv \qquad (22)$$

Differentiating h_0, yields from Equation (19)

$$dh_0 = du + \frac{1}{\rho}\,dp + pdv + \frac{1}{2g_0}\,dC^2 + \frac{g}{g_0}\,dz \qquad (23)$$

or combining with Equation (22) to eliminate $du + pdv$

$$dh_0 = \frac{1}{\rho}\,dp + \frac{1}{2g_0}\,dC^2 + \frac{g}{g_0}\,dz \qquad (24)$$

Then, if it is desirable to look only at changes in the direction of the streamline,

$$\frac{\partial h_0}{\partial s} = \frac{1}{\rho}\frac{\partial p}{\partial s} + \frac{1}{2g_0}\frac{\partial C^2}{\partial s} + \frac{g}{g_0}\frac{\partial z}{\partial s} \qquad (25)$$

This equation may be combined with Newton's law (15) to give finally

$$\frac{\partial h_0}{\partial s} = -\frac{1}{g_0}\frac{\partial C}{\partial t} \quad \text{for reversible, adiabatic flow.} \qquad (26)$$

This equation states the surprising fact that, in a frictionless adiabatic flow (compressible or incompressible), the spatial rate at which the stagnation enthalpy (or head, in an incompressible flow) is changing in the direction of the instantaneous velocity at a point is proportional *to the time rate of change of fluid velocity of the field at that instant, at that point.* In other words, if the flow is steady, $\partial C/\partial t = 0$; the stagnation enthalpy h_0 is constant along streamlines, and the steady-flow energy equation

$$-W_x = h_{0_2} - h_{0_1} \qquad (27)$$

where the subscripts 1 and 2 represent two stations along the streamline, indicates again that the shaft work must be zero.

Equation (26) turns out to be rather difficult to use in practice since the direction s is constantly changing as the streamline lashes about in an unsteady flow. This difficulty can be avoided by dealing with the rate of change of a particle's stagnation enthalpy *as it is followed along.* Such "following" brings in again the substantial derivative D, which is expressed as a result of arguments similar to those leading to equation (14) by

$$\frac{Dh_0}{Dt} = \frac{\partial h_0}{\partial t} + C\frac{\partial h_0}{\partial s} \qquad (28)$$

The second term on the right is given by Equation (26) while the first on the right is easily obtained from Equation (23) by considering changes in time only at a point

$$\frac{\partial h_0}{\partial t} = \frac{1}{\rho}\frac{\partial p}{\partial t} + \frac{C}{g_0}\frac{\partial C}{\partial t} + \frac{g}{g_0}\frac{\partial z}{\partial t} \qquad (29)$$

The $\partial z/\partial t$ term will be ignored, since a point stationary in Newtonian space cannot change elevation z in the earth's gravitational field. Then combining equations (28), (26), and (29),

$$\frac{Dh_0}{Dt} = \frac{1}{\rho}\frac{\partial p}{\partial t} \quad \text{for reversible, adiabatic flow.} \qquad (30)$$

For an incompressible fluid, since

$$h_0 = g/g_0 H \qquad (31)$$

then

$$\frac{D(g/g_0 H)}{Dt} = \frac{1}{\rho}\frac{\partial p}{\partial t} \qquad (32)$$

---

[3] See Keenan, "Thermodynamics," p. 85.

[4] Ibid., p. 83.

These expressions state that *the rate at which a particle's stagnation enthalpy (or head) changes with time is proportional to the instantaneous rate of pressure fluctuation at the point where the particle finds itself at any given time.*

Thus *if work is to be done on the particle by pressure forces in order to change its stagnation enthalpy (or head), the pressure must fluctuate at a point and the flow is, as a consequence, unsteady.*[5] If shear, electrical, magnetic, or capillary forces are utilized to do work on the particle, the flow may be steady.

Physical Interpretation

If a hole were bored through a turbine casing directly above the rotor blade tips, and the pressure were measured there, something like Fig. 3 would be recorded.

This pressure trace results from the pressure field of the blades moving under the pressure-tapping hole. Looking at the trace, it can be seen that $\frac{\partial p}{\partial t}$ is negative. This fact, according to Equation (30), implies that the stagnation enthalpy of the fluid particles passing through the turbine is decreasing. This conclusion is known to be true for a turbine.

In an axial compressor, the reader can construct a similar argument and arrive at a conclusion exactly reversed from the turbine case above.

To drive home the theoretical arguments given, a machine, say a centrifugal blower, will be analyzed in just the reverse fashion to the preceding development. Imagine a blower doing work steadily on a flowing gas. The only means that the rotor has at hand to impart those forces which do the work on the fluid is through a local pressure difference between the two sides of each impeller vane. For simplicity, assume that the pressure, high on the driving vane face and low on the trailing face, varies linearly in the tangential direction across the space between the vanes. Then, as the rotor turns by, stationary observers note that the pressure varies relative to them. In fact, if the pressure difference across the blade is Δp and the time between vane passings is

$$\Delta t = \left(\frac{2\pi r}{Z}\right)\frac{1}{r\Omega} \tag{33}$$

where

r = radius of the observation point from the center of rotation

Z = number of blades

Ω = angular velocity of impeller in radians/sec

then the rate of pressure variation $\partial p/\partial t$ is

$$\frac{\partial p}{\partial t} \simeq \frac{\Delta p}{\Delta t} = \frac{(\Delta p)Z\Omega}{2\pi} \tag{34}$$

Now consider the mass particle of fluid ds, dn, $\frac{2\pi r}{Z}$ shown in Fig. 4. The net torque about the axis acting upon this particle in the direction of impeller rotation is

$$\Sigma\tau = (\Delta p)rdsdn \tag{35}$$

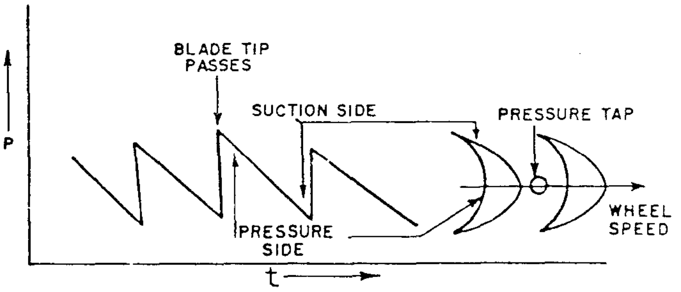

Fig. 3 Schematic of the pressure variation with time at a casing pressure tap in a turbine

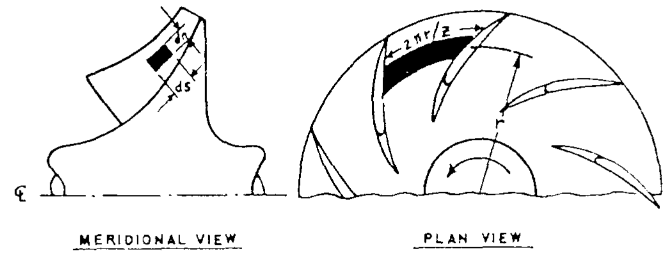

Fig. 4 Centrifugal compressor impeller

where Δp is the pressure difference across a vane at radius r. The rate at which work is done on the particle by this torque is $\tau\Omega$. This power applied to the particle equals the rate at which the particle's stagnation enthalpy (or head) is increasing in adiabatic flow according to the first law of thermodynamics or

$$\frac{Dh_0}{Dt} = \frac{(\Delta p)rdsdn\Omega}{\rho dsdn\, 2\pi r/Z} \tag{36}$$

which is divided by the particle mass, since h_0 is the stagnation enthalpy per unit mass.

Then, on combining (36) and (34), it can be seen again that

$$\frac{Dh_0}{Dt} = \frac{1}{\rho}\frac{\partial p}{\partial t} \tag{37}$$

This is exactly the expression derived before from more abstract (but more exact) considerations. Thus, if work is done on or by the fluid, it must be exposed to boundaries which impose a net pressure force and which must move creating by their motion a pressure that fluctuates in time at a stationary point.

Some Further Considerations

When idealizing turbomachines, an infinite number of blades is often assumed in order to produce axisymmetric flow. It is important to realize that, if the total amount and spatial distribution of the work done by the impeller is assumed to be unaffected by this idealization, then *the rate of pressure variation at each point $\partial p/\partial t$ must be unaltered* according to Equations (30) and (37). In other words, the pressure variations must resemble Fig. 5. The slope of the "saw teeth" must be independent of the number of blades.[6] As a consequence, although the flow becomes axisymmetric for an infinite number of blades, *it does not become steady.* Euler's and Bernoulli's equations do not apply in the idealized impeller.

The idea comes to mind, that the distribution of work addition or extraction within fluid machines could be determined by measuring $\partial p/\partial t$. Modern pressure probes make this measurement fairly easy.

---

[5] The pressure must fluctuate at a point stationary in the coordinate system relative to which we measure work and stagnation enthalpy (or head). Conventionally, this would be relative to the machine casing. Relative to the machine rotor (i.e. to an observer riding on the rotor), if the relative flow is steady, then no work can be or is observed by the rotating observer. If the relative flow is unsteady (e.g., due to the disturbances of stationary upstream or downstream blades, struts, and so forth), the rotating observer will see work done, although a different amount than the stationary observer. It is also interesting to note that the rotating observer would regard the stators as the work-producing elements of the machine.

[6] This follows also from simple reasoning, i.e., twice as many blades give one half the distance and one half the passing time between blades and one half the load or pressure difference across each blade. Therefore, $\partial p/\partial t$ is independent of the number of blades.

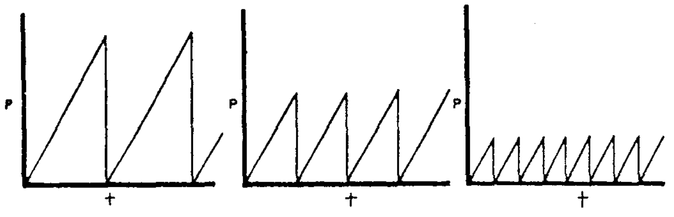

Fig. 5 Schematic of the alteration of the pressure variation with time at a casing pressure tap of a fluid machine as the number of blades is increased.

Summary and Conclusion

It has been shown that:

1 The flow in fluid machines doing useful work by pressure forces must be unsteady.

2 Euler's and Bernoulli's equations are for steady flow and do not apply through the working region of the machine even if the events therein are cyclic.

3 The steady-flow energy equation does apply over the working region if the processes are cyclic, for such are "steady" as far as that equation is concerned.

4 The time rate of increase of a particle's stagnation enthalpy (or head), on passing through the working region of the machine, is proportional to the local time rate of pressure fluctuation at a point stationary relative to the machine casing.

5 Conclusion 4 can be explained readily in terms of the forces that moving blades or vanes exert on the fluid in order to do work.

6 Idealizing the machine to an axisymmetric flow produced by an impeller with an infinite number of blades cannot make the flow steady.

7 Measurement of the local flow unsteadiness might be a useful new technique to determine work distribution in impellers.

Shock Waves and shock Tubes
15th International Symposium of Shock Waves and Tubes
Berkeley, Calif. July 28- Aug. 2, 1985, Editors Daniel Bershaden and Ronald Hanson
Stanford University Press, 1986
p.179-185

WAVE AND THERMAL PHENOMENA IN H.S.-TUBES WITH AN AREA CONSTRICTION

E. Brocher and M. Kawahashi*

Institut de Mécanique des Fluides
de Marseille, 1, rue Honnorat,
13003 Marseille, France

*Department of Mechanical Engineering
Faculty of Engineering, Saïtama University
255 Shimo-Okubo, Urawa, 338 Japon

The propagation of waves in a Hartmann-Sprenger tube having an area constriction is studied both theoretically and experimentally. It is found that there are several possible modes of oscillations within the tube. The observed mode depends on the diameter - and length - ratios of the upstream and downstream parts of the tube. The mode also depends on the Mach number of the exciting jet. In the "first" mode, the shock wave generated in the upstream cavity is transmitted trough the area change and strongly amplified. In higher modes, the incident wave in the upstream cavity meets, near the area change, a shock wave traveling in the opposite direction in the downstream cavity. For a given total length, the oscillation frequency of the 3rd and 5th modes are approximately 3 and 5 times the frequency of the 1st mode, respectively. The thermal effects, essentially due to repetitive shock heating, strongly depend on the oscillation mode. In the 1st mode, the temperature steadily increases along the tube, with a steep temperature gradient in the downstream cavity. In the 3rd mode, a steep temperature gradient is observed near the area constriction whereas the temperature is high and almost constant in the downstream cavity. The influence of the shape of the joining section between the upstream and downstream cavities has been investigated. The highest shock intensities and thermal effects have been observed with a sinusoïdal converging section.

1. INTRODUCTION

At the 13th International Symposium on Shock Waves and Tubes, it was shown[1] that a Hartmann-Sprenger tube (HS-tube) presenting a sudden change in cross section could produce high amplitude pressure waves. The configuration studied is shown in Fig. 1. A high speed jet flows out of a "needle" nozzle[2] and drives flow oscillations within a tube with constriction. A simplified wave diagram for the flow within the tube was proposed. A theoretical amplification was derived and experimental values were in good agreement with the predicted ones. Subsequently, it was found that several modes of oscillations are possible[3]. The wave diagram as well as the thermal effects are quite different for each mode. This is important when one considers the H.S.-tube as an igniter for pyrotechnic compositions[4].

Linear acoustic theory gives some idea on the possible oscillation modes. However, it cannot predict which one of these modes will be observed. Also, because the oscillation amplitude is very large and can attain several bars, it is not surprising if one finds substantial deviation between measured and calculated frequencies. The agreement between numerical experimental values and computations made with the so-called FLIC-method (fluid-in-cell) is much better.

2. LINEAR THEORY

The basic scheme of the linear theory applied to the single-step H.S tube is as follows. The acoustic pressure in each cavity is given by the superposition of waves moving in upstream and downstream directions

$$p_1 = Ae^{j(\omega t - kx)} + Be^{j(\omega t + kx)} , \qquad (1)$$

$$p_2 = Ce^{j(\omega t - kx)} + De^{j(\omega t + kx)} ,$$

where p, ω, k, x, and t represent acoustic pressure, angular frequency, wavenumber, axial coordinate, and time, respectively; j is the imaginary unit and subsripts 1 and 2 indicate the upstream and downstream cavities, respectively.

The complex constants A, B, C, and D are determined by boundary conditions. These are given first by the reflection coefficients at the junction and at the downstream end, and second, by consideration of the impedance at the mouth. The reflection factors R_{12} and R_{21} at the junction are given by

$$R_{12} = \frac{(D_1/D_2)^2 - 1}{(D_1/D_2)^2 + 1} , \qquad R_{21} = \frac{(D_2/D_1)^2 - 1}{(D_2/D_1)^2 + 1}$$

The reflection factor at the downstream end is equal to unity. Moreover, if the amplitude of acoustic velocity at the mouth is kept constant, i.e., $|u| = u_0$. the unknown complex constants A, B, C, and D are functions of u_0. When geometrical parameters are given, the acoustic impedance $Z \equiv p/u$ at the mouth is a function of frequency only. The eigenfrequencies are those frequencies for which the impedance vanishes. The eigenfrequencies calculated with this procedure are plotted in Fig. 4.

Particular values of eigenfrequencies are

$$f_1 = a/4(L_1 + L_2) \quad \text{if} \quad D_1 = D_2 \qquad \text{(1st mode)}$$

$$f_3 = 3\ |a/4(L_1 + L_2)| \quad \text{if} \quad D_1 \neq D_2 \text{ and } L_2 = 2L_1 \qquad \text{(3rd mode)}$$

$$f_5 = 5\ |a/4(L_1 + L_2)| \quad \text{if} \quad D_1 \neq D_2 \text{ and } L_2 = 4L_1 \qquad \text{(5th mode)}$$

When the frequencies are close to one of these particular frequencies, the oscillations are called 1st mode-, 3rd mode-, or 5th mode-oscillations, respectively.

3. NON LINEAR THEORY

The wave phenomena are computed with a numerical method (FLIC method) on a two-dimensional model of the tube. The basic equations used are the continuity and momentum equations

$$\frac{D\rho}{Dt} + \rho \nabla V = 0 , \qquad \rho \frac{DV}{Dt} = - \nabla p$$

when ρ , V, p and t represent the density, velocity, pressure and time, respectively. In these equations, friction and heat conductivity are not taken into account, but artificial viscous pressure is introduced for the stability of the shock computation.

Wave diagrams obtained by this method are shown on Fig. 3. The diagramm for $L_2/L_1 = 5$ shows very clearly the head-on collision of shock-waves at the step (Fig. 3a) and corresponds to the 5th mode. The computed frequencies are indicated on Fig. 4.

4. EXPERIMENTAL SET-UP

In Fig. 1, the H-S tube with constriction and the supersonic "needle nozzle" are shown in schematic fashion. The length (L_1) of the upstream cavity has a fixed value (80 mm) whereas the length (L_2) of the downstream cavity can take several values ranging from 80-480 mm so that the length ratio L_2/L_1 can be varied from 1-6. The inner diameter D_1 of the upstream cavity is 18 mm and the diameter D_2 of the downstream cavity is 9, 6, or 3 mm, so that the diameter ratio D_1/D_2 takes the values 2, 3, or 6. The diameter D_N of the nozzle exit is identical to D_1. Since non-linear theory[5] applied to a sudden area change (step) shows that the flow near the constriction has a two-dimensional character, it can no longer be said that the step corresponds to a velocity node, as linear theory does. It therefore appears that if a sudden change in cross-section is replaced by a con[illegible]sly changing section, the amplification of pressure amplitude and thermal effects could be further increased. Three different shapes of transition section, with length L_t, have been tested (Fig. 2).

Pressure histories and time-average pressures are determined at various positions in axial direction of the tube. Instantaneous pressure is measured by piezoelectric transducers and mean pressure by a manometer. Three different shapes of the needle laid upon the nozzle axis were used in the test. They were giving correctly expanded supersonic jet for 3 Mach numbers : 1.2, 1.68 and 2.07.

5. EXPERIMENTAL RESULTS

4.1. Oscillation frequency

The oscillation frequency f in a constant area H-S tube is nearly equal to the 1st mode of the acoustic frequencies of a pipe closed at one end, i.e., $f \approx f_0 = a_a/4L$, where a_a represents the ambient speed of sound and L the pipe length. The oscillation frequency is a slightly decreasing function of the jet Mach number. Whereas the ratio f/f_0 is almost equal to unity for low values of M_j, it is about 0.88 for $M_j = 2$.[6] . The oscillation frequency of the constant area tube is not very sensitive to the length ratio L/D, except for small values of this parameter where end effects become important. In contrast, the oscillation frequency in a single-step H-S tube strongly depends on its geometrical configuration, the main parameters being the length ratio L_2/L_1 and the diameter ratio D_1/D_2.

All the measurements reported in section 4.1. were made with the step configuration (sudden change).

4.1.1. Influence of length ratio

In Fig. 4, experimental results of oscillation frequency in a single-step H-S tube with $D_1/D_2 = 2$ are shown and compared with the values calculated by linear acoustic theory and by the FLIC method for two values of M_j. The measured frequencies are normalized with the acoustical frequency f_0 of the total tube length, that is, $f_0 = a_a/4(L_1+L_2)$.

It is seen that over a certain range, the experimental value of the oscillation frequency slightly increases with the length ratio until it reaches a domain of instability. In this domain, the frequency discontinuously changes from 1st-3rd mode. Then comes a range in which the frequency gradually increases until it reaches another domain of instability in which the oscillation discontinuously changes from 3rd to 5th mode. It is also observed that the frequencies given by the FLIC method are closer to experimental values than frequencies given by linear theory. The jump from one mode to the other, however, is not predicted accurately.

Fig. 5 shows the pressure histories for each mode at the middle position of the downstream cavity and at the closed end of the same cavity. Pressure fluctuations at the middle position are seen to be very different for each mode. In the 1st mode they are similar to those of a constant area tube and in the 5th mode, they are almost identical to the fluctuations at the closed end.

In the 3rd mode, however, the situation is quite different because the compression wave is not canceled by the rarefaction wave as happens in the acoustical case. This is because in nonlinear wave motions with traveling shock waves, pressure increases discontinuously across the shocks whereas it gradually decreases across the isentropic rarefaction wave bundle.

4.1.2. Influence of diameter ratio

In all the tests reported above, the diameter ratio D_1/D_2 had a value of 2. This ratio is also an important geometric parameter for the wave motion in a single-step H-S tube. If D_1/D_2 increases, the oscillation frequency generally decreases, the oscillation mode being unchanged. Also, the domain of length ratio for which the oscillations are unstable becomes wider. Moreover, the critical length ratio for mode change is a decreasing function of D_1/D_2. Figure 6 shows the effect of diameter ratio on frequency and on oscillation mode for a single-step H-S tube having a fixed length ratio ($L_2/L_1 = 2$). It can be observed that, for this length ratio, the 1st-mode frequency is an increasing function of D_1/D_2, whereas the 3rd-mode has a constant value corresponding to upstream cavity resonating at quarter-wavelength frequency and downstream cavity resonating at half-wave frequency. The critical diameter ratio for mode change at high jet Mach number lies in the region $2<D_1/D_2<3$, whereas for $M=1.2$, it is smaller than 2. This is in agreement with the result reported in Ref.5, where the critical diameter ratio for mode change was found to be 1.3 for low jet Mach number ($M_j \simeq 1.34$).

4.2. Thermal effects

The temperature distribution of the tube wall depends very strongly on the oscillation mode.

4.2.1. 1st-mode

For this mode, the incident shock wave is amplified by the constriction so that maximum temperatures are observed at the end wall. The shape of the constriction has a strong effect on the temperature, especially for large diameter ratios (Fig. 7). In the 1st-mode, mixing of the driving and driven gas limits the temperature in the upstream part of the cavity (Fig. 8).

4.2.2. 3rd-mode

For this mode, the incident shock is reflected at the constriction. Mixing of the gas oscillating in the downstream cavity with the cold driving gas is much reduced, so that an almost uniform temperature is observed in this cavity. The shape of the constriction section has less effect on the temperature (Fig. 9).

5. CONCLUSION

The influence of various parameters on the oscillation mode of Hartmann-Sprenger tubes presenting an area change has been studied both experimentally and theoretically. It has been shown that the oscillation mode has a strong effect on the maximum attainable temperature, as well as on the temperature distribution. These results are interesting for applications, such as the so called "fluidic" igniter.

REFERENCES

1. BROCHER, E.,"Amplification of non-linear standing waves in a cylindrical cavity with varying cross section", Proceedings of the 13 th International Symposium on Shock Waves and Shock Tubes, State University of New-York Press, Albany N.Y., 1981, p. 209

2. BROCHER, E., "Contribution à l'étude des générateurs acoustiques à jet d'air" ACUSTICA, Vol. 32, n° 4, 1975, p. 227

3. KAWAHASHI, M., BOBONE, R. and BROCHER, E., "Oscillations modes in single step Hartmann-Sprenger tubes", J. Acoust. Soc. Am. 75(3), March 1984, p. 780

4. MARCHESE, V.P., RAKOWSKY, E.L. and BEMENT, L.J., "A fluidic sounding rocket motor ignition system", J. Spacecraft, Vol. 10, n° 11, 1973, p. 731

5. KAWAHASHI, M., KURUTA, R. and SUZUKI, M., Trans. JSME 49, 1983, p. 1224 (in japanese)

6. BROCHER, E., MARESCA, M. and BOURNAY, M.H., "Fluid Mechanics of the Resonance Tube", J. Fluid Mech. 43, 1970, p. 369

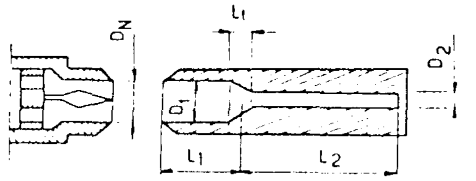

Fig. 1 : H.S. tube with area constriction

D_N = nozzle diameter ; L_1, D_1 = length and diameter of upstream cavity; L_2, D_2 = length and diameter of downstream cavity; L_t = length of transition section.

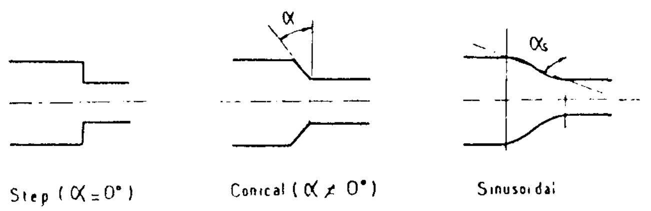

Fig. 2 : Different shapes of transition section tested.

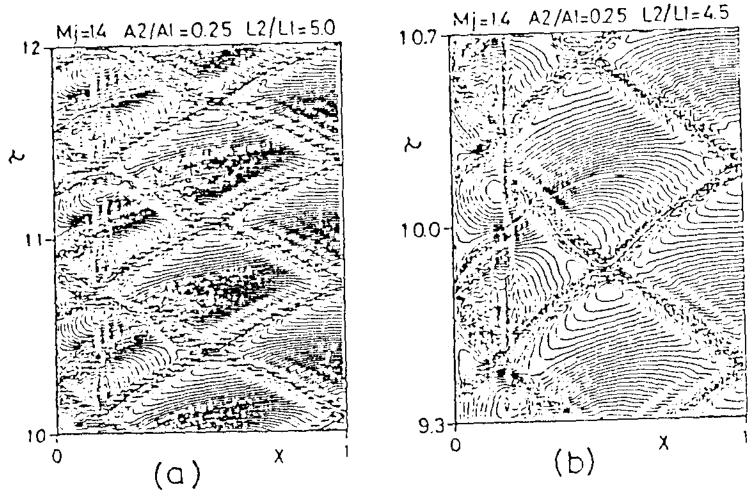

Fig. 3 : Wave diagrams for two different length ratios

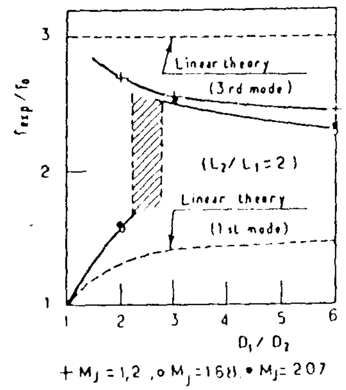

Fig. 6 : Effect of diameter ratio on the oscillation mode

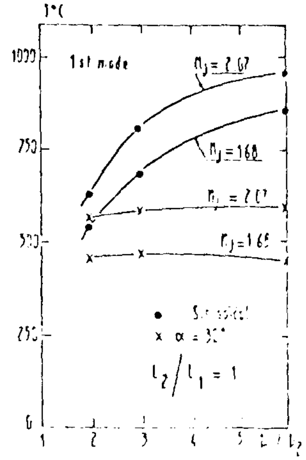

Fig. 7 : Effect of diameter ratio on end wall temperature

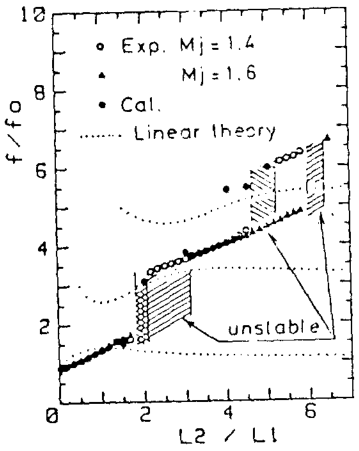

Fig. 4 : Frequency of oscillation as a function of the length ratio

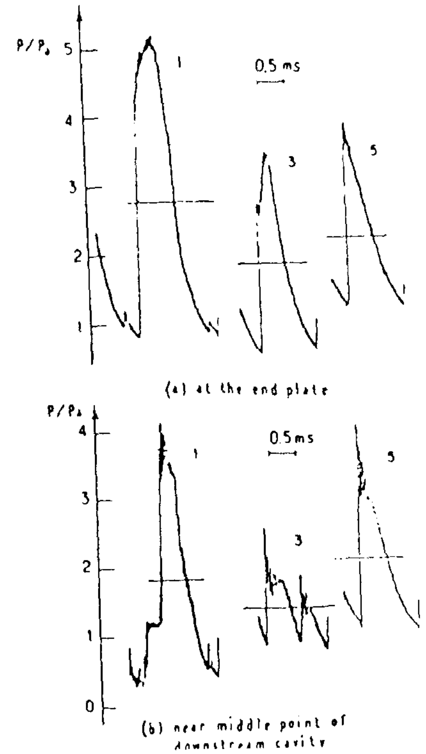

Fig. 5 : Pressure histories for the 1st, 3rd and 5th modes

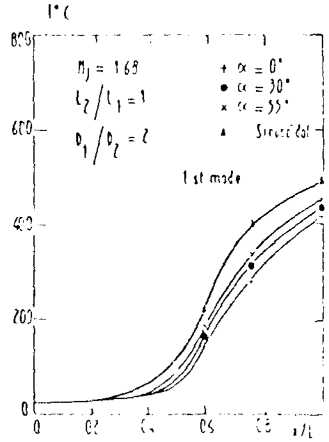

Fig. 8 : Temperature distribution along the tube (1st mode)

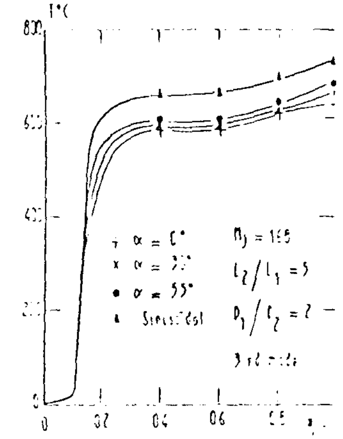

Fig. 9 : Temperature distribution along the tube (3rd mode)

FACTORIES BLOW SMOKE RINGS

Factory chimneys of the future will be shorter and fatter, if an American scientist has his way. Instead of dribbling smoke into the air in a continuous stream, they will puff smoke rings, like a contented cigar smoker. Dr. Timothy Fohl, a physicist from Boston, has been studying industrial smoke production and air pollution problems for some years. He observed that smoke rings travel much more quickly through the air than "unstructured smoke emissions" and sought to apply this principle to the rapid dispersal of industrial smoke. Dr. Fohl has calculated that a short, relatively plump factory chimney equipped with a shutter and pump mechanism to puff out smoke rings will push the smoke to heights of 10,000 feet before it disperses. The tallest conventional chimney does not send smoke higher than 2500 feet, he says. It is also reckoned that chimney blown smoke rings will be less affected by wind than are ordinary smoke plumes.—*Compressed Air*, May 1968.

Postfix

BY ALEXANDER ROCA

Killer Air Ray

The end result of the Army's vortex-weapon research.

MAMMOTH SMOKE RINGS DOWN ENEMY BOMBERS! MONSTER MACHINE CREATES MAN-MADE TORNADOES! It was a fantastic idea, and it approached reality during World War II. The client? The U.S. government.

In recent decades wingtip vortices generated by jumbo jets have been known to disrupt the flights of smaller aircraft following nearby, turning them upside down in seconds. Imagine hostile pilots in close formation and laden with armaments and explosives encountering such whirlwinds.

That was the goal of a wartime plan hatched by the U.S. Army Chemical Warfare Service (USACWS) at the Dugway Proving Ground in Utah. The department did research not only on chemical agents but also on the means of delivering them. That's where vortices came in, because they can improve the penetration of a gas charge through the air. A Colonel Esmond of the USACWS hired Thomas Shelton to work on the idea with Philip Leighton of Stanford University. Shelton was a genius inventor and aerodynamicist noted for his twin-boom, twin-engine 1935 Crusader, an aircraft that cruised at 200 miles per hour on just 312 horsepower. Its efficiency stemmed from Shelton's careful wind-tunnel-tested streamlining. At cruising speed the teardrop-shaped cabin alone generated substantial lift. And fuselage-to-wing filleting prevented the interference drag that plagued other, later twin-boomed aircraft. (For example, early Lockheed P-38 Lightnings suffered from tail buffeting until fairings were added to their wing roots.)

Shelton quickly developed a clever vortex maker. A bell-shaped chamber, acted on by a piston or an explosion, would send a packet of gas out its narrow end as a high-velocity vortex. The vortex enhanced the speed, distance, accuracy, and penetration through crosswinds of any vapor being shot out of the bell, just as rifling improves bullet performance. It could be used with vapor-based herbicides and insecticides, as well as with chemical and biological weapons.

Shelton envisioned another way to use his device: Vortices from a huge generator might disrupt aircraft in flight, and the equivalent of a giant smoke ring might break up high-altitude enemy bomber formations. To test his thesis, he built a scale model. Powered by a shotgun shell, it shot an 18-inch smoke ring 150 yards. And it made an eerie howling sound—potent psychological weaponry.

According to Shelton, the Army Air Corps brass at Wright Field, in Dayton, Ohio, seriously considered a version with high-explosive power and a business end yards wide. It would rocket a deadly accurate and invisible ring of air at near-supersonic speed thousands of feet skyward. There the vortex would wreak havoc, spinning target aircraft wildly out of control, crashing into other craft, and falling to earth.

This top-secret stratagem died unfulfilled as offensive weapons garnered war-research resources. But after the war Shelton patented miniature versions of his vortex generator as children's toys. The Flash Gordon Air Ray Gun, manufactured by the Budson Company of Chula Vista, California, knocked over targets with a puff of air and cost only $2.49. It was named "Toy of the Year" in 1949 by *Popular Mechanics* magazine.

Later, with backing from an investor named Paul Zifrin, Shelton developed the Magic Ray Gun, for the Nu-Age Company. It shot miniature smoke rings from small pellets developed by the Lion Match Company. The pellets, in book-match form, neither flamed nor flared but safely smoked prodigiously. Shelton based his idea on a toy made from a cylindrical oatmeal carton by his father, who was himself an industrialist and inventor of no small repute. When filled with cigarette smoke and tapped on one end, it would eject a ring from a hole in the other end. In the 1960s Wham-O Manufacturing revived the Budson gun as the Air Blaster, cleverly configured with targets built into the cardboard box it came in.

Today "death ray" fantasies are back as prototypes for ground- and satellite-based laser and particle-beam weapons. Tom Shelton's idea—which also projected disruptive, destructive energy—looked forward almost half a century. Perhaps it was merely too far ahead of its time. ★

Alexander Roca is the author of Crusader: The Story of the Shelton Flying Wing *(Rare Birds Publishing, Berlin, Mass.).*

AMERICAN HERITAGE CENTER, UNIVERSITY OF WYOMING, LARAMIE

KEN MARTEN Earthtrust

Ring Bubbles of Dolphins

A number of bottlenose dolphins in Hawaii can create shimmering, stable rings and helices of air as part of play

by Ken Marten, Karim Shariff, Suchi Psarakos and Don J. White

KEN MARTEN, SUCHI PSARAKOS AND DON J. WHITE *Earthtrust*

Below the towering cliffs of Makapuu Beach on the island of Oahu, Hawaii, is a unique laboratory dedicated to the study of dolphins. Project Delphis, run by the nonprofit conservation organization Earthtrust, in cooperation with Sea Life Park Hawaii, conducts research ranging from investigating dolphin self-awareness to exploring the animals' intelligence using an underwater computer touch screen. The scientists in the lab do not use food as a reward, so all the behavior observed is of the dolphins' own volition.

One of the most fascinating activities we have seen in our research involves no high-tech human toys at all. Instead the dolphins fashion their own entertainment by swirling the water with their fins and blowing bubbles into the resulting vortices to produce rings and helices of air. Furthermore, the physics behind the air rings turns out to be quite interesting. Few people doubt that dolphins are highly intelligent animals, but these observations demonstrate just how imaginative they can be.

As air breathers, dolphins blow bubbles whenever they exhale underwater. Dolphin behaviorists have noted that when dolphins are excited, surprised or curious, they will sometimes expel air from their blowholes, generating large, amorphous bubbles that rise quickly to the surface. The animals occasionally emit streams of small bubbles when they make sounds; the bubbles might add another component, detectable by sight or sonar, to the vocal message.

Dolphins can also create more exotic types of bubbles for less prosaic reasons. In recent years, researchers at several oceanariums around the world have reported that a variety of marine mammals can blow smooth, stable rings of air that linger in the water for several seconds. Because of the intricate techniques and practice required to form such rings, as well as the helices we have seen, these bubbles are clearly not a spontaneous response to alarm or a standard part of communication. Wolfgang Gewalt of the Duisburg Zoological Gardens in Germany observed untrained Amazon river dolphins (*Inia geoffrensis*) producing bubbles in unusual and playful ways. The animals emitted air from their mouths to yield necklaces of bubbles, which they would pass through or bite.

Elsewhere, at Marine World Africa USA in Vallejo, Calif., Diana Reiss and Jan Ostman-Lind noticed bottlenose dolphins (*Tursiops truncatus*) at the aquarium playing with rings similar to the ones we have seen. Kenneth S. Norris of the University of California at Santa Cruz described beluga whales (*Delphinapterus leucas*) at the Vancouver Aquarium that expelled bubbles from their blowholes and then sucked them into their mouths as part of playful behavior. Some people have even witnessed air rings in the wild. The behavioral biologist Karen Pryor observed male Pacific spotted dolphins (*Stenella attenuata*) blowing rings during social encounters; Denise Herzing of Florida Atlantic University has viewed similar displays in free-ranging Atlantic spotted dolphins (*Stenella frontalis*). And the marine mammal photographer Flip Nicklin has seen beluga whales living in Lancaster Sound in Baffin Bay, Canada, that released rings of air as they repeatedly clapped their jaws together, possibly in a display of aggression.

KAIKO'O (*left*), an adult bottlenose dolphin at Sea Life Park Hawaii, generates a rising ring of air to play with. The laboratory at the park (*above, right*) offers a window into the world of dolphins.

Hawaiian Ring Culture

During the past five years at Sea Life Park Hawaii, we have studied 17 bottlenose dolphins; nine of them, ranging in age from 1.5 to 30 years old, generated air rings. Based on our observations at other oceanariums and consultations with colleagues at various sites, we believe ring blowing is more common at Sea Life Park Hawaii than at other aquariums; the dolphins here appear to have created a "ring culture" in which novice dolphins learn to make rings in the presence of experts that, in a sense, pass down the tradition.

Ring making is a leisurely pastime, so the animals generate rings only when they want to—not on command or for a reward of food. Furthermore, ring making does not seem to be associated with functional behaviors such as eating or sexual activity. Because ring blowing is unpredictable, we have had some difficulty documenting it. But over time we have captured most of the dolphins at play in photographs and on videotape. (Additional photographs can be seen on the World Wide Web at http://earthtrust.org, and a Quicktime movie can be found at http://www.sciam.com/) Unfortunately, neither of these media does the dolphins justice. But the archived images do reveal important information about the physics of the rings.

From what we have seen, the dolphins employ three basic techniques to form the rings. In the simplest method (also

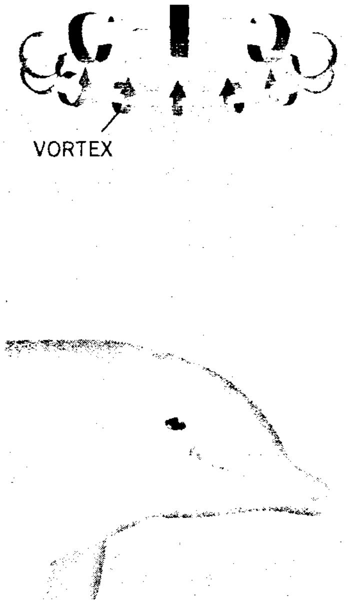

LAURIE GRACE

HALO OF AIR becomes thinner and expands in radius as it is carried to the surface by the vortex flow (*arrows*) through the center of the ring. The vortex also serves to stabilize the ring, preventing it from breaking up into smaller bubbles. Here Kaiko'o produces a ring and follows it up through the water (*video stills, bottom to top*).

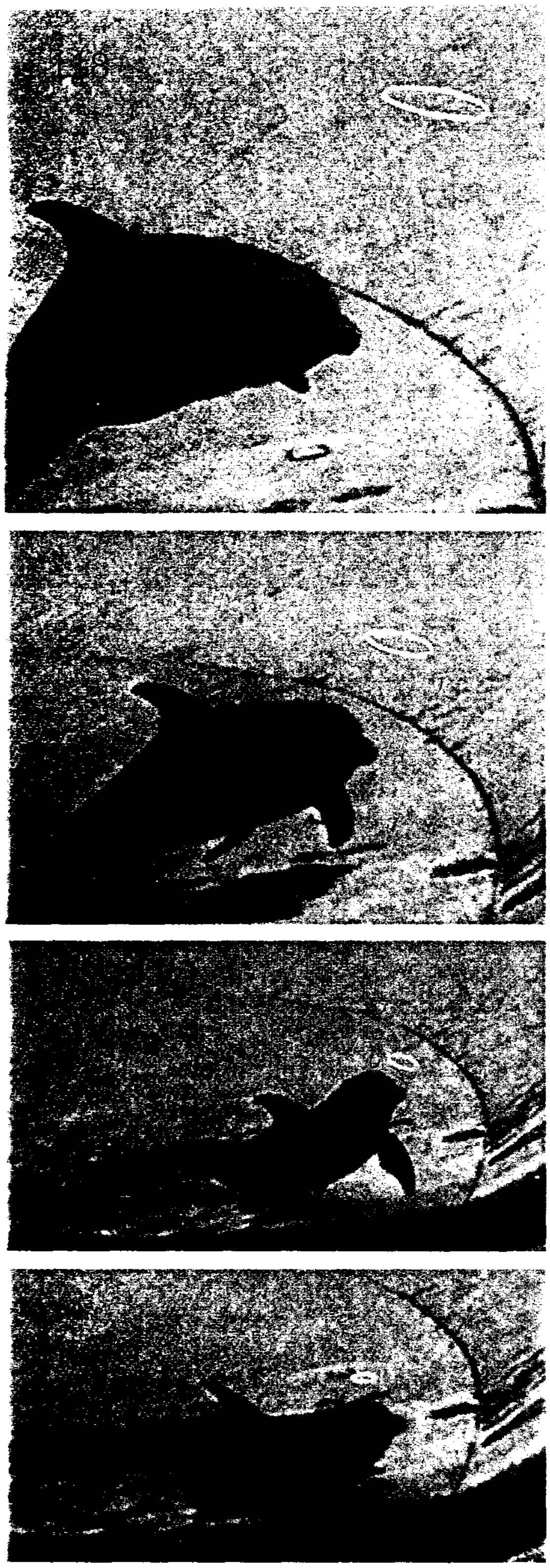

MARTEN, PSARAKOS AND WHITE *Earthtrust*

used by human divers), dolphins puff out bubbles from their blowholes; these bubbles become halos of air that expand in radius while decreasing in thickness as they rise to the surface [*see illustration above*]. One of the dolphins we watched, the adult male Kaiko'o, could emit two rings in succession and then fuse them into a single, large ring.

The physics behind this type of ring is relatively straightforward: any spherical bubble bigger than about two centimeters in diameter will quickly become a ring because of the difference in water pressure above and below the bubble. Water pressure increases with depth, so the bottom of the bubble experiences a higher pressure than the top does. The pressure from below overcomes the surface tension of the sphere, punching a hole in the center to create a doughnut shape.

As water rushes through this hole, a vortex forms around the bubble. Any vortex ring travels in the same direction as the flow through its center; in the case of these simple air rings, the vortex flow, in combination with the air's natural buoyancy, propels the bubbles toward the surface. Although the process of making air-filled rings is fairly simple, dolphins cannot blow stable ones without some practice, suggesting that additional factors—such as the viscosity of the water and how the air is ejected from the blowhole—need to be taken into account.

In a more elaborate approach, the dolphins fabricate rings that travel horizontally and sometimes even downward in the water. For instance, a dolphin might swim forward rapidly on its side so that its normally horizontal flukes (that is, its tail fin) are vertical. By thrusting its flukes vigorously to one side, the animal generates an invisible, ring-shaped vortex that travels horizontally and slightly downward. After quickly turning around, the dolphin finds the vortex and injects a bubble into it from the blowhole. (The dolphin often produces an audible series of clicks before the release of air, suggesting that sonar may be employed to locate the invisible vortex.) The pressure inside a vortex is lowest in the center, or "eye," of the swirl; when the dolphin exhales into the vortex, the air migrates to the region of lowest pressure and is drawn out along the core of the ring-shaped vortex [*see illustrations at top of pages 86 and 87*].

The resulting ring can be up to 60 centimeters (two feet) across and just over a centimeter thick, traveling horizontally in the water. Once again, the movement of the ring reflects the direction of the flow through its center; in the case of the vortex created by the dolphin tail fin, this flow is horizontal and sometimes even downward. With a sideways toss of its rostrum, or jaws, the dolphin can pull a small ring off the larger one and then steer it through the water.

Making a vortex with flukes and planting a bubble in it can be done in a variety of ways—the adult female Laka often positions herself vertically in the water with her head pointed down and tail up. Laka then flips her tail fin down to stir up a vortex. She fills the vortices not only with air from her blowhole but also with air from her mouth. Occasionally, Laka will capture air from above the water with a downward thrust of her flukes. In addition, we have watched Laka release from her mouth small bubbles that pass along her body; when the bubbles reach her flukes, she flips them into a ring. And she can even augment a ring by injecting more air into it.

Experimenting with Bubbles

The third type of air-filled vortex dramatically reveals the dolphins' capacity for experimentation. On a few occasions, we watched the young female dolphin Tinkerbell, Laka's daughter, construct long helices of air, using the most complicated technique we have seen. These more complex structures no doubt result from considerable refinement through trial and error. Tinkerbell has developed two very different methods for making helices. In one approach, she releases a group of small bubbles while swimming in a curved path near the wall of the tank. She then turns quickly, and as the dorsal fin on her back brushes past the bubbles, the vortex formed by the fin brings the bubbles together and coils them into a helix three

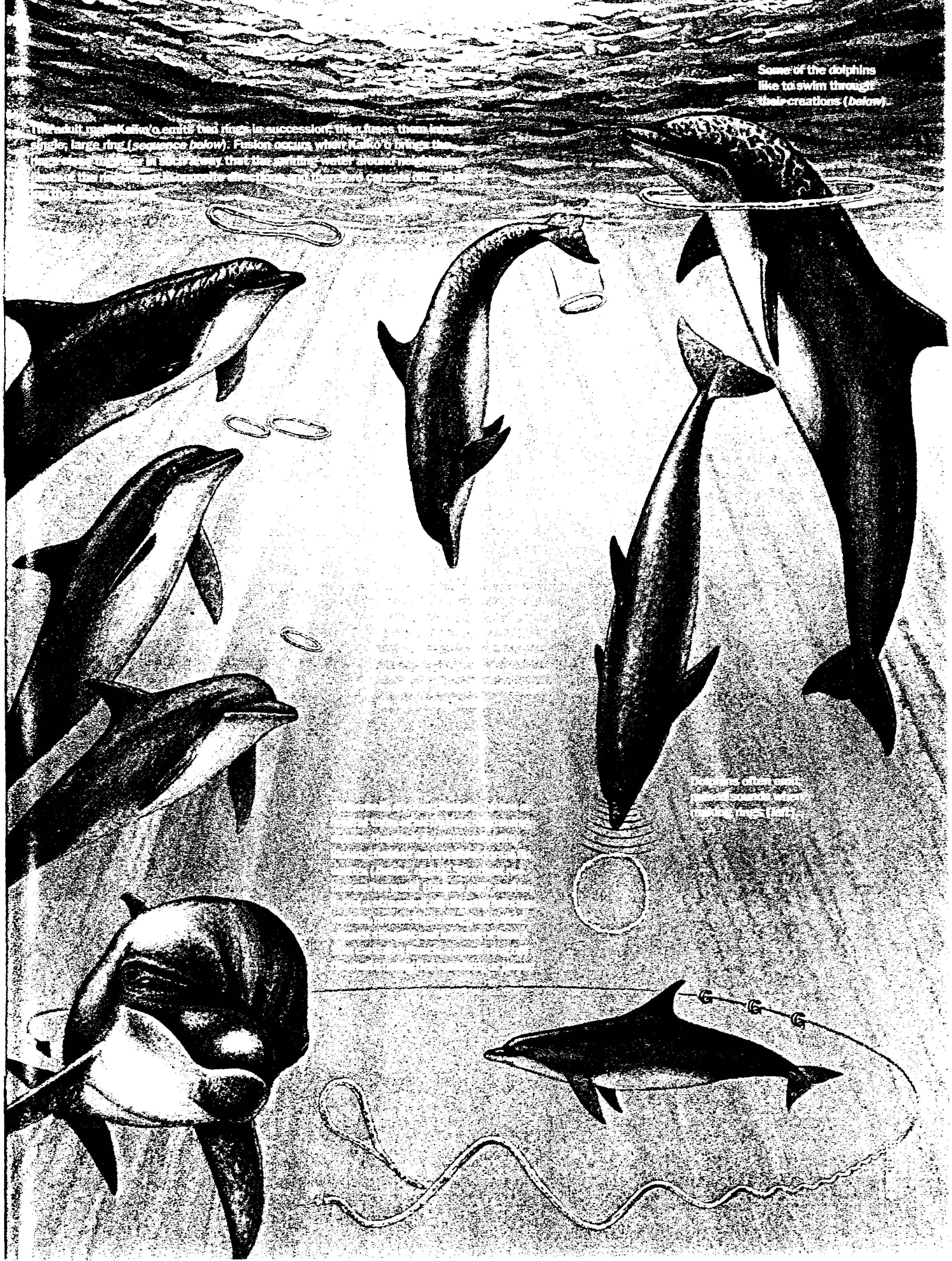

Some of the dolphins like to swim through their creations (*below*).

The adult male Kaiko'o emits two rings in succession, then fuses them into a single, large ring (*sequence below*). Fusion occurs when Kaiko'o brings the rings close together in such a way that the spinning water around neighboring sections of the rings moves in opposite directions and therefore cancels out, and [illegible]

[illegible]

Dolphins often emit pulsed sounds when making rings (*left*).

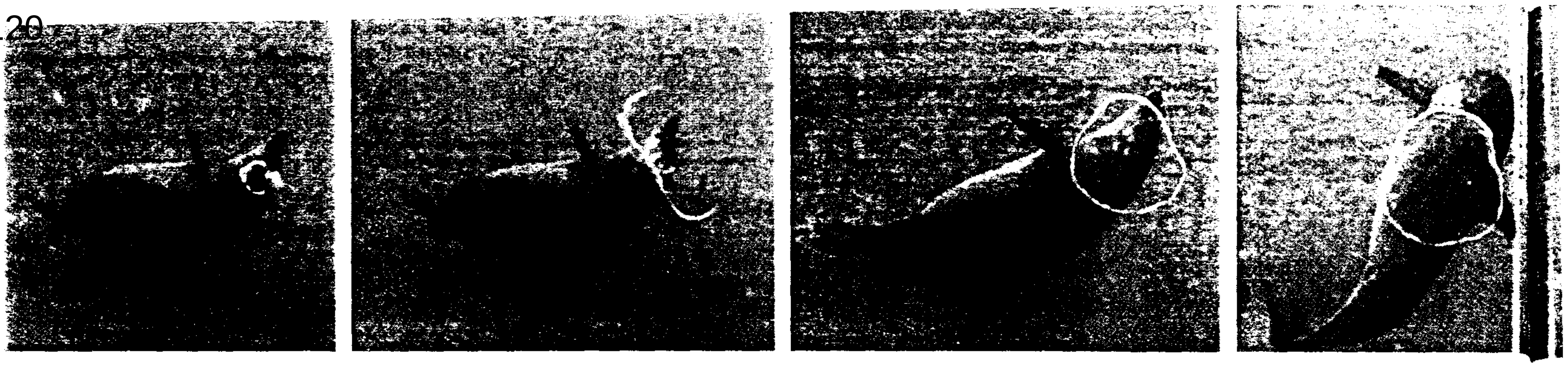

to five meters (10 to 15 feet) long [*see illustrations at bottom of these two pages*]. We have also seen Tinkerbell swim across the tank in a slightly curved path, leaving behind an invisible dorsal fin vortex. She then retraces the path and injects a stream of air into the vortex, producing a long helix that shoots out in front of her.

Again, because the pressure in a vortex is lowest in the eye, once the bubbles are inside the vortex, they move toward the center, merge and elongate into a helical tube. Usually a tube of air in water is unstable and breaks up into smaller bubbles. But all the dolphins' rings and helices are shiny and smooth because the variation of pressure inside the vortex (low pressure at the center, building up to higher pressure at the edges) actually works to stabilize the tube by smoothing the ripples that would otherwise break up the large bubble.

Although we did not see any dolphins other than Tinkerbell generating helices, the practice of making rings spread through the population of dolphins, as some of the individuals learned the technique in the presence of their ring-blowing companions. We had the opportunity to watch one young dolphin's rings evolve over a period of two months from unstable, sloppy bubbles that dissipated rapidly to stable, shimmering rings that lingered in the water for several seconds. Older dolphins also needed time to acquire the talent. One adult male, Keola, lived in the research tank for two years with dolphins that did not produce air rings, and during that time we did not see him generate any. But when his younger, ring-blowing sibling Kaiko'o moved into the same tank, Keola watched for long stretches while Kaiko'o blew rings; within a couple of months, Keola began making his own rings, which slowly progressed in quality.

We have noticed that other dolphins also monitor their ring-blowing tank mates intently, suggesting that the exhibition interests the animals or offers a learning opportunity for them. On several occasions we saw the two brothers Keola and Kaiko'o lying side by side on the bottom of the tank, repeatedly blowing large doughnut rings either simultaneously or within a second of each other. We have also seen one female, swimming closely behind another female who was blowing rings, produce her own bursts of small bubbles as she watched.

The dolphins have drawn humans into their play as well: one day during a period of intense ring making, Tinkerbell repeatedly blew a ring and then came to the lab window where one of us (Psarakos) was videotaping, as if to include her in the activity. Once, we blew soap bubbles inside the lab in front of the dolphins' window, and within a few minutes one of the dolphins joined in by blowing simple, rising doughnut rings

MARTEN, PSARAKOS AND WHITE *Earthtrust*

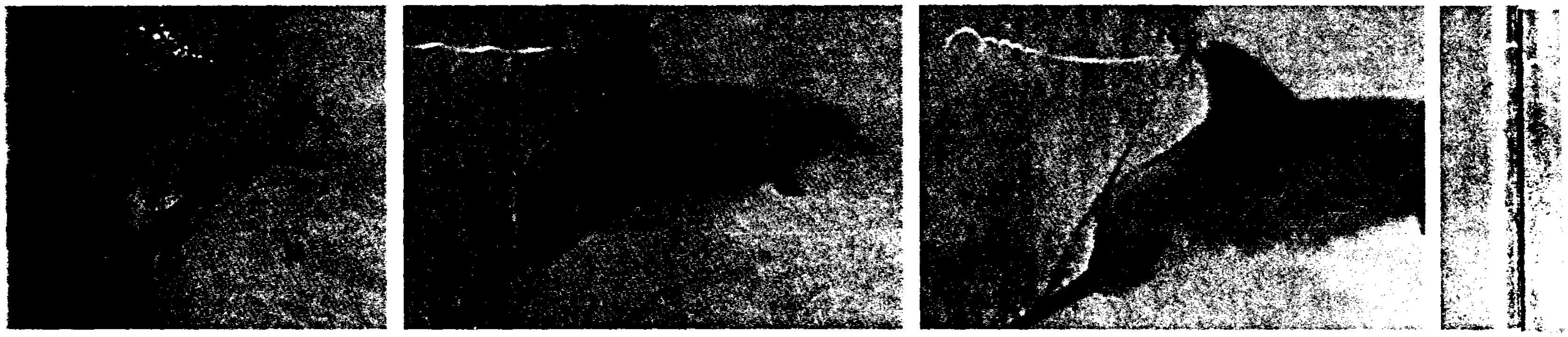

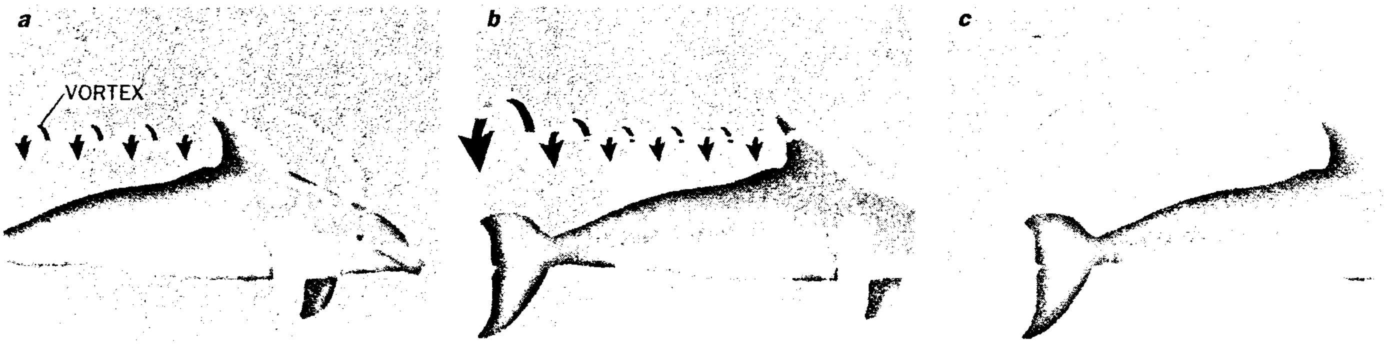

LAURIE GRACE

CORKSCREWS OF AIR are uncommon: the authors have observed only Tinkerbell (*video stills, above*) create them. In one technique, Tinkerbell emits a burst of bubbles while producing a spiral vortex off the dorsal fin (*a*). When the bubbles encounter the vortex (*b*), they are drawn into it, then merge and elongate into a long helix of air (*c*).

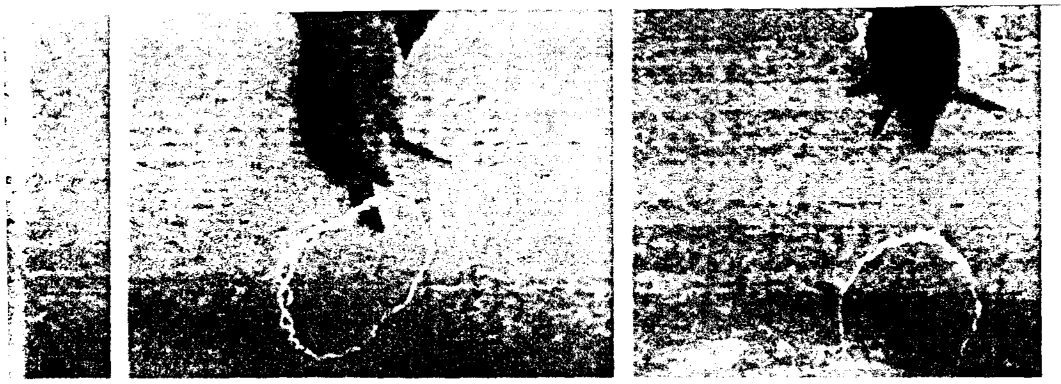

HORIZONTALLY MOVING RING forms when a dolphin flicks its tail while swimming on its side. The horizontal and slightly downward motion of the fin creates a vortex traveling in the same direction (*a*). The dolphin then turns around and injects air into the swirling flow (*b*); the air is drawn along the core of the vortex (*c*), forming a ring that moves in the direction of flow through its center. The adult female Laka is pictured (*left*) exhaling into the vortex and examining her creation.

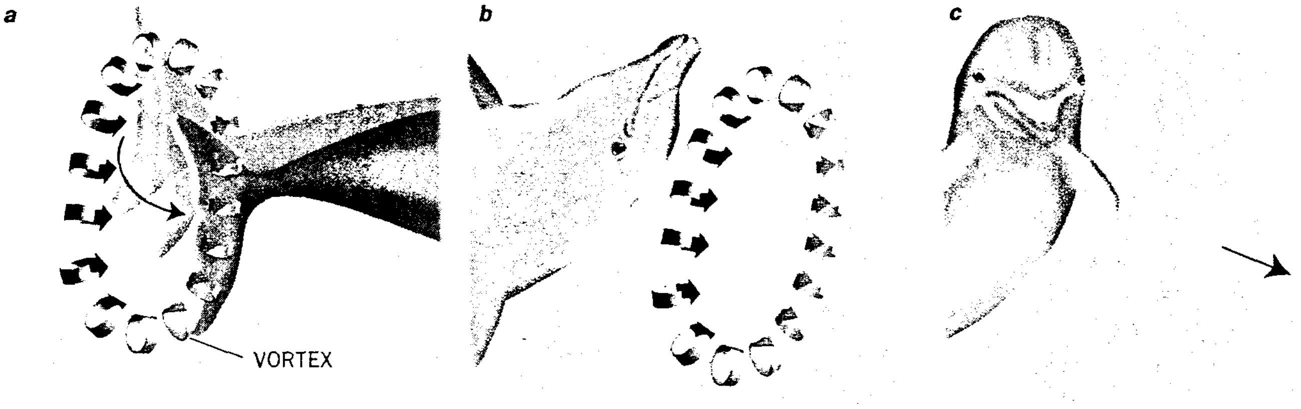

LAURIE GRACE

near the lab window. The real surprise came when the dolphin swam away from the window and made several fluke vortex rings—so different from what we each blew at the window.

Our study of the bottlenose dolphins at Sea Life Park Hawaii continues in the hope of better understanding their behavior. As the only nonprimates that have shown strong indications of self-awareness, these dolphins may teach us about the nature of intelligence through their experimentation and play. But as we consider their remarkable abilities, we are haunted by the knowledge that many cultures, including our own, regard dolphins as expendable. Dolphins continue to be targeted by tuna nets, to become ensnared in expansive drift nets and gill nets, to be canned as mock whale meat and to be shot for crab bait or to be hunted for sport. Earthtrust and its sponsors work to address these issues, but we believe only a basic change in human behavior will make a permanent difference. It is our fervent hope that by providing new views into the dolphin mind, we may yet convince people to stop the indiscriminate slaughter of these fascinating creatures. ◼

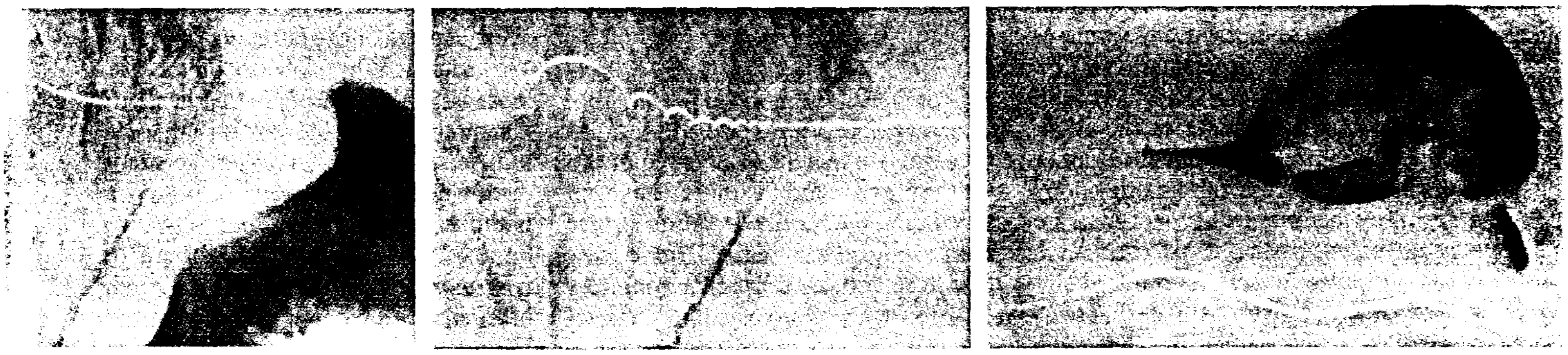

The Authors

KEN MARTEN, KARIM SHARIFF, SUCHI PSARAKOS and DON J. WHITE have worked together in the study of dolphin rings for the past two years. Marten, who studies bioacoustics as well as dolphin behavior, is director of research for Project Delphis at Earthtrust. Shariff specializes in fluid dynamics at the National Aeronautics and Space Administration Ames Research Center. Psarakos is the computer scientist and co-director of the wild dolphin research project at Project Delphis. White founded Earthtrust in 1976 to promote the conservation of marine mammals; he is currently spearheading a new campaign in the area of nonintrusive dolphin research and public education. The authors gratefully acknowledge the support of the staff at Sea Life Park Hawaii. Information on Earthtrust is available from earthtrust@aloha.net or 25 Kaneohe Bay Drive, Kailua, HI 96734.

Further Reading

VORTEX RING BUBBLES. T. S. Lundgren and N. N. Mansour in *Journal of Fluid Mechanics*, Vol. 225, pages 177–196; March 1991.

EVIDENCE OF SELF-AWARENESS IN THE BOTTLENOSE DOLPHIN (*TURSIOPS TRUNCATUS*). Ken Marten and Suchi Psarakos in *Self-Awareness in Animals and Humans: Developmental Perspectives*. Edited by S. T. Parker, R. W. Mitchell and M. L. Boccia. Cambridge University Press, 1994.

USING SELF-VIEW TELEVISION TO DISTINGUISH BETWEEN SELF-EXAMINATION AND SOCIAL BEHAVIOR IN THE BOTTLENOSE DOLPHIN (*TURSIOPS TRUNCATUS*), by Ken Marten and Suchi Psarakos, pages 205–224, and related articles on animal consciousness in *Consciousness and Cognition*, Vol. 4, No. 2, pages 205–269; June 1995.

General information on dolphin cognition research and the organization Earthtrust is available on the World Wide Web at http://earthtrust.org

p. 113 – 115

VORTEX MOTION.

Every one has noticed the symmetrical wreaths of smoke and steam occasionally projected high into the air on a still day by a locomotive; similar rings may often be noticed after the firing of a gun. It is not uncommon to see a smoker forming such wreaths with his mouth. These rings are simply whirling masses of air revolving upon axes curved in annular form, the smoke serving to mark the projected and whirling body of air, thus distinguishing it from the surrounding atmosphere. The whirls would exist without the smoke, but they would, of course, be invisible.

All the apparatus needed for producing vortex rings at will is an ordinary pasteboard hat box, having a circular hole of 4 or 5 inches diameter in the cover. Two pads of blotting paper are prepared, each consisting of six or eight pieces. Upon one pad is poured a small quantity of muriatic acid and upon the other a similar quantity of strong aqua ammonia. These pads are placed in the box and immediately a white cloud is formed, which consists of particles of chloride of ammonium so minute as to float in the air.

By smartly tapping opposite sides of the box, a puff of air is sent through the circular opening of the cover, carrying with it some of the chloride of ammonium. The friction of the air against the edges of the cover retards the outer portion of the projected air column, while the inner portion passes freely through, thus imparting a rotary motion to the body of air adjoining the edge of the cover, the axis of revolution being annular. After the ring is detached, the central portion of the air column continues to pass through it, thus maintaining the rotary motion.

When two rings are projected in succession in such a manner as to cause one to collide with the other, they behave much like elastic solid bodies. By making the aperture in the box cover elliptical, the rings will acquire a vibratory motion.

By fastening the box cover loosely at the corners, the box may be turned upon its side and rings may be projected horizontally.

It is obvious that smoke may be used in this experiment in lieu of the chloride of ammonium.

Fig. 116.

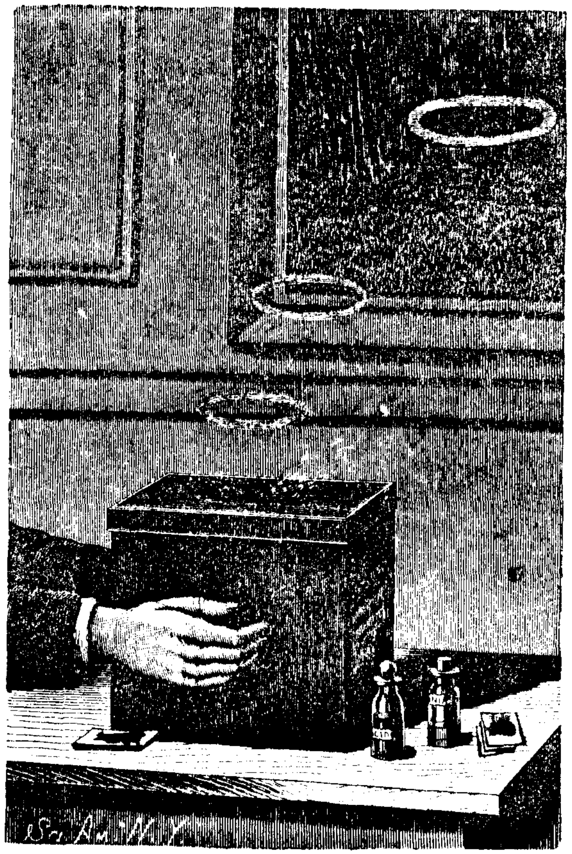

Vortex Rings.

Popular Science. August 1942. p. 33-35.

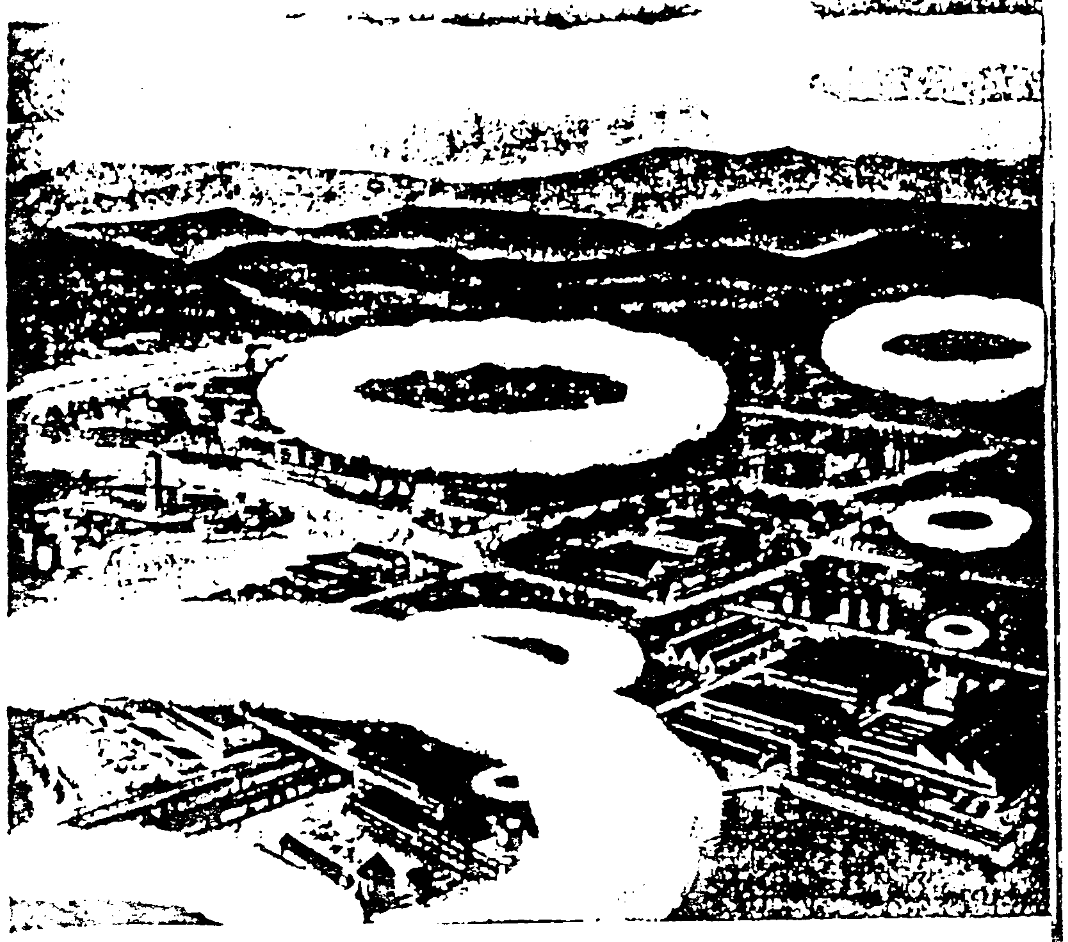

Whirling Smoke Rings to Free Cities of Soot

VORTEX GUNS CAN SHOOT FACTORY GASES SKYWARD

DR. PHILLIPS THOMAS, research engineer of the Westinghouse Electric & Manufacturing Company, picked up what appeared to be a small copper and brass drum with an aperture some two inches in diameter in its head. By means of a tubular peep sight affixed to the top of the drum, he aimed the aperture at one of a row of lighted candles about ten feet away, and then tapped the back of the drum with a rubber hammer. Instantly the candle was extinguished. He repeated the performance half a dozen times, and each time the striking of the metal drum was followed by the extinguishing of a candle. He pointed the aperture at a gong, tapped the drum, and the gong rang. In each case, it was as though an unseen projectile had been fired from the strange device.

These seemingly miraculous feats were accomplished by an invisible ring of air, a smoke ring without the smoke, shot from the aperture by the force with which Dr. Thomas struck the back of the drum. Called a vortex gun and designed on the basis of elaborate mathematical calculations by Westinghouse scientists, this device embodies the first practical application of the well-known principle of vortex motion. Good examples of this motion are the common smoke ring which almost all smokers can blow, and the tunnel-shaped twister cloud familiar to anyone who has lived in the tornado and cyclone belts of the Middle West. The twister, however, is only half of a vortex; it moves only if a wind is blowing, and always travels at right angles to the ground. A smoke ring, which is a true vortex ring, will move in any direction, according to the initial impulse, and owing to the vortex motion the smoke will remain in the ring as long as it is moving. The more rapid the motion, the farther the ring will go before breaking up.

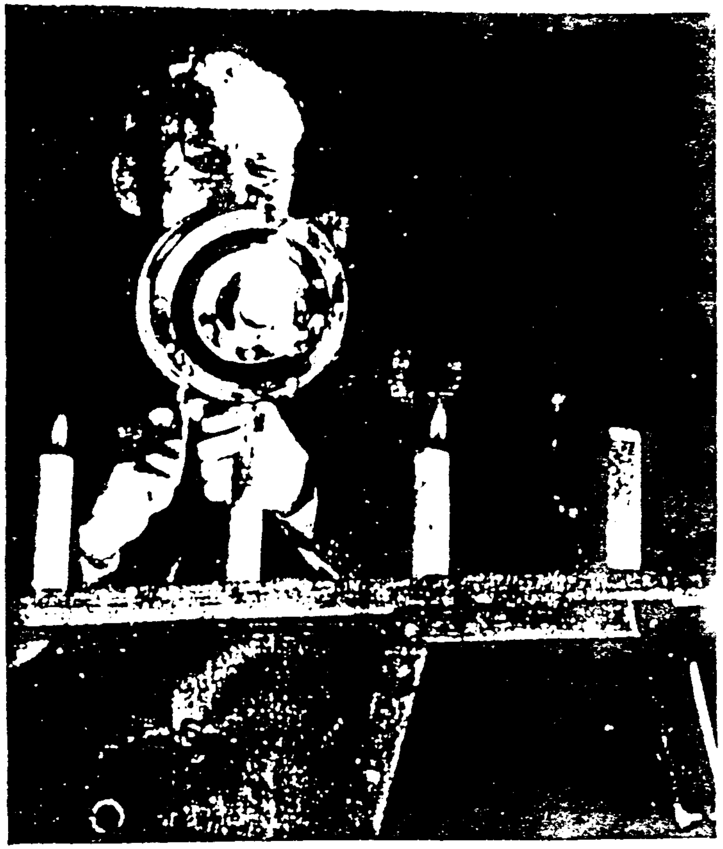

Shot from this vortex gun like bullets from a rifle, whirling air rings will extinguish candles at a distance of 15 feet. The hand machine at left will send out vortex rings at a speed of 20 feet a second. They carry so much force that their impact can be felt at about 25 feet

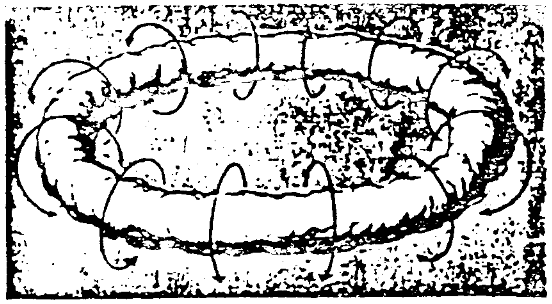

These rings are true vortexes governed by the same principle as that of the familiar rings blown by nearly all smokers. They go in the direction of the initial impulse, keeping smoke trapped as long as they move

The rings or miniature whirlwinds shot from the vortex gun conform to the behavior pattern of the smoke ring as blown from the mouth. Their size and velocity, and the distance traveled, depend upon the dimensions of the gun and the force with which it is struck. They are always invisible unless smoke or some other visible substance is put into the gun.

Westinghouse engineers have constructed experimental vortex guns in two sizes. The hand model, demonstrated by Dr. Thomas as part of the equipment of a traveling laboratory with which he has been touring the country, is about eight inches in diameter. It shoots a vortex ring, with a diameter of from two to three inches, which travels approximately 20 feet a second. The impact of the ring can be felt at about 25 feet, and at from ten to 15 feet will extinguish candles and ring gongs. Mechanically operated, this gun will put out lighted candles at the rate of two a second, and could probably be geared to operate several times that fast.

The other model, with which tests are being conducted at the Westinghouse research laboratories in Pittsburgh, is about 6½ feet in diameter, and shoots an 18-inch ring at a speed of 90 miles an hour. It will blow out candles at from 60 to 70 feet, and at 20 feet will knock a man off balance unless he is braced to receive the blow. Guns of from 12 to 14 feet in diameter, constructed of heavy steel, are now being planned. They will be fired with a TNT cartridge, so that a real wallop will be obtained, and will shoot a four or five-foot vortex ring a distance of one mile at the speed of sound, roughly from 800 to 1,000 miles an hour, depending upon atmospheric conditions. A ring of air traveling at this velocity will strike anything in its path with terrific force, and could conceivably knock a heavy airplane out of control. Theoretically, at least, even larger guns, with correspondingly greater range and power, can be built. According to Dr. Thomas there is no practical limit as to size, provided machines can be devised to give sufficient striking force.

Some of the experiments now under way at Pittsburgh are military secrets, but others deal with the possible use of vortex rings in peacetime. The most promising of these applications so far has to do with the elimination of smoke from industrial areas. Dr. Thomas suggests that it may prove feasible to trap the smoke of a manufacturing plant in huge vortex guns installed just below or above the roof. Powerful automatic hammers would strike the guns at periodic intervals, and the smoke would be sent into the air in the form of vortex rings. Then, instead of low-lying clouds of disagreeable smoke, the air above an industrial plant would be clean and pure, filled with gigantic smoke rings hurtling heavenward at terrific speed. Smokestacks would be unnecessary, and there would also be a war-defense application too, for as Dr. Thomas pointed out, "war planes now find that smokestacks make handy targets."

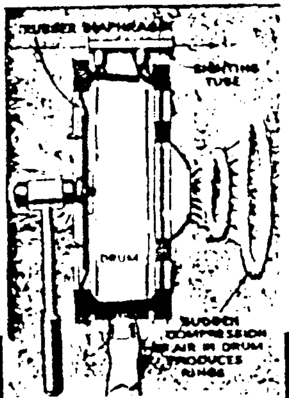

Striking the back of the drum with a rubber hammer, as shown by Dr. Phillips Thomas, research engineer, starts this miniature cyclone on its way. Rings are shot through the front opening

How the vortex gun works can be seen in the cross section at the left. A larger model, operated mechanically, shoots rings at a speed of 90 miles an hour, and really huge guns are in prospect

THE JOURNAL OF THE ACOUSTICAL SOCIETY OF AMERICA VOLUME 27, NUMBER 6 NOVEMBER, 1955

Structure and Velocity of the Periodic Vortex-Ring Flow Pattern of a *Primary Pfeifenton* (Pipe Tone) Jet

A. B. C. Anderson
Michelson Laboratory, U. S. Naval Ordnance Test Station, Inyokern, China Lake, California

(Received April 25, 1955)

Visualization of the vortex flow pattern in typical ***primary Pfeifenton*** jets was made by means of shadowgraph techniques to show the transition in form of the vortex pattern as it moves downstream in the jet, as well as, the dependence of the downstream translational vortex velocity and the geometry of the vortex pattern on the Reynolds number of the jet.

Results of experiment are compared with available theory. These studies were carried out with carbon dioxide jets discharging into the atmosphere. The flow channel geometry consisted of a pipe ⅜ in. in diameter, 12.013 in. long effectively, open at one end which was inserted into a large stilling tank and terminated at the other end by an orifice plate containing a sharp-edged circular orifice, 0.250 in. in diameter and 0.093 in. thick.

INTRODUCTION

As Reynolds number Re of the flow through a circular sharp-edged orifice terminating a pipe (resonant-chamber orifice combination) is gradually changed, discrete ranges of self-excited eigenfrequencies, *Pfeifentöne*, are produced inside the pipe.[1,2] The *primary Pfeifenton* frequency is the one associated with the low Re end of each of the discrete ranges of pipe tones.

Experimental evidence,[1–4] including that to be presented here, supports the view that the mechanism for excitation of the *Pfeifentöne* may be periodic fluctuations of the effective aerodynamic orifice area produced by the growth and periodic shedding of vortices (the boundary layer) from side walls of the orifice. Fluctuation of effective orifice area would then create periodic fluctuations in discharge rate and, therefore, fluctuations in pressure inside the pipe in the vicinity of the orifice. These periodic pulses propagate upstream in the pipe. If the frequency of the pulses is equal to or a multiple of one of the resonant eigenfrequencies of the pipe-orifice combination, the column of gas in the pipe sings out especially clearly to give a pronounced *Pfeifenton*.

Associated with the *Pfeifenton* is a jet, emerging from the orifice, composed of a periodic arrangement of vortex rings. As first shown by Kelvin,[4] the axial velocity of translation v of an isolated vortex ring in a perfect fluid is

$$v=\frac{k}{4\pi R}\left[\ln\left(8\frac{R}{r}\right)-\frac{1}{4}\right],$$

where the radius r of the circular cross section (core) of vortex has been assumed small compared with ring radius R, and where k is the strength of the whole vortex.

Considerations leading to the development of this expression lead to the deduction that if a number of vortex rings co-exist, each ring will move without sensible change of shape or size and with nearly uniform velocity in the direction of its rectilinear axis until it comes within a short distance of a second ring. If the two circular vortices have the same rectilinear axis and the same sense of rotation, the two rings will advance in the same direction. Owing to their interaction, the ring radius of the downstream vortex will increase causing its axial velocity of translation to decrease. The ring radius of the upstream vortex will decrease causing its axial velocity of translation to increase. It may, therefore, happen that the upstream vortex ring will overtake and pass through the downstream ring.

Studies have been made indicating that the foregoing expression is helpful in explaining the nature of the downstream movement of liquid vortices generated at the sharp-edged entrance of a circular pipe.[5] The quantities v, r, and R were evaluated from the flow pattern of colored liquid tracer filaments injected upstream by a hypodermic needle. The vortices, and therefore the circulation in the vortices, appeared to be generated in the *Totwasser* space between the *vena contracta* and the tube walls at the tube entrance. They were formed by the rolling up of lengths of transition layer[6–8] assumed equal to the vortex separation l.

For laminar flow this leads to vortices of core radius r having a circumference $l=2\pi r$. Circumferential velocity of the vortices was assumed to be $\bar{u}/\alpha$ where $\bar{u}$ is the mean velocity of flow in the pipe and α is the contraction area ratio at the *vena contracta* (cross section of the *vena contracta* divided by the pipe cross section). Therefore, the strength of each vortex $k=2\pi r(\bar{u}/\alpha)=l(\bar{u}/\alpha)$ all quantities of which are experimentally measurable. The resultant vortex strength of a downstream vortex resulting from the coalescence of two or more of these was considered equal to the sum of the component strengths.

---

[1] A. B. C. Anderson, J. Acoust. Soc. Am. 25, 541–545 (1953).
[2] A. B. C. Anderson, J. Acoust. Soc. Am. 24, 675–681 (1952).
[3] A. B. C. Anderson, J. Acoust. Soc. Am. 25, 626–631 (1953).
[4] Horace Lamb, ***Hydrodynamics*** (Dover Publications, New York, 1945), pp. 241, 242.
[5] Hermann Kurzweg, Ann. Physik 18, 193–216 (1933).
[6] L. Schiller, 3. Intern. Kongr. Tech. Mech. Teil I, 226–233, Stockholm (1931).
[7] A. Naumann, *Forsch. Gebiete Ingenieurw. 2, 85–98 (1931).*
[8] H. Hahnemann, Forsch. Gebiete Ingenieurw. 8, 226–237 (1937).
[9] A. B. C. Anderson, J. Acoust. Soc. Am. 27, 13 (1955).

For turbulent flow downstream in the pipe, larger and more well-defined vortices were observed in the *Totwasser* space. Observation suggested that the diameter of these vortices should be taken as equal to the distance $2r=(d/2)(1-\sqrt{\alpha})$ between the *vena contracta* and the pipe wall,[6,7] where d is the internal pipe diameter. The circumferential velocity around the vortex was again assumed $\bar{u}/\alpha$, so that the vortex strength is now $k=\pi\bar{u}d(1-\sqrt{\alpha})/2\alpha$.

Kelvin's expression has also been used with apparent success[10,11] *to account for some of the* behavior of vortices in a jet where, again, the vortex strength k of each vortex was taken as $(\bar{u}/\alpha)l$. Associated with this was also the deduction that vortex separation, orifice diameter and vortex-ring diameter should be approximately equal to each other. On the other hand, an analysis has also been made to show that there should exist no stable value for the ratio of vortex-ring diameter to vortex-ring separation,[12] as in the case of the Kármán vortex street.[13]

A vital distinction exists between interaction of separate vortices in a perfect fluid and interaction of separate vortices in a viscous fluid.[14] *In the former*, the vortices during their interplay will always retain their separate identities regardless of their relative strengths and signs. In the latter, experiment shows that a vortex may change in intensity by directly absorbing any number of others, the system coalescing into one or more distinct vortices, while at the same time their combined energies degrade gradually into heat.

The present paper is concerned with visualization of the vortex-flow pattern in typical ***primary Pfeifenton*** jets by means of shadowgraph techniques, the transition in form of the pattern as it moves downstream, and the dependence of the downstream translational vortex velocity on Re of the jet.

APPARATUS

These studies were carried out with carbon dioxide jets discharging into the atmosphere. The flow channel geometry consisted of a pipe ⅜ in. in diameter, 12.013 in. long effectively, open at one end which was inserted into a large stilling tank, and terminated at the other end by an orifice plate containing a sharp-edged circular orifice, 0.250 in. in diameter and 0.093 in. thick. The equipment was the same as described elsewhere,[1,2] except for the shadowgraph arrangement shown schematically, Fig. 1.

To obtain successive pictures of the same jet, and therefore, to observe the transition in form of the jet vortex pattern with elapse of time, two sparks S_1 and S_2[15] were mounted as in Fig. 1. After S_1 discharged producing an image of jet J on one-half of film F, S_2 discharged at a suitable predetermined time later producing a second image of jet J on the other half of the same film F. Knife edges E_1 and E_2 define the borders of the two shadowgraph pictures. A part of the stroboscopic wheel W, having equally spaced holes punched around its periphery and rotating at a known constant velocity, was placed so that part of it shaded film F and was coplanar with it. The dot separation, produced photographically by the holes on the shadowgraphs, permitted a direct determination of the time interval between the two shadowgraph exposures.

Measurements on the shadowgraphs were greatly facilitated by the use of a Universal Telereader Type 17-A developed by the Telecomputor Corporation, Burbank, California. An expression of appreciation to Dr. A. G. Hoyem and W. C. Ward of the Aviation Ordnance Department for having made th [illegible] ment available is hereby acknowledged; also a [illegible] on is extended to Dr. George Kretschmar and [illegible] gley for development and perfection of the timing and triggering circuits.

EXPERIMENTAL RESULTS

Figures 2 to 8 show typical side views of the periodic vortex-ring structure observed. The jets are all discharging upward from the orifice located at the bottom of each shadowgraph. The shadowgraphs occur in pairs, the right-hand showing the jet at a slightly later time then the left.

The time interval between the two shadowgraphs of a pair is determined from the separation of two sets of dots at the top of each pair produced by the stroboscope wheel W, Fig. 1. These are shown only at top of Fig. 2, having been blanked off from the other figures for economy of space. This time interval at the principle sound frequency observed in the resonant cavity and other related data, are shown in the legends. The numbers in parentheses denote the laboratory notebook number of the shadowgraph picture. The length scale used in evaluating the geometry of each pair of shadowgraphs is given by the separation (0.500 cm) of the notches on the posts on each side of each pair of shadowgraphs.

Most of the shadowgraphs show vortex coalescence. Figure 2 shows pairs of vortices of seemingly equal strength coalescing downstream. The original photographs are much clearer and show far more detail. Figures 3 and 4 show two successive stages in the coalescence of a small amplitude second harmonic vortex near orifice with a large amplitude vortex a bit farther ***upstream***. *Figures 5 and 6, on the other*

---

[10] Henning von Gierke, "Über schneidentöne an kreisrunden gasstrahlen und ebenen lamellen," dissertation, Technischen Hochschule Karlsruhe (1944).
[11] Henning von Gierke, Z. angew. Phys. 2, 97–106 (1950).
[12] H. Levy and A. G. Forsdyke, Proc. Roy. Soc. (London) A114, 594–604 (1927).
[13] Th. v. Kármán, Gesselischaft Wiss. Göttingen 5, 547–556 (1911–1912).
[14] H. Levy, Phil. Mag. 2, 844–851 (1926).
[15] Frank N. Miller, *"A short-duration collimated light source,"* US NOTS, Inyokern NAVORD Rept. 3350, July 16, 1954.

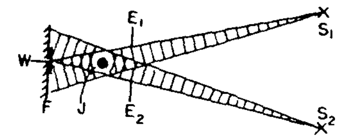

FIG. 1. Shadowgraph arrangement.

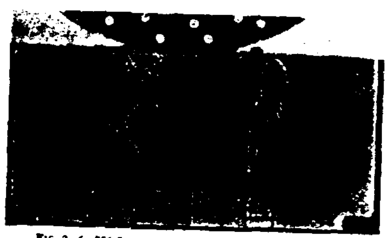

FIG. 2. $f=756.5$ cps, Re $=583$, $\Delta t=1.17\times10^{-3}$ sec (497).

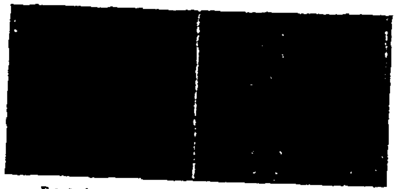

FIG. 3. $f=362$ cps, Re $=738$, $\Delta t=0.889\times10^{-3}$ sec (787).

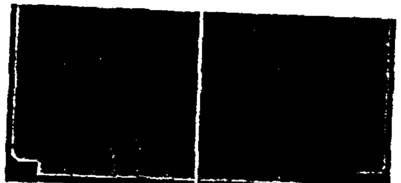

FIG. 4. $f=362$ cps, Re $=738$, $\Delta t=0.889\times10^{-3}$ sec (789).

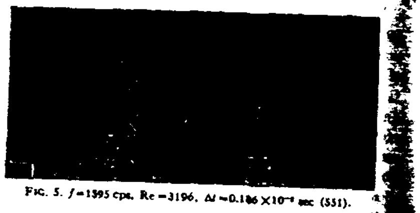

FIG. 5. $f=1595$ cps, Re $=3196$, $\Delta t=0.186\times10^{-3}$ sec (551).

FIG. 6. $f=1595$ cps, Re $=3196$, $\Delta t=0.186\times10^{-3}$ sec (553).

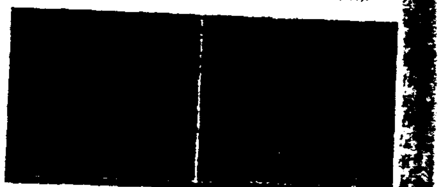

FIG. 7. $f=745$ cps, Re $=1355$, $\Delta t=0.565\times10^{-3}$ sec (900).

FIG. 8. $f=2498$ cps, Re $=4348$, $\Delta t=0.139\times10^{-3}$ sec (956).

FIGS. 1–8. Shadowgraph arrangement and typical side views of the periodic vortex ring structure observed. Jets are all discharging upward from the orifice located at bottom of each shadowgraph. The shadowgraphs occur in pairs, the right-hand showing the jet at a slightly later time Δt than the left. The length scale used in evaluating the geometry of each pair of shadowgraphs is given by the separation (0.500 cm) of the notches on the posts on each side of each pair of shadowgraphs. Number in parentheses denotes laboratory notebook number of the shadowgraph picture.

hand, show two successive stages in the coalescence of a small amplitude second harmonic vortex near orifice with a large amplitude vortex a *bit farther downstream*. In one case, Figs. 3 and 4, a resultant attraction appears between a small vortex ring and a large one *upstream*; in the other case, Figs. 5 and 6, a resultant attraction appears between a small vortex ring and a large one *upstream*; in the other case, Figs. 5 and 6, a resultant attraction appears between a small vortex ring and a large one *downstream*.

Figure 8 also illustrates vortex coalescence. A combination of vortices in the left shadowgraph, just above the orifice, coalesce into a larger more organized single vortex on the right.

Generally, during the close approach of two or more vortices, the following occurs entailing vortex coalescence: The downstream vortex expands and slows down; the upstream contracts and speeds up, finally to overtake and coalesce with the downstream vortex. This behavior is to be expected from a consideration of the interaction of the fields of circulation about the vortices. Frequently, especially when vortex coalescence

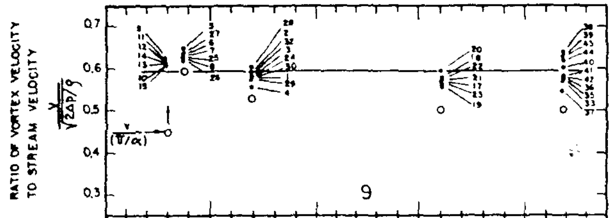

FIG. 9. Experimental dependence of ratio $v/(2\Delta p/\rho)^{\frac{1}{2}}$ [of vortex velocity v in jet to the jet stream velocity expressed as $(2\Delta p/\rho)^{\frac{1}{2}}$, where Δp is the pressure across the orifice and ρ is gas density] on Re of jet (expressed as $\rho l(\Delta p/\rho)^{\frac{1}{2}}/\mu$ where l is thickness of orifice plate and μ viscosity of gas). Large hollow circles show the theoretical dependence of $v/(\bar{u}/\alpha)$ on Re, where $\bar{u}$ is mean velocity of flow through orifice and α is contraction area ratio of flow at *vena contracta*.

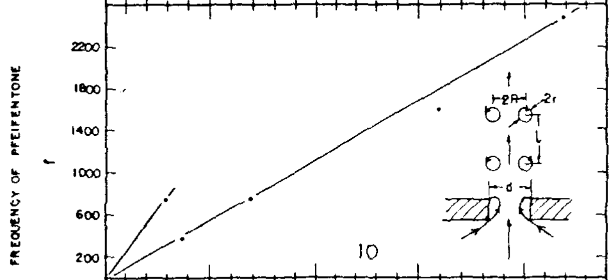

FIG. 10. Dependence of *primary Pfeifenton* frequency f on Re. Deviation of point at Re $=3196$ from straight line due to fact that this jet was a little above the *primary Pfeifenton* condition. This in no way, however, invalidates the results in Figs. 9, 11, and 12. Diagram at right serves to define terms used in the geometrical description of vortex train.

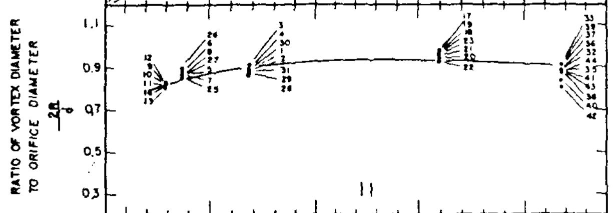

FIG. 11. Dependence of ratio $2R/d$, of vortex diameter $2R$ to orifice diameter d, on Re.

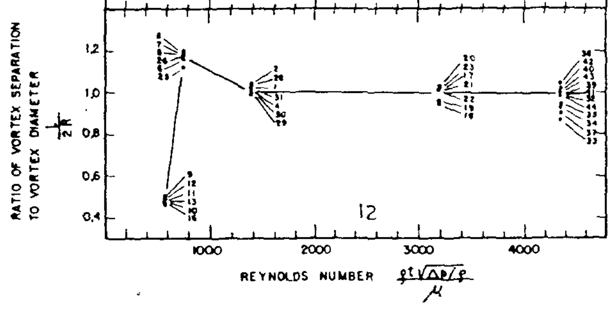

FIG. 12. Dependence of ratio $l/2R$, of vortex separation l to vortex diameter $2R$, on Re. Numbers attached to points denote the laboratory notebook number of the shadowgraph picture according to following code:

1, 393; 2, 394; 3, 395; 4, 396; 5, 411; 6, 412; 7, 413; 8, 414; 9, 485; 10, 486; 11, 491; 12, 492; 13, 495; 14, 496; 15, 497; 16, 498; 17, 550; 18, 553; 19, 555; 20, 556; 21, 564; 22, 565; 23, 566; 24, 586; 25, 774; 26, 780; 27, 788; 28, 900; 29, 901; 30, 906; 31, 907; 32, 908; 33, 948; 34, 922; 35, 949; 36, 950; 37, 953; 38, 955; 39, 956; 40, 960; 41, 962; 42, 963; 43, 964; 44, 965.

is not significant, as in Fig. 7, the jet vortices continue to move downstream very evenly without appreciable change of shape, separation, or translational velocity.

Calculation of the vortex shedding frequency from the displacement of the vortices in each pair of shadowgraphs always showed that the shedding frequency of the largest vortices equaled the frequency of the tone of largest amplitude recorded by the sound pickup.

Figure 9 presents the ratio $v/[2\Delta p/\rho]^{\frac{1}{2}}$, of the vortex velocity in the jet to the jet stream velocity u [expressed as $[2\Delta p/\rho]^{\frac{1}{2}}$, where Δp is pressure difference across the orifice and ρ is the gas density] as a function of Re of the jet [expressed as $\rho l(\Delta p/\rho)^{\frac{1}{2}}/\mu$, where l is thickness of orifice plate and μ viscosity of gas][1,2]. These ratios were determined from a number of shadowgraphs of which Figs. 2 to 8 are typical. Within experimental scattering the ratio appears fairly independent of Re even though the frequency of the principal tone inside the resonant cavity and the rate of shedding of the vortices downstream from the orifice vary over the wide range shown in Fig. 10. Variation of the jet stream velocity $(2\Delta p/\rho)^{\frac{1}{2}}$ with change of Re also parallels Fig. 10 since the orifice number $lf/(\Delta p/\rho)^{\frac{1}{2}}$ has been shown to be relatively constant[14] where f is pipetone frequency.

All the *primary Pfeifentöne* observed, with the pipe-orifice combination used in this study, are presented in this paper except the one around 1150 cps. This one has been *omitted* because of its different and very unusual vortex flow pattern which showed an amazing and reproducible splitting of the jet (upon emergence from the orifice) into *two distinct circular vortex trains.* The axes of these vortex trains made a considerable angle with respect to the normal to the orifice plate. The two trains always lay in a plane passing through the normal to the plate. The geometrical form of the forked vortex train may be described by the fact that *alternate* vortices *emerging* from the orifice were always thrown into one and the same branch of the forked train. Details on this will be presented in a later paper.

Figure 11 shows the ratio $(2R/d)$ of vortex diameter to orifice diameter as a function of Re. These terms are defined as indicated schematically in Fig. 10. In general, vortex diameter is a bit smaller than orifice diameter and is relatively constant with change of Re.

Figure 11 also gives the mean calculated values of the ratio (R/r), of vortex ring radius to vortex core radius for the different pipe tones. This ratio is involved in the Kelvin expression for vortex-ring translational velocity. Some arbitrariness is of necessity involved in the definition and experimental determination of the vortex core radius r from the shadowgraphs. All the visible cross section in the shadowgraph associated with a vortex was *not* assumed to be vortex core, only the part enclosed by the dark innermost ring or arc of each vortex cross section. Inside this ring, the photographic darkening of the shadowgraph appears relatively uniform. This is clearly visible in all originals of shadowgraphs, Figs. 3 to 8. In Fig. 2, the position of the dark ring, however, could only be estimated from the position of the relatively white ring that usually accompanies and partly surrounds the dark ring. Absence of any visible appearance of the dark ring, Fig. 2, and not in the others, is not unreasonable because the derivative of the gas density gradient (which determines photographic contrast in a shadowgraph) across the vortex cores of this pipe tone jet should be less than for any of the others.

Figure 12 shows the ratio $(l/2R)$, of vortex separation to vortex-ring diameter as function of Re. The means of this ratio for the different pipe tones are not all equal and neither are they always approximately equal to unity. The latter appears at variance with conclusions deduced theoretically elsewhere[10,11] which seem to conclude that one should find $l/2R \approx 1$.

DISCUSSION

Kelvin's expression for vortex translational velocity was derived for a free and *isolated* vortex. For a train of circular vortices such as found in the present studies, the expression would seem most appropriate for vortices least involved in vortex coalescence, that is, where the vortex-ring diameter $2R$ and vortex separation l of the different vortices remain relatively constant with elapse of time as the vortices move downstream. This appears true in Fig. 7, in the downstream part of Figs. 3, 4, 5, 6, 8, and possibly to some extent in the upstream part of Fig. 2.

The expression would seem least appropriate where the vortices are close enough so that their interaction leads rather quickly to vortex coalescence. In this case, when two vortices are in the process of coalescing, the vortex diameter of the downstream vortex increases while its vortex velocity decreases; the diameter of the upstream vortex *decreases* while its vortex velocity increases. This appears especially true in the upstream parts of Figs. 3, 4, 5, 6, 8 and possibly, to some extent, in the upstream part of Fig. 2.

In this paper, also, let it be assumed[8-9,10,11] that the vortex strength $k = l(\bar{u}/\alpha)$. This expression may be justified in the present case on the basis that the circulation generated per second in the jet transition boundary layer is $kf = v(\bar{u}/\alpha)$. Since $v = lf$, the circulation generated per second becomes $lf\bar{u}/\alpha$, and therefore the circulation generated per vortex (vortex strength) is $k = l\bar{u}/\alpha$. Substituting this into Kelvin's expression, as well as the appropriate experimental values of $l/2R$ and R/r obtained from Figs. 11 and 12 and listed in Table I, gives the values of the vortex translational velocity in the last column, Table I, expressed in the form $v/[\bar{u}\alpha]$. These values are indicated in Fig. 9 by large hollow circles.

Insofar as $\bar{u}/\alpha$ (the jet stream velocity through the *vena contracta*) equals $(2\Delta p/\rho)^{\frac{1}{2}}$ (the jet stream velocity according to the Bernoulli equation) Fig. 9 gives a comparison of experimental and theoretical values of vortex velocity expressed in terms of stream velocity.

It is somewhat difficult to make a meaningful numerical comparison between values of $v/(2\Delta p/\rho)^{\frac{1}{2}}$ obtained here for pipe tones and values of $v/\bar{u}$ obtained elsewhere[10,11] for jet tones because of the different measures of stream velocity used in the two studies. The two sets of values are comparable, however. Visualization of vortices in the latter study was accomplished by adding white ammonium chloride smoke upstream of the jet and viewing the jet with a stroboscope.

Although the experimental values of the velocity ratio appear to fall somewhat above the theoretical, Fig. 9, the trend in the ratio, with change of Re, appears the same in both. According to the convention for determining vortex-core radius r adopted and described earlier, only in the case of the vortices obtained at Re 583 was there any great indecision as to the proper value to take for vortex core diameter. For more precise determinations of the vortex velocity ratio than possible here, it would be desirable to know how the velocity distribution across the jet (in the orifice and a bit downstream from the orifice) varies with Re, how closely the appropriate velocity in the expression for the strength k of the vortices agrees with $(2\Delta p/\rho)^{\frac{1}{2}}$, and to have a better understanding of the relation between what is seen photographically in the shadowgraph of a vortex and the velocity and density distribution in the vortex.

Figure 12 indicates there is no one single preferred vortex separation l for vortices just emerging from the circular orifice. This appears somewhat at variance with other studies[10,11] which seem to conclude that one should find $l \approx 2R$. The other studies, however, appear to have been carried out on jet tones from circular orifices generally having $l/d \approx 1$. Figures 2 to 8 indicate, nevertheless, that vortices in a circular vortex train whose $l/2R \ll 1$ prefer and endeavor to coalesce downstream into a train whose $l/2R$ is considerably greater.

TABLE I.

Primary *Pfeifenton* frequency f	Ratio of vortex separation to vortex diameter $l/2R$	Ratio of vortex ring radius to vortex core radius R/r	Reynolds numbers Re	Calculated ratio of vortex translational velocity to jet velocity through vena contracta $\frac{v}{\bar{u}\alpha}$
756	0.485	50 or greater	583	0.45
362	1.19	3.51	738	0.58
745	1.00	4.37	1378	0.53
1595	0.99	3.87	3196	0.50
2490	0.985	3.80	4348	0.50

This increased tendency towards instability and vortex coalescence of vortices in a vortex train having $l/2R \ll 1$ may result from the greater degree of interaction existing between vortices that are closer together, superimposed on any inequalities in the strength and relative separation of the vortices leaving [illegible]

Although Figs. 2 to 8 and 12 might lea[illegible]fer that all circular vortex trains tend to app[illegible] ≈ 1 *before dissolution by viscosity, this broa*[illegible]*aliza*tion is not considered substantiated here. An analysis has been made elsewhere to show that there exists no stable value for the ratio $l/2R$ of a circular vortex train as exists for the Kármán street.[11]

---

[14] A. B. C. Anderson, J. Acoust. Soc. Am. 26, 21-25 (1954).

Jets and Cavities--International Symposium. ed. J. H. Kim,
O. Furuya, B. R. Parkin. (NY: ASME, 1985). p. 21-33

MECHANICS AND APPLICATIONS OF SELF-RESONATING CAVITATING JETS

G. L. Chahine and V. E. Johnson, Jr.
Tracor Hydronautics, Inc.
Laurel, Maryland

ABSTRACT

Self-resonating jets take advantage of the natural tendency of an axisymmetric jet to organize into large structures. If a feedback mechanism at the nozzle exit isprovided, the energy content of the jet natural frequency can be dramatically amplified with a resonant chamber. The submerged jet shear layer then organizes in large ring vortices emitted from the nozzle at a discrete frequency and could cavitate to form toroidal bubbles. These cavities grow, collapse, and interact with a nearby impact surface and generate very high pressure fluctuations. Associated with these fluctuations are the usually undesirable phenomena of noise and erosion. These effects can, however, be taken advantage of in important applications such as deep hole drilling, cleaning, cutting, underwater sound generation,...etc. In deep hole drilling, jet structuring is shown to improve on conventional cavitating jets by increasing the cavitation inception number, aiding in chip removal, and improving drilling rates. Cavitating jets are known to be noisy. Self-resonance of the jet makes these fluctuations not only two to three orders of magnitude higher but also concentrates the energy into discrete frequencies. This makes self-resonating cavitating jets very good candidates for controlled high intensity discrete frequency underwater noise generators.

In order to understand the mechanics of these self-resonating cavitating jets, several fundamental studies have been conducted and are still on-going. These cover the areas of nozzle design, flow field description, and jet nozzle, jet target interaction. In this paper, the principle of operation of these jets will be described. The importance of the various parameters will be discussed, and results of tests as related to the various aspects presented. Analytical and numerical studies related to the bubble ring dynamics and interactions are presented. Finally, jet simulation by the replacement of the shear layer with a succession of ring vortices is shown to allow the study of important effects such as: jet structuring; jet shear layer - nozzle lip interaction; and jet wall interaction.

INTRODUCTION

Cavitation is mainly known for its harmful effects, namely, loss of performance, erosion, and noise. The usual procedure to prevent these deleterious effects is to avoid the phenomenon by proper design and by limiting the operating conditions. However, attempts to induce and harness cavitation for useful purposes have been increasingly successful. Ultrasonic cavitation methods take advantage of the erosive power of cavitation for cleaning, emulsification, and mixing. In high-pressure jets, cavitation has for some time now been purposely induced in order to increase their drilling, cutting, and cleaning capabilities, (Johnson et al, 1972). The noise associated with cavitation is being used as a means of sensing cavitation when it becomes destructive and, hence, could allow for alleviating its damaging effects. More recently, we have developed a more direct utilization of cavitation noise: underwater sound generation (Chahine, Johnson, Lindenmuth, and Frederick, 1985).

Experimental observations of submerged jets show the tendency of the turbulent eddies in their shear layer to organize in large structures. Excitation of an air jet with periodic acoustic signals produced upstream of the nozzle by transducers or loud speakers shows a remarkable change of the jet structure into discrete ring vortices when the excitation frequency, f, matches the predominant natural frequencies of the non-excited jet (Crow and Champagne, 1971 and Kibens, 1979). This corresponds to a Strouhal number, S_d, close to 0.3 or one of its first integer multiples. V and d being the velocity and the diameter of the jet, the Strouhal number is defined as

$$S_d = fd/V, \qquad (1)$$

This "natural tendency" of a submerged jet to organize in large structures is of great interest in aerodynamics for air jet noise studies. Crow and Champagne (1971) studied this phenomenon extensively and showed experimentally that forced excitation of the jet at the preferred frequency ($S_d \approx 0.3$) enhances the structuring. The vorticity is then mainly concentrated in ring-shaped, large structures.

The potential of such a phenomenon for submerged water jets was recognized (Johnson et al, 1984), and a unique technology was developed related to achieving useful submerged jets having very high amplitude, periodic, oscillatory discharge without using moving parts in the supply system. The passive excitation is obtained hydroacoustically and structures the shear layer of the jet into discrete, well defined ring vortices when the excitation frequency, f, matches the jet's preferred value. This can be obtained by (a) feeding the final jet-forming nozzle with various types of acoustic chambers (for example, Helmholtz chambers or organ-pipe tubes) tuned to resonate at the desired frequency; and (b) shaping the nozzle so as to feed back the pressure oscillations which occur at the exit. Such devices are forms of "whistles" which self-excite and thus are totally passive. These STRATOJETs have shown enhanced erosivity from increased cavitation activity. The large pressure oscillations associated with the intensification of cavitation, with resonance in the nozzle assembly, and with the production and disappearance of large vortical structures greatly improve the erosion and cleaning capabilities of the jet and make a very effective noise generator.

The principal types of STRATOJET configurations that we have studied and developed are shown in Figure 1. The PULSER (Fig. 1-a) and PULSER-FED (Fig. 1-c) configurations consist of a Helmholtz oscillator whose volume is tuned to coincide with the jet preferred Strouhal number. Another type of STRATOJET which has been the subject of extensive study and development at Tracor Hydronautics uses an organ-pipe acoustic chamber as illustrated in Figure 1-b. In this device the organ-pipe resonant frequency is selected to match the desired structuring frequency defined by the critical Strouhal number of the jet. This concept offers the simplest system design and has been used successfully for erosion studies and noise generation. Although PULSER and PULSER-FED nozzle systems have many important uses and continue to be studied at Tracor Hydronautics, we limit our discussion in this paper to the Organ-Pipe STRATOJET.

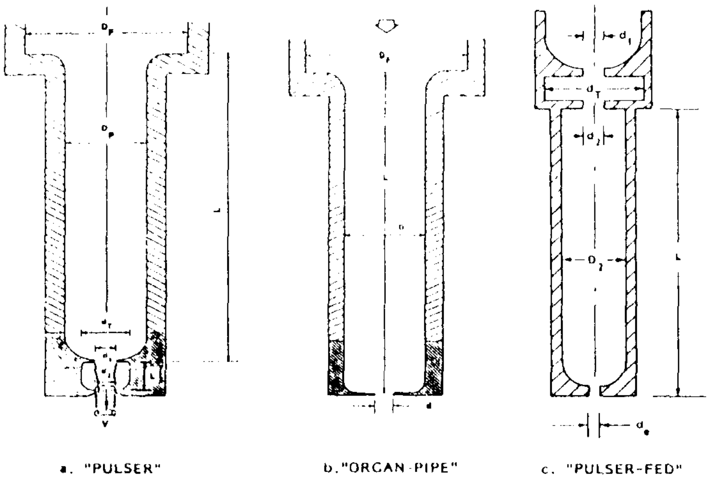

a. "PULSER" b. "ORGAN-PIPE" c. "PULSER-FED"

Figure 1 - Self-Resonating Nozzle System Concepts

PRINCIPLES OF OPERATION OF AN ORGAN-PIPE STRATOJET

Acoustic resonance is achieved in the nozzle feed-tube assembly when a standing wave forms in the "organ-pipe" section [length: L, diameter: D in Figure 1-b]. This section is created by the upstream contraction, (D_f/D) and the nozzle contraction (D/d). Peak resonance will occur when the fundamental frequency of the organ-pipe is near the preferred jet structuring frequency. The exact resonance frequency is dependent on the contractions at each end of the organ pipe; for instance, if both (D_F/D) and (D/d) are large, then the first mode resonance in the pipe will occur when the sound wavelength in the fluid is approximately four times L. When D/d is close to one, resonance occurs when the wavelength is approximately two times L. Although, there are interesting applications where quarter wave organ pipes are applicable, most of our studies to date have involved half wave length systems.

The major problem when designing an ORGAN-PIPE system is the generation of the initial excitation of the oscillations in the organ-pipe chamber. This is successfully achieved through a feedback mechanism at the exit section of the nozzle. Empirical acoustic analysis (Chahine, et al., 1984) have led to the following approximation, useful for estimating the length of the organ pipe:

$$L/d \approx K_n/MS_d\,(1+\beta) \qquad (2)$$

where the "mode parameter" K_n is given, for $D_F/D > 1$, by

$$K_n = \text{func}\left(n, \frac{D}{d}, M\right) = \begin{cases} \dfrac{2n-1}{4}; & \text{for } \dfrac{D}{d} > \dfrac{1}{\sqrt{M}}, \qquad (3) \\[2ex] \dfrac{n}{2}; & \text{for } \dfrac{D}{d} < \dfrac{1}{\sqrt{M}}. \qquad (4) \end{cases}$$

In these expressions, n is the mode number of the organ pipe, S_d the preferred Strouhal number, M the Mach number (ratio of jet velocity to sound speed), and β is an end correction. Figure 2 represents some experimental results for half-wave modes and the relation

$$M = \frac{n}{2\,S_d}\left[\frac{d}{L} - 0.86\left(\frac{d}{L}\right)^2\right] , \qquad (5)$$

where β has been evaluated.

The principles of operation and noise generation of an ORGAN-PIPE STRATOJET are schematically represented in Figure 3.Two predominant sources of pressure fluctuations can be distinguished in addition to the classical nonexcited turbulent shear layer between the jet and the surrounding liquid. One of these sources is easy to define and corresponds to the volume fluctuations of the moving vortex bubble rings formed in the center of the large structures of the self-excited jet. The other source of pressure fluctuations is more complex and relates to the exit area of the jet where high amplitude oscillations of the main flow characteristics are interrelated with the shear layer-nozzle lip interaction. Basically, the two sources of pressure fluctuations are simultaneously sources of jet excitation and noise generation. The acoustic signals from both areas are forcing functions to the resonating chamber in the nozzle assembly.

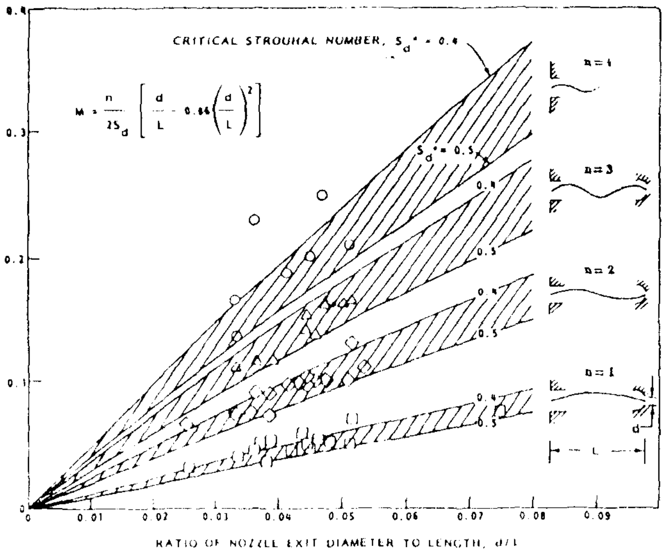

Figure 2 - Correlation of Optimum Mach Number and Organ-Pipe STRATOJET Geometry

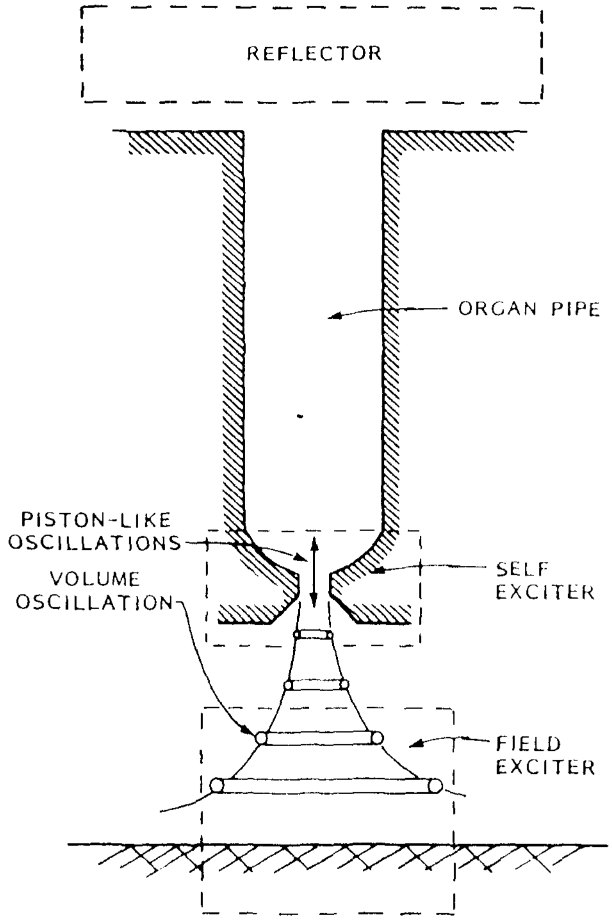

Figure 3 - STRATOJET-Noise Generator. Schematic of Operation

These signals strongly interact; they are both fed back and amplified by the organ pipe of the STRATOJET.

CUTTING AND CLEANING APPLICATIONS

It is generally accepted in the deep-hole drilling industry that bit hydraulics has a major effect on the rate of penetration. The actual drilling rate is always equal to or less than the rate which can be achieved if chips are removed as soon as they are created. Chips are removed from the bottom of the hole by the drilling fluid. Most roller bits utilize the hydraulic horsepower available by ejecting the fluid at the maximum velocity possible from single orifices located in the sectors between the roller cones. Further increases in the jet velocity would improve the cleaning and thus the drilling rate; but, for the most part, the problems involved in working with higher pressure equipment have postponed development of this option. Using cavitating jets is a very effective way of significantly improving cutting efficiency without expenditure of additional power. However, with increasing depth, cavitation becomes harder to achieve.

A. Effects of Jet Structuring on Cavitation Inception

The parameter defining cavitation is the cavitation number, σ,

$$\sigma = \frac{p_a - p_v}{\frac{1}{2}\rho V^2} , \qquad (6)$$

where p_a is the ambient or far field pressure, p_v is the vapor pressure of liquid, ρ is the liquid density, and V is the characteristic velocity, the jet mean velocity. In the case of high-pressure submerged jets used in deep-hole drilling, $p_a >> p_v$, and for well-designed nozzles $1/2\rho V^2$ may be approximated by the pressure drop, Δp, across the nozzle. Thus

$$\sigma = \frac{p_a}{\Delta p} . \qquad (7)$$

The particular value at which cavitation is incipient is defined as

$$\sigma_i = \left(\frac{p_a}{\Delta p}\right)_{\text{at inception}} . \qquad (8)$$

Thus, if the operating conditions for a submerged jet are such that $\sigma/\sigma_i < 1$ then cavitation will occur and as σ/σ_i continues to decrease below unity the amount of cavitation will increase. When a cavitatiang jet is impinged against a surface, so that the cavities formed by the jet are collapsed on that surface, very high pressures ($>>1/2\rho V^2$) are generated, and the resulting cleaning or cutting action is substantially greater than when the jet is not cavitating. In deep-hole drilling, the ambient pressure is hydrostatic and p_a is directly related to hole depth.

Figure 4 indicates zones of cavitation for jets in drill bits under various operating conditions. For a given fluid density, the ordinate may be related to hole depth. In Figure 4, the right side ordinate is shown for a drilling mud density of 10 lb/gal (1.2 gm/cm^3). For typical drill bit nozzles, σ is approximately 0.7. Therefore, cavitation will take place at an operating pressure drop of 2000 psi (13.8 MPa) at depths less than about 2500 ft (760 m). If σ_i is multiplied by a factor of three, as is the case with the STRATOJET, the depth over which cavitation contributes to improved drilling rate becomes significant even at current rig mud pump operating pressures. Figure 5 shows for various nozzle geometries the improvement in σ_i as a function of the relative pressure fluctuations, $p'/\Delta P$, at mid-length of the ORGAN PIPE.

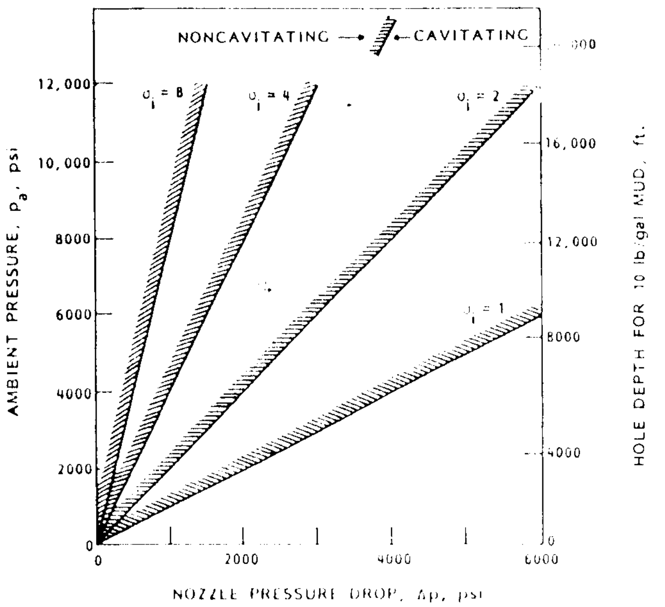

Figure 4 - The Influence of σ_i on the Possibility of Cavitation Utilization for Deep-Hole Drilling

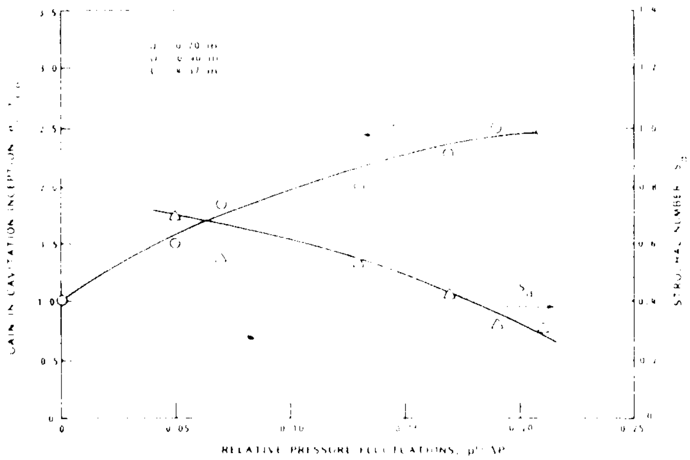

Figure 5 - Gain in STRATOJET Cavitation Inception Index as Compared to Conventional Nozzles as a Function of Relative Pressure Fluctuations at Organ Pipe Mid-Length

There are two reasons why structured jets should be of interest in the context of improving drill bit performance. Both of these reasons may be revealed by estimating the expected differences between an unstructured and a structured jet in local pressures in the flow field and at the surface on which the jets are impinging.

Figure 6 shows the velocity distribution in a line vortex having a rotational core radius denoted as r_c and a velocity at r_c equal to V_c. Such a Rankine vortex is a reasonable approximation of vortices which exist in real, viscous fluids. For such a single line vortex, the value of the pressure drop from the ambient pressure, p_a, to the minimum pressure, p_{min}, which exists at the center of the core (and reaches the vapor pressure, p_v, at inception) is

$$\frac{p_a - p_{min}}{\frac{1}{2}\rho V^2} = \frac{\Gamma^2}{2\pi^2 V^2 r_c{}^2} = \sigma_{i,(\text{vortex center})} \qquad (9)$$

where Γ is the circulation around the vortex.

Since σ_i is desired to be as high as possible in order to cause increased cavitation and erosion, it is preferable for a given nozzle, liquid and speed to have Γ as large as possible. For unexcited jets, the shear zone has many small vortices (Γ is small and of order of the product jet velocity by turbulence length-scale) which roll up into a statistical distribution of sizes; whereas, for an excited jet that becomes structured into discrete ring vortices, Γ is of the order of the product jet diameter by jet velocity.

The preceding analysis is not exact because of the various simplifying assumptions made, (for example, the detailed pressure distribution in a ring vortex system is more complex) but the important result shown is that, qualitatively, σ_i- structured is much greater than σ_i-nonstructured.

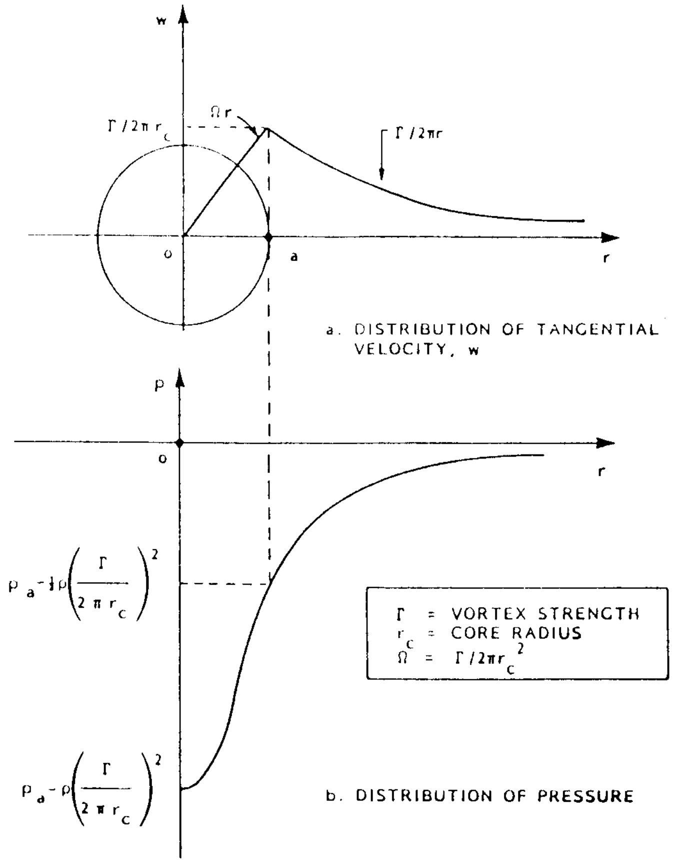
w
$\Gamma/2\pi r_c$
Ωr
$\Gamma/2\pi r$
o
a
r
a. DISTRIBUTION OF TANGENTIAL VELOCITY, w
p
o
r
$p_a - \frac{1}{2}\rho\left(\frac{\Gamma}{2\pi r_c}\right)^2$
$p_a - \rho\left(\frac{\Gamma}{2\pi r_c}\right)^2$
Γ = VORTEX STRENGTH
r_c = CORE RADIUS
$\Omega = \Gamma/2\pi r_c{}^2$
b. DISTRIBUTION OF PRESSURE

Figure 6 - Distribution of Tangential Velocity and Pressure Associated with a Vortex

B. Effects of Jet Structuring on Hole Bottom Cleaning

The normal procedure to resist "blow outs" in bit holes is to operate with an overbalance in pressure. That is, the mud density is selected so as to produce a hydrostatic pressure at the hole bottom greater than the formation pore pressure (Johnson, et al., 1984). Thus there is a flow of fluid into the formation and a resulting "filter cake" buildup across the hole bottom. Consequently, the fluid passing over the hole bottom to remove chips must "lift" them against a very large pressure gradient - creating a hold-down force which is many times larger than the force caused by gravity. Drilling rate decreases dramatically as the pressure difference across the hole bottom is increased. The formation of large structures in the STRATOJET (vortex rings) has the advantage of providing, even in the absence of cavitation, the needed lift force. The passage of each ring vortex across the hole bottom generates a substantial pressure fluctuation at this surface. These pulsations of negative pressure, estimated (for an inviscid fluid) to be an order of magnitude greater than the nozzle pressure drop, should readily overcome most normal hold-down pressures, and thus lift the chips previously created by the mechanical bit action, even at depths where cavitation is suppressed. This phenomenon has been modeled as follows (Genoux and Chahine, 1984a.)

Neglecting the fine structure of the jet's shear layer and assuming that the major features of the flow field are associated with the large structures, the excited jet is modelled with large vortex rings emitted from the nozzle orifice at constant time intervals which correspond to the frequency of the pulsing jet. Each of these vortex rings is allowed to move and change shape under the influence of its self-induced velocity as well as the velocities induced by the other ring vortices present in the field. The presence of the wall is accounted for by applying the method of images since no viscous effects are considered. Knowing the location and characteristics of all rings at any time allows the computation of the generated pressure field.

For a bubble ring of initial section radius, R_0, small as compared with the initial overall ring radius, A_0, the self-induced velocity of the ring is

$$V_{self} = \frac{\Gamma}{4\pi R_0}\,\frac{\varepsilon}{A}\,\left[\mathrm{Log}\,\frac{8\bar{A}}{\varepsilon} - \frac{1}{2} + \frac{W_s^{-1}}{\Omega_s}\right] + 0(\varepsilon) \quad . \qquad (10)$$

W_S^{-1} is the inverse of the Weber number and Ω_S is the circulation number. They measure respectively the relative importance of the surface tension and the pressure drop due to circulation relative to the ambient pressure. These are written as:

$$W_s^{-1} = \gamma/(R_0 P_\infty) \ , \qquad (11)$$

$$\Omega_s = \rho(\Gamma/2\pi R_0)^2/P_\infty \ . \qquad (12)$$

The other terms in (10) are defined as follows

$$\varepsilon = R_0/A_0 \ll 1 \ , \ \bar{A} = A/A_0 \ . \qquad (13)$$

A similar expression is known for vortex rings with a viscous liquid core. In that case ε is replaced by δ, the ratio between the core size and the torus radius, A, the surface tension term is null, and the constant 1/2 is replaced by 1/4 (Safman, 1970)

$$V_{viscous} = \frac{\Gamma}{4\pi R_0}\,\delta\,\left[\mathrm{Log}\frac{8\bar{A}}{\delta} - \frac{1}{4}\right] + 0(\delta) \qquad (14)$$

The interaction of different vortex rings is obtained using the velocity potential induced by each vortex ring at a field point M:

$$\phi = \frac{-\Gamma}{4\pi}\int_S \frac{\underline{PM}\cdot\underline{e}_z}{|\underline{PM}|^3}\,ds \quad . \qquad (15)$$

S is any surface limited by the circular vortical line representing the vortex ring. P is a field point on this surface and thus $\underline{PM}$ is the vector connecting P and M. $\underline{e}_z$ is the unit vector on the ring axis. The translation velocity of vortex ring due to the incoming flow generated by the other vortex rings is equal to the fluid velocity at its location.

Figure 7 shows an example of vortex trajectories obtained numerically. Two distinct trajectories for odd and even number rings are seen. As a result, the even number rings get very close to the wall and therefore generate great tangential velocities and pressure drop on the wall along their trajectory. Comparison with high-speed movie observation of a STRATOJET ring shows a fair qualitative agreement.

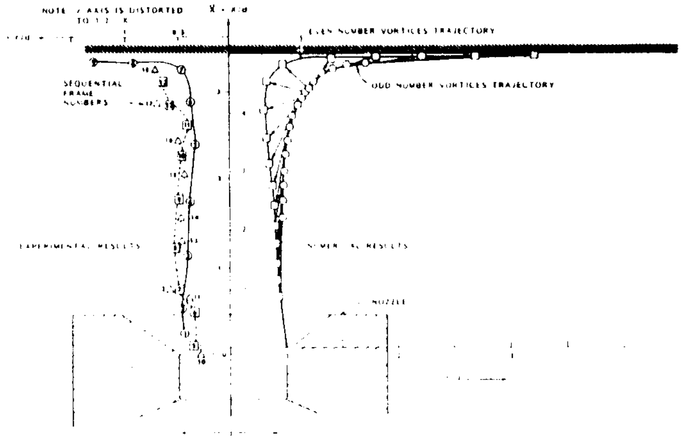

Figure 7 - Trajectories of Structured Jet Vortices, S ≈ 0.25

Figures 8 and 9 show the tangential velocities and pressures induced in five different locations on the solid wall versus time. The spikes correspond to the passage of a vortex ring. It is interesting to notice that both the amplitude and the frequencies of the locally sensed velocity and pressure spikes are dependent on the point of observation. The occurence of the pressure and velocity spikes are very well correlated as well as their amplitudes. Both seem to indicate that the predominant factor is the distance at a given time between the ring and the wall. This explains why the highest negative pressure peaks are at an optimum value of X. Both the high intensification of the tangential velocities and of the suction pressures on the wall due to the passage of organized structures indicate a significant enhancement of the cleaning capability of water jets through excitation. This is possible through an increased shearing action and lifting forces on the solid chips at the wall.

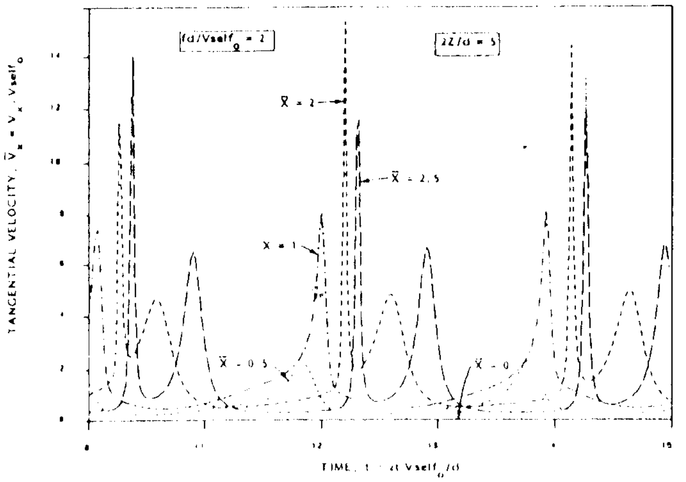

Figure 8 - Tangential Velocities Induced at Different Locations, X, on the Impacted Wall Versus Time

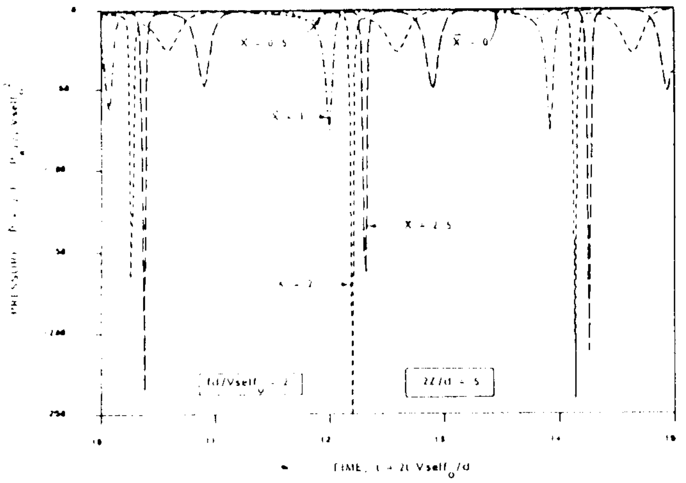

Figure 9 - Pressures Induced at Different Locations, X, on the Impacted Wall, Versus Time

c. Effect of Jet Structuring on Cavitation Erosion

The aspect of the shear layer of a submerged cavitating jet is modified when excited from scraggly random quasilinear vapor vortices to structured well-organized ring vortices moving along the jet periphery. Figure 10 shows a comparison of cavitation appearance in three nozzle types. The self-resonating nozzle is seen, even at a higher cavitation number, to heavily cavitate. Figure 11 shows a high-speed film strip of the bubble ring motion. The behavior of these bubble rings as they collapse on a target is responsible for improved cavitation erosion when using the **STRATOJET**. We have modelled the dynamics of these bubbles when the ratio, ε, between the characteristic size, R_0, of the cross-section of the ring and the overall ring radius, A_0, is small (Chahine and Genoux, 1983; Genoux and Chahine, 1984b.)

The existence of two length scales R_0 and A_0 allowed the use of the method of matched asymptotic expansions. In the "outer region" (macroscale A_0) the torus appears as a distribution of singularities on a moving circle of radius $A(t)$. In the "inner region" (microscale R_0) the torus is reduced to a cylinder of variable section $R(t)$. At high orders of approximation deviation from the circular symmetry, motion of the vortex ring and modification of its overall radius, $A(t)$, also appear. Assuming the fluid inviscid and the irrotational, one has to solve in the liquid the Laplace equation subjected to the boundary conditions at the torus wall, at infinity and eventually at a nearby target. The presence of the solid wall is taken into account by the use of the method of images: the wall is replaced by a symmetrical singularity distribution.

In a matched asymptotic approach, the two boundary conditions at the bubble wall - namely the kinematic and dynamic conditions, apply only in the "inner problem," while the at-infinity condition and the solid wall boundary condition are to be verified only in the "outer problem." The two problems are linked with a matching condition.

In order to simplify the analytical formulation, we follow the bubble during its motion, and we subject the frame of reference to move with the vortex. Therefore, the origin of coordinates in the inner problem is also the location of the vortex center. The first order equation for the normalized cross-section radius, $R^0 = R^0(t)/R_0$, of a bubble ring interacting with a solid wall initially at a distance $d_0 = d_0/A_0$ from the ring center is the following:

$$(\tilde{R}^0\ddot{\tilde{R}}^0 + \dot{\tilde{R}}^{0^2})\left[\mathrm{Log}\,\frac{\varepsilon}{8} + \mathrm{Log}\,\tilde{R}^0 - \alpha_0 K(\alpha_0)\right] + \frac{\dot{\tilde{R}}^{0^2}}{2} = \frac{T^2\Delta P}{\rho R_0^2}\left[\tilde{P}_\infty(t) + \mathscr{P} - \frac{\Omega}{2\tilde{R}^{0^2}} - \frac{\tilde{P}_{g_0}}{\tilde{R}^{0^{2k}}} + \frac{w_e^{-1}}{\tilde{R}^0}\right]. \tag{16}$$

In this expression, T is the characteristic time of the bubble dynamics. $P_\infty(t)$ being the time dependent imposed ambient pressure of characteristic amplitude, ΔP, the parameters in (16) are defined with:

$$\alpha_0 = (1+d_0)^{-1/2}\ , \quad \tilde{P}_\infty(t) = \left[P_\infty(t) - P_\infty(0)\right]\Delta P,$$

$$\tilde{P}_{g_0} = P_{g_0}/\Delta P\ , \quad w_e = R_0\Delta P/\gamma,\ \Omega = \rho(\Gamma/2\pi R_0)^2/\Delta P, \tag{17}$$

$$\mathscr{P} = (P_\infty(0) - P_v)/\Delta P = \tilde{P}_{g_0} + \Omega^2/2 - w_e^{-1}.$$

P_{g_0} is the initial gas pressure in the bubble, K the polytropic coefficient of compression, and P_v is the vapor pressure. The characteristic time T is obtained by balancing the predominant terms between the left and right hand side of the dynamic equation (16),

$$T = R_0\left[\rho\Delta P^{-1}\ \mathrm{Log}(8/\varepsilon)\right]^{1/2}\ ;\ \bar{d}_0 = O(1)\ , \tag{18a}$$

This result is the same as for a torus collapsing in an infinite medium since it assumes that $\alpha_0 K(\alpha_0)$ is of order 1. In a more general case where d_0 is small compared to A_0, the characteristic time T increases when d_0 decreases. Its expression can then be written, provided that $d_0 << 1$,

$$T_0 = R_0\left[\rho\Delta P^{-1}\ \mathrm{Log}\ (32/\varepsilon\bar{d}_0)\right]^{1/2};\ \bar{d}_0 << 1. \tag{18b}$$

Equation (16) as well as higher order equations describing bubble ring motion and deformation can be solved numerically using a Runge-Kutta procedure. This was achieved for a large set of values of P_{g_0}, ε, Ω, and d_0. (Chahine, Genoux, Johnson, and Frederick, 1984). The most important conclusions are the

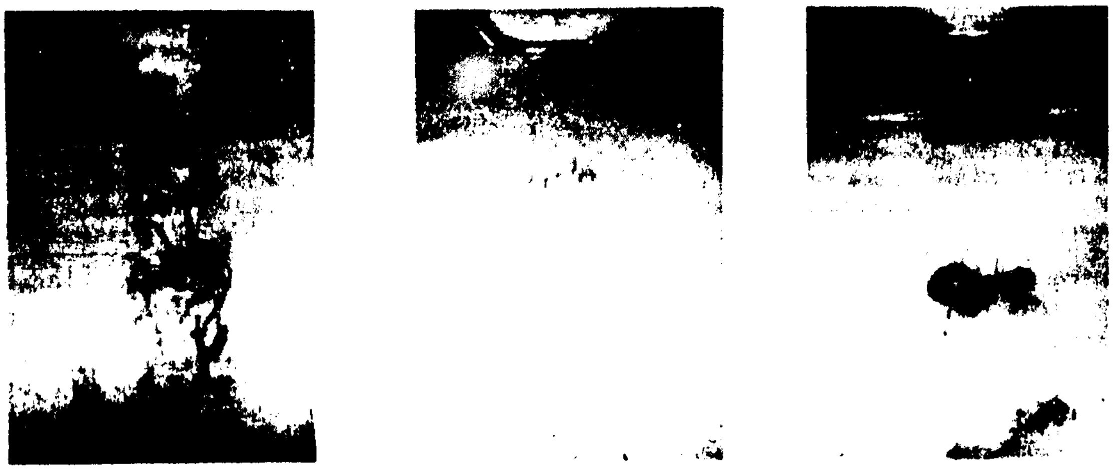

SMITH NOZZLE

Pa = 28 psi
ΔP = 90 psi
$\sigma \simeq 0.31$

CAVIJET NOZZLE NO LIP

Pa = 27 psi
ΔP = 102 psi
$\sigma \simeq 0.26$

CAVIJET NOZZLE THICK LIP

Pa = 40 psi
ΔP = 72 psi
$\sigma \simeq 0.56$
f ~ 700 Hz

FIGURE 10 - COMPARISON OF CAVITATION APPEARANCE IN THREE NOZZLE TYPES (ONLY THE LAST IS SELF-RESONATING)

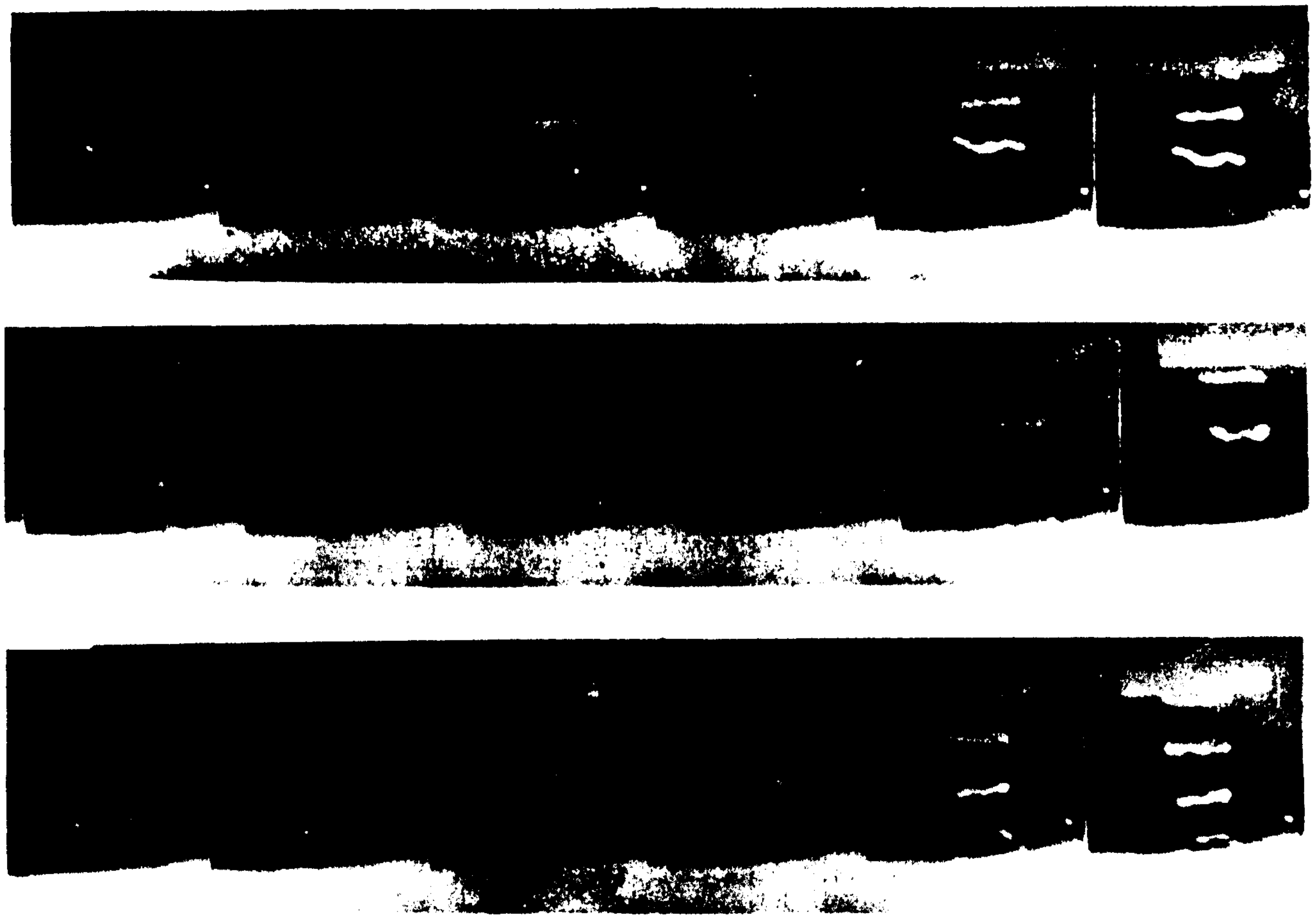

FIGURE 11 - HIGH SPEED MOVIE SEQUENCES OF RING MOTION AND EMISSION FROM A STRATOJET

following. The intensity of the collapse of a bubble ring is of the same order as a spherical bubble but is spread on a larger area. Therefore, a higher erosive power is expected with bubble ring collapse However, the efficiency of this implosion depends largely on the circulation parameter Ω. Let us restate that Ω is a measure of the amount of the pressure drop due to the vortical motion relative to the characteristic amplitude of dynamic pressure variations. Figure 12 ilustrates the importance of Ω. Increasing the vortical motion is seen to have the same effect on the torus behavior as increasing the amount of noncondensible gas in the bubble.

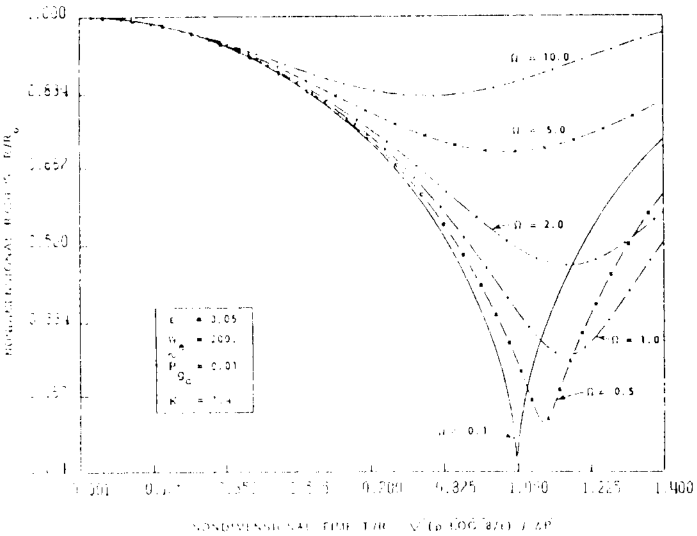

Figure 12 - Vortex Strength Influence on Bubble Ring Collapse

This result is logical once we consider Equation (16). It is seen that changing P_{g_0} or Ω has a comparable effect, and for K = 1 (isothermal compression) the two parameters, P_{g_0} and Ω, can be combined into a single variable. Physically this is understandable since increasing Ω implies decreasing the local ambient pressure at the torus boundary and thus reducing the driving collapse pressure. The same remark applied for P_{g_0}, since increasing the initial gas pressure, while keeping the ambient pressure constant, will also reduce the driving pressure for the implosion. This observation on the influence of Ω has important consequences. For example, when attempting to increase the erosion caused by a jet, increasing Ω has two opposite effects: (a) cavitation inception will appear earlier, and (b) the collapse is damped. This indicates the existence of an optimum Ω for given conditions and the need for an in-depth examination of the criterion required to determine this optimum value. The research of this optimum constitutes our main effort toward the design of an optimized STRATOJET device.

In the presence of a solid wall, numerical solutions have shown the possibility of the formation of a reentering jet as observed for an initially spherical bubble. We have not as yet observed experimentally the existence of such a "conical" jet due to the very short time duration of the phenomenon and to camera frame rate limitations. Figure 13 shows the numerically generated bubble ring sections at different times during the collapse. Three cases are shown: a bubble ring in an infinite medium and a bubble ring at distances of the same order as the overall ring radius and of $\varepsilon^{1/2}$ times this radius. It is interesting to notice that during the collapse stage, there is a change in the direction of the reentering jet as the bubble approaches the wall.

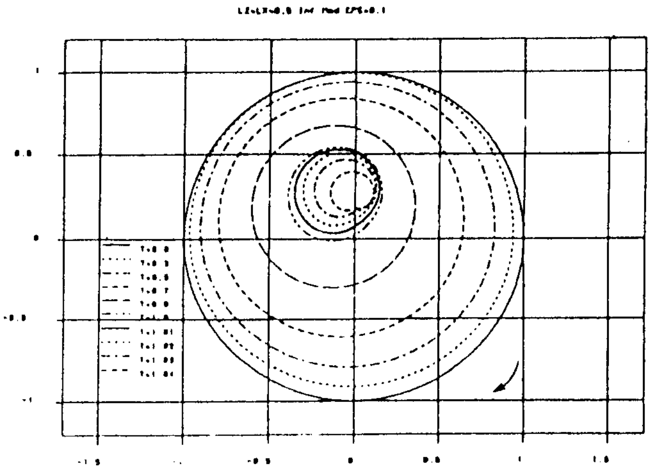

a. INIFINITE MEDIUM

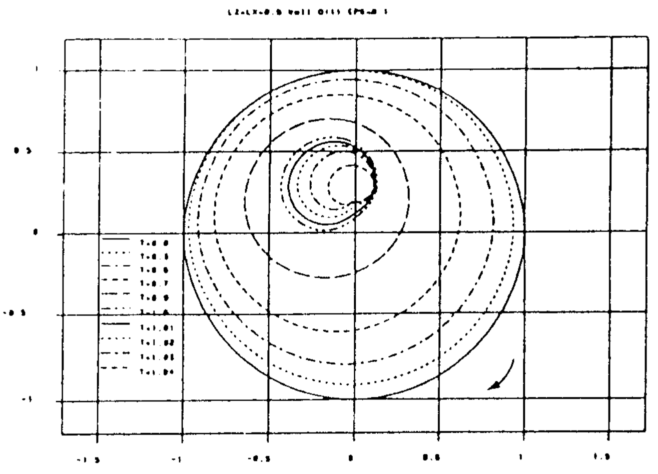

b. d = O (A_0)

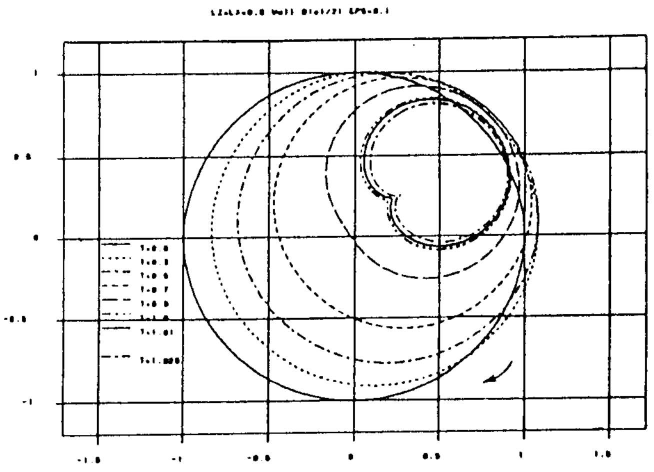

c. d = O $(\sqrt{R_0 A_0})$

Figure 13 - Collapse of a Bubble Vortex Ring Near a Wall. Cross Section Shape at Successive Times

In the infinite medium case, the formation of this asymmetry in the bubble shape is only due to the vortex bubble self-induced motion, i.e., its translation motion relative to the ambient fluid due to both the vortex and the source distribution on the ring center line. In this case, the reentering jet is directed towards the ring axis in the direction of motion of the bubble ring vortex. In the presence of the wall, an opposite force is generated by the bubble ring image. Its importance increases with the closeness to the wall. For instance, in the case $\bar{d}_0 = O(\epsilon^{1/2})$, the force exerted by the wall overtakes the self-induced force, and the reentrant jet is directed away from the ring axis (i.e., the jet axis for the case of a submerged self-resonating cavitating jet). For $\bar{d}_0 = O(1)$, the wall influence is weak, and the same behavior as in an infinite medium is observed. The comparison of Figures 13b and 13c leads to the speculation that there is a distance, $\bar{d}_0$, for a given circulation for which the reentering jet of the collapsing ring is directed perpendicular to the wall. Since reentering jets constitute a basic erosive mechanism of cavitation bubbles, there is a practical application for this observation.

Actual erosion tests of STRATOJETs versus conventional nozzles show a significant intensification of cavitation erosion with the jet oscillations. Table 1 shows some typical results in Indiana Limestone for pressure drops across the nozzle of about 2500 psi. Except at the very low cavitation number of 0.067, the organ-pipe CAVIJET nozzle system cut this limestone to a depth 2 to 2.5 times greater than the standard Smith system. Figure 14 shows similar results in aluminum at a nozzle pressure drop of 7000 psi. After a 5-minute jetting period, the STRATOJET does much better then both conventional CAVIJET and SMITH nozzles.

NOISE GENERATION APPLICATIONS

Noise from submerged cavitating jets has been extensively studied. The early study of Jorgensen (1961) covered most of the ground to be investigated and remains highly relevant to any study of cavitating jets. Jorgensen studied the intensity and frequency content of the noise generated by a submerged jet, investigating the scaling effect associated with nozzle size and the influence of the cavitation number. The acoustic energy upstream was found, for all cases investigated, to peak at a preferred normalized frequency or Strouhal number S_d. The value of S_d was found to be strongly dependent on the cavitation number σ. This "natural tendency" of a submerged jet to organize in large structures, and thus of its acoustic frequency content to peak near a discrete normalized frequency, is taken advantage of in the STRATOJET. The self-excitations enhance pressure oscillations in the Organ-Pipe feed tube and the formation of large structures in the jet shear layer. The nozzle-orifice area can be considered as a piston-like noise radiator, and the acoustical pressure p' generated at a distance r from the radiator can be approximated by

$$p' = \rho c v' K\, d^2 / 8r, \qquad (19)$$

when the wavelength is large compared to the piston diameter. In Equation (19), v' is the velocity oscillation of the radiator, K is the wave number of the oscillations, c is the speed of sound in the fluid, ρ is its density, and d the jet diameter. This can be written

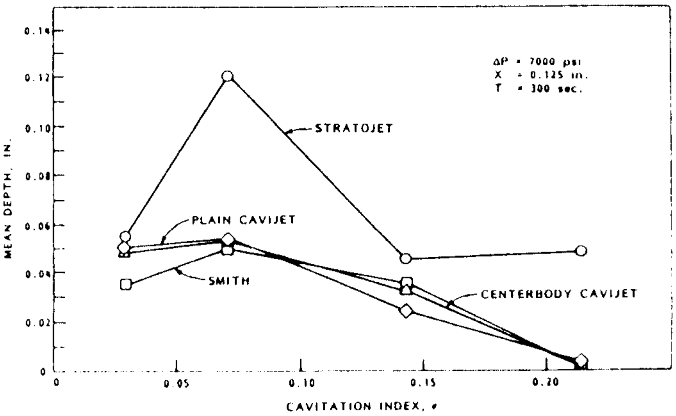

Figure 14 - Comparison of Mean Depth of Erosion for Four Nozzles in Aluminum

$$\frac{p'}{\Delta p} = \alpha \; \frac{d}{r}\,, \qquad (20)$$

where the jet acoustical pressure coefficient α is given by

$$\alpha = (\pi/2) S_d (v'/V). \qquad (21)$$

v'/V is the relative amplitude of the velocity oscillations, and Δp is the pressure drop across the nozzle. Similarly, the acoustic efficiency η of the jet, defined as the ratio of the radiated sound power to the hydraulic power, can be written:

$$\eta = 8\alpha^2 M, \qquad (22)$$

where M is the jet Mach number, $M = V/c$.

Equation (22) contains the basic information needed to optimize such a noise source. The highest coefficient of proportionality between $p'/\Delta P$ and d/r is needed as well as the highest possible jet velocity (or Mach number). These two factors are, in fact, dependent since maximizing the nozzle oscillations corresponds to a determination of the Mach number (see Equation (5)). Therefore, criteria for compromise depending on the sound generation requirements and on the physical constraints must be sought.

Maximizing the nozzle oscillations also depends on maximizing the forcing function arising from the bubble ring collapse described in the preceding section. A measure of the cavitation amplification factor, A_{cav}, is the ratio between the pressure generated by a bubble ring collapse and the pressure fluctuation, p'. One can show that A_{cav} is bounded by (Chahine, Johnson, Lindenmuth, and Frederick, 1985)

$$A_{cav} > \frac{\sigma}{2\alpha} \; \dot{\tilde{R}}^2 \qquad (23)$$

When the jet is excited and α is dramatically increased, A_{cav} is reduced. This result reflects the fact that a part of the cavitation energy is then transferred into jet oscillation. Since the pressure driving the collapse is the ambient pressure around the jet, while the pressure scaling the jet noise is Δp, the relative importance of the cavitation noise is inversely proportional to the degree of cavitation. Fortunately, a lower bound for A_{cav} is proportional to $\tilde{R}^2$. Maximizing $\tilde{R}^2$ is a logical requirement to maximize A_{cav}, since it means an increase in the collapse intensity. Numerical values of $\tilde{R}$ of order 10 were obtained. This would indicate for the experimental tests reported below a significantly high cavitation amplification factor, $A_{cav} \geq 125$.

In order to evaluate the STRATOJET noise generation characteristics, minimize reflections, avoid standing waves in the range of frequencies of interest, and be able to vary σ for constant jet velocity, we used the Hydronautics Ship Model Basin. The basin is 128 m long, 7.6 m wide, and 4 m deep. In addition, the presence in this basin of a well 13 m deep and 3.35 m in diameter allowed us, by locating the nozzle at various depths, to control the ambient pressure at the nozzle exit. This enabled the variation of the cavitation number while keeping the jet velocity constant without the drawbacks of a small enclosed tank and wall reflections.

The nozzle assembly tested for noise generation consisted of a plenum with an 8.25 cm diameter feeding a straight stainless steel pipe of length L and 2.5 cm diameter. This pipe, which acted as an organ pipe, discharged into the ambient liquid through a nozzle having a hemispherical shape with a sharp edge. The nozzle lip was shaped and sized such as to provide a feedback of the preferred natural frequencies of the jet oscillations to the organ pipe which amplified them. That lip consisted of a cylindrical section of length e, followed by a conical bevel of length t. A pressure transducer, located at the midpoint of the organ pipe, allowed for comparisons between the pressure oscillations in the pipe and the noise measurements in the field surrounding the jet. An example of the correspondence between the signal of the transducer located in the pipe and the hydrophone signal can be seen in Figures 15 and 16. A good agreement was observed at the low frequencies, especially at the main organ-pipe frequency. However, the high frequencies sensed by the hydrophone which are probably due to cavitation were filtered by the organ-pipe chamber and hence were not strong in the pipe.

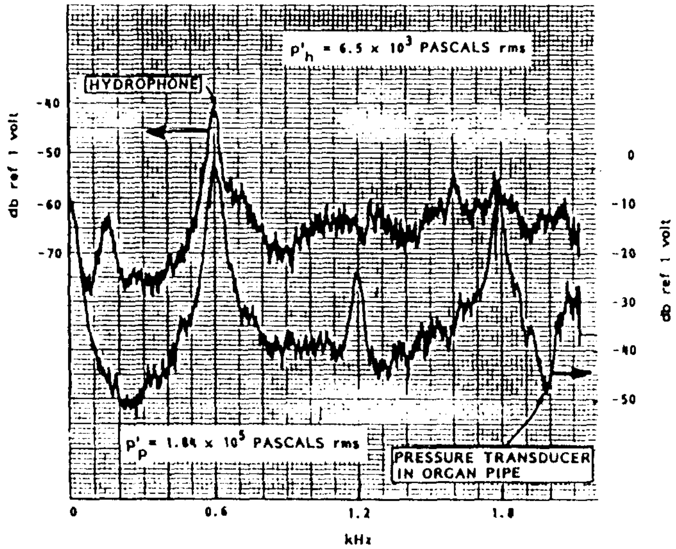

Figure 15 – Frequency Spectrum of Pressure Fluctuations in Pipe and of Acoustic Pressures at r = 0.92 m, θ = 18°, Hydrophone 3.4 x 10^4 Pascals/volt, Transducer 1.4 x 10^5 Pascals/volts, d = 1 cm, ΔP 0.35 MPa

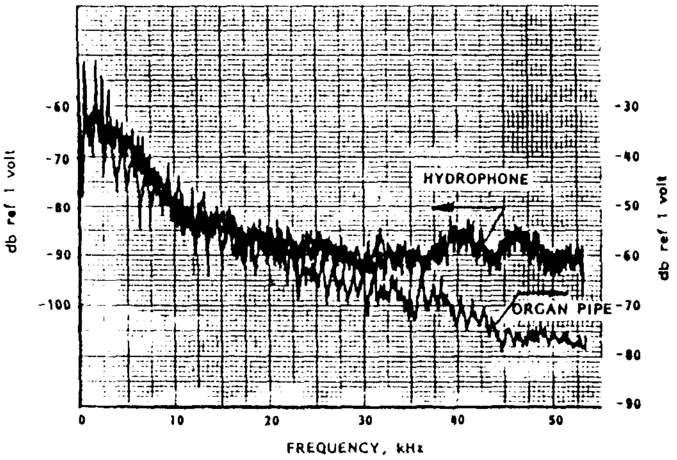

Figure 16 – Frequency Spectrum of Pressure Fluctuations in Pipe and of Acoustic Pressures at r = 0.92 m, θ = 18°, Hydrophone: 1 volt = 1.4 x 10^4 Pascals. Transducer: 1 volt = 1.4 x 10^5 Pascals/volts, d = 1 cm, ΔP = 0.35 MPa

For a practical noise generator it is of great importance to determine the decay function of the generated noise with distance from the nozzle. Figure 17 shows, for two nozzles of diameters 1 cm and 0.5 cm, the results obtained at distances of up to 500 nozzle diameters. These results give the most important indication of the effectiveness of the STRATOJET as a noise generator. Both the rms value of the acoustic pressure and the amplitude of the fundamental frequency of the noise detected by the hydrophone decayed with the distance r from the nozzle as 1/r, with a slope α (Equation 20).

The measured value of α for the conditions presented in Figure 17 was for θ<60°:

$$\alpha \approx 0.18, \text{ for } d{=}1\text{cm}, \qquad (24)$$

$$\alpha \approx 0.11, \text{ for } d{=}0.5 \text{ cm}.$$

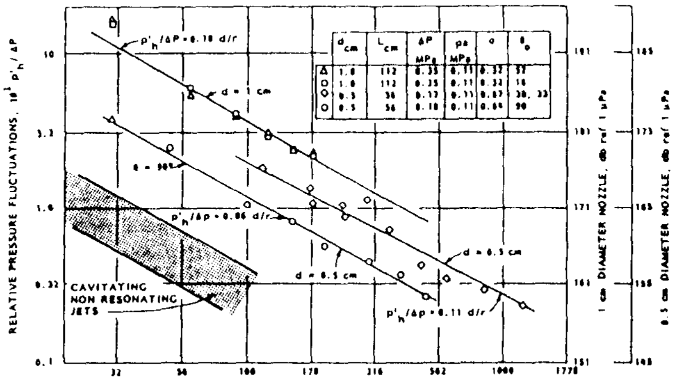

Figure 17 – Attenuation of the RMS Value of the Pressure Fluctuations with Normalized Radial Distance from Nozzle Orifice

The difference between these two values was related to the acoustical performance of the two nozzles with relation to the cavitation number. The acoustical performance of the self-resonating nozzle was much better than a nonresonating cavitating jet. Expressed in terms of the coefficient α, such non-resonating jets would have the value (Jorgensen, 1961)

$$0.008 < \alpha < 0.02. \qquad (25)$$

The acoustic efficiency, η, for these STRATOJETs is:

$$\eta \approx 0.268 \text{ M, for } d \approx 1 \text{cm},$$
$$\eta \approx 0.093 \text{ M, for } d \approx 0.5 \text{ cm}. \qquad (26)$$

Jorgensen reports for a conventional cavitating nozzle:

$$0.0005 \text{ M} < \eta < 0.003 \text{ M}. \qquad (27)$$

These values for conventional cavitating jets, even if an order of magnitude higher than noncavitating jets, are two to three orders of magnitude lower than the efficiency of the STRATOJETs used in these experiments. In terms of decibels, the 1-cm- diameter nozzle, working at a pressure drop of 0.35 MPa, generated about 176 dB re: 1 μPa at a distance of 1 m. This value can be increased by increasing nozzle diameter, pressure across the nozzle, and by improving the nozzle efficiency with better design. Limitation on this increase would, however, come from scaling effects and practical limitations on geometrical size and pump power. Recent tests have also shown that the generated signal could be easily modulated with relatively high frequency (more than half the main frequency for these tests).

NUMERICAL SIMULATION OF JET STRUCTURING

The understanding of the basic mechanisms by which self-resonance and intense oscillations of the flow are initiated and sustained is essential for further development and use of these new nozzle systems. Our first efforts have used systematic experimentation to determine the satisfactory nozzle shape and piping size which achieve strong oscillations at predetermined flow conditions. Problems appeared later when scaling effects, different liquids, (e.g., drilling mud), and lower cavitation number conditions had to be dealt with. This has justified our concentrated effort on an analytical and experimental program to improve our knowledge and establish general guidelines for the optimization of the nozzle/piping assembly design for any prescribed conditions.

Many investigators have theoretically examined jet structuring, and, based on experimental observations, several attempts have been carried out to model a jet with a discrete distribution of vortex rings. Axially symmetric vortex rings with a viscous core have been investigated, and the numerical schemes were able satisfactorily to reproduce experimental measurements or observations. For instance, Acton (1980) represented the upstream portion of the jet with a double row of ring vortices which were allowed to interact and move freely downstream of the nozzle exit. The roll up of the vortex sheet into large axisymmetric structures was numerically demonstrated. Artificial excitation of the jet by periodically modulating the strength of the emitted vortices exhibited the same features as observed experimentally, namely the existence of an optimal Strouhal number.

In an ongoing program, we follow the same approach and introduce, in addition, a potential flow model for the flow inside the feed section to the nozzle orifice. The interaction between the free emitted vortices and the nozzle walls in the separated area of the nozzle (Figure 18) is allowed. The interaction in this region between the jet shear layer and the walls controls the feedback mechanism, and its study is fundamental for the understanding and the control of this mechanism.

As sketched in Figure 18, the flow field under study is divided into three regions. a) The first region, noted U for upstream, is constituted of a semi-infinite cylinder. The flow in that region is reproduced by a cylindrical vortex sheet of uniform intensity ω_{up}. b) The second region is noted N and corresponds to the nozzle walls both in the wetted and separated areas. In that region the flow is reproduced by cylindrical distributions of vortices of intensity ω and of sources of intensity s. c) The last region is the jet region and is noted S for the shear layer. The jet shear layer is replaced by a succession of discrete rings emitted from the nozzle, of spacing λ, which are free to move and interact together and with the upstream singularities. The circulation of any ring k, $\Gamma(k)$ can be modulated, oscillate with time, and be tied to the organ pipe oscillations.

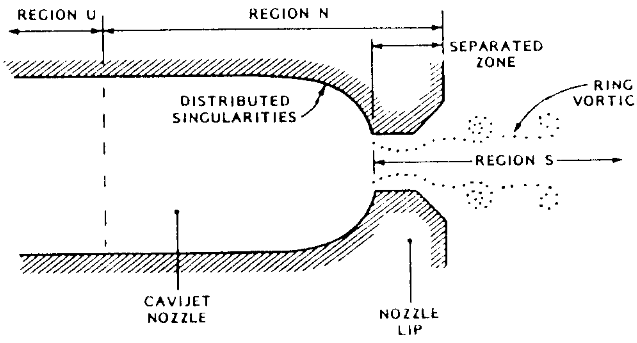

Figure 18 - Schematics of Nozzle Assemblies for Flow Visualization and Numerical Simulation

The distribution of singularities in region U is constant with time and constitutes a "boundary condition" for the rest of the flow. However, the intensity of the singularities in region N constantly varies with time and is such that there is no cross-flow at the nozzle walls. This intensity is mainly controlled by the positions of all freely moving rings, and by the influence at the considered point of the rest of the singularity sheet. Similarly, the motion of each vortex ring is a combination of its self-induced velocity, the velocity induced by the other rings, and the velocity due to the singularity distributions in regions U and N.

For the numerical simulation, the solid boundaries are discretized into axisymmetrical panels of small size on which the distribution of singularities is uniform. For a given nozzle shape, the flow induced by a distribution of sources and vortices on the panel "i" of the nozzle is computed at any discrete point "j". This allows the definition of matrices of influence which are a function only of the nozzle geometry and independent of the rings emitted at the exit. This simplifies considerably the numerical procedure and the computation time. These matrices and their inverses are computed once and for all for a given nozzle and then become inputs for the actual flow problem. Outside the nozzle, the ring-vortices emitted interact together and with the upstream singularities in the same manner as described in preceding sections.

The computations are done in the following sequence (Chahine, Genoux, and Liu, 1984). Two matrices of influence, defined as follows, are computed. The matrices, $\underline{\underline{AS}}$ and $\underline{\underline{AV}}$ are such that the components AS_{ij} and AV_{ij} are the normal velocities induced at the location of an element E_i by a uniform distribution of sources and vortices of unit intensity on the element E_j. We define, in addition, the vectors, $\underline{AV}_{up}$ and $\underline{V}_{TN}$, whose components are the normal velocities at each element E_i due respectively to a vortex sheet of unit intensity in the region U and to the discrete ring vortices in region S. $\underline{\underline{AV}}$, $\underline{\underline{AS}}$, and $\underline{AV}_{up}$ are not time-dependent and are computed once for a given nozzle geometry. However, $\underline{V}_{TN}$ has to be computed at each time step.

With the above definitions, the condition of zero normal velocity at the nozzle wall can be written:

$$0 = \underline{\underline{AS}} \cdot \underline{s} + \underline{\underline{AV}} \cdot \omega + \omega_{up} \underline{AV}_{up} + \underline{V}_{TN}, \tag{28}$$

where the vectors s and ω have as components the actual unknown source and vortex intensities at each element E_i. The system has one degree of freedom, and s or ω could be imposed. If we preselect the value of ω, then the source intensity distribution is obtained by the following expression:

$$s = - \underline{\underline{AS}}^{-1} \cdot (\underline{\underline{AV}} \cdot \omega + \omega_{up} AV_{up} + V_{TN}). \tag{29}$$

Since V_{TN} changes at each time step, s is recomputed accordingly. We have implemented such a computation code, and two test cases are presented in Figures 19 and 20. Figure 19 shows the case of a Smith nozzle with a cylindrical whistler mouth added to it. The time evolution of the ring position, the strong fluctuations in the whistler, and the tendency to structuring can be seen. However, large computation times are needed to introduce enough ring elements to observe distinct structuring. Figure 20 shows a case where t>>1. Structuring is here very clear. In order to use the code as a reasonable tool for resonating nozzle design, we are presently working on means to reduce the computation time. This involves automated schemes to recognize clustering of vortices in a large structure and the replacement of this structure with a single high circulation vortex.

CONCLUSIONS AND ACKNOWLEDGMENTS

In this paper we have described some aspects of the mechanics and principles of operation of self-resonating cavitating jets. We have tried to highlight the principal advantages of these jets, namely, early cavitation inception, improved cleaning capabilities and chip removal, enhanced cavitation erosion, and intense noise generation. We have tried, within the space limitations, to describe our contributions to the modeling of the various aspects of these jets. We ask the interested reader to consult

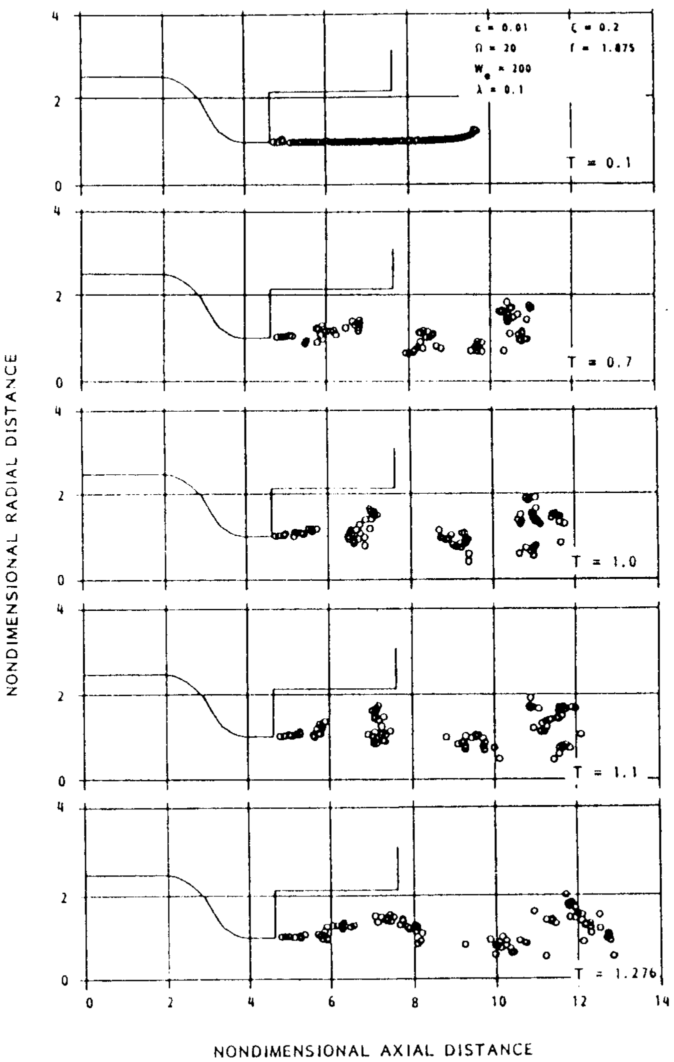

Figure 19 - Simulation f Jet Nozzle Interaction. Smith Nozzle with Whistler Mouth - Oscillating Vortex Strength

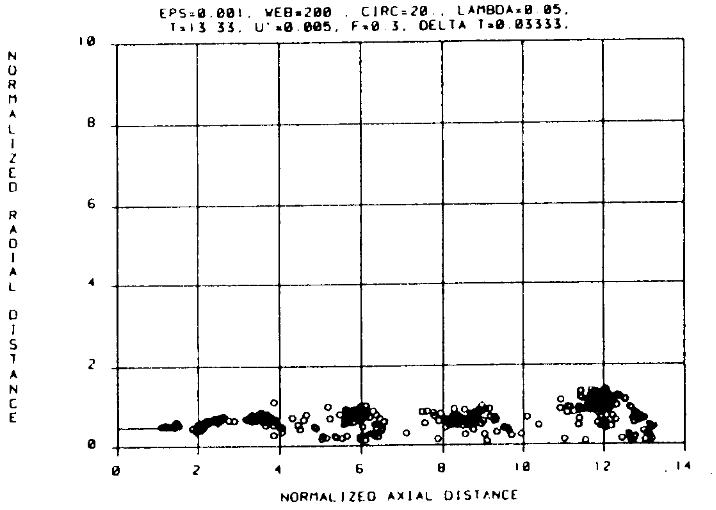

Figure 20 - Simulation of Jet Shear Layer Structuring. T = 13

earlier publications on the various details. Several aspects of the mechanics of these jets are still unclear and our ongoing efforts are concentrating on these aspects. For instance, the fundamental understanding of the feedback mechanism at the nozzle orifice, viscous effects, the optimization of ring vortex circulation, and the influence of the cavitation number on self-oscillations are important questions which need investigation.

This work was supported in part by the U.S. Department of Energy, Division of Geothermal Energy, under SANDIA Laboratories Contract No. 13-5129, and by the Office of Naval Research, Contract N00014-82-C-0678. We would like to thank Ph.F. Genoux from the Direction des Recherches Etudes et Techniques, Paris, France for his significant contribution while at Tracor Hydronautics to the theoretical work associated with this study; H.L. Liu for his contribution to the numerical simulation; and to the many colleagues at Tracor Hydronautics for their contributions.

REFERENCES

1. Acton, E., (1980), "A Modelling of Large Eddies in an Axisymmetric Jet," J. Fluid Mech. 89, 1-31.
2. Chahine, G. L. and Genoux, Ph. F., (1983), "Collapse of a Cavitating Vortex Ring " ASME J. Fluid Eng. 105, (4), 400-405.
3. Chahine, G. L., Genoux, Ph. F., Johnson, Jr., V. E., and Frederick, G. S., (1984), "Analytical and Experimental Study of the Acoustics and the Flow Field Characteristics of Cavitating Self-Resonating Water Jets," Tracor Hydronautics Technical Report 82009-1; Sandia Report SAND84-7142.
4. Chahine, G. L., Genoux, Ph. F., and Liu, H. L., (1984), "Flow Visualization and Numerical Simulation of Cavitating Self-Oscillating Jets," International Symposium Seventh Jet Cutting Technology, Ottawa, Canada, BHRA, 13-33.
5. Chahine, G. L., Johnson, Jr., V. E., Lindenmuth, W. T., and Frederick, G S., (1985), "The Use of Self-Resonating Cavitating Water Jets for Underwater Sound Generation," Journal of the Acoustical Society of America 77 (1), January, 113-126.
6. Crow, S. C. and Champagne, F. H., (1971), " Orderly Structure in Jet Turbulence," J. Fluid Mech., 547-591.
7. Fung, Y. T., Lui, C H., and Gunzburger, M. D., (1979), "Simulation of the Pressure Near a Jet Randomly Distributed Vortex Rings," AIAA Journal, Vol. 17, 553-557.
8. Genoux, Ph. F. and Chahine, G. L., (1984a), "Simulation of the Pressure Field Due to a Submerged Oscillating Jet Impacting on a Solid Wall," Journal of Fluids Engineering, Vol. 106, 491-495.
9. Genoux, Ph. F. and Chahine, G. L., (1984b), "Collapse of a Toroidal Bubble Near a Solid Wall," Cavitation and Multiphase Flow Forum, ASME, FED VOl. 9, 49-73.
10. Johnson, Jr., V. E., Kohn, R. E., Thiruvengadam, A., and Conn, A. F., (1972), "Tunneling, Fracturing, Drilling, and Mining With High Speed Water Jets Utilizing Cavitation Damage," 1st International Symposium on Jet cutting Technology (Coventry, England), Paper A3, 19.
11. Johnson, Jr., V. E., Chahine, G. L., Lindenmuth, W. T., Conn, A. F., Frederick, G. S., and Giacchino, Jr., G. J., (1984), "Cavitating and Structured Jets for Mechanical Bits to Increase Drilling Rate," A.S.M.E. Journal of Energy Resources Technology, Vol. 106, 282-294.
12. Jorgensen, D. W., (1961), "Noise From Cavitating Submerged Jets," J. Acoust, Soc. Am., 33, 1334-1338.
13. Kibens, V., (1979), "Discrete Noise Spectrum Generated by an Acoustically Excited Jet," Paper 75-0592, AIAA, 5th Aeroacoustics Conference.
14. Safman, P. G., (1970), "The Velocity of Viscous Vortex-Rings," Studies Applied Mathematics, Vol. 49, 371-380.

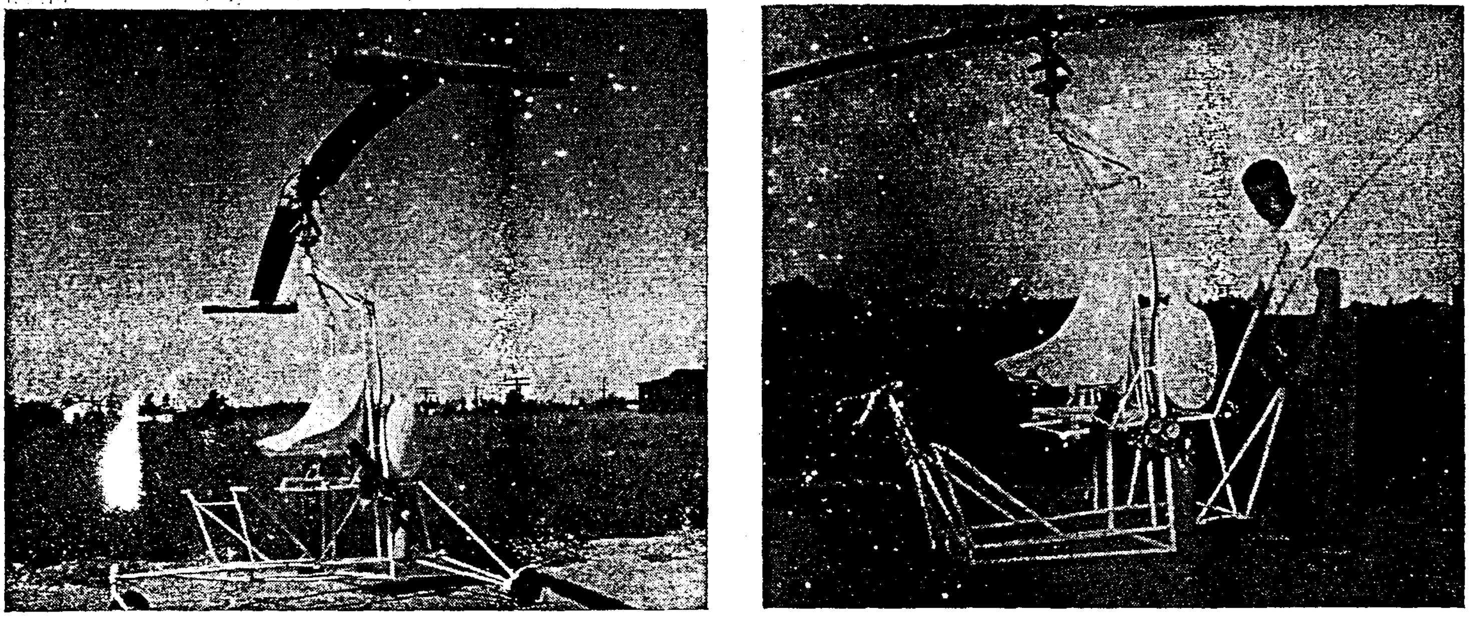

ONE-LITTER AMBULANCE for frontline use is mission envisaged for Para-Copter rotorcraft by inventor, George Schmidt.

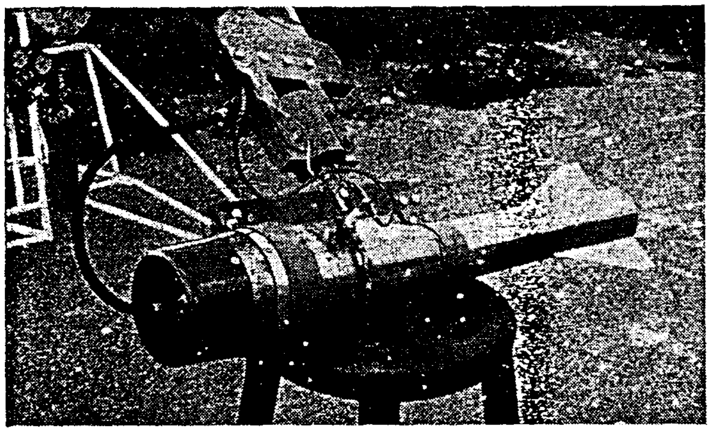

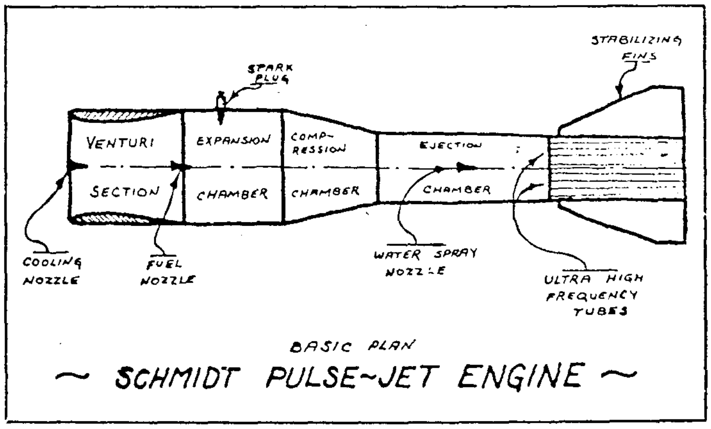

"ALMOST SILENT" PULSEJET ENGINE used by Schmidt delivers 105 lb. of thrust on special kerosene-base fuel.

Noise Is Cut in New Pulsejet Engine

A small pulsejet-powered helicopter, designed and built by George Schmidt as a combat evacuation craft, is nearing completion at the former Focke-Wulf engineer's Brentwood, N. Y., factory.

Military interest has been shown in the Para-Copter 2 (Aviation Week Sept. 7, p. 9), intended as a one-litter ambulance to fly wounded soldiers from front line areas to points of safety.

▶ "Silent" Operation—Schmidt engineered and constructed the 105-lb.-thrust twin pulsejet engines for his new craft, developed a special kerosene-base fuel called JPX, and devised a silencing system that he claims will make the helicopter powerplants approximately 80% quieter than other existing types.

"Almost silent" operation of the machine is projected as a top selling point for military operation and in the civilian market, if the engineer develops a civil configuration of his copter.

▶ Adjustable CG—Schmidt based the Model 2 on an earlier, smaller strap-on type of helicopter that he built and flew successively.

The Para-Copter is constructed of welded steel tubing, stands 8 ft. 7 in. high, and has a folding tricycle landing gear of 7-ft. base.

An aluminum seat, located directly under the rotor hub, is adjustable fore and aft for center of gravity balance. The single litter is carried directly under the pilot seat.

▶ Little Torque—Schmidt designed rotor controls that extended from the rotor hub but now is installing conventional floor configuration demanded by the latest military specifications.

Practically no compensation for torque is required in the Para-Copter's control surfaces, the designer says, because the only torque existing in the craft is caused by bearing friction. A small fin may be added to correct the friction effect, however, if the need is indicated by future flight tests.

▶ Powerful Pulsejet—Schmidt developed several innovations in design, operation and mounting of the helicopter pulsejet engines.

Each powerplant is 32 in. long, 5 in. in major diameter and weighs 17.5 lb. Although smaller than the new British pulsejet developed by Saunders-Roe for copters (story on next page), the Schmidt engine delivers more than twice the former's 45 lb. thrust.

The engine shell is constructed of welded 347 stainless steel.

▶ Menthol Mixture—To preserve the life of four valves in each pulsejet, a mixture of menthol crystals dissolved

p. 41-42

in alcohol and mixed with water is bled from a high pressure tank into a fuel line mounted just ahead of the throttle regulator. One pint of this coolant is required for each hour of engine operation.

In operation, a small amount of coolant mixed with fuel is sprayed into the pulsejet just ahead of the venturi through a .004-in. hole. The same fuel-coolant mixture is injected into an expansion chamber of the engine through a No. 60 hole.

This combination, Schmidt claims, keeps valves much cooler, preserves their life and gives a better fuel mixture for operation.

▶ **Muffled Pops**—The Para-Rotor's silencing system probably is the first to cut down noise of a pulsejet engine.

Schmidt deadens the loud, pulsating pop in two operations:

- Nozzle of .007 in. diameter sprays water into the ejection chamber, where the 1,700F heat turns it into a steam mass that muffles noise. Each engine uses approximately one quart of steam an hour.
- Thirty-two tubes of 7-in. long stainless steel are mounted in the tail of the pulsejet ejection chamber, where they change noise that escapes the steam muffle into a high-pitched sound above the level of human reception.

Schmidt claims his silencing system also gives the pulsejet 15-20% greater thrust.

▶ **Folding Package**—Rotor blades on the new copter have a straight chord of 9 in., are hinged to fold at the semi-rigid, see-saw hub.

When the rotors and landing gear are folded, the Para-Copter is a small package that can be stowed aboard a cargo transport and dropped by parachute into forward combat areas.

The Clark Y airfoil of the copter's rotor blades, made of eight layers of laminated sitka spruce and seven layers of nylon, may be shaped and mass-produced by unskilled workers on a special machine designed by Schmidt.

A 7-ft. blade can be cut in six minutes on this machine, he reports.

▶ **Pressurized System**—Fuel system of the new helicopter is a pressure type up to the rotor head, where it becomes centrifugal.

Rotor blades currently have integrally built fuel lines, but they will be removable in the future to facilitate maintenance.

An 18-gal. fuel tank, located behind the pilot seat, gives the Para-Copter an endurance of 1 hr. 10 min. Air pressure of 35-40 lb. in the tank is used to start the pulsejets, but centrifugal forces keeps the fuel flowing after the engines begin burning.

A bottle containing 92 cu. in. of compressed air is carried for starting purposes.

▶ **Simple Overhaul**—Major overhaul of the Schmidt pulsejets after 60 hr. of operation requires less than an hour for each powerplant:

- Nose venturis are removed by taking out four screws.
- Valve plate assembly is lifted out.
- New assembly is installed.

Unlike conventional rotor-tip jet units, the Schmidt engines are not attached solidly to the rotor blade but are installed on a ball-bearing mount that permits the powerplant to swing freely within limits in an up-and-down motion.

Small fins at the tail of the pulsejets and the center-of-gravity mounting keep the engines in a horizontal position regardless of the angle of attack changes of the rotor blades.

A manufacturer has quoted Schmidt a price of $85 per pulsejet for the first lot of 50 powerplants.

▶ **Strap-On Copter**—Schmidt flew his early strap-on helicopter to an altitude of nearly 12,000 ft. in July of last year. The craft was demolished on a second flight when the designer, unfamiliar with the flying characteristics of his new copter, allowed the rotor-craft to be blown sideways and tipped over by a strong gust of wind.

But Schmidt says he expects to rebuild the small copter.

▶ **Achgelis Engineer**—The German-born engineer worked on Focke-Wulf's Achgelis helicopter before he came to the United States in 1939. He has been employed by several major U.S. aircraft firms during the past 14 years.

Working with Schmidt on the Para-Copter are T. McGeough, chief engineer of the independent company, and engineer M. Simbrow.

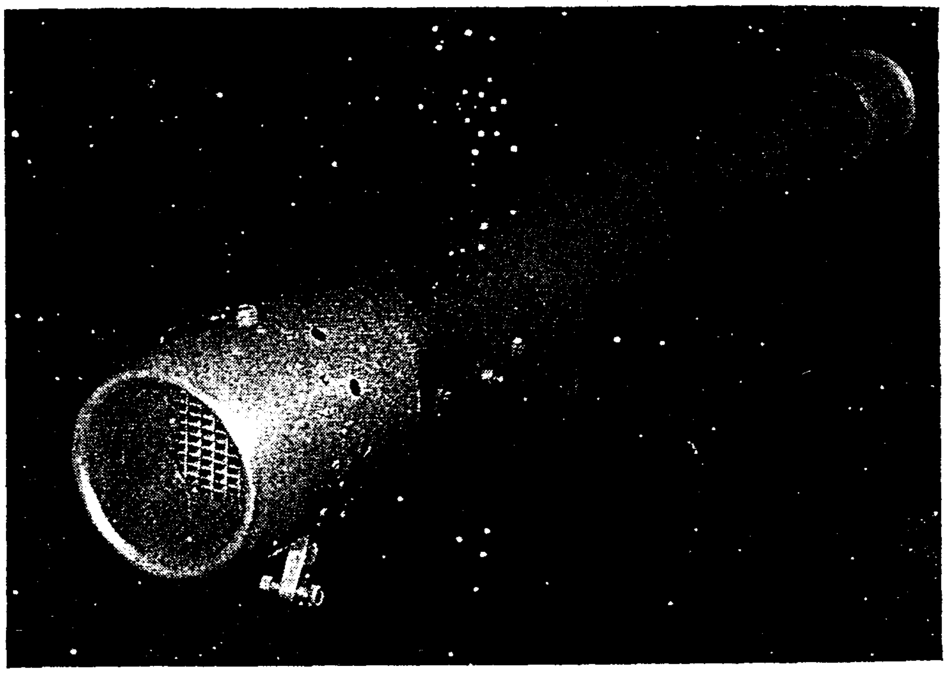

British Pulsejet to Power Copters

The pulsejet engine is the most promising means for tip propulsion of rotors, says the Helicopter Division of Saunders-Roe, Ltd., British aircraft firm.

After a year of experimenting, the company has developed a 45-lb.-thrust unit that has logged many hours of test and is working on a 120-lb.-thrust engine.

▶ **First British Pulsejet**—This is the first British pulsejet to propel or lift any aircraft, although similar U.S. engines have powered American Helicopter's XH-26 and Marquardt's M-14 for some time.

The pulsejet, one of the family of aerothermodynamic engines that includes the ramjet, was used by the Germans during World War II to power V-1 buzz-bombs.

▶ **Operation**—A pulsejet engine consists of simple parts: A cylindrical combustion chamber with a spring-loaded, normally open intake valve, and a tailpipe.

In operation, a mixture of fuel and air is ignited in the combustion chamber. The resulting explosion forces gases out the exhaust pipe at high speed and closes the intake valve.

The discharge lowers combustion chamber pressure to a point where the spring-loaded valve is able to open again, and a fresh charge of air is sucked and rammed in. The cycle then repeats.

▶ **Acoustic Tuning**—The Saunders-Roe unit is "tuned" by the acoustic properties of the chamber and tailpipe to a frequency of 120 cycles per second. It can be varied to a maximum of approximately 200 cps. or a minimum of 46 cps.

Engine weighs only about 15 lb. for its 45-lb. thrust. It is 47.5 in. long, and 5.5 in. in diameter.

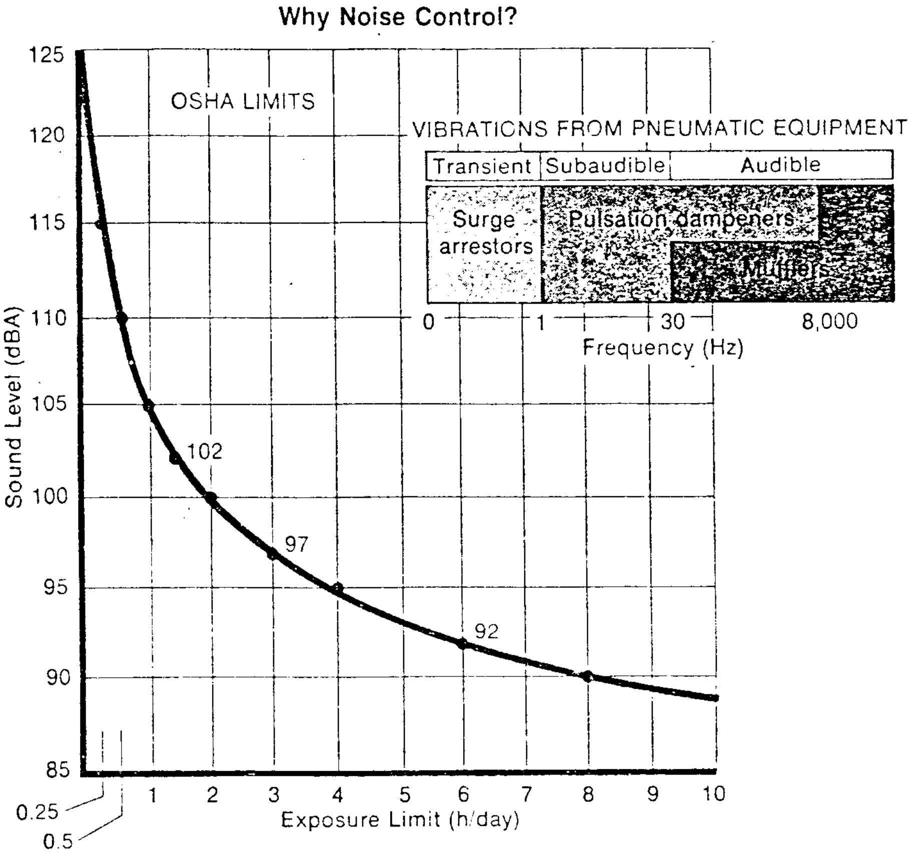

Recommended noise exposure limits are a major factor in the decision to institute a noise control program. Air equipment produces vibrations ranging from the subaudible (below [illegible] Hz) to the limits of human perception. Depending on the environment, noise control usually should be considered for equipment vibrating at frequencies over 30 Hz and producing noise above 90 dBA.

Beating OSHA to the punch by SILENCING PNEUMATIC EQUIPMENT

Air compressors and vacuum pumps are prime sources of noise in offices and plants. With OSHA about to issue a standard limiting allowable exposure to 90 dBA, users and manufacturers alike are scrambling to find ways to quiet their pneumatic components. Generally, the technology to reduce noise in air-powered equipment is readily available and easy to apply.

ROBERT MOFFATT
Gast Mfg. Corp.
Benton Harbor, Mich.

MACHINE DESIGN
March 20, 1980
p. 74-77

PNEUMATIC components in equipment as diverse as packing machines and computer peripherals can produce noise exceeding daily exposure limits mandated by OSHA. Besides being dangerous to hearing, such noise can interfere with communications, contribute to lowered productivity, and cause frequent errors and inattention. Also, the vibrations that produce the noise can damage machinery and pipes.

Fortunately, noise generated by air systems is comparatively easy to control and can be kept

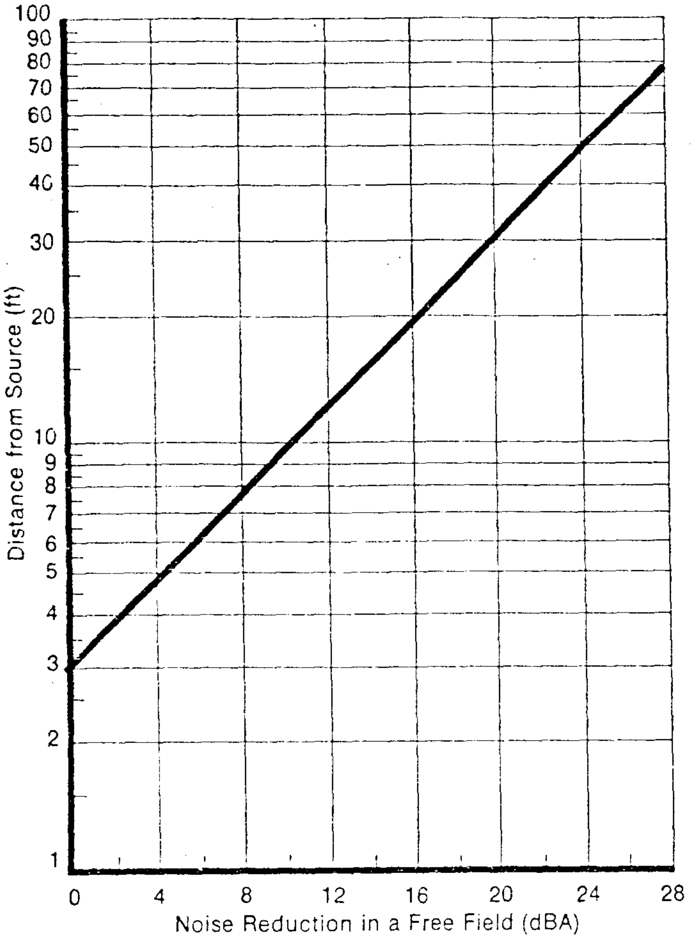

How Noise Dissipates

Noise exposure often can be reduced to acceptable levels by simply separating the noise source from personnel. This graph shows free-field dBA reduction produced by increasing the distance between a noise source and a listener. The chart's usefulness depends on knowing the dBA level at 3 ft. For example, a piston-driven vacuum pump rated at 73 dBA at 3 ft produces only 62.6 dBA at 10 ft and 54.7 dBA at 25 ft.

well below OSHA limits. Although the burden of noise control normally falls on the user, information on noise characteristics and noise control is readily available from manufacturers. The decision on how to control noise generally depends on a consideration of costs, operating environment, worker comfort, and legal requirements.

When Is Noise a Problem?

The determination of whether noise is a problem depends on how people react to the sound emitted. Many factors about noise are relative and subjective, a fact that should be taken into account when planning a noise-attenuation program. For instance, a compressor operating in a metal-stamping plant might go unnoticed, but the same compressor in a dental office could be quite annoying.

To establish whether a problem exists at the objective level, the sound must be analyzed with a sound level meter or an octave-band analyzer. Such equipment is useful in determining potential hearing damage, annoyance, and speech interference.

Annoyance level and loudness may not be synonymous, although a loud noise is usually more annoying than the same sound that is somehow muted. Given the same sound pressure level, higher-frequency sounds (above 2,000 Hz) are usually more annoying than lower-frequency sounds.

The vibrations produced by air equipment range from the subaudible to the limit of human perception. A low-speed pump, for instance, can produce low-frequency vibrations (less than 15 Hz) that are felt rather than heard. As frequency rises, the vibrations are accompanied by noise, with the audible range beginning at about 30 Hz. In this range, noise control usually becomes an important consideration.

Two Ways To Reduce Noise

Generally, noise is reduced at two locations: the source or the listener's ear (by changing the sound path). The first correction involves installing equipment such as dampeners and mufflers at the intake or discharge end of a compressor, vacuum pump, or air motor. Or the equipment can be placed in a specially built enclosure.

Noise reduction at the listener's ear can involve simply moving either people or equipment to another location. The relationship between noise level and distance is shown in the noise reduction graph.

The sound path also can be changed by modifying the acoustical environment or placing appropriate barriers between the source and listener. Sound follows a line-of-sight path; obstructing the path reduces noise. The intent of these methods is not necessarily to silence the equipment, but to reduce noise to levels that are physically and psychologically tolerable and to reduce vibrations to levels that pose no danger to the equipment itself.

There are many types of noise attenuation devices for air equipment. Dampeners and mufflers covering the range of pulsations from 1 to 20,000 Hz are available. Some are based on the phase-shift principle, which is analogous to cancelling out or stabilizing three-phase alternating current. Also, absorptive and dissipating mufflers, in which the compressed air passes over perforations that lead to sound-absorbing materials, can be used.

One of the most economical and most effective devices to attenuate noise over a wide spectrum is the low-pass filter. This filter, which can be as simple as a glass or plastic jar, allows only lower-frequency sound waves to pass through. In more sophisticated versions, a succession of tubes with different cross-sectional areas and lengths act as a low-pass filter for sound waves passing through them. The ratios of the cross-sectional areas to each other and to the tube lengths determine the frequency range of the sounds that are attenuated and passed. A tube with equally spaced side

How Phase-Shift Mufflers Work

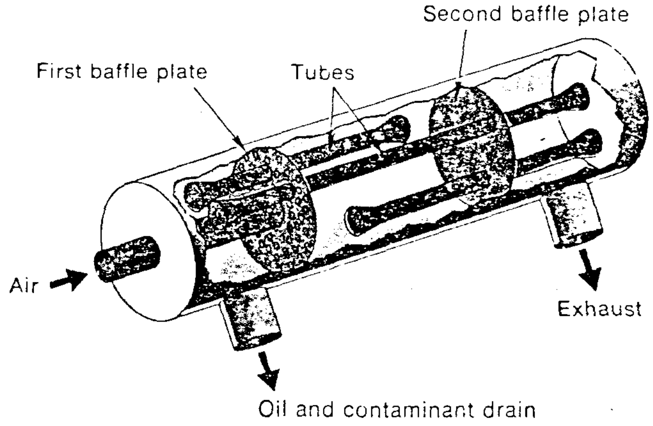

Muffler based on the phase-shift principle lowers frequency peaks of entering air by splitting the air stream into two branches and shifting them 180° out of phase. In operation, some air passes through the small holes in the first baffle plate, and some rebounds and enters the flared ends of the tubes. The tubes are of different lengths, so some air flows to the muffler exhaust and some bounces off the second baffle plate. The second air stream then enters another tube and flows to the exhaust.

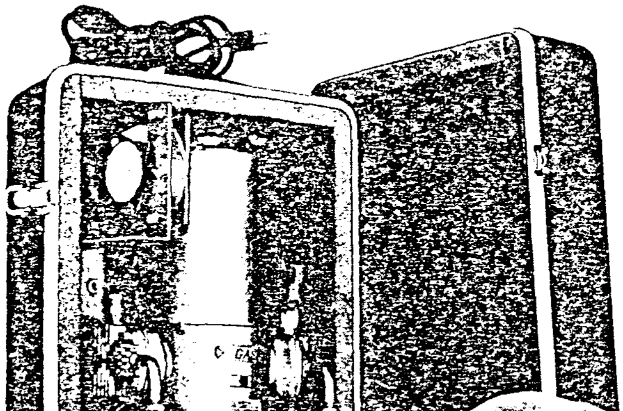

An acoustically insulated cabinet (quiet box) can cut rotary and piston pump noise by up to 17 dBA. The portable enclosure holds the pump on vibration isolators inside a foam-lined, baffled, 20-gage steel cabinet. A fan maintains the proper temperature inside the cabinet.

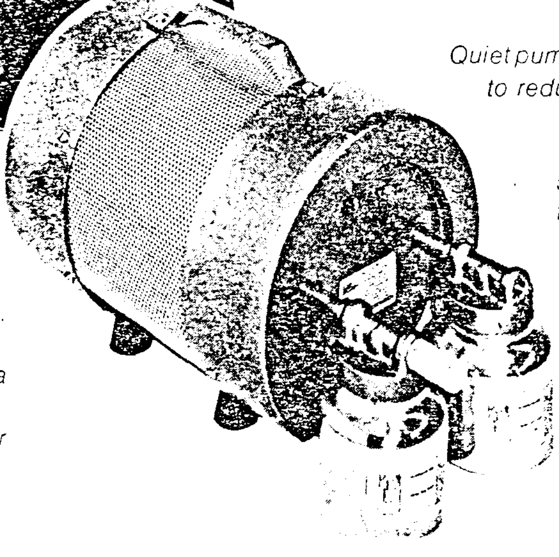

Quiet pump shown here has been modified to reduce operating noise by as much as 15 dBA, compared with the standard pump. The motor is suspended on brackets within a foam-insulated canister, and the unit has rubber mounting feet. A cartridge muffler was also added.

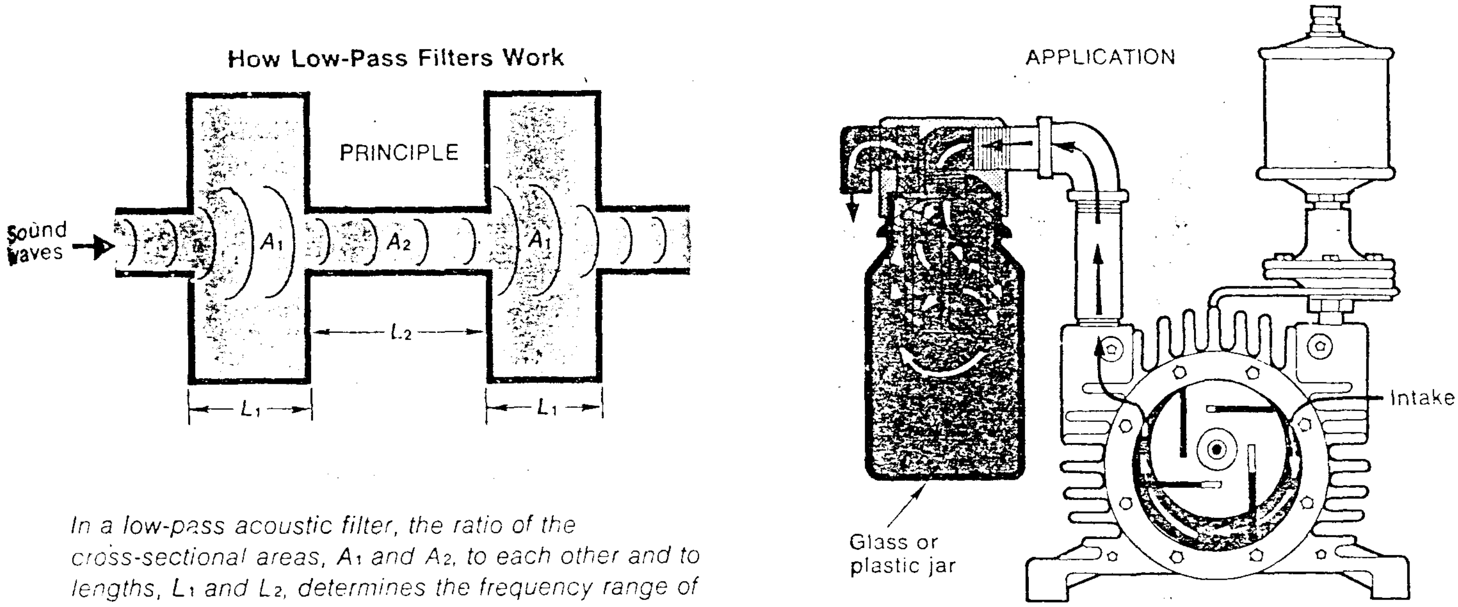
How Low-Pass Filters Work

In a low-pass acoustic filter, the ratio of the cross-sectional areas, A_1 and A_2, to each other and to lengths, L_1 and L_2, determines the frequency range of sound that is attenuated and passed through. Such a filter can be as simple as a glass or plastic jar mounted on a pump outlet.

orifices acts as a high-pass filter.

The effect of a low-pass filter is the same as that produced by passing the sound waves through alternating layers of different media, each transmitting only certain frequencies. The power transmission ratio—the ratio of average power emerging from the medium to that entering it—can be calculated to determine the influence of the layer. This ratio depends on medium thickness and specific acoustic resistance for a plane wave. (For instance, water has a specific acoustic resistance 3,800 times that of air.) Various types of media thus could be used to build an acoustic filter that either blocks or selectively transmits waves of certain frequencies.

Compressors and vacuum pumps also can be modified by inserting a plastic-foam liner directly into the units. This can reduce pump and compressor noise by up to 14 dBA, depending on the amount of pressure or vacuum being generated. Modification of a unit with a readily available kit is easy; the end plate is removed and the liner simply slipped between the shroud and body of the pump or compressor.

Acoustically insulated cabinets are also available to reduce air-equipment noise to office levels (about 50 dBA). One version of such an enclosure quiets—by as much as 17 dBA—the equipment by holding it on a vibration isolator inside a foam-lined, baffled cabinet.

Compressors and vacuum pumps engineered to run quietly are, of course, the best choices for applications that require noise levels even lower than those mandated by any "official" standard—in dental and medical offices, for example. One such unit reduces noise output by as much as 15 dBA because its motor is suspended on brackets within a plastic-foam-insulated canister. The unit also is fitted with rubber mounting feet. (The standard unit, by contrast, is rigidly mounted directly to the motor.) The quiet model also can be fitted with a double-length cartridge muffler to reduce noise even further.

Noise Trade-offs

The technology and data required to reduce noise in air equipment are readily available. The major criterion for selecting a method is to buy only as much quietness as is required. Indeed, it may be more difficult to define required noise attenuation—regulatory, comfort, and aesthetic considerations could have significant impact—than it is to select a muffling technique.

The least expensive cure is to simply increase the distance between the noise source and the listener. However, this may not be possible if space is already at a premium.

Applying the various sound-deadening techniques costs somewhat more than merely moving equipment around. Minor modifications such as quiet boxes or kits are the least expensive, add-ons such as larger mufflers are moderately expensive, and specially engineered units are the most expensive.

Combustion Science and Technology, 1987, Vol. 52, pp. 107–119
0010-2202/87/5203-0107$20.00/0

© 1987 Gordon and Breach Science Publishers, Inc.
Printed in Great Britain

Development of a Low Noise Pulse Combustor

ISAO INUI, KENJI OKAMOTO, MITSUYOSHI NAKAMOTO and MASATO HOSAKA *Central Research Laboratories, Matsushita Electric Industrial Co., Ltd., Moriguchi, Osaka, Japan*

(Received October 28, 1985; in final form August 6, 1986)

Abstract—A low noise pulse combustor has been developed based on experiments. Combustion noise has been reduced by dividing the heat input into two equal quantities and burning them with two small burners. When the two pulse burners whose combustion frequencies were slightly different were operated side by side, an annoying beating occurred. The beat was suppressed by bringing two burners into synchronized combustion. This was achieved by a new construction which included a communicating passage between two exhaust decouplers to allow the pressures in them to interact on each other. The construction was simple, but it was confirmed by experiments that the means offered a reliable way to synchronize multiple pulse combustions. It was found that the pulse combustion noise as a noise source could be reduced by 6.5 dB applying this construction to a two-burner combustor.

1 INTRODUCTION

To improve the efficiency of fossil energy utilization, it is necessary to make the most of the latent heat energy contained by burned gases. As is generally known, pulse combustion, which is a series of repeated explosions, seems to be a suitable combustion form to recover the latent heat for its pulsive and rapid exhaust flow. Hanby (1969) reported the results of investigation on the heat transfer coefficient obtained with pulse combustion in comparison with the conventional methods. Using the pulse combustion principle, a useful apparatus to efficiently use the heat energy produced may be realized without incorporating any exhaust fan but using a simple heat exchanger.

Griffiths and Weber (1969) reported a method of designing flapper-valve-type pulse combustors. After the oil crisis, a number of analytical and experimental reports appeared. Ahrens *et al.* (1980), Blomquist *et al.* (1980) and Soedel *et al.* (1982) reported fundamental phenomena and heat transfer characteristics of the pulse combustion. Computer simulations of the pulse combustion phenomena were carried out, and Dhar *et al.* (1982) reported one of the results.

On the other hand, the noise of the pulse combustion is inherently large. It is necessary to reduce the noise before the pulse combustion can be used widely. The pulse combustors are quite different from conventional residential burners, and a drastic noise reduction has to be done. Sran and Kentfield (1982) and Briffa and Staddon (1982) studied phase cancelling methods and pulse combustors without flapper valves. They reported the possibility of drastic noise reduction by means of phase cancelling.

Based on the experimental work, the authors developed a method to reduce the pulse combustion noise by operating two burners in-phase. The combustion method to reduce the combustion noise and the method to suppress the accompanying beat are described in this paper. A part of this paper was released in 1984 by Nakamoto *et al.* (in Japanese).

2 EXPERIMENTAL APPARATUS

Schematic drawings of experimental apparatus are shown in Figures 1 and 2. The pulse burners used in this work are of Helmholtz resonator type and both gas and air valves are of flapper type. The combustion chambers and exhaust decouplers shown in Figure 1 are cylindrical. Each combustion chamber has three tail-pipes. The combustion chamber is 97.6 mm in diameter and 250 mm in length and a tail-pipe is 26.8 mm in diameter and 1134 mm in length. The experiment to reduce the pulse combustion noise using multiple identical burners was achieved with the apparatus shown in Figure 1. This apparatus is consisted of variable number of identical burners, but Figure 1 shows a case of dual-burner construction.

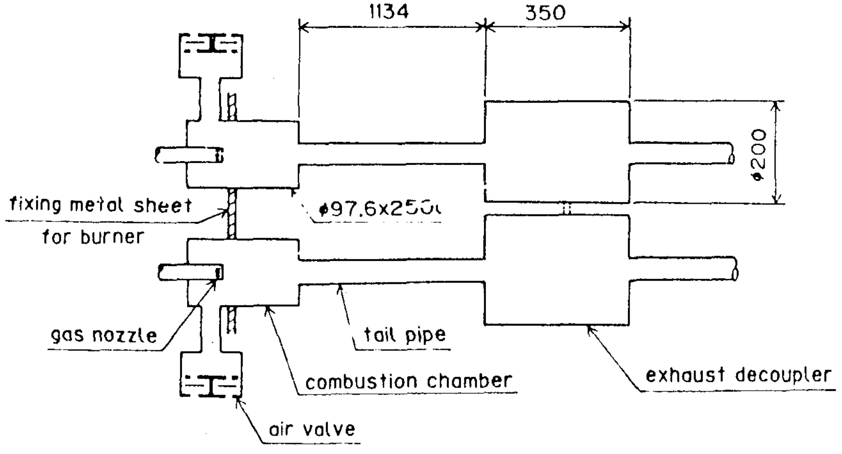

FIGURE 1 Experimental apparatus.

The apparatus shown in Figure 2 was used to study the conditions for synchronized combustions. In this apparatus, a single cylindrical chamber was divided by a partition into two equal sections each forming an exhaust decoupler for each burner. In our experimen [illegible] otal communicating area shared by the two exhaust decouplers was varied by changing the number of holes provided in the partition, each 6 mm in diameter, and by changing the clearance between the partition and the bottom wall of chamber.

3 EXPERIMENTAL RESULTS AND DISCUSSIONS

3.1 *Combustion Noise*

The relation between pulse combustion noise level and heat release rate was investigated. The noise levels were measured at a point 1.05 m height from the floor and 1 m in front of the tail pipe end, which extends 200 mm from the combustion chamber end. The burner has no intake or exhaust decouplers. The experiment was carried out with propane gas. The results of the measurements are shown in Figure 3. The relation between the heat release rate Q kcal/h and the noise level N dB (A) can be expressed by Eq. (1).

Coefficients obtained from the measured data are: $a = 2.1$, $N_0 = 97$ dB(A) at $Q_0 = 10{,}000$ kcal/h.

$$N = N_0 + 10\log(Q/Q_0)^a \text{ dB(A)}. \qquad (1)$$

The noise level of the pulse combustor which has been developed in this work can be expressed by the following equation:

$$N = 97 + 21\log(Q/10^4)\ \mathrm{dB(A)}. \qquad (2)$$

It is found by measurement that the pressure amplitude P of the combustion chamber is proportional to the heat release rate Q shown in Figure 4. If the sound pressure of this combustor is assumed to be proportional to the pressure P in the combustion chamber, the sound pressure level can be expressed as $10\log(P/P_s)^2$ or $10\log(Q/Q_s)^2$, where P_s is the reference pressure in the combustion chamber and Q_s is the reference heat release rate. So, it is reasonable that the value of a in Eq. (1) is about 2.

From Eq. (2), it is found that the noise level at a heat release rate of 30,000 kcal/h is approximatey 107 dB(A). It means that the noise has to be reduced by 60 dB so as to develop a low noise appliance having a noise level less than 50 dB(A). The noise propagated in the ducts and the noise emitted from the inlet and outlet of a combustor can be diminished by using a decoupler and muffler. If a practical reduction level by these means would be about 50 dB, it is still necessary that the remaining 10 dB has to be reduced at the noise source. The combustion noise as a noise source may be reduced by changing the combustion intensity or the air ratio. However, using these means, the operational pressure in our combustor became low, resulting in unstable combustions. The methods decreasing the operational pressure should be avoided, because most of the mufflers designed for drastic noise reduction have large flow resistances. Instead of them, it was chosen to divide heat input into n equal portions and to burn them with n equal scale burners.

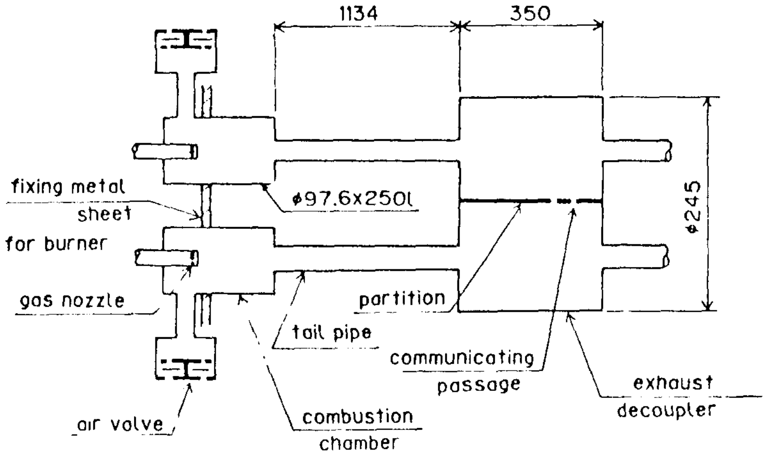

FIGURE 2 Experimental apparatus.

3.2 *Combustor Consisting of Two Pulse Burners*

Using the burner of which the noise level can be calculated from Eq. (2), the resultant noise level N_n of the pulse combustor consisting of n equal scale burners may be expressed by the following:

$$N_n = N_{Qm} + 10\log(n)\ \mathrm{dB(A)}. \qquad (3)$$

From Eq. (1), when a is about 2.0, the noise level N may be expressed by the following:

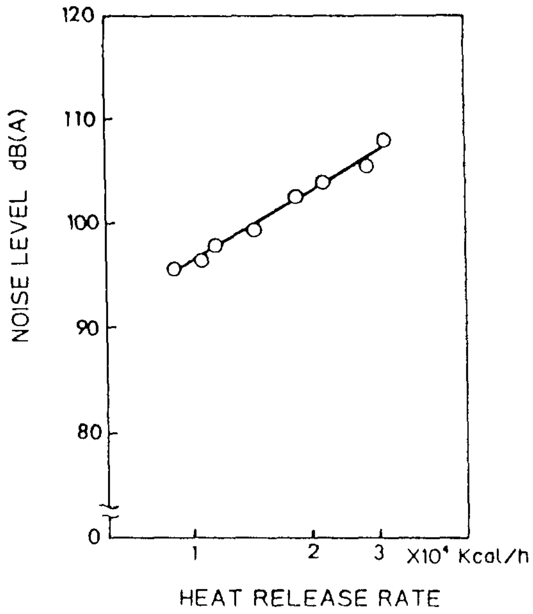

FIGURE 3 Combustion noise level vs. heat release rate.

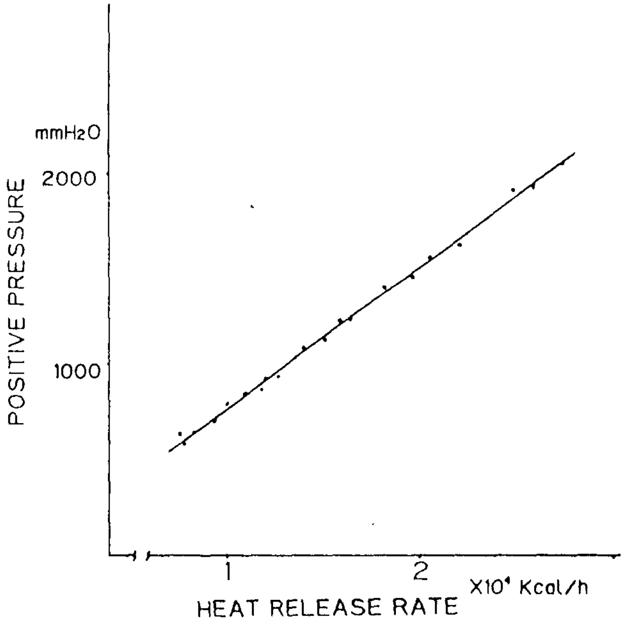

FIGURE 4 Positive pressure vs. heat release rate.

$$N = N_{Qm} + 20\log(n)\ \mathrm{dB(A)}. \qquad (4)$$

With Eqs. (3) and (4), the noise level N_n can be presented by the following:

$$N_n = N - 10\log(n)\ \mathrm{dB(A)} \qquad (5)$$

Where:

N_n Noise level when the total heat release rate Q kcal/h is obtained using n equal scale burners.
N_{Qn} Noise level when the heat release rate Q/n kcal/h is obtained using a single small burner.
N Noise level when the heat release rate Q kcal/h is obtained using a single big burner.
n Number of burners used.

According to the Eq. (5), it is found that the noise level N_n is smaller than N by $10 \log(n)$ dB. The calculated result of the relation between the number of burners n and the noise level N_n is shown by the dotted curve in Figure 5. The experimental result of the noise levels taken by obtaining the total heat input using 2 to 5 burners is shown by the solid curve in the same figure. The measurements are accomplished at a total heat release rate of 30,000 kcal/h. The difference between these two curves, 3 to 3.5 dB, is considered to be due to the noise reduction gained by mechanically combining multiple burners. Furthermore, fixing these burners to a supporting board and forming a unified structure as shown in Figure 1 increases the mechanical strength of the combustion chamber.

It is found from Figure 5 that 10 dB reduction is realized by obtaining the total heat release rate using five burners. It is found also that the increase rate of the reduction effect decreases as the number of burners, n, increases. The reduction effect improves by only 1.8 dB when the number of burners increases from 2 to 3. From cost/performance considerations, a two-burner configuration was chosen, and a noise reduction of 6.5 dB was obtained without spoiling the combustion stability.

The combustion characteristics of one of the burners shown in Figure 1 are shown in Figure 6 and the combustion frequency and the heat release rate of each burner are shown in Table I. From the Table I, it is found theat there is some difference between the combustion frequencies of the two burners. When these two burners were operated together, a beating occurred. The level of the beating noise varied by about 9 dB, from 76.5dB(A) to 67 dB(A), at a frequency of about 3.5 Hz. The noise was measured under the conditions that the two air valves were installed in an intake decoupler and the exhaust decouplers were attached to the tail-pipes of each burner. The beat is quite annoying and has to be suppressed to utilize the combustion noise reduction effect obtained by the use of a multiple-burner construction.

TABLE I
Characteristics of the two burners

	Heat release rate	Pulse combustion frequency	CO_2	CO
Burner A	16320 kcal/h	85 Hz	11.7%	0.009%
Burner B	15970 kcal/h	80 Hz	12.1%	0.015%

3.3 *Combustion Frequency Synchronization*

It seems that the difference in frequency was caused mainly by the some difference between the heat release rates of the two burners. The difference in heat release rate is due to the difference in dimensions within the tolerance of manufacturing and assembly of the components. The thermal and the density distributions of the fluid in the combustion chamber and the tail-pipe become different between the two burners because of the difference in the heat release rate. And then, it seems that a little difference in pulse combustion frequency between the two burners occurs and results in beating. As the results of further experiments, it was found that the synchronization of pulse combustions could be obtained by connecting the two burners A and B at their exhaust decouplers. The dotted lines in Figure 1 show the communicating passage. The apparatus with which a condition of synchronization was investigated experimentally is shown in Figure 2. From the experiments performed with this apparatus, it is found that the stability of synchronization of the two pulse combustions is governed by the area of the communicating passage. The relation

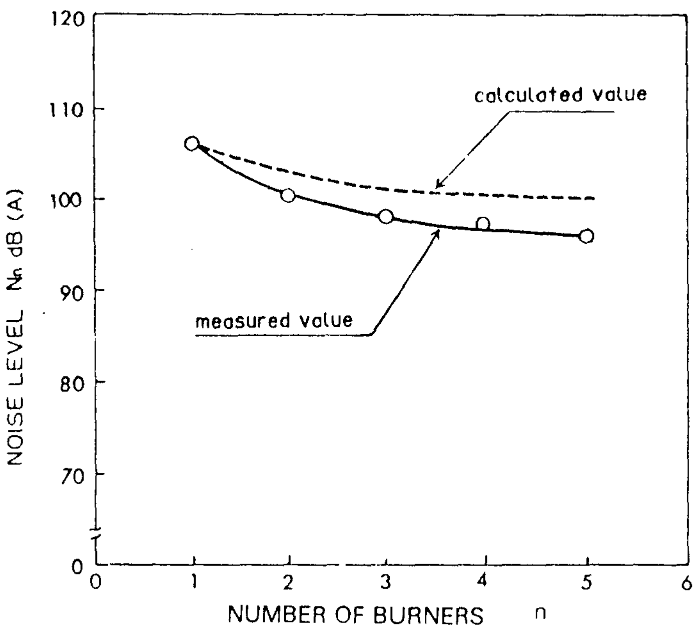

FIGURE 5 Combustion noise level vs. number of burners.

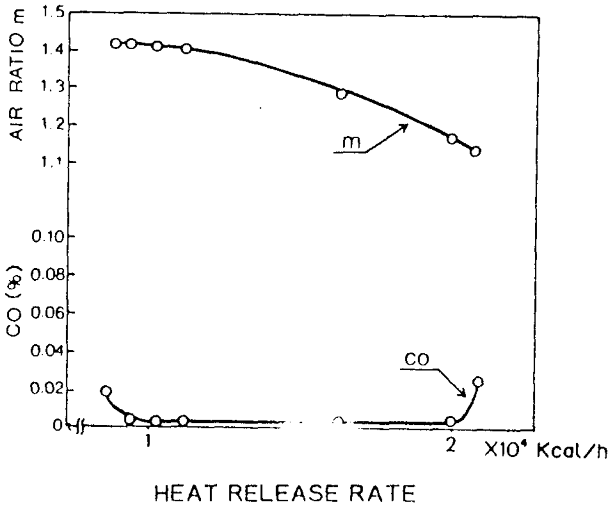

FIGURE 6 CO content and air ratio vs. heat release rate.

between the communicating area and the situation of combustions is shown in Table II. The total area of 3 holes which are provided in the partition and are 6 mm in diameter is equal to 85 mm^2 and the total area of 6 holes is equal to 170 mm^2. When the number of holes, each 6 mm in diameter, was less than 3, beating occurred. When the communicating area was increased to more than 170 mm^2, an irregular combustion sound occurred occasionally. As the communicating area was increased from 170 mm^2 to 520 mm^2, the irregular combustion sound occurrence was increased. When the communicating area became larger than 520 mm^2, irregular explosions happened frequently at the starting time, and it became somewhat difficult to establish a stable pulse combustion. Even after the irregular explosion disappeared, if the igniter was stopped, the combustions stopped within a few seconds. When the partition between the exhaust decouplers was removed, irregular explosions resulted and stable pulse combustions were not established. As previously mentioned the communication area that ensure stable synchronized combustions of the burners was from 85 mm^2 to 170 mm^2. When the combustions were synchronized, the combustion frequency was 83 Hz and the noise level was about 76 dB(A). The noise level was near the upper value, which was recorded when beating occurred. The noise reduction which was expected with an acoustical system consisting of two exhaust decouplers and a passage between them was not gained. And viscous dissipation due to communicating passage was assumed to be negligibly small because the passage is extremely short in length. The condition for synchronized combustions could be expressed with the ratio of the communicating area S_C to the cross sectional area S_T of tail-pipe or exhaust pipe as the following equation:

$$1/20 < S_C/S_T < 1/10 . \tag{6}$$

The cross sectional area of the burner's tail-pipes or exhaust pipe was about 1700 mm^2.

TABLE II
Relation between communicating area and synchronizing state

Communicating area in mm^2	0 to 85	85 to 170	170 to 520	above 520
Synchronizing state	beat	sychronized combustion	unstable combustion	not start

3.4 *Mechanism of Synchronization*

The pressures in the combustion chambers and the exhaust decouplers when the two burners A and B shown in Table I were operated individually were measured. The results of measurement are superposed and shown in Figure 7 and Figure 8. In a stable pulse combustion, the phase relation between the pressures in combustion chamber and in exhaust decoupler was nearly antiphase. In Figure 7, it is supposed that the pressures in the combustion chambers of two burners peak at the time t_0. For the sake of explanation, it is supposed that the phase relation between the pressures of the combustion chamber and the exhaust decoupler are exactly antiphase. The different pressures and combustion frequencies of the two burners are shown rather exaggerated. As shown in Figures 7 and 8, during the period t_0 to t_1, the pressure relation between the two burners is expressed by the following equations:

$$P_A > P_B , \tag{7}$$

$$|P_{DA}| > |P_{DB}| . \tag{8}$$

If communication is made between the exhaust decouplers of the two burners through the holes provided in the partition, the difference in pressure ΔP_D shown by Eq. (9) appears at the holes. And then, a part of the exhaust gas from the burner B flows through the holes from the decoupler B into the decoupler A.

$$\Delta P_D = P_{DB} - P_{DA} > 0 . \tag{9}$$

As the result of it, the burned gas flows out more easily from the combustion chamber B and the flow velocity becomes higher than when the burner B operated alone. As the consequence, the time P_B or P_{DB} is equal to the atmospheric pressure P_0 comes earlier than t_3 and the inertia of the burned gas flow flowing out from the combustion chamber is increased. Due to the increase of the flow inertia, the degrees of the negative value of P_B and of the positive value of P_{DB} during the period t_3 to t_4 are larger than those when the burner B is operated, as shown by the arrows in Figures 7 and 8. On the other hand, as a result of it, the flow velocity of the burned gas flowing out from the combustion chamber of the burner A will be slightly decreased. Consequently, the time P_A or P_{DA} becomes equal to the atmospheric pressure, P_0, comes later than t_2. The inertia of burned gas flow will be decreased, then the degrees of the negative value of P_A and of the positive value of P_{DA} during the period t_2 to t_4 will be smaller than those when the burner A is operated alone. At a time anywhere between t_2 and t_4, the suction process starts at the combustion chambers. Due to the effect of the communicating passage as mentioned previously, the volumes of fuel gas and air used will be increased on the part of the burner B and decreased on the part of the burner A when compared to the volumes that would be used if the burners are operated individually.

At a time anywhere between t_4 and t_5, a part of the burned gas flows from the exhaust decouplers back to the combustion chambers. During this period, because P_{DA} is higher than P_{DB}, the value of ΔP_D calculated from Eq. (10) becomes negative. So, the pressure difference ΔP_D acts at the holes in the direction opposite to that during the period t_0 to t_1.

$$\Delta P_D = P_{DB} - P_{DA} < 0 . \qquad (10$$

A part of the burned gas starts flowing through the communicating holes from the decoupler A into the decoupler B. Since the exhaust decoupler's pressure P_{DB} of the burner B is higher than that expected when the burner B is operated alone, the quantity of the reverse flow to the combustion chamber B will be increased and the timing of the reverse flow will come earlier. Thus, the timing of explosion comes early and the explosive force becomes larger. Concerning the burner A, the timing of the explosion will be delayed and the explosive force will become somewhat reduced. As shown with the arrows in Figures 7 and 8, the pressures of burners A and B become closer to each other because of the effect of the communicating passage. The difference in pressure between the two burners will become smaller. After several cycles with such interaction, both burners A and B begin exploding and exhausting at the same timing.

It was found that when the combustor provided with this communicating passage was operated, the combustions of the two burners become synchronized during the early period between the start and the time stable pulse combustion is established. The combustion chamber's pressures of the two burners were measured simultaneously and the results of them are shown in Figure 9. It may be found from the Figure 9 that there are three types of synchronizing process.

1) The first explosions at the two burners start at the same time but the following explosions occur alternately with increasing pressure amplitudes. After the pressure increases level off, the function of synchronization acts on combustions and synchronization little by little.

2) The combustions start at the same time. In the process of the pressure amplitudes increasing, two explosions become suddenly nearly identical in phase and frequency. At this time, the function of synchronization starts acting on combustions.

3) The first explosions start at the same time and following explosions keep their combustion phases and frequencies nearly identical with increasing pressure amplitudes. The function of synchronization starts acting on combustions in the same manner as case (1).

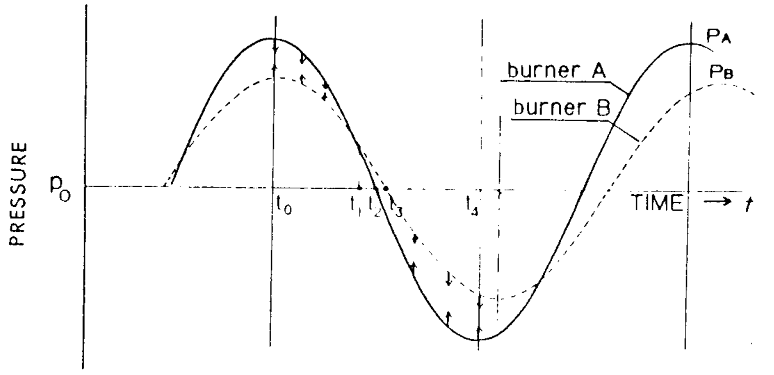

FIGURE 7 Pressure oscillation amplitude of combustion chamber.

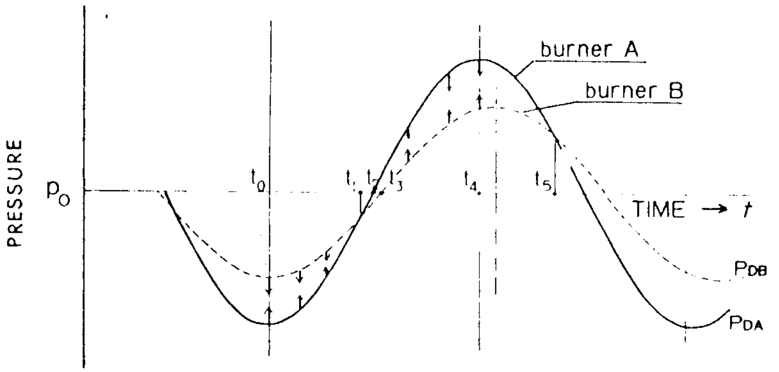

FIGURE 8 Pressure oscillation amplitude of exhaust decoupler.

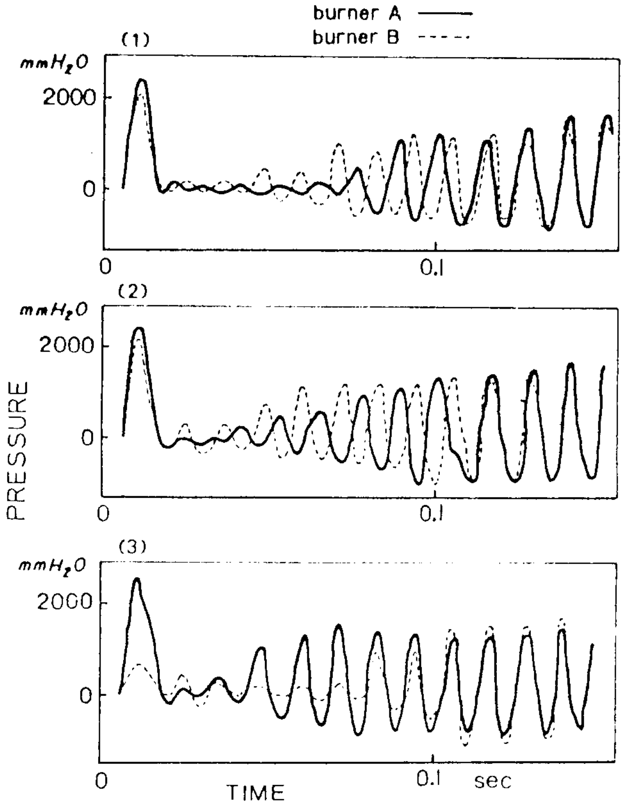

FIGURE 9 Pressure oscillation waves of two burners from start to stable pulse combustion.

In any of the above cases, it seems that after the pressure amplitude increases level off, the function of synchronization starts acting on the combustions. It is found that synchronization is accomplished before the amplitudes become constant. And in any case, it takes ten to several tens of cycles to establish stable synchronized pulse combustions. Or, in terms of time, stable synchronized pulse combustions are established within one-fourth to one-half second after the starting time. There is no significant beat since synchronization is established at an early stage. The reasons why the function of synchronization does not act on combustions before the pressures level off and why the relation between two combustions changes suddenly in case (2) were not investigated in this work. They would better be subjects for future theoretical studies. Figure 10 shows a record of pressure amplitude observed in a combustion chamber while a pulse burner continues stable combustion. When examined closely, it will be noticed that both the amplitude and the period of cycle waveforms fluctuate from cycle to cycle. It can be said that, even though a pulse combustion involves rather complicated phenomena, a mechanically simple communicating mechanism secures synchronization very reliably.

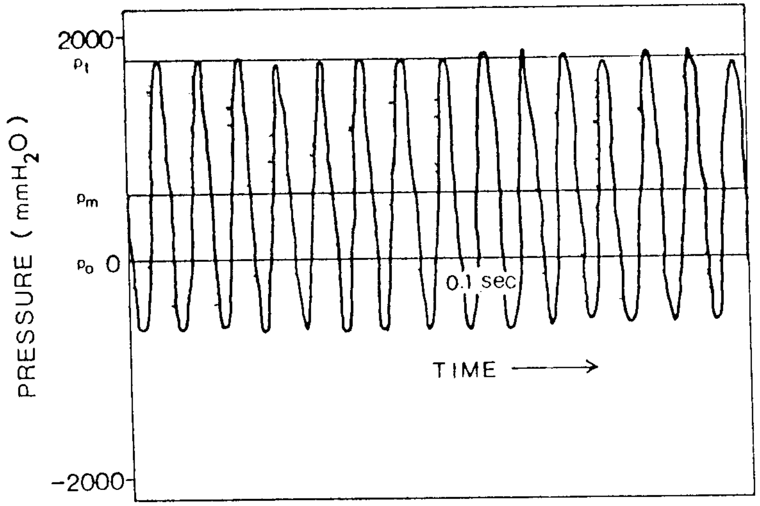

FIGURE 10 Pressure oscillation wave of stable pulse combustion.

5 CONCLUSIONS

The pulse combustion noise could be reduced by 10 log(*n*) dB by obtaining total heat input using *n* identical burners. A further noise reduction was possible with an appropriate mechanical design that integrated these *n* burners. The noise reduction effect of the mechanical construction was about 3.5 dB. It was rather a greater effect than expected. Based on these findings, a pulse combustor which consisted of two burners was developed. The combustion noise as a noise source was reduced by 6.5 dB. These burners were designed not to change the best condition of air ratio. Annoying beating occurs when two pulse burners which have slightly different combustion frequencies are operated side by side. It can be suppressed by synchronizing two combustion frequencies. A communicating passage provided between two exhaust decouplers was tested for synchronization of pulse combustion frequencies of two burners. Though mechanically very simple, this scheme was found to offer a reliable and stable synchronizing function. The appropriate range of communicating areas giving a stable synchronized condition for pulse combustions were experimentally determined to be from 85 to 170 mm^2. It is expressed as $1/20 < S_C/S_t < 1/10$, where S_C is the area of the communicating passage provided between two exhaust decouplers and S_t (1700 mm^2) is the area of the tail-pipe which is one of the main design factors.

ACKNOWLEDGEMENT

The authors acknowledge the support and the encouragement given by the management of Matsushita Housing Products Co., Ltd., in the course of water heater development.

REFERENCES

Ahrens, F. W., and Clinch, J. M. (1980). Pulse combustion technology for heating applications, quarterly progress report, October 1-December 31, Argonne National Laboratory Report ANL/EES-TM-78.

Blomquist, C. A., Clinch, M. J., and Ahrens, F. W. (1980). Pulse combustion technology for heating applications, quarterly progress report, January 1-March 31. Argonne National Laboratory Report ANL/EES-TM-85.

Briffa, F. E. J., and Staddon, P. W. (1982) An application of fluid-logic techiques to pulsed combustion. *Proceedings Symposium on Pulse-Combustion Application*, Vol. 1 Atlanta, Georgia, March 2–3.

Dhar, B., Huang, H. C. G., Lee, J. H., S[illegible] and Schoenhals, R. J. (1982). *Dynamic and thermal characteristics of a pulse-combustion gas-fired water heater*. Proceedings Symposium on Pulse-Combustion Application, Vol.1, Atlanta, Georgia, March 2–3.

Griffiths, J. C., and Weber, E. J. (1969). The design of pulse combustion burners. American Gas Association Laboratories Research Bulletin 107, June.

Hanby, V. I (1969), Convective heat transfer in a gas-fired pulsating combustor. Transactions of A.S.M.E., Series A, **91**, 48.

Nakamoto, M., Hosaka, M., Inui, I., and Okamoto, K. (1984). Pulse-combustion technology for water heater, (in Japanese), National Technical Report, Vol. 30, No.5, Oct. 1984.

Soedel, W., Schoenhals, R. J., Lee, J. H., and Huang. H. C. G. (1984). Experimental and analytical investigation of a pulse combustion water heater. Final report (October 1979–January 1984).

Sran, B. S., and Kentfield, J. A. C. (1982). Twin valveless pulse combustors coupled to operate in antiphase. *Proceedings Symposium on Pulse-Combustion Application*, Vol. 1 Atlanta, Georgia, March 2–3.

(word processor parameters LM=8, RM=75, TM=2, BM=2)
Taken from KeelyNet BBS (214) 324-3501
Sponsored by Vangard Sciences
PO BOX 1031
Mesquite, TX 75150
There are ABSOLUTELY NO RESTRICTIONS
on duplicating, publishing or distributing the
files on KeelyNet except where noted!
February 26, 1993
NOISECNC.ASC

This file is from the Dallas Morning News of
Saturday, February 13, 1993 - Business section.

The following file is most intriguing and applies to one of the root studies of Vangard Sciences and KeelyNet. Keely used compound vibrations and we believe at various phasing differentials. This phase adjustment is known in modern terms as interference or phase conjugation and can be either constructive (additive) or destructive. Use of such principles can lead to phenomena beyond simple cancellation of a signal, but we will stay within the context of the article as given.

Technology Report

Silence is gold for companies

Experiments seek noise reduction

by Rebecca Smith

San Jose, Calif. - Imagine summer without the earsplitting roar of power lawn mowers, flying without hearing the whining din of jet engines, running the dishwasher without having to shout over the noise.

Companies that make noisy products are looking at an ingenious breakthrough technology that enables them to dramatically reduce unwanted sounds.

"Active noise reduction" systems represent the broadest assault on noise pollution since invention of the muffler. Products employing the technology will begin showing up in mass consumer products later this year.

In what could be a boost for U.S. competitiveness, about 75 patents covering product-specific applications of the technology are controlled by two U.S. companies.

"It'll be part of the next wave of luxury home appliances and cars," says technology analyst Dan Hutcheson, president of VLSI Research in San Jose. "Right now, it's expensive, but the cost should come down fairly fast as volumes build."

The idea of active noise reduction dates back to a 1936 patent for a "process of silencing sound oscillations" by German inventor Paul Lueg. But commercial execution required invention of the microchip.

The concept is simple. Fight fire with fire.

Here's how it works :

Start with an irritating noise, say, that of an air compressor. A microphone samples the noise and sends a signal to a microchip analog-to-digital converter, which translates the sound waves into computer language. It creates a digitized blueprint of the sound, then passes the blueprint to a digital signal processing chip that analyzes the sound's magnitude and frequency.

The digital sound processor (DSP) then computes WHAT pattern of sound waves would be EQUAL but OPPOSITE - a MIRROR IMAGE. (180 degree shifted for perfect cancellation...Vangard)

That sound profile (signature) is then converted back from a digital to an analog representation. An audible sound wave is created and amplified through speakers or a headset. When the yin-and-yang sound patterns collide - the whole process takes a fraction of a second - they largely cancel each other out. The loud air compressor noise becomes a quiet hum. Advanced systems continuously sample the ambient noise level, correcting and re-correcting. They follow noises as they change, such as engines accelerating.

"Most of these systems are still in the experimental stage," says Mike Collins, a manager of digital signal operations at Motorola Corp. in Austin. "In a couple of years, it has the potential to become a commonplace consumer item that will make quieter dishwashers, quieter airplanes and so forth."

Most of the patents required to make a DSP-based noise reduction system work are owned by two small U.S. companies : privately held Active Noise and Vibration Technology in Phoenix and publicly held Nose Cancellation Technologies in Stamford, Conn. They are working with Motorola and Analog Devices of Norwood, Mass. to develop the best chips. Other companies are expected to become active players in coming years, at least at the chip-production level.

Active Noise says it will have headsets on the market this year carrying a price tag of about $250. They'll be marketed primarily to workers in noisy industrial settings, where they will replace earplugs as safety equipment.

Unlike earplugs, which block sounds indiscriminately, the headsets will be programmed to target low-frequency, repetitive sounds that bother most people. A jackhammer operator, at least theoretically, will be able to operate his or her machine and still converse with a co-worker without shouting. As brilliant as noise reduction technology sounds, not everybody is getting on board yet.

"The more mainstream approach is to try to reduce noise at the source," says engineer Tom Mitchell, head of the Noise Technology Center at General Motors Corp's Power Train Division in Pontiac, Mich. "Anything you add to a vehicle to susceptible to failure, and there's some added cost associated with a noise reduction system."

Mr. Mitchell says GM has devoted considerable resources to reducing unwanted vibrations and noise in automobiles. Fluid-filled engine mounts, developed eight years ago, are an example of a simple device that eliminates noise by reducing the transfer of vibrations from the engine to the frame of the car.

"I could bore you for hours with all the stuff we've developed," says Mr. Mitchell. "Like double-wall, insulated exhause pipes and sound absorbers in the headliner. We devote a lot of energy to reducing noise, because customers tell us it's one of the best mechanisms they have for assessing quality." Reducing noise can get kind of tricky. Nobody wants road noise, thus tire makers have sound standards to meet.

"On the other hand, nobody wants absolute silence. They want some feedback that the engine is there. That's where an electric car can be eerie," Mr. Mitchell says.

The key to the noise-cancellation feature of DSP systems rests in the software that's built into the chips. That's where most research and development energies are being expended. The chip has to be told which sounds to attack and which to leave alone.

"You don't want to cancel the sound of a great Porsche engine," says Tom Hesse, founder and chief executive officer of Active Noise in

Phoenix. In some cases, noise suppression systems actually do more than eliminate an irritation or a safety hazard. They can improve performance. Systems are being developed to replace the entire exhaust system and muffler, thus eliminating the back pressure that the muffler creates.

"As a result, you get up to a 5 percent improvement in gas mileage," says John McCoy, president of Noise Cancellation Technologies.

Many companies - including Boeing Co., Mercedes Benz and Whirlpool Corp. - confirm they are looking at noise reduction systems but don't want to comment on their research progress because they don't want to tip off their competitors about the timing of the introduction of improved devices. "I know there's a lot of work going on here, but it's highly proprietary," says Boeing spokesman Tom Cole.

Meanwhile, designers at Noise Cancellation and Active Noise are busy drumming up interest. So far, most of their income has come from licensing big companies to develope their own systems for specific products. When they come to market, there may be some interesting twists.

"We could use it to do more than reduce noise. It could create sounds," says Active Noise's Mr. Hesse. "We probably could make a Honda Civic sound like a Ferrari."

Better yet, how about one that can tune out, "Are we there yet?"

If you have comments or other information relating to such topics as this paper covers, please upload to KeelyNet or send to the Vangard Sciences address as listed on the first page.
Thank you for your consideration, interest and support.
Jerry W. Decker.........Ron Barker...........Chuck Henderson
Vangard Sciences/KeelyNet

If we can be of service, you may contact
Jerry at (214) 324-8741 or Ron at (214) 242-9346
